

ATTACHMENT 3

M180008

NEDO-33866

Model 2000 Radioactive Material Transport Package
Safety Analysis Report, Revision 2, December 2017

Non-Proprietary Information – Class I (Public)

NOTICE

This is a non-proprietary version of NEDE-33866P, Revision 2, which has the proprietary information removed. Portions of the document that have been removed are indicated by white space with an open and closed bracket as shown here [[]].

IMPORTANT NOTICE REGARDING CONTENTS OF THIS REPORT

Please Read Carefully

The information contained in this document is furnished for the purpose of licensing the Model 2000 Radioactive Material Transport Package. The use of this information by anyone other than that for which it is intended is not authorized; and with respect to any unauthorized use, GEH makes no representation or warranty, and assumes no liability as to the completeness, accuracy, or usefulness of the information contained in this document.



HITACHI

GE Hitachi Nuclear Energy

NEDO-33866

Revision 2

January 2018

Non-Proprietary Information - Class I (Public)

Model 2000 Radioactive Material Transport Package Safety Analysis Report

*Copyright 2016, 2017 GE-Hitachi Nuclear Energy Americas LLC
All Rights Reserved*

INFORMATION NOTICE

This is a non-proprietary version of the document NEDE-33866P, Revision 2, which has the proprietary information removed. Portions of the document that have been removed are indicated by an open and closed bracket as shown here [[]].

IMPORTANT NOTICE REGARDING CONTENTS OF THIS REPORT

Please Read Carefully

The information contained in this document is furnished for the purpose of licensing the Model 2000 Radioactive Material Transport Package. The use of this information by anyone other than that for which it is intended is not authorized; and with respect to any unauthorized use, GEH makes no representation or warranty, and assumes no liability as to the completeness, accuracy, or usefulness of the information contained in this document.

TABLE OF CONTENTS

List of Tables	viii
List of Figures.....	xiii
Revision Summary	xix
Acronyms.....	xxxviii
1 GENERAL INFORMATION	1-1
1.1 Introduction.....	1-1
1.2 Package Description.....	1-1
1.2.1. Packaging	1-2
1.2.2. Contents.....	1-4
1.2.3. Special Requirements for Plutonium.....	1-5
1.2.4. Operational Features	1-5
1.3 Appendix.....	1-12
1.3.1. Drawings	1-12
1.3.2. Material Specifications.....	1-37
1.4 References.....	1-38
2 STRUCTURAL EVALUATION	2-1
2.1 Description of Structural Design	2-1
2.1.1. Discussion	2-1
2.1.2. Design Criteria	2-3
2.1.3. Weights and Centers of Gravity	2-4
2.1.4. Identification of Codes and Standards for Package Design	2-6
2.2 Materials	2-7
2.2.1. Material Properties and Specifications.....	2-7
2.2.2. Chemical, Galvanic, or Other Reactions.....	2-13
2.2.3. Effects of Radiation on Materials.....	2-13
2.3 Fabrication and Examination	2-14
2.3.1. Fabrication.....	2-14
2.3.2. Examination	2-14
2.4 General Requirements for All Packages.....	2-14
2.4.1. Minimum Package Size.....	2-14

2.4.2.	Tamper-Indicating Feature.....	2-14
2.4.3.	Positive Closure.....	2-14
2.5	Lifting and Tie-Down Standards for All Packages.....	2-15
2.5.1.	Lifting Devices.....	2-15
2.5.2.	Tie-Down Devices.....	2-18
2.6	Normal Conditions of Transport.....	2-20
2.6.1.	Heat	2-20
2.6.2.	Cold	2-26
2.6.3.	Reduced External Pressure.....	2-26
2.6.4.	Increased External Pressure	2-26
2.6.5.	Vibration.....	2-26
2.6.6.	Water Spray.....	2-27
2.6.7.	Free Drop.....	2-27
2.6.8.	Corner Drop.....	2-72
2.6.9.	Compression.....	2-72
2.6.10.	Penetration.....	2-72
2.7	Hypothetical Accident Conditions.....	2-72
2.7.1.	Free Drop.....	2-72
2.7.2.	Crush	2-98
2.7.3.	Puncture.....	2-98
2.7.4.	Thermal	2-99
2.7.5.	Immersion - Fissile Material	2-101
2.7.6.	Immersion - All Packages	2-101
2.7.7.	Deep Water Immersion Test (for Type B Packages Containing More than 10^5 A ₂)	2-101
2.7.8.	Summary of Damage.....	2-101
2.8	Accident Conditions for Air Transport of Plutonium.....	2-101
2.9	Accident Conditions for Fissile Material Packages for Air Transport.....	2-101
2.10	Special Form.....	2-102
2.11	Fuel Rods	2-102
2.12	Appendix.....	2-102
2.12.1.	LS-DYNA Evaluation of the Model 2000 Transport Package	2-102
2.12.2.	Lead Slump Calculation	2-154
2.12.3.	Lifting and Tie-Down Analysis.....	2-160
2.12.4.	Cask Closure Bolt Evaluation	2-199
2.12.5.	Model 2000 Scale Model Drop Test Report	2-215
2.12.6.	Fabrication Stresses.....	2-264
2.13	References.....	2-276

3	THERMAL EVALUATION	3-1
3.1	Description of Thermal Design	3-4
3.1.1.	Design Features	3-4
3.1.2.	Content's Decay Heat.....	3-4
3.1.3.	Summary Tables of Temperatures	3-4
3.1.4.	Summary Tables of Maximum Pressures.....	3-7
3.2	Material Properties and Component Specifications	3-8
3.2.1.	Material Properties	3-8
3.2.2.	Component Specifications.....	3-11
3.3	Thermal Evaluation under Normal Conditions of Transport	3-11
3.3.1.	Heat and Cold.....	3-34
3.3.2.	Maximum Normal Operating Pressure	3-42
3.4	Thermal Evaluation under Hypothetical Accident Conditions	3-42
3.4.1.	Initial Conditions.....	3-43
3.4.2.	Fire Test Conditions.....	3-47
3.4.3.	Maximum Temperatures and Pressure.....	3-48
3.4.4.	Maximum Thermal Stresses.....	3-56
3.4.5.	Accident Conditions for Fissile Material Packages for Air Transport.....	3-56
3.5	Appendix	3-57
3.5.1.	Model 2000 Transport Package with HPI and No Material Basket.....	3-57
3.6	References	3-67
4	CONTAINMENT	4-1
4.1	Description of Containment System	4-1
4.1.1.	Containment Vessel.....	4-1
4.1.2.	Closure	4-1
4.1.3.	Containment Penetrations	4-1
4.2	Containment Under Normal Conditions of Transport	4-5
4.3	Containment Under Hypothetical Accident Conditions	4-6
4.4	Leakage Rate Tests for Type B Packages	4-6
4.5	References	4-7
5	SHIELDING EVALUATION	5-1
5.1	Description of Shielding Design	5-1
5.1.1.	Design Features	5-1

NEDO-33866 Revision 2
Non-Proprietary Information – Class I (Public)

5.1.2.	Summary Table of Maximum Radiation Levels	5-2
5.2	Source Specification.....	5-3
5.2.1.	Gamma Source	5-4
5.2.2.	Neutron Source.....	5-6
5.3	Shielding Model.....	5-6
5.3.1.	Configuration of Source and Shielding.....	5-6
5.3.2.	Material Properties	5-14
5.4	Shielding Evaluation.....	5-16
5.4.1.	Methods.....	5-16
5.4.2.	Input and Output Data	5-17
5.4.3.	Flux-to-Dose-Rate Conversion	5-17
5.4.4.	External Radiation Levels	5-19
5.5	Appendices.....	5-22
5.5.1.	ORIGEN-S Irradiated Hardware and Byproduct Source Term Calculation	5-22
5.5.2.	Cobalt-60 Isotope Rod Activity Distribution	5-31
5.5.3.	Radionuclide Decay Heat Conversion Factors.....	5-37
5.5.4.	Irradiated Hardware and Byproduct Loading Table	5-39
5.5.5.	Combined Content Shipments.....	5-41
5.6	References.....	5-42
6	CRITICALITY EVALUATION.....	6-1
7	OPERATING PROCEDURES	7-1
7.1	Package Loading.....	7-1
7.1.1.	Preparation for Loading	7-2
7.1.2.	Loading of Contents.....	7-3
7.1.3.	Closing the Cask and Performing Leakage Tests.....	7-3
7.1.4.	Preparation for Transport	7-5
7.2	Package Unloading	7-5
7.2.1.	Receipt of Package from Carrier	7-5
7.2.2.	Removal of Contents.....	7-7
7.3	Preparation of Empty Packaging for Transport.....	7-7
7.3.1.	Cask Cavity Inspection.....	7-7
7.3.2.	Installation of the Cask Closure Lid.....	7-8
7.3.3.	Assembly Verification Leakage Testing.....	7-8
7.3.4.	Preparing the Empty Cask for Transport.....	7-8
7.4	Other Operations	7-8

7.5	Appendix.....	7-9
7.5.1.	Irradiated Hardware and Byproduct Loading Table	7-9
7.5.2.	Verification of Compliance for Cobalt-60 Isotope Rods	7-13
7.5.3.	Combined Contents	7-15
7.6	References.....	7-17
8	ACCEPTANCE TESTS AND MAINTENANCE PROGRAM	8-1
8.1	Acceptance Test.....	8-1
8.1.1.	Visual Inspections and Measurements	8-1
8.1.2.	Weld Examinations	8-1
8.1.3.	Structural and Pressure Tests	8-2
8.1.4.	Fabrication Leakage Tests.....	8-2
8.1.5.	Component and Material Tests	8-3
8.1.6.	Shielding Tests	8-4
8.1.7.	Thermal Tests.....	8-4
8.1.8.	Miscellaneous Tests	8-5
8.2	Maintenance Program	8-7
8.2.1.	Structural and Pressure Tests	8-7
8.2.2.	Leak Tests	8-8
8.2.3.	Component and Material Tests	8-8
8.2.4.	Thermal Tests.....	8-9
8.2.5.	Miscellaneous Tests	8-9
8.3	Appendix.....	8-9
8.4	References.....	8-9

LIST OF TABLES

Table 1.3-1.	Model 2000 Packaging Licensing Drawings.....	1-12
Table 2.1-1.	Structural Design Criteria for Model 2000 Cask.....	2-4
Table 2.1-2.	Structural Design Criteria for HPI and Material Basket	2-4
Table 2.1-3.	Summary of Maximum Weights	2-5
Table 2.1-4.	Overpack Base Weight.....	2-5
Table 2.2-1.	Structural Properties of Type 304 Stainless Steel	2-7
Table 2.2-2.	Structural Properties of ASME Type [[]]	2-8
Table 2.2-3.	Structural Properties of ASME Type [[]]	2-9
Table 2.2-4.	Structural Properties of Depleted Uranium Metal.....	2-9
Table 2.2-5.	Structural Properties of Lead.....	2-10
Table 2.2-6.	Bolt – ASTM A-540 Grade B21 Class 3.....	2-10
Table 2.2-7.	Internal Thread – ASME SA-182 F304	2-11
Table 2.2-8.	ASTM A-193 B6 Bolt Properties.....	2-12
Table 2.2-9.	ASTM A-540 Grade B22 Class 3 Bolt Properties	2-12
Table 2.5.1-1.	Summary of Cask Lifting Device Stresses.....	2-17
Table 2.5.2-1.	Tie-Down System Stress Analysis Results	2-18
Table 2.6.1-1.	Temperature Results, NCT (in Shade and with Insolation)	2-23
Table 2.6.1-2.	Radial Thermal Expansion Evaluation for HPI and Material Basket	2-24
Table 2.6.1-3.	Axial Thermal Expansion Evaluation for HPI and Material Basket	2-24
Table 2.6.1-4.	NCT Thermal Stress Results (psi).....	2-24
Table 2.6.1-5.	Model 2000 Cask NCT Stress Analysis Summary (psi)	2-25
Table 2.6.7-1.	LS-DYNA Results.....	2-28
Table 2.6.7-2.	NCT End Drop Section 1 Stress Results (psi).....	2-40
Table 2.6.7-3.	NCT End Drop Section 1 Stress Results (psi).....	2-40
Table 2.6.7-4.	NCT End Drop Section 2 Stress Results (psi).....	2-43
Table 2.6.7-5.	NCT End Drop Section 2 Stress Results (psi).....	2-43
Table 2.6.7-6.	NCT Side Drop Section 3 Stress Results (psi).....	2-46
Table 2.6.7-7.	NCT Side Drop Section 3 Stress Results (psi).....	2-46
Table 2.6.7-8.	NCT Side Drop Section 4 Stress Results (psi).....	2-48
Table 2.6.7-9.	NCT Side Drop Section 4 Stress Results (psi).....	2-48
Table 2.6.7-10.	NCT Side Drop Section 5 Stress Results (psi).....	2-50
Table 2.6.7-11.	NCT Side Drop Section 5 Stress Results (psi).....	2-50
Table 2.6.7-12.	LS-DYNA NCT Impact Results Summary	2-58
Table 2.6.7-13.	NCT Case 1 HPI Body Top 30 Results.....	2-63
Table 2.6.7-14.	NCT Support Disk Case 1 Results	2-64
Table 2.6.7-15.	NCT Case 2 HPI Body Top 30 Results.....	2-66

NEDO-33866 Revision 2
 Non-Proprietary Information – Class I (Public)

Table 2.6.7-16.	NCT Support Disk Case 2 Results	2-67
Table 2.6.7-17.	NCT End Drop Stress Summary	2-68
Table 2.6.7-18.	Moment of Inertia Calculation	2-71
Table 2.7.1-1.	LS-DYNA Results.....	2-73
Table 2.7.1-2.	HAC End Drop Section 6 Stress Results (psi)	2-76
Table 2.7.1-3.	HAC End Drop Section 6 Stress Results (psi)	2-76
Table 2.7.1-4.	HAC End Drop Section 7 Stress Results (psi)	2-78
Table 2.7.1-5.	HAC End Drop Section 7 Stress Results (psi)	2-78
Table 2.7.1-6.	HAC Side Drop Section 8 Stress Results (psi).....	2-80
Table 2.7.1-7.	HAC Side Drop Section 8 Stress Results (psi).....	2-81
Table 2.7.1-8.	HAC Side Drop Section 9 Stress Results (psi).....	2-83
Table 2.7.1-9.	HAC Side Drop Section 9 Stress Results (psi).....	2-83
Table 2.7.1-10.	HAC End Drop Stress Summary	2-86
Table 2.7.1-11.	HAC Case 1 HPI Body Top 30 Results	2-87
Table 2.7.1-12.	HAC Support Disk Case 1 Results.....	2-88
Table 2.7.1-13.	HAC Case 2 HPI Body Top 30 Results	2-89
Table 2.7.1-14.	HAC Support Disk Case 2 Results.....	2-90
Table 2.7.1-15.	Moment of Inertia Calculation	2-96
Table 2.7.1-16.	Summary Temperatures for HAC	2-99
Table 2.7.4-1.	Summary of HAC Stress Results	2-100
Table 2.12.1-1.	Summary of Drop Cases and Results	2-104
Table 2.12.1-2.	Benchmark Runs and the Drop Parameters.....	2-106
Table 2.12.1-3.	Normal Condition of Transport Runs and the Drop Parameters	2-107
Table 2.12.1-4.	Hypothetical Accident Condition of Transport Runs and the Drop Parameters	2-108
Table 2.12.1-5.	Shallow Angle Drop Runs and the Drop Parameters	2-109
Table 2.12.1-6.	HAC Drop Cases with Pin Puncture	2-109
Table 2.12.1-7.	Mechanical Properties of SS304 at Temperature of Interest.....	2-110
Table 2.12.1-8.	Stress Strain Curve of SS304 at -40°F	2-110
Table 2.12.1-9.	Stress Strain Curve of SS304 at Ambient Temperature	2-111
Table 2.12.1-10.	Stress Strain Curve of SS304 at 300°F.....	2-112
Table 2.12.1-11.	Lead Temperature Dependent Properties	2-115
Table 2.12.1-12.	Strain-Rate Factors that elevated the Stress-Strain Curves of SS304	2-116
Table 2.12.1-13.	Component Temperature Range and Justification	2-117
Table 2.12.1-14.	Comparison of Benchmark Simulations and Drop Tests Acceleration.....	2-153
Table 2.12.1-15.	Comparison of Benchmark Simulations and Drop Tests Deformations	2-153
Table 2.12.1-16.	Comparison of Shallow Angle Drop Analyses	2-154
Table 2.12.2-1.	Compressive Stress in Lead Shield	2-157
Table 2.12.3-1.	Bolt Loading Per Ear Design and Load Case.....	2-173
Table 2.12.3-2.	Lifting Ear Bolt Percent Proof Load	2-175

NEDO-33866 Revision 2
 Non-Proprietary Information – Class I (Public)

Table 2.12.3-3.	Summary of Ear Analysis for Model 2000	2-179
Table 2.12.3-4.	Tie-Down Ropes Tension Forces	2-192
Table 2.12.3-5.	Tie-Down System Stress Analysis Results	2-199
Table 2.12.4-1.	Input Parameters.....	2-201
Table 2.12.4-2.	Lid Bolt Evaluation Input Parameters	2-202
Table 2.12.4-3.	Calculation of Required Length of Engagement at 150°F	2-204
Table 2.12.4-4.	Model 2000 Stress Analysis Design Input Parameter	2-205
Table 2.12.4-5.	Forces/Moments Results (NCT).....	2-211
Table 2.12.4-6.	Forces/Moments Results (HAC)	2-212
Table 2.12.4-7.	Total Loads/Bolt Stresses (NCT)	2-212
Table 2.12.4-8.	Total Loads/Bolt Stresses (HAC).....	2-213
Table 2.12.4-9.	Fatigue Analysis Results	2-215
Table 2.12.6-1.	Dimensions of Stainless Steel Shells.....	2-264
Table 2.12.6-2.	Dimensions of Inner and Outer Shell at 620°F	2-268
Table 2.12.6-3.	Dimensions of Shells at 70°F	2-270
Table 2.12.6-4.	Summary of Stresses Due to Lead Pouring, Solidification, and Shrinkage	2-275
Table 3-1.	Insolation Data per 10 CFR 71.71	3-1
Table 3.1.3-1.	Temperature Limits	3-5
Table 3.1.3-2.	NCT Temperature Summary and Comparison with Allowable Temperatures	3-5
Table 3.1.3-3.	HAC Maximum Temperature Summary and Comparison with Allowable Temperatures	3-7
Table 3.1.4-1.	Maximum Pressures	3-7
Table 3.2.1-1.	Thermal Properties of Solid Regions in the Model 2000 Finite Element Thermal Model.....	3-9
Table 3.2.1-2.	Thermal Properties of Gaseous Regions in the Finite Element Thermal Model.....	3-10
Table 3.3-1.	Typical Thermal Contact Conductance Values from Open Literature.....	3-19
Table 3.3-2.	TCC Values Used in the Thermal Analyses.....	3-20
Table 3.3-3.	Thermal Contact Resistance Levels Assigned to the Modeled Contact Elements.....	3-21
Table 3.3-4.	Thermophysical Properties of Dry Air (from Reference 3-3).....	3-27
Table 3.3-5.	Constants 'C' and 'm' for the Nusselt Number Calculation of a Cylinder in Cross Flow (from Reference 3-3, Table 7.2)	3-29
Table 3.3.1-1.	Temperature Results, NCT (in Shade and with Insolation)	3-37
Table 3.3.1-2.	Comparison of Mixed and Perfect Thermal Contact for NCT with Insolation.....	3-40
Table 3.3.1-3.	Model 2000 Transport Package Temperatures for Exposure to -40°F in Shade	3-41
Table 3.4.3-1.	Temperature Results, Hypothetical Accident Conditions	3-49

NEDO-33866 Revision 2
 Non-Proprietary Information – Class I (Public)

Table 5.5-4.	Cr-51 Gamma Emission Energy Spectrum	5-26
Table 5.5-5.	Mn-54 Gamma Emission Energy Spectrum.....	5-26
Table 5.5-6.	Co-58 Gamma Emission Energy Spectrum.....	5-26
Table 5.5-7.	Fe-59 Gamma Emission Energy Spectrum	5-26
Table 5.5-8.	Co-60 Gamma Emission Energy Spectrum.....	5-26
Table 5.5-9.	Zn-65 Gamma Emission Energy Spectrum.....	5-27
Table 5.5-10.	Nb-92m Gamma Emission Energy Spectrum	5-27
Table 5.5-11.	Nb-94 Gamma Emission Energy Spectrum	5-27
Table 5.5-12.	Zr/Nb-95 Gamma Emission Energy Spectrum	5-27
Table 5.5-13.	Sb-124 Gamma Emission Energy Spectrum	5-28
Table 5.5-14.	Sb-125 Gamma Emission Energy Spectrum	5-28
Table 5.5-15.	Sb-126 Gamma Emission Energy Spectrum	5-29
Table 5.5-16.	Cs-134 Gamma Emission Energy Spectrum	5-29
Table 5.5-17.	Cs-137 (Ba-137m) Gamma Emission Energy Spectrum	5-29
Table 5.5-18.	Hf-175 Gamma Emission Energy Spectrum	5-30
Table 5.5-19.	Hf-181 Gamma Emission Energy Spectrum	5-30
Table 5.5-20.	Ta-182 Gamma Emission Energy Spectrum	5-30
Table 5.5-21.	Cobalt-60 Isotope Rod Shielding Analysis Case Summary	5-32
Table 5.5-22.	Cobalt-60 Isotope Rod Shielding Analysis NCT Dose Rate Results	5-36
Table 5.5-23.	Cobalt-60 Isotope Rod Shielding Analysis Maximum NCT Dose Rates	5-36
Table 5.5-24.	Isotope Decay Heat Data	5-38
Table 5.5-25.	Example Irradiated SS304 Radionuclide Inventory	5-40
Table 5.5-26.	Example Zr-95 Radionuclide Inventory	5-40
Table 5.5-27.	Example Hf Poison Rod Radionuclide Inventory	5-40
Table 5.5-28.	Example SS304 Irradiated Hardware and Byproduct Loading Table	5-41
Table 5.5-29.	Example Zr-95 Irradiated Hardware and Byproduct Loading Table	5-41
Table 5.5-30.	Example Hf Poison Rod Irradiated Hardware and Byproduct Loading Table.....	5-41

NEDO-33866 Revision 2
 Non-Proprietary Information – Class I (Public)

Figure 2.6.7-26.	Case 1, NCT, Stress Intensity Result (psi)	2-64
Figure 2.6.7-27.	Case 2, NCT, Stress Intensity Result (psi)	2-67
Figure 2.6.7-28.	HPI NCT End Drop Results – Peak Stress Intensity (psi) and Displacement (inches)	2-69
Figure 2.7.1-1.	HAC End Drop Cask Body Stress Intensity (total stress psi)	2-75
Figure 2.7.1-2.	HAC End Drop Linearized Stress Location (Section 6)	2-75
Figure 2.7.1-3.	HAC End Drop Lid Stress Intensity (total stress psi)	2-77
Figure 2.7.1-4.	HAC End Drop Linearized Stress Location (Section 7)	2-77
Figure 2.7.1-5.	HAC Side Drop Cask Body Stress Intensity (total stress psi).....	2-79
Figure 2.7.1-6.	HAC Side Drop Linearized Stress Location (Section 8).....	2-80
Figure 2.7.1-7.	HAC Side Drop Lid Stress Intensity (total stress psi).....	2-81
Figure 2.7.1-8.	HAC Side Drop Linearized Stress Location (Section 9).....	2-82
Figure 2.7.1-9.	HPI HAC End Drop Results – Peak Stress Intensity (psi) and Displacement (in)	2-85
Figure 2.7.1-10.	Case 1, HAC, Stress Intensity Result (psi).....	2-88
Figure 2.7.1-11.	Case 2, HAC, Stress Intensity Result (psi).....	2-90
Figure 2.7.1-12.	Overpack Loading, HAC Side Drop	2-92
Figure 2.7.1-13.	Free Body Diagram of Overpack Top	2-93
Figure 2.7.1-14.	Overpack Junction	2-94
Figure 2.12.1-1.	Model 2000 Solid Model.....	2-105
Figure 2.12.1-2.	Drop Orientations	2-106
Figure 2.12.1.5-1.	Shallow Angle Drops	2-108
Figure 2.12.1.7-1.	Stress-Strain Curve of SS304 at -40°F	2-113
Figure 2.12.1.7-2.	Stress-Strain Curve of SS304 at Ambient Temperature.....	2-114
Figure 2.12.1.7-3.	Stress-Strain Curve of SS304 at 300°F	2-115
Figure 2.12.1.7-4.	Temperature Effect of Honeycomb Material	2-116
Figure 2.12.1.8-1.	Model 2000 Overpack and Cask Finite Element Model	2-118
Figure 2.12.1.8-2.	Rigid Plane and Pin Model for the End Drop Configuration	2-119
Figure 2.12.1.8-3.	Rigid Plane and Pin Model for the Side Drop Configuration	2-119
Figure 2.12.1.8-4.	Deformed Geometry of the Overpack after a 30 foot End Drop.....	2-120
Figure 2.12.1.8-5.	Deformed Geometry of the Overpack after a 30 foot Side Drop	2-121
Figure 2.12.1.11-1.	Case 1 Deformed Overpack Shape (Effective Plastic Strain)	2-124
Figure 2.12.1.11-2.	Case 1 Payload Acceleration Time History	2-124
Figure 2.12.1.11-3.	Case 1 Impact Energy Plot	2-125
Figure 2.12.1.11-4.	Case 1 Interface Sliding Energy Time History	2-125
Figure 2.12.1.11-5.	Case 2 Deformed Overpack Shape (Effective Plastic Strain)	2-126
Figure 2.12.1.11-6.	Case 2 Payload Acceleration Time History	2-126
Figure 2.12.1.11-7.	Case 2 Impact Energy Plot	2-127
Figure 2.12.1.11-8.	Case 2 Interface Sliding Energy Time History	2-127
Figure 2.12.1.11-9.	Case 3 Deformed Overpack Shape (Effective Plastic Strain)	2-128

NEDO-33866 Revision 2
Non-Proprietary Information – Class I (Public)

Figure 2.12.1.11-10.	Case 3 Payload Acceleration Time History	2-128
Figure 2.12.1.11-11.	Case 3 Impact Energy Plot.....	2-129
Figure 2.12.1.11-12.	Case 3 Interface Sliding Energy Time History	2-129
Figure 2.12.1.11-13.	Case 4 Deformed Overpack Shape (Effective Plastic Strain).....	2-130
Figure 2.12.1.11-14.	Case 4 Payload Acceleration Time History	2-130
Figure 2.12.1.11-15.	Case 4 Impact Energy Plot.....	2-131
Figure 2.12.1.11-16.	Case 4 Interface Sliding Energy Time History	2-131
Figure 2.12.1.11-17.	Case 5 Deformed Overpack Shape (Effective Plastic Strain).....	2-132
Figure 2.12.1.11-18.	Case 5 Payload Acceleration Time History	2-132
Figure 2.12.1.11-19.	Case 5 Impact Energy Plot.....	2-133
Figure 2.12.1.11-20.	Case 5 Interface Sliding Energy Time History	2-133
Figure 2.12.1.11-21.	Case 6 Deformed Overpack Shape (Effective Plastic Strain).....	2-134
Figure 2.12.1.11-22.	Case 6 Payload Acceleration Time History	2-134
Figure 2.12.1.11-23.	Case 6 Impact Energy Plot.....	2-135
Figure 2.12.1.11-24.	Case 6 Interface Sliding Energy Time History	2-135
Figure 2.12.1.11-25.	Case 7 Deformed Overpack Shape (Effective Plastic Strain).....	2-136
Figure 2.12.1.11-26.	Case 7 Payload Acceleration Time History	2-136
Figure 2.12.1.11-27.	Case 7 Impact Energy Plot.....	2-137
Figure 2.12.1.11-28.	Case 7 Interface Sliding Energy Time History	2-137
Figure 2.12.1.11-29.	Case 8 Deformed Overpack Shape (Effective Plastic Strain).....	2-138
Figure 2.12.1.11-30.	Case 8 Payload Acceleration Time History	2-138
Figure 2.12.1.11-31.	Case 8 Impact Energy Plot.....	2-139
Figure 2.12.1.11-32.	Case 8 Interface Sliding Energy Time History	2-139
Figure 2.12.1.11-33.	Case 9 Deformed Overpack Shape (Effective Plastic Strain).....	2-140
Figure 2.12.1.11-34.	Case 9 Payload Acceleration Time History	2-140
Figure 2.12.1.11-35.	Case 9 Impact Energy Plot.....	2-141
Figure 2.12.1.11-36.	Case 9 Interface Sliding Energy Time History	2-141
Figure 2.12.1.11-37.	Case 10 Deformed Overpack Shape (Effective Plastic Strain).....	2-142
Figure 2.12.1.11-38.	Case 10 Payload Acceleration Time History	2-142
Figure 2.12.1.11-39.	Case 10 Impact Energy Plot.....	2-143
Figure 2.12.1.11-40.	Case 10 Interface Sliding Energy Time History	2-143
Figure 2.12.1.11-41.	Case 11 Deformed Overpack Shape (Effective Plastic Strain).....	2-144
Figure 2.12.1.11-42.	Case 11 Payload Acceleration Time History	2-144
Figure 2.12.1.11-43.	Case 11 Impact Energy Plot.....	2-145
Figure 2.12.1.11-44.	Case 11 Interface Sliding Energy Time History	2-145
Figure 2.12.1.11-45.	Case 12 Deformed Overpack Shape (Effective Plastic Strain).....	2-146
Figure 2.12.1.11-46.	Case 12 Payload Acceleration Time History	2-146
Figure 2.12.1.11-47.	Case 12 Impact Energy Plot.....	2-147
Figure 2.12.1.11-48.	Case 12 Interface Sliding Energy Time History	2-147
Figure 2.12.1.11-49.	Case 13 Deformed Overpack Shape (Effective Plastic Strain).....	2-148

NEDO-33866 Revision 2
 Non-Proprietary Information – Class I (Public)

Figure 2.12.1.11-50.	Case 13 Payload Acceleration Time History	2-148
Figure 2.12.1.11-51.	Case 13 Impact Energy Plot.....	2-149
Figure 2.12.1.11-52.	Case 13 Interface Sliding Energy Time History	2-149
Figure 2.12.1.11-53.	Case 14 Deformed Overpack Shape (Effective Plastic Strain).....	2-150
Figure 2.12.1.11-54.	Case 14 Payload Acceleration Time History	2-150
Figure 2.12.1.11-55.	Case 14 Impact Energy Plot.....	2-151
Figure 2.12.1.11-56.	Case 14 Interface Sliding Energy Time History	2-151
Figure 2.12.1.11-57.	Strain Contour of Package after 30 ft End Drop and Pin Puncture Sequence.....	2-152
Figure 2.12.1.11-58.	Strain Contour of Package after 30 ft Side Drop and Pin Puncture Sequence.....	2-152
Figure 2.12.3-1.	Structural Locations for Ear Analysis	2-160
Figure 2.12.3-2.	Magnitude and Direction of Loading in Model 2000 Cask.....	2-161
Figure 2.12.3-3.	Ear Hole Cross Section.....	2-163
Figure 2.12.3-4.	Standard Ear Load Case I or III.....	2-165
Figure 2.12.3-5.	Auxiliary Ear, Case I and Case II Weld Stresses	2-167
Figure 2.12.3-6.	Standard Ear, Case I and Case II Weld Stresses	2-170
Figure 2.12.3-7.	Lifting Ear Contact Bearing Stresses	2-176
Figure 2.12.3-8.	Design Fatigue Curves For High Strength Steel Bolting Above 700°F	2-178
Figure 2.12.3-9.	Analytical Model of Lifting Lug	2-181
Figure 2.12.3-10.	Loading on the Weld Area	2-182
Figure 2.12.3-11.	Stresses Acting on the Weld.....	2-183
Figure 2.12.3-12.	Tie-Down of Transport Package to Vehicle.....	2-185
Figure 2.12.3-13.	Tie-Down Wire Ropes.....	2-187
Figure 2.12.3-14.	Wire Rope Extension at Small Angle (θ) Rotation	2-187
Figure 2.12.3-15.	Final Length of Rope 5.....	2-188
Figure 2.12.3-16.	Final to Initial Rope Length Ratio per Small Angle Rotation.....	2-190
Figure 2.12.3-17.	Tie-Down Rib Hole Loading.....	2-194
Figure 2.12.3-18.	Weld Pattern of Top Tie Down Rib	2-195
Figure 2.12.3-19.	Weld Geometry of Tie-Down Rib and Gusset to Overpack	2-197
Figure 2.12.4-1.	Seal with Contact Width Dimension	2-201
Figure 3-1.	Model 2000 Transport Package (High Performance Insert and Material Basket Not Shown)	3-3
Figure 3.3-1.	Finite Element Model of the Model 2000 Transport Package	3-14
Figure 3.3-2.	Finite Element Model of the Model 2000 Transport Package - Air and Helium Not Shown.....	3-15
Figure 3.3-3.	Finite Element Model of the Model 2000 Transport Package - Exploded View	3-16
Figure 3.3-4.	Heat Transfer Through the Contact Plane Between Two Solid Surfaces	3-17
Figure 3.3-5.	Thermal Contact Pair Locations in the Finite Element Model.....	3-24
Figure 3.3-6.	Natural Convection Boundary Conditions for NCT.....	3-31

NEDO-33866 Revision 2
 Non-Proprietary Information – Class I (Public)

Figure 3.3-7.	Natural Convection and Thermal Radiation Coefficients for NCT	3-32
Figure 3.3-8.	Contents Heat Flux Applied to Material Basket [[]]	3-34
Figure 3.3.1-1.	Solar Heat Flux Boundary Conditions for NCT.....	3-36
Figure 3.3.1-2.	Steady-State Temperature Distribution—NCT	3-38
Figure 3.3.1-3.	Overpack Steady-State Temperatures, 100°F Ambient Temperature	3-39
Figure 3.4.1-1.	Three-Dimensional Finite Element Model of the Model 2000 (Half Symmetry).....	3-44
Figure 3.4.1-2.	LINK34 Incorporated to Simulate HAC Side Contact and Puncture Damage.....	3-45
Figure 3.4.1-3.	Natural Convection Boundary Conditions for HAC	3-46
Figure 3.4.1-4.	Natural/Forced Convection and Thermal Radiation Coefficients for HAC	3-47
Figure 3.4.2-1.	Solar Heat Flux Boundary Conditions for HAC (Post-Fire Cool-Down).....	3-48
Figure 3.4.3-1.	Temperature-History of the Material Basket and Overpack for HAC	3-50
Figure 3.4.3-2.	Temperature-History of the HPI and Cask for HAC.....	3-51
Figure 3.4.3-3.	Temperature-History of the Cask Ports for HAC.....	3-52
Figure 3.4.3-4.	Temperature-History of the HPI and Cask Fill Gases.....	3-53
Figure 3.4.3-5.	Temperature Contours During HAC 30-Minute Fire and Cool-Down ...	3-54
Figure 3.4.3-6.	Gap Between HPI [[]]and Cask Cavity Bottom (INCH)	3-56
Figure 3.5.1-1.	3D FEA Model of the Model 2000 Transport Package with HPI and No Material Basket (Half Symmetry) - Elements Representing Air and Helium Not Shown for Clarity	3-58
Figure 3.5.1-2.	Package Temperature Contours for NCT with 100°F Ambient Temperature in Shade and with Insolation.....	3-61
Figure 3.5.1-3.	Package Exterior Surface Temperature Contours for NCT with 100°F Ambient Temperature in Shade.....	3-62
Figure 4.1.3-1.	Cask Containment Boundary.....	4-3
Figure 4.1.3-2.	Cask Port Configuration (Assembled View).....	4-4
Figure 4.1.3-3.	Cask Lid Seal Design	4-4
Figure 4.1.3-4.	Cask Port Configuration (Exploded View)	4-5
Figure 5.3-1.	MCNP6 Point / Line Source Locations	5-8
Figure 5.3-2.	NCT MCNP6 Shielding Model.....	5-11
Figure 5.3-3.	HAC MCNP6 Shielding Model	5-12
Figure 5.3-4.	NCT MCNP6 Tallies with 10% Margin to the Regulatory Limit.....	5-13
Figure 5.3-5.	HAC MCNP6 Tallies with 10% Margin to the Regulatory Limit	5-14
Figure 5.5-1.	HPI Material Basket with ‘Realistic’ Source Geometry Locations	5-31
Figure 5.5-2.	‘Realistic’ Source Arrangement for Bottom Dose Rates	5-32
Figure 5.5-3.	‘Bounding’ Source Arrangement for Bottom Dose Rates.....	5-33
Figure 5.5-4.	‘Realistic’ Source Arrangement for Top Dose Rates.....	5-33
Figure 5.5-5.	‘Bounding’ Source Arrangement for Top Dose Rates	5-34

NEDO-33866 Revision 2
Non-Proprietary Information – Class I (Public)

Figure 5.5-6.	‘Realistic’ Source Arrangement for Side Dose Rates	5-34
Figure 5.5-7.	‘Bounding’ Source Arrangement for Side Dose Rates – Case 1	5-35
Figure 5.5-8.	‘Bounding’ Source Arrangement for Side Dose Rates – Case 2.....	5-35
Figure 7.5.1-1.	Irradiated Hardware and Byproduct Loading Table.....	7-10
Figure 8-1.	Cask Shielding Inspection Points	8-5
Figure 8-2.	Thermocouple Locations	8-6

REVISION SUMMARY

Changes from Revision 0 to Revision 1 are listed in the following table. No revision bars are used for these changes. Changes from Revision 1 to Revision 2 are listed in a separate table immediately following this one.

Location	Description of Change (Rev. 0 to Rev. 1)	Reason for Change
Chapter 1		
Section 1.1	Deleted “fissile materials” from the first paragraph.	Responses to RAIs 5.1, 5.2, and 5.6.
Section 1.1	Deleted Reference 1-1, as 10 CFR 71 does not need to be a chapter reference. Adjusted all other reference numbers accordingly in Chapter 1. Added pointer to Section 5.1.2 for discussion of exclusive use shipment.	Administrative change.
Section 1.1	Reworded last sentence of first paragraph – CSI not applicable due to removal of fissile content from SAR, as stated in the responses to RAIs 5.1, 5.2, and 5.6.	Responses to RAIs 5.1, 5.2, and 5.6.
Section 1.2	Modified third bullet under “Contents” consistent with removal of fissile material from SAR.	Responses to RAIs 5.1, 5.2, and 5.6.
Section 1.2.1.1	Second paragraph – regarding the cask lid seal, deleted the information associated with Configuration 2.	Removing reference to decay heat configurations and Configuration 2 seal material per response to RAI 4.1.
Section 1.2.1.1	Fourth paragraph – regarding the cask lid seal, deleted the information associated with Configuration 2.	Removing reference to decay heat configurations and Configuration 2 seal material per response to RAI 4.1.
Section 1.2.2.1	Added “nominally” for the HPI dimensions, as the supporting drawing lists the dimensions as nominal.	Change made for clarity.
Section 1.2.2.3	Removed “and fissile materials” from the first sentence. Removed irradiated fuel rods and special nuclear material from the second sentence.	Responses to RAIs 5.1, 5.2, and 5.6.
Section 1.2.2.3	Item d) rewritten to remove reference to Configuration 1 and 2 and clarify the decay heat basis for the SAR.	Removing reference to decay heat configurations consistent with the response to RAI 4.1.

NEDO-33866 Revision 2
Non-Proprietary Information – Class I (Public)

Location	Description of Change (Rev. 0 to Rev. 1)	Reason for Change
Table 1.2-1	Deleted due to the changes to Section 1.2.2.3 Item d).	Removing reference to decay heat configurations consistent with the response to RAI 4.1.
Section 1.2.2.3	Removed Irradiated [[]] Fuel Rods and Special Nuclear Material as contents for shipment. Also, updated the Cobalt-60 Isotope Rods Item c. to reflect consistency with Section 5.5.2.	Responses to RAIs 1.1, 5.1, 5.2, and 5.6.
Section 1.2.3	Reworded to clarify that fissile material is not an approved content.	Responses to RAIs 5.1, 5.2, and 5.6.
Section 1.2.4	Administratively updated wording related to the additional shoring. Deleted last part of last sentence in fourth paragraph, as there are no longer multiple decay heat configuration designs.	Removing reference to decay heat configurations consistent with the response to RAI 4.1.
Section 1.2.4	Updated the reference to the Chapter 3 section that discussed the protective personnel barrier.	Administrative change.
Table 1.3-1	Updated revision numbers for licensing drawings.	Update made because drawings have been revised since SAR Revision 0 was issued.
Section 1.3.1	Provided revised licensing drawings and associated parts lists in accordance with Table 1.3-1.	Update made because drawings have been revised since SAR Revision 0 was issued.
Section 1.3.2.1	Rewritten to only address the one seal material (originally associated with Configuration 1). References 1-3 and 1-5 deleted, as they are specific to the Former Configuration 2 seal material. Reference 1-4 revised to only provide information for the one seal material (and the reference renumbered due to the other reference deletions).	Responses to RAIs 4.1, 4.2, and 4.3.
Section 1.4	Deleted Reference 1-1 as discussed above. Deleted References 1-3 and 1-5 per the changes to Section 1.3.2.1.	Response to RAIs 4.1, 4.2, and 4.3.
Chapter 2		
Chapter 2	Changed the title of Chapter 2 from “Structural Analysis” to “Structural Evaluation”.	For strict adherence to Regulatory Guide 7.9.
Section 2	Created paragraph 2 explaining the licensing basis (1500 W) and the Chapter 2 analysis basis (3000 W).	Elimination of Configuration 2.

NEDO-33866 Revision 2
Non-Proprietary Information – Class I (Public)

Location	Description of Change (Rev. 0 to Rev. 1)	Reason for Change
Section 2	Removed bullet 5 concerning support of criticality analysis assumptions.	Criticality analysis has been removed from Chapter 6. Fissile material is no longer in content scope.
Section 2.1.1	Removed Configuration 2 seal materials.	Elimination of Configuration 2.
Table 2.1-3	Removed HPI component weights.	Consistent with GEH licensing drawings 001N8425, 001N8427 and 001N8428
Table 2.1-4	Added for overpack base weight.	Response to RAI 7.2.
Section 2.4.3	Changed closure bolt torque from 500 ft-lb to 720±30 ft pound.	Response to RAI 7.2.
Table 2.5.1-1	Updated lifting device bolt stresses and margins of safety.	Response to RAI 7.2.
Section 2.5.1.2	Changed lifting ear bolt expected life from 12.5 to 11 years.	Response to RAI 7.2.
Section 2.5.2.1	Added missing word “shows”.	Editorial correction.
Section 2.6.1	Removed “maximum” from description of internal power generation.	1500 W is maximum, 3000 W bounding for structural analysis.
Section 2.6.1.1	Removed references to Configuration 2 and Configuration 1, replaced with 3000W and 1500W.	GE2000 with HPI is licensed for 1500W with 3000W bounding for structural evaluation.
Section 2.6.1.2	Subsection Radial Thermal Expansion, added “worst case” and changed difference in diameters from 0.19” to 0.020”.	Worst case dimensions used consistent with GEH licensing drawings 001N8424R2,001N8425R2, 101E8718R17 and 105E9520R9; difference in diameters consistent with revised Table 2.6.1-2.
Section 2.6.1.2	Subsection Axial Thermal Expansion, added “worst case” and changed difference in lengths from 0.23” to 0.13”.	Worst case dimensions used consistent with GEH licensing drawings 001N8424R2,001N8425R2, 101E8718R17 and 105E9520R9; difference in diameters consistent with revised Table 2.6.1-3.
Figure 2.6.1-1	Updated to reflect HPI support disk diameter as built condition.	Consistent with GEH licensing drawing 001N8425 R2.
Figure 2.6.1-2	Updated to reflect material basket as built condition.	Consistent with GEH licensing drawing 001N8424 R2.
Figure 2.6.1-3	Updated to reflect HPI inside diameter as built condition.	Consistent with GEH licensing drawing 001N8425 R2.

NEDO-33866 Revision 2
Non-Proprietary Information – Class I (Public)

Location	Description of Change (Rev. 0 to Rev. 1)	Reason for Change
Table 2.6.1-2	Updated for worst case as built dimensions and corrected maximum component temperatures consistent with supporting calculations.	Consistent with as built condition per GEH licensing drawing 001N8425R2 and temperature error correction.
Table 2.6.1-3	Updated for worst case as built dimensions for MB height and corrected maximum component temperatures consistent with supporting calculations.	Consistent with as built condition per GEH licensing drawings 001N1824R2, 001N8425R2, 101E8718 and 105E9520 and temperature error correction.
Table 2.6.1-5	Updated stress component $P_m + P_b + Q$ values and margins of safety as appropriate, deleted stress component Q for all cases because there is no acceptance criteria secondary stress.	Response to RAI 7.2; additional analysis for cask body stresses due to increase in cask lid bolt preload.
Section 2.6.7.1.1	Under subsection “Closure Lid Bolt Preload”, replace 32,000 lb preload with 48,000 lb preload consistent with a maximum torque of 750 ft-lb.	Response to RAI 7.2.
Figure 2.6.7-2	Updated for 48,000 lb cask closure bolt preload.	Response to RAI 7.2; additional analysis for cask body stresses due to increase in cask lid bolt preload.
Figure 2.6.7-4	Updated for 48,000 lb cask closure bolt preload.	Response to RAI 7.2; additional analysis for cask body stresses due to increase in cask lid bolt preload.
Section 2.6.7.1.2	Updated paragraph 2 & 3 margin of safety for $P_m + P_b + Q$ consistent with changes to Table 2.6.1-5.	Response to RAI 7.2; additional analysis for cask body stresses due to increase in cask lid bolt preload.
Figure 2.6.7-6	Updated consistent with 48,000 lb cask closure bolt preload.	Response to RAI 7.2; additional analysis for cask body stresses due to increase in cask lid bolt preload.
Table 2.6.7-3	Updated consistent with 48,000 lb cask closure bolt preload.	Response to RAI 7.2; additional analysis for cask body stresses due to increase in cask lid bolt preload.
Figure 2.6.7-8	Updated consistent with 48,000 lb cask closure bolt preload.	Response to RAI 7.2; additional analysis for cask body stresses due to increase in cask lid bolt preload.
Table 2.6.7-5	Updated consistent with 48,000 lb cask closure bolt preload.	Response to RAI 7.2; additional analysis for cask body stresses due to increase in cask lid bolt preload.
Section 2.6.7.1.3	Updated paragraph 3 and 4 margin of safety for $P_m + P_b + Q$ consistent with changes to Tables 2.6.7-9 and Table 2.6.7-10.	Response to RAI 7.2; additional analysis for cask body stresses due to increase in cask lid bolt preload.

NEDO-33866 Revision 2
Non-Proprietary Information – Class I (Public)

Location	Description of Change (Rev. 0 to Rev. 1)	Reason for Change
Figure 2.6.7-10	Updated consistent with 48,000 lb cask closure bolt preload.	Response to RAI 7.2; additional analysis for cask body stresses due to increase in cask lid bolt preload.
Table 2.6.7-7	Updated consistent with 48,000 lb cask closure bolt preload.	Response to RAI 7.2; additional analysis for cask body stresses due to increase in cask lid bolt preload.
Figure 2.6.7-12	Updated consistent with 48,000 lb cask closure bolt preload.	Response to RAI 7.2; additional analysis for cask body stresses due to increase in cask lid bolt preload.
Table 2.6.7-9	Updated consistent with 48,000 lb cask closure bolt preload.	Response to RAI 7.2; additional analysis for cask body stresses due to increase in cask lid bolt preload.
Figure 2.6.7-14	Updated consistent with 48,000 lb cask closure bolt preload.	Response to RAI 7.2; additional analysis for cask body stresses due to increase in cask lid bolt preload.
Table 2.6.7-11	Updated consistent with 48,000 lb cask closure bolt preload.	Response to RAI 7.2; additional analysis for cask body stresses due to increase in cask lid bolt preload.
Section 2.6.7.1.6	Added new section for cask overpack NCT end drop bolt evaluation.	Response to RAI 7.2.
Section 2.6.7.3	Deleted 2 nd sentence in paragraph 1, added NCT end drop case to material basket evaluation.	Response to RAI 2.1.
Section 2.7.1.2.5	Added new section for cask overpack HAC end drop bolt evaluation.	Response to RAI 7.2.
Section 2.7.1.3	Added material basket HAC end drop evaluation.	Response to RAI 2.2.
Section 2.7.1.3	Added subsection title “HAC Side Drop”.	Editorial change.
Section 2.7.1.3	Corrected “NCT side drop. . .” to “HAC side drop. . .” in G definition.	Editorial correction.
Section 2.7.5	Changed paragraph to state that the Model 2000 Transport Package is not licensed to transport fissile material.	Criticality analysis has been removed from Chapter 6. Fissile material is no longer in content scope.
Section 2.12.3.1	Subsection “Bolt Preload”, updated for 600±20 ft-lb lifting ear bolt torque.	Response to RAI 7.2.
Figure 2.12.3-7	Label added to figure showing lifting ear contact bearing stresses.	Editorial change
Table 2.12.3-2	Added new table for summarizing lifting ear bolt percent preload.	Response to RAI 7.2.

NEDO-33866 Revision 2
Non-Proprietary Information – Class I (Public)

Location	Description of Change (Rev. 0 to Rev. 1)	Reason for Change
Section 2.12.3.1	Subsection “Bolt Fatigue Analysis”, updated for 600±20 ft-lb lifting ear bolt torque.	Response to RAI 7.2.
Table 2.12.2-3	Updated bolt and thread stresses and margins of safety.	Response to RAI 7.2.
Section 2.12.4.1	Updated based on a cask lid closure bolt torque of 720±30 ft-lbs.	Response to RAI 7.2.
Section 2.12.4.1	Removed soft steel and stainless steel gasket retainer options.	Elimination of Configuration 2.
Table 2.12.4-1	Updated removing carbon steel and stainless steel parameters.	Elimination of Configuration 2.
Table 2.12.4-2	Deleted – Bolt torque sizing analysis removed.	Response to RAI 7.2 and elimination of Configuration 2.
Table 2.12.4-3	Deleted – Cask lid bolt torque sizing analysis removed.	Response to RAI 7.2 and elimination of Configuration 2.
Table 2.12.4-4	Deleted– Cask lid bolt torque sizing analysis removed.	Response to RAI 7.2 and elimination of Configuration 2.
Table 2.12.4-7 (now Table 2.12.4-4)	Updated existing parameters consistent with cask lid bolt torque and low temperature aluminum cask seal, added additional parameters from deleted Table 2.12.4-2 required for the bolt load and stress evaluation.	Response to RAI 7.2 and elimination of Configuration 2.
Table 2.12.4-8 (now Table 2.12.4-5)	Updated consistent with revised cask closure bolt load analysis.	Response to RAI 7.2 and elimination of Configuration 2.
Table 2.12.4-9 (now Table 2.12.4-6)	Updated consistent with revised cask closure bolt load analysis.	Response to RAI 7.2 and elimination of Configuration 2.
Table 2.12.4-10 (now Table 2.12.4-7)	Updated consistent with revised cask closure bolt load analysis.	Response to RAI 7.2 and elimination of Configuration 2.
Table 2.12.4-11 (now Table 2.12.4-8)	Updated consistent with revised cask closure bolt load analysis.	Response to RAI 7.2 and elimination of Configuration 2.
Section 2.12.4.2.16	Updated results consistent with revised cask closure bolt load analysis.	Response to RAI 7.2 and elimination of Configuration 2.
Section 2.12.4.2.17	Updated results consistent with revised with cask closure bolt load analysis.	Response to RAI 7.2 and elimination of Configuration 2.
Table 2.12.4-12 (now Table 2.12.4-9)	Updated consistent with revised cask closure bolt load analysis.	Response to RAI 7.2 and elimination of Configuration 2.

NEDO-33866 Revision 2
Non-Proprietary Information – Class I (Public)

Location	Description of Change (Rev. 0 to Rev. 1)	Reason for Change
Chapter 3		
Section 3	Removed Configurations 1 and 2, added 2 nd paragraph explaining the licensing basis (1500W) and the Chapter 3 analysis basis (3000W).	Elimination of Configuration 2.
Section 3.1.1	Updated 3 rd paragraph, cask lid seal discussion.	Elimination of Configuration 2.
Section 3.1.2	Removed “configurations” from first sentence, removed irradiated fuel as a content, deleted last sentence.	Elimination of Configuration 2 and revised content scope.
Section 3.1.3	Removed Configuration 2.	Elimination of Configuration 2.
Table 3.1.3-1	Changed note c to “See Chapter 4 for additional discussion”.	Chapter 4 provides the 1500 W decay heat licensing basis temperatures for the seal locations.
Section 3.1.3.1	Removed Configuration 2.	Elimination of Configuration 2.
Table 3.1.3-2	Added note c callouts to lid seal and O-ring allowable temperatures and added note c “See Chapter 4 for additional discussion”.	Chapter 4 provides the 1500 W decay heat licensing basis temperatures for the seal locations.
Section 3.1.3.2	Removed Configuration 2.	Elimination of Configuration 2.
Table 3.1.3-3	Added note b callouts to lid seal and O-ring allowable temperatures and added note b “See Chapter 4 for additional discussion”.	Chapter 4 provides the 1500 W decay heat licensing basis temperatures for the seal locations.
Section 3.2.2	Removed Configuration 2, updated description of seal, O-ring and retainer materials.	Elimination of Configuration 2.
Section 3.3	Removed Configuration 2.	Elimination of Configuration 2.
Figure 3.3-1	Removed Configuration 2 from title.	Elimination of Configuration 2.
Figure 3.3-2	Removed Configuration 2 from title.	Elimination of Configuration 2.
Figure 3.3-3	Removed Configuration 2 from title.	Elimination of Configuration 2.
Section 3.3.1.1.2	Removed Configuration 2.	Elimination of Configuration 2.
Figure 3.3.1-2	Removed Configuration from title.	Elimination of Configuration 2.
Section 3.3.1.1.3	Removed Configuration 2.	Elimination of Configuration 2.
Figure 3.3.1-3	Removed Configuration from title.	Elimination of Configuration 2.
Section 3.4	Removed Configuration 2.	Elimination of Configuration 2.
Section 3.4.3	Removed Configuration 2.	Elimination of Configuration 2.
Table 3.4.3-1	Removed Configuration 2 from title.	Elimination of Configuration 2.
Figure 3.4.3-1	Removed Configuration 2 from title.	Elimination of Configuration 2.

NEDO-33866 Revision 2
Non-Proprietary Information – Class I (Public)

Location	Description of Change (Rev. 0 to Rev. 1)	Reason for Change
Figure 3.4.3-2	Removed Configuration 2 from title.	Elimination of Configuration 2.
Figure 3.4.3-3	Removed Configuration 2 from title.	Elimination of Configuration 2.
Figure 3.4.3-4	Removed Configuration 2 from title.	Elimination of Configuration 2.
Figure 3.4.3-5	Removed Configuration 2 from title.	Elimination of Configuration 2.
Table 3.4.3-2	Removed Configuration 2 from title.	Elimination of Configuration 2.
Figure 3.4.3-6	Removed Configuration 2 from title.	Elimination of Configuration 2.
Section 3.5.1	Removed Configuration 1 and Configuration 2 from section title and text.	Elimination of Configuration 2.
Figure 3.5.1-1	Removed Configuration 1 from title.	Elimination of Configuration 2.
Table 3.5.1-1	Removed Configuration 1 from title.	Elimination of Configuration 2.
Table 3.5.1-2	Removed Configuration 1 from title.	Elimination of Configuration 2.
Table 3.5.1-3	Removed Configuration 1 from title.	Elimination of Configuration 2.
Figure 3.5.1-2	Removed Configuration 1 from title.	Elimination of Configuration 2.
Figure 3.5.1-3	Removed Configuration 1 from title.	Elimination of Configuration 2.
Table 3.5.1-4	Removed Configuration 1 from title.	Elimination of Configuration 2.
Table 3.5.1-5	Removed Configuration 1 from title, updated note a, deleted note b.	Elimination of Configuration 2.
Table 3.5.1-6	Removed Configuration 1 from title.	Elimination of Configuration 2.
Table 3.5.1-7	Removed Configuration 1 from title.	Elimination of Configuration 2.
References	Updated References 3-4 and 3-7.	Response to RAI 3.1.
Chapter 4		
Section 4	Removed “primary” from 4 th sentence in response to RAI 8.2. Reference 4-1 has been deleted – see basis in description of change for Section 4.6.	Response to RAI 8.2.
Section 4.1	Reworded section to clarify thermal decay heat basis for Chapter 4.	Removes reference to decay heat configurations and establishes the basis for Chapter 4.
Section 4.1.2	Revised the cask lid closure torque, consistent with the response to RAI 7.2.	Response to RAI 7.2.
Section 4.1.3	Deleted Reference 4-2 – see basis in description of change for Section 4.6.	Administrative change.
Section 4.1.3.2	Eliminated reference to the configuration numbers, as well as the lid seal for the 3000 W case, as the 1500 W decay heat case forms the basis for Chapter 4 as stated in Section 4.1.	Removes reference to decay heat configurations and establishes the basis for Chapter 4. Changes are consistent with the responses to RAIs 4.2 and 4.3.

NEDO-33866 Revision 2
Non-Proprietary Information – Class I (Public)

Location	Description of Change (Rev. 0 to Rev. 1)	Reason for Change
Figure 4.1.3-3	Replaced the figure by removing the material options for the lid gasket.	Removes Configuration 2 seal material.
Section 4.1.3.3	<p>Added wording to note that the cask port O-rings and covers are outside the containment boundary, consistent with the response to RAI 4.1.</p> <p>Eliminated reference to the configuration numbers, as well as the O-ring material for the 3000 W case, as the 1500 W decay heat case forms the basis for Chapter 4 as stated in Section 4.1.</p>	Removes reference to decay heat configurations and establishes the basis for Chapter 4. Changes are consistent with the responses to RAIs 4.2 and 4.3.
Section 4.2.1	Section heading has been deleted, and the text has been moved to Section 4.2. Maximum pressure during NCT has been updated in the second paragraph to reflect the 1500 W case.	Removes reference to decay heat configurations and establishing the basis for Chapter 4.
Section 4.2.2	Section has been deleted in its entirety.	The 1500 W case forms the basis for Chapter 4 as stated in Section 4.1, and Configuration 2 has been removed per the response to RAI 4.2.
Section 4.3.1	Section heading 4.3.1 has been deleted. Maximum pressure during HAC has been updated to reflect the 1500 W case. Clarification has been added for the cask drain and test ports exceeding the 400°F seal material design temperature consistent with the response in RAI 4.1.	Response to RAI 4.1.
Section 4.3.2	Section has been deleted in its entirety.	The 1500 W case forms the basis for Chapter 4 as stated in Section 4.1, and Configuration 2 has been removed per the response to RAI 4.2.
Section 4.4	Eliminated reference to the configuration numbers and stated the values for the 1500 W decay heat thermal basis. Clarified the conditions used in the acceptance testing.	Removes reference to decay heat configurations and establishes the basis for Chapter 4.
Section 4.5	Section in its entirety has been deleted, as it refers to Configuration 2 results.	Removes reference to decay heat configurations and establishes the basis for Chapter 4.

NEDO-33866 Revision 2
Non-Proprietary Information – Class I (Public)

Location	Description of Change (Rev. 0 to Rev. 1)	Reason for Change
Section 4.6	Renumbered to Section 4.5 based on the change above. References 4-1 and 4-2 have been deleted. Reference 4-1 points to 10 CFR 71, which does not need a reference, and Reference 4-2 is redundant to the licensing drawings listed in Section 1.3.1. Remaining references have been renumbered.	Administrative change.
Chapter 5		
Section 5.1.1	Removed “and solid fissile materials”.	Fissile material is no longer an approved shipping content per responses to RAI 5.1, RAI 5.2 and RAI 5.6.
Section 5.1.2	Changed from three content types to two content types.	Fissile material is no longer an approved shipping content per responses to RAI 5.1, RAI 5.2 and RAI 5.6.
Table 5.1-2	Removed row of Content 1 and updated dose rates; changed note from 1 and 2 to a and b.	Fissile material is no longer an approved shipping content per responses to RAI 5.1, RAI 5.2 and RAI 5.6. Update the dose rates due to the elimination of Configuration 2 (3000W) per response to RAI 5.5.
Table 5.1-3	Removed row of Content 1 and updated dose rates; changed note from 1 and 2 to a and b.	Fissile material is no longer an approved shipping content per responses to RAI 5.1, RAI 5.2 and RAI 5.6. Update the dose rates due to the elimination of Configuration 2 (3000W) per response to RAI 5.5.
Section 5.2	In first paragraph, removed the content regarding irradiated fuel and special nuclear material.	Fissile material is no longer an approved shipping content per responses to RAI 5.1, RAI 5.2 and RAI 5.6.
Section 5.2	Removed description of Irradiated Fuel.	Fissile material is no longer an approved shipping content per responses to RAI 5.1, RAI 5.2 and RAI 5.6.
Section 5.2	Removed description of Special Nuclear Material.	Fissile material is no longer an approved shipping content per responses to RAI 5.1, RAI 5.2 and RAI 5.6.

NEDO-33866 Revision 2
Non-Proprietary Information – Class I (Public)

Location	Description of Change (Rev. 0 to Rev. 1)	Reason for Change
Section 5.2.1.1	Deleted Section 5.2.1.1.	Fissile material is no longer an approved shipping content per responses to RAI 5.1, RAI 5.2 and RAI 5.6.
Section 5.2.1.2 (now 5.2.1.1)	Added ORIGEN-S description.	Carry over from deleted Section 5.2.1.1.
Section 5.2.1.3 (now 5.2.1.2)	Changed from 3000W to 1500W and from 194,500 Ci to 97,250 Ci.	Configuration 2 (3000W) is no longer an approved configuration per response to RAI 5.5.
Table 5.2-4 (now 5.2-2)	Changed from 194,500 Ci to 97,250 Ci and reduce source strength to half.	Configuration 2 (3000W) is no longer an approved configuration per response to RAI 5.5.
Section 5.2.2.1	Deleted Section 5.2.2.1.	Fissile material is no longer an approved shipping content per responses to RAI 5.1, RAI 5.2 and RAI 5.6.
Section 5.3.1.1	Removed description of Irradiated Fuel.	Fissile material is no longer an approved shipping content per responses to RAI 5.1, RAI 5.2 and RAI 5.6.
Section 5.3.1.1	Editorial modification under Irradiated Hardware and Byproducts and Cobalt-60 Isotope Rods.	For consistency and match shielding model.
Section 5.3.1.3	Added “(except cavity radius which is nominal)” to the third sentence of Section 5.3.1.3.	Drawing 001N8425 Revision 2 includes a tolerance.
Table 5.3-1	Added Note d.	Drawing 001N8425 Revision 2 includes a tolerance.
Section 5.3.1.3	Editorial modification due to removal of neutron shielding model because it is not applicable to irradiated hardware and byproduct and Co-60 isotope rod.	Fissile material is no longer an approved shipping content per responses to RAI 5.1, RAI 5.2 and RAI 5.6.
Table 5.3-1	Changed from MCNP to MCNP6, delete MCNP Surface column, change Dimension column to Parameter column, change value columns to Dimension columns, change note from 1-3 to a-c, add description in Parameter column.	For consistency.
Figure 5.3-2	Removed neutron shielding model because it is not applicable to irradiated hardware and byproduct and Co-60 isotope rod.	Fissile material is no longer an approved shipping content per responses to RAI 5.1, RAI 5.2 and RAI 5.6.

NEDO-33866 Revision 2
Non-Proprietary Information – Class I (Public)

Location	Description of Change (Rev. 0 to Rev. 1)	Reason for Change
Section 5.3.1.4	Editorial modification due to removal of neutron shielding model because it is not applicable to irradiated hardware and byproduct and Co-60 isotope rod.	Fissile material is no longer an approved shipping content per responses to RAI 5.1, RAI 5.2 and RAI 5.6.
Figure 5.3-3	Removed neutron shielding model because it is not applicable to irradiated hardware and byproduct and Co-60 isotope rod.	Fissile material is no longer an approved shipping content per responses to RAI 5.1, RAI 5.2 and RAI 5.6.
Section 5.3.1.5	Changed from MNCP to MCNP6 and delete tally description.	Tally description is not needed because it is consistent with 10 CFR 71.47 and 10 CFR 71.51.
Tables 5.3-2	Deleted Table 5.3-2.	Tally description is not needed because it is consistent with 10 CFR 71.47 and 10 CFR 71.51.
Tables 5.3-3	Deleted Table 5.3-3.	Tally description is not needed because it is consistent with 10 CFR 71.47 and 10 CFR 71.51.
Section 5.3.2	Removed description of neutron shielding model because it is not applicable to irradiated hardware and byproduct and Co-60 isotope rod.	Fissile material is no longer an approved shipping content per responses to RAI 5.1, RAI 5.2 and RAI 5.6.
Section 5.4.1.1	Editorial modification due to removal of neutron shielding model because it is not applicable to irradiated hardware and byproduct and Co-60 isotope rod.	Fissile material is no longer an approved shipping content per responses to RAI 5.1, RAI 5.2 and RAI 5.6.
Section 5.4.1.2	Editorial modification due to removal of neutron shielding model because it is not applicable to irradiated hardware and byproduct and Co-60 isotope rod.	Fissile material is no longer an approved shipping content per responses to RAI 5.1, RAI 5.2 and RAI 5.6.
Section 5.4.1.3	Deleted Section 5.4.1.3.	Fissile material is no longer an approved shipping content per responses to RAI 5.1, RAI 5.2 and RAI 5.6.
Section 5.4.3	Deleted description of neutron conversion factor.	The neutron conversion factor is not applicable to irradiated hardware and byproduct and Co-60 isotope rod.
Table 5.4-2	Deleted Table 5.4-2.	The neutron conversion factor is not applicable to irradiated hardware and byproduct and Co-60 isotope rod.

NEDO-33866 Revision 2
Non-Proprietary Information – Class I (Public)

Location	Description of Change (Rev. 0 to Rev. 1)	Reason for Change
Section 5.4.4	Changed from three content types to two content types.	Fissile material is no longer an approved shipping content per responses to RAI 5.1, RAI 5.2 and RAI 5.6.
Section 5.4.4.1	Deleted previous Section 5.4.4.1.	Fissile material is no longer an approved shipping content per responses to RAI 5.1, RAI 5.2 and RAI 5.6.
Section 5.4.4.2 (now 5.4.4.1)	Changed from 3000 W to 1500 W.	Configuration 2 (3000W) is no longer an approved configuration per response to RAI 5.5.
Table 5.4-15 (now 5.4-4)	Updated activity limit in Table 5.4-15 (now 5.4-4) due to 1500W thermal limit	Configuration 2 (3000W) is no longer an approved configuration per response to RAI 5.5.
Table 5.4-16 (now 5.4-5)	Updated dose rate in Table 5.4-16 (now 5.4-5) due to 1500W thermal limit.	Configuration 2 (3000W) is no longer an approved configuration per response to RAI 5.5.
Section 5.4.4.3 (now 5.4.4.2)	Changed from 3000 W to 1500 W.	Configuration 2 (3000W) is no longer an approved configuration per response to RAI 5.5.
Table 5.4-19 (now 5.4-8)	Updated dose rate in Table 5.4-19 (now 5.4-8) due to 1500W thermal limit.	Configuration 2 (3000W) is no longer an approved configuration per response to RAI 5.5.
Section 5.4.4.4 (now 5.4.4.3)	Removed irradiated fuel related text.	Fissile material is no longer an approved shipping content per responses to RAI 5.1, RAI 5.2 and RAI 5.6.
Section 5.5.1	Deleted Section 5.5.1.	Fissile material is no longer an approved shipping content per responses to RAI 5.1, RAI 5.2 and RAI 5.6.
Section 5.5.2 (now 5.5.1)	Added a sentence to the end of the first paragraph.	Updated per responses to RAI 5.3 and RAI 7.3.
Table 5.5-7 (now 5.5-2)	Changed note from 1 to a.	For consistency.
Section 5.5.3 (now 5.5.2)	Removed Configuration 2 from the sentence before Table 5.5-28 (now 5.5-23).	Configuration 2 (3000W) is no longer an approved configuration per response to RAI 5.5.
Table 5.5-28 (now 5.5-23)	Changed note from 1 to a.	For consistency.
Section 5.5.3 (now 5.5.2)	Deleted the last 5 paragraphs.	Paragraphs are not needed per response to RAI 5.4.

NEDO-33866 Revision 2
Non-Proprietary Information – Class I (Public)

Location	Description of Change (Rev. 0 to Rev. 1)	Reason for Change
Table 5.5-29	Deleted Table 5.5-29.	Table is not needed per response to RAI 5.4.
Section 5.5.4 (now 5.5.3)	Removed Configuration 1 and Configuration 2 from the first sentence.	Configuration 2 (3000W) is no longer an approved configuration per response to RAI 5.5.
Table 5.5-30 (now 5.5-24)	Changed note from 1 and 2 to a and b; removed isotopes Sn-117 and Sn-119.	Consistent with Table 5.5-7 (now 5.5-2).
Section 5.5.5	Deleted Section 5.5.5.	Fissile material is no longer an approved shipping content per responses to RAI 5.1, RAI 5.2 and RAI 5.6.
Section 5.5.6 (now 5.5.4)	Removed the sentence (related to Configuration 2) before Table 5.5-40 (now 5.5-28).	Configuration 2 (3000W) is no longer an approved configuration per response to RAI 5.5.
Table 5.5-39 (now 5.5-27)	Updated the total activity.	Configuration 2 (3000W) is no longer an approved configuration per response to RAI 5.5.
Table 5.5-40 (now 5.5-28)	Changed the decay heat limit from 3000 W to 1500 W.	Configuration 2 (3000W) is no longer an approved configuration per response to RAI 5.5.
Table 5.5-41 (now 5.5-29)	Changed the decay heat limit from 3000 W to 1500 W.	Configuration 2 (3000W) is no longer an approved configuration per response to RAI 5.5.
Table 5.5-42 (now 5.5-30)	Changed the decay heat limit from 3000 W to 1500 W and update values.	Configuration 2 (3000W) is no longer an approved configuration per response to RAI 5.5.
Section 5.5.7 (now 5.5.5)	Removed irradiated fuel related text.	Fissile material is no longer an approved shipping content per responses to RAI 5.1, RAI 5.2 and RAI 5.6.
Table 5.5-43	Deleted Table 5.5-4.	Fissile material is no longer an approved shipping content per responses to RAI 5.1, RAI 5.2 and RAI 5.6.
References	Deleted References 5-3 and 5-10.	Fissile material is no longer an approved shipping content per responses to RAI 5.1, RAI 5.2 and RAI 5.6.
Chapter 6		
Chapter 6	Replaced Chapter 6 content with a paragraph.	Fissile material is no longer an approved shipping content per responses to RAI 6.1 and RAI 6.2.

NEDO-33866 Revision 2
Non-Proprietary Information – Class I (Public)

Location	Description of Change (Rev. 0 to Rev. 1)	Reason for Change
Chapter 7		
Chapter 7 has been modified to reflect the global removal of the 3000W configuration and text associated with irradiated fuel rods and special nuclear material. In addition to the changes listed below to address the RAIs provided, Chapter 7 has been modified to incorporate operational experiences and current lessons learned.		
Section 7.1.1.3:b	Inserted “± 20”.	In response to RAI 7.2.
Section 7.1.2.2	Deleted.	Removal of Irradiated Fuel Rods from the Cask scope and in response to RAI 7.5.
Section 7.1.2.2.c (Previously Section 7.1.2.3.c)	Deleted second sentence. Inserted “The HPI material basket may be used as shoring, but is not required.”	Clarification in response to RAI 7.1.
Section 7.1.2.4	Deleted.	Removal of Special Nuclear Material from the Cask scope and in response to RAI 7.5.
Section 7.1.3.2.a	Inserted “500” deleted, “720±30”.	Correction to the required torque bolt and in response to RAI 7.2.
Section 7.1.4.1.e	Inserted “±5”.	Addition of tolerance in response to RAI 7.2.
Section 7.2.1.3.c	Inserted “±20”.	Addition of tolerance in response to RAI 7.2.
Section 7.2.2.1	Removed reference to irradiated fuel.	Removal of Irradiated Fuel Rods from the Cask scope.
Section 7.2.2.2	Deleted “/ 500 grams U-235 Equivalent Mass of SNM”.	Removal of Special Nuclear Material from the Cask scope and in response to RAI 7.5.
Section 7.2.2.2	Deleted “either” and “or 500 grams U-235 equivalent mass of SNM”.	Removal of Special Nuclear Material from the Cask scope.
Section 7.2.2.3.b	Inserted “Install the spacer, if one came with the packaging” deleted, “If spacer was provided, confirm it is secured to the HPI top plug”.	Clarification on spacer use and in response to RAI 7.2.
Section 7.3.2.b	Inserted “500” deleted, “720±30”.	In response to RAI 7.2.
Section 7.5.1 (Previously Section 7.5.2)	Inserted second to last bullet “criticality” deleted, “activity.”	In response to RAI 8.3.
Section 7.5.1 – 2.	Inserted “(alpha and beta emitters)”; inserted “A list of radionuclides for consideration to include in the loading plan is provided in, but not limited to, Table 5.5-24.”	In response to RAI 7.3.

NEDO-33866 Revision 2
Non-Proprietary Information – Class I (Public)

Location	Description of Change (Rev. 0 to Rev. 1)	Reason for Change
Section 7.5.2 – 1.	Changed to “Verify that the peak activity in any axial 1-inch increment in the HPI cavity is in accordance with Section 5.5.2.”	In response to RAI 7.4.
Section 7.5.2 – 1.	All bullets deleted.	Clarification in response to RAI 7.4.
Section 7.5.4 – 1.	Deleted.	Removal of Irradiated Fuel Rods from the Cask scope.
Section 7.5.5	Deleted.	Removal of Special Nuclear Material from the Cask scope and in response to RAI 7.5.
Chapter 8		
Section 8	Removed Reference 8-1, which points to 10 CFR 71, which does not need a reference. Other references have been renumbered.	Administrative change.
Section 8.1.5.2	Eliminated reference to the configuration numbers, as well as the lid seal material for the 3000 W case, as the 1500 W decay heat case forms the basis for containment as stated in Section 4.1. Clarified the lid seal test conditions.	The lid seal material is based on the 1500 W decay heat case, as stated in Section 4.1.
Section 8.1.7	Added clarification at the end of the section denoting the decay heat basis.	Because the thermal testing is designed for 2000 W, it was necessary to clarify that the thermal basis for the cask is 3000 W, even though the allowable decay heat for shipping is 1500 W.
Section 8.2	Clarified the end of the second.	In response to RAI 8.1.
Section 8.2.1.2	Clarified the first sentence.	In response to RAI 8.1.
Section 8.2.2.2	Clarified the end of the second.	In response to RAI 8.1.
Section 8.2.3.1	Eliminated reference to Configuration 2.	There is no Configuration 1/Configuration 2 designation for contents as seen in Section 1.2.2.3.
Section 8.4	Along with the deletion of Reference 8-1, as stated previously, References 8-8, 8-9, 8-10, 8-12, and 8-13 have been deleted (and citations in the text removed). These are internal GEH specifications and reports that normally are not cited in a SAR.	Administrative change.

NEDO-33866 Revision 2
Non-Proprietary Information – Class I (Public)

Changes from Revision 1 to Revision 2 are listed in the following table. Revision bars are used for these changes.

Location	Description of Change (Rev. 1 to Rev. 2)	Reason for Change
Revision Summaries	Clarified that the Revision Summary for Revision 0 to Revision 1 is maintained, while this Revision Summary for Revision 1 to Revision 2 is added. Revision bars are used only for Revision 2 changes.	Clarification.
Various	Unredacted “support disk” in various locations.	Consistency change.
Section 1.2	Moved bulleted information for the high performance insert and the HPI material basket from “Contents” to “Packaging”.	The HPI and material basket are packaging, not contents.
Former Section 1.2.2.1 New Section 1.2.1.3	Moved former Section 1.2.2.1, High Performance Insert, from Section 1.2.2, Contents, to Section 1.2.1, Packaging. It is now Section 1.2.1.3.	The HPI is packaging, not a content.
Former Section 1.2.2.2 New Section 1.2.1.4	Moved former Section 1.2.2.2, HPI Material Basket, from Section 1.2.2, Contents, to Section 1.2.1, Packaging. It is now Section 1.2.1.4.	The material basket is packaging, not a content.
Former Section 1.2.2.3 Now Section 1.2.2.1	Renumbered this section due to relocating Sections 1.2.2.1 and 1.2.2.2. Also, in Item a), defined “payload” as all cask internals and contents. This is consistent with existing information in Revision 1 (e.g., as stated in Section 2.12.1.2).	Administrative and clarification change.
Section 1.2.3	In the second sentence in the section, changed the pointer for package content from Section 1.2.2.3 to Section 1.2.2.1.	Administrative change.
Chapter 2	In the chapter lead-in discussion, second paragraph, first bullet, changed: “Ensure the maximum content weight does not exceed 5,450 pounds.” To: “Ensure the maximum payload weight does not exceed 5,450 pounds.”	Clarification change.

NEDO-33866 Revision 2
Non-Proprietary Information – Class I (Public)

Location	Description of Change (Rev. 1 to Rev. 2)	Reason for Change
Table 2.1-3	<p>In the first data row, first column, changed “Total Packaging Weight” to “Total Overpack plus Cask Weight”.</p> <p>In the fifth data row, first column, changed “Allowed Contents Weight” to “Payload Weight”.</p> <p>Changed footnotes “*” and “**” to “1” and “3”, respectively. In footnote 3, changed “If material basket is not included in contents...” to “If material basket is not used...”.</p> <p>Added footnote 2: “The HPI plus material basket plus radioactive contents (with shoring) is defined as payload for purposes of this report”.</p>	The HPI and material basket are packaging, not contents.
Section 2.6.7.1.1	<p>In the second sentence under subheading “Cask Contents Loading – End Drop” (below Table 2.6.7-1), changed “one half the contents weight of 5,450 lb” to “one half the payload weight of 5,450 lb (see Table 2.1-3)”.</p> <p>Also, in the second sentence under subheading “Cask Contents Loading – Side Drop”, changed “produced by the 5,450 lb contents weight” to “produced by the 5,450 lb payload weight”.</p>	Clarification change.
Table 2.12.4-4	Changed the data entry cell “Weight of Cask Contents” to “Weight of Cask Payload”.	Clarification change.
Section 3.1.1	In the last sentence of the section, changed the pointer for information on the high performance insert from Section 1.2.2.1 to Section 1.2.1.3.	Administrative change.
Section 3.3	In the first sentence of the second paragraph under subheading “Heat Generation by Contents,” (below Figure 3.3-7), changed the pointer for information on the material basket from Section 1.2.2.2 to Section 1.2.1.4.	Administrative change.
Section 4.1	In the first sentence of the section, changed the pointer for package content from Section 1.2.2.3 to Section 1.2.2.1.	Administrative change.
Section 5.5.5	In the last sentence of the section, changed the pointer for package content from Section 1.2.2.3 to Section 1.2.2.1.	Administrative change.
Chapter 6	In the first sentence of the chapter, changed the pointer for package content from Section 1.2.2.3 to Section 1.2.2.1.	Administrative change.

NEDO-33866 Revision 2
 Non-Proprietary Information – Class I (Public)

Location	Description of Change (Rev. 1 to Rev. 2)	Reason for Change
Section 7.5.1	In procedure step 2, first bullet, changed the parenthetical “alpha and beta emitters” to “alpha, beta, and gamma emitters”.	Clarification change.
Section 7.5.2	Modified the procedure steps by explicitly stating the allowable per inch activity level and clarifying use of the Combined Contents Loading Table.	Clarification change.
Section 7.5.3	Added a new procedure sub-step 2.1 to address the allowable per inch activity level to include point source values. Also, corrected the pointer to the previous steps from “Steps 1 through 3” to “Steps 1 and 2”.	Clarification change.
Section 8.1.7	In the fourth sentence of the section, changed the pointer for package content from Section 1.2.2.3 to Section 1.2.2.1.	Administrative change.

ACRONYMS

Term	Definition
3D	Three-Dimensional
Amb.	Ambient
ANSI	American National Standards Institute
APDL	ANSYS Parametric Design Language
ASM	American Society for Metals
ASME	American Society of Mechanical Engineers
ASNT	American Society for Nondestructive Testing
ASTM	American Society for Testing and Materials
Aux.	Auxiliary
B&PVC	Boiler and Pressure Vessel Code
CFR	Code of Federal Regulations
C.G.	Center of Gravity
CSI	Criticality Safety Index
DOF	Degree-of-Freedom
DR	Total Dose Rate
DU	Depleted Uranium
[[]]
FEA	Finite Element Analysis
GE	General Electric
GEH	GE-Hitachi Nuclear Energy Americas LLC
HAC	Hypothetical Accident (Transport) Conditions
HEPA	High Efficiency Particulate Air
HPI	High Performance Insert
IAEA	International Atomic Energy Agency
ID	Inner Diameter
MCNP	Monte Carlo N-Particle
MS	Margin of Safety

NEDO-33866 Revision 2
 Non-Proprietary Information – Class I (Public)

Term	Definition
MSLD	Mass Spectrometer Leak Detector
NBS	National Bureau of Standards
NCT	Normal Conditions of Transport
NDE	Nondestructive Examination
Nom.	Nominal
NPT	National Pipe Taper (Thread)
NRC	Nuclear Regulatory Commission
OD	Outer Diameter
OR	Outer Radius
PNNL	Pacific Northwest National Lab
QAP-1	GEH Quality Assurance Program
S/N	Serial Number
SS	Stainless Steel
Std.	Standard
TCC	Thermal Contact Conductance
UNC	Unified Coarse
U.S.	United States

1 GENERAL INFORMATION

1.1 Introduction

The Model 2000 Radioactive Material Transport Package was developed at Vallecitos Nuclear Center. The primary use of the packaging is to provide containment, shielding, impact resistance, criticality safety, and thermal resistance for its contents during normal and hypothetical accident conditions. The packaging is designed to transport Type B quantities of radioactive materials. It complies with the Nuclear Regulatory Commission (NRC) regulations contained in the Code of Federal Regulations, Title 10, Part 71 (10 CFR 71). The package is to be shipped in all modes of transportation, except air. The Model 2000 Transport Package may only be shipped exclusive use, as discussed in Section 5.1.2. No Criticality Safety Index (CSI) is determined, as a criticality evaluation is not required as discussed in Chapter 6.

Calculations, engineering logic, and all related documents that demonstrate compliance with regulations are presented in subsequent sections of this report.

The GEH Quality Assurance Program (QAP-1) (Reference 1-1) controls design, purchase, fabrication, handling, shipping, storing, cleaning, assembly, inspection, testing, operation, maintenance, repair and modification of the packages. The NRC has approved QAP-1 under docket number 71-0171 upon demonstration that the QA plan meets the requirements of Subpart H of 10 CFR 71.

1.2 Package Description

The Model 2000 Transport Package, shown in Figure 1.2-1, is transported exclusive use, in the upright position. The approximate overall packaging dimensions are 131.5 inches in height and 72 inches in diameter. The approximate total weight of the package (packaging plus the contents) is 33,550 lb. Table 2.1-3 shows the breakdown of the component weights for the Model 2000 Transport Package.

The Model 2000 Transport Package and contents are described below:

Packaging

- Cask
- Overpack
- High performance insert (HPI)
- HPI material basket

Contents

- Solid radioactive materials

1.2.1. Packaging

1.2.1.1. Cask

The cask body (the containment vessel), shown in Figure 1.2-2, is constructed of two concentric, 1-inch thick stainless steel (SS) SS304 cylindrical shells (ASTM A240 / ASME SA 240). The shells are joined at the bottom end by a type SS304 forging (ASTM A182 / ASME SA 182). A SS304 forging connects the cask shell and cavity shell at the top end of the cask. This flange is part of the cask lid sealing joint and has an electropolished finish on the sealing surface. The annulus between the two shells is approximately 4 inches thick and filled with lead. The cask body height is approximately 71 inches and the outer diameter (OD) is approximately 38.5 inches. The cavity is approximately 26.5 inches in diameter and 54 inches deep.

The cask lid is made of SS304 and lead. It has a stepped design and is fully recessed into the cask top flange. The lid sealing surface is on the underside of the top flange and has an electropolish finish. The cask lid seal is composed of four rings of contoured [[]] material (two on the top and two on the bottom) bonded to a [[]] thick metal retainer with an OD of 34 inches. The area between the inner and outer seal is designed to permit flow for a seal test port to verify leak-tightness of the package by evaluating the performance of the inner seal. The cask lid [[]] and metal retainer material design is evaluated to support 1500 W decay heat. The cask lid seal is a [[]] retainer with four Parker Compound No. [[]] rings. The material specifications are included in Section 1.3.2.1. The cask lid is secured to the cask body by fifteen (15) 1¼-inch diameter socket head screws.

The cask has three penetrations. Only two of the three penetrations are within the cask containment boundary. They include: the drain and vent ports for the cask cavity. The drain port hole leads from the center of the cavity bottom out the side of the outer shell. The vent port line spirals through the cask lid near the cask centerline. The third penetration, that is not within the containment boundary, is the test port, which is used to test the adequacy of the seal joint after the cask body and lid are assembled. The test port path leads from the side of the top forging to the region between the inner and outer seals and is sealed in the same manner as the other penetrations.

All of the cask port seals are composed of ½ National Pipe Taper (NPT) thread socket head pipe plugs, followed by an exterior plug cover with O-ring to seal the port. The plug cover and O-ring provide a backup seal to the pipe plug, and they are not considered part of the containment boundary. The O-ring [[]] compound.

The cask body utilizes attachment plates for lifting devices that are detached during transport and rendered inoperable. There are three types of lifting devices use in the Model 2000 cask: (1) standard ears used for crane and fork truck handling; (2) auxiliary ears used for crane only handling; and (3) optional ears that function as a trunnion. Except for these devices, there are no other devices or features of the cask that could be used for lifting the package, once the cask is within the overpack.

1.2.1.2. Overpack

The cask is positioned inside a protective overpack, shown in Figure 1.2-3, for transport. The overpack is constructed of two 0.5-inch thick SS304 concentric cylindrical shells (ASTM A240/ASME SA 240), which are separated radially by eight equally spaced tubes along the length of the shells, and by two tube sections around the perimeter of the shells. A toroidal shell impact limiter made of SS304 is attached to each end of the overpack shells. The overpack opens just above the lower impact limiter for access to the cask. The top section of the overpack is joined to the base by fifteen (15) 1³/₈-inch diameter shoulder screws. Gussets on the top and bottom impact limiters provide tie-down points for the package.

Additional impact protection is provided by aluminum honeycomb impact absorbers permanently positioned on the inside of the overpack at the top and bottom ends of the cask.

The cask sits on a 0.5-inch thick, 42-inch diameter plate called the cask support plate. It features eight square cross-section prongs welded to the plate perimeter to ensure cask concentricity within the overpack. The cask support plate material of construction is SS304; however, there are two cask support plate options. One option is solid SS304, while the other option includes a tungsten insert.

1.2.1.3. High Performance Insert

The Model 2000 Transport Package is equipped with an HPI, shown in Figure 1.2-4, to increase the shielding capability of the package. The HPI is nominally [[

]] The HPI body consists of [[]] SS concentric cylindrical shells. The annulus between the two shells is filled with [[]] thick depleted uranium. The HPI body is positioned in the cask cavity by five [[]] support disks [[]] to provide uniform support. The support disks are joined together by [[]] arms that function as the primary lifting fixture. The HPI body assembly is completed with the addition of ASME [[]] at each end of the cylindrical sub-assembly.

Closure of the HPI is provided by top and [[]] The [[]] is a stepped design comprised of a [[]] thick depleted uranium cylinder encapsulated by a [[]] shell. Holes are machined in the [[]] on the HPI body. The [[]]

]] The top plug is a stepped design comprised of a [[]] depleted uranium cylinder encapsulated by a [[]] shell. To facilitate lifting of the top plug, [[]] circular plate. The top plug is held in position by [[]] Attachment of the top and [[]] does not produce a pressure boundary. Grooves are cut into the surface of the plugs to allow moisture to escape during the vacuum drying process.

1.2.1.4. HPI Material Basket

The material basket is shown in Figure 1.2-5 with an example of supplemental dunnage. The material basket is constructed of [[

]] pattern and are identified as Item 1 on Drawing 001N8424. See Figure 1.2-6 for material basket details. The outer [[]] of the material basket form a composite section with the addition of [[

]] The center location of the material basket is a developed cell, which is created by the surrounding [[]] To allow for the proper insertion of supplemental dunnage and facilitate fabrication, [[]] are inserted at the top and bottom of the developed cell and are identified as Item 2 on Drawing 001N8424. Therefore, the exterior view of the material basket shows [[

]] facilitate loading and positioning of the material basket within the HPI cavity. Parts List 001N8424G001 is provided in Section 1.3.

1.2.2. Contents

1.2.2.1. Radioactive Material Contents

The Model 2000 Transport Package is designed to transport Type B quantities of radioactive materials. This may include irradiated hardware and byproducts or Co-60 isotope rods. The following are requirements for all shipments:

- a) The maximum quantity of material per package shall not exceed 5,450 lb, including all cask internals and contents (defined as “payload” for purposes of this report – see Table 2.1.3).
- b) All contents shipped shall be in solid form.
- c) All configurations require the use of the HPI.
- d) The decay heat for shipping all contents shall be limited to no more than 1500 W. However, a decay heat of 3000 W is conservatively used as the design basis for the Model 2000 Transport Package, where applicable. There are a few exceptions as noted within this SAR where 1500 W forms the basis; while a 1500 W decay heat is used in these sections, it is demonstrated that the 3000 W design basis is bounding.

The specific radioactive contents transported in the Model 2000 cask are:

1. Irradiated Hardware and Byproducts
 - a. Irradiated hardware components composed of stainless steels, carbon steels, nickel alloys, and zirconium alloys.
 - b. Irradiated byproducts such as control rods and/or blades composed of hafnium and boron carbide.
 - c. Minimum decay time shall be at least 30 days prior to shipment.
 - d. Refer to loading table provided in Section 7.5.2
2. Cobalt-60 Isotope Rods
 - a. Must be shipped with the HPI material basket in the upright position and confined per 2.b and demonstrated to meet NCT.

- b. Content shall be in the form of pellets or cylindrical solid rods with the source(s) evenly distributed and encapsulated in normal or special form.
- c. Total activity in any axial 1-inch increment in the HPI cavity must be $\leq 17,000$ Ci (see Section 5.5.2).

Shipment of combined contents is allowed.

1.2.3. Special Requirements for Plutonium

Fissile material is not an approved content of the Model 2000 Transport Package. Thus, any plutonium present in the Model 2000 Transport Package is negligible due to the insignificant quantities of crud build-up on the Section 1.2.2.1 approved content.

1.2.4. Operational Features

The Model 2000 Transport Package description in Section 1.2.1 shows that the packaging is not a complex system. There are no valves or items that require specialized knowledge for proper operation, and cooling is provided through natural convection and radiation. [[]] during installation, and only normal practices for seal handling (e.g., cleanliness) are required.

The Model 2000 Transport Package operation is described in Chapter 7. The loading operation is a dry or wet-loaded operation. If wet-loaded, the cask and cask internals contain features to allow easy drainage of water for underwater loading. To vacuum dry the cask, its cavity pressure is reduced below the vapor pressure of water and maintained at or below this pressure level for a period of time.

Content shoring may include components such as the rod [[]] holders shown in Figure 1.2-5. This example shoring is designed to fit into the HPI material basket (Drawing 001N8424), but other shoring components may be placed directly into the HPI cavity (Drawing 001N8423). The HPI material basket is loaded into the HPI cavity (Figure 1.2-4) if required for a specific content.

When the HPI top plug is installed (Drawing 001N8427), additional shoring may be added, as necessary, to ensure the [[]] between the bottom of the cask lid and the top of the HPI does not exceed 0.25 inches. However, no credit for shoring is given in the Normal Conditions of Transport (NCT) and Hypothetical Accident Conditions (HAC) evaluations. The required evaluations are included in this application to demonstrate safe transport of the Model 2000 Transport Package for the included contents with specified required internals.

Once the package is loaded onto the transport vehicle, external temperature measurements are taken of the loaded overpack. If any temperature exceeds 185°F, a protective personnel barrier is installed around the package to block access as discussed in Section 3.3.1.1.3. The cask containment boundary is illustrated in Figure 4.1.3-1.

[[

]]

Figure 1.2-1. Model 2000 Packaging with High Performance Insert

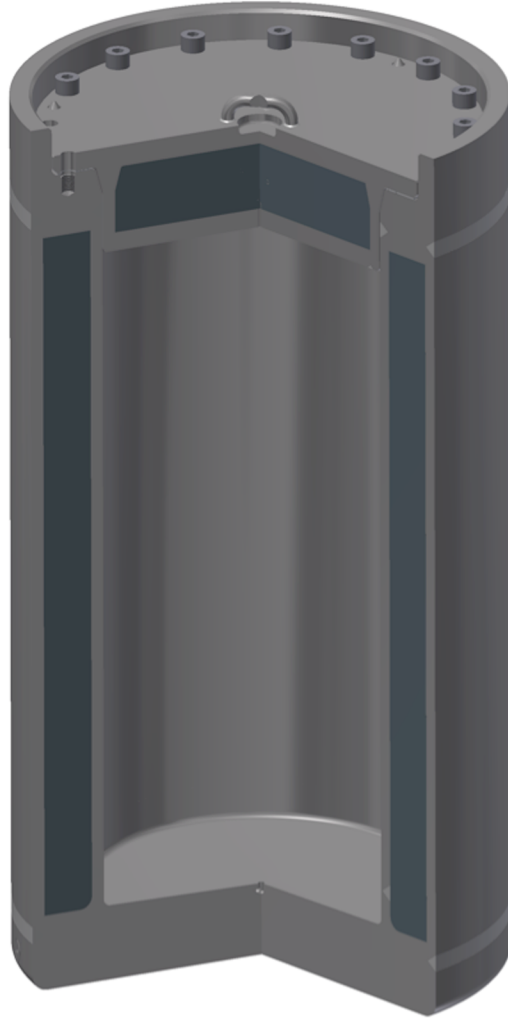


Figure 1.2-2. Model 2000 Cask



Figure 1.2-3. Model 2000 Overpack

[[

]]

Figure 1.2-4. Model 2000 High Performance Insert with Material Basket

[[

]]

Figure 1.2-5. Material Basket and Rod [[]] Holder

[[

]]

Figure 1.2-6. Material Basket Details

1.3 Appendix

1.3.1. Drawings

This section contains the Model 2000 Transport Package licensing drawings and bill of materials. Table 1.3-1 provides a list of current licensing drawings, which follow, and current revision level.

Table 1.3-1. Model 2000 Packaging Licensing Drawings

Drawing Number	Title	Revision
001N8422	GE 2000 HPI and Material Basket Licensing Drawing	3
001N8423	GE 2000 HPI Licensing Drawing	2
001N8424	GE 2000 HPI Material Basket Assembly Licensing Drawing	2
001N8425	GE 2000 HPI Body Licensing Drawing	2
001N8427	GE 2000 HPI Top Plug Assembly Licensing Drawing	2
001N8428	GE 2000 HPI [[]] Assembly Licensing Drawing	2
101E8718	Model 2000 Shipping Cask S/N 2001	17
105E9520	Model 2000 Shipping Cask all S/N's Except S/N 2001	9
129D4946	Model 2000 Transport Container Assembly	12
101E8719	Model 2000 Shipping Cask Overpack S/N 2001	14
105E9521	Model 2000 Shipping Cask Overpack all S/N's Except S/N 2001	7

NEDO-33866 Revision 2
Non-Proprietary Information – Class I (Public)

PARTS LIST 001N8422G001

[[

]]

NEDO-33866 Revision 2
Non-Proprietary Information – Class I (Public)

DWG 001N8422 DRAWING

Proprietary in its Entirety

[[

]]

NEDO-33866 Revision 2
Non-Proprietary Information – Class I (Public)

PARTS LIST 001N8423G001

]]

]]

NEDO-33866 Revision 2
Non-Proprietary Information – Class I (Public)

DWG 001N8423 DRAWING

Proprietary in its Entirety

[[

]]

PARTS LIST 001N8424G001

[[

]]

NEDO-33866 Revision 2
Non-Proprietary Information – Class I (Public)

DWG 001N8424 DRAWING
Proprietary in its Entirety

[[

]]

PARTS LIST 001N8425G001

[[

]]

NEDO-33866 Revision 2
Non-Proprietary Information – Class I (Public)

DWG 001N8425 DRAWING
Proprietary in its Entirety

[[

]]

PARTS LIST 001N8427G001

[[

]]

NEDO-33866 Revision 2
Non-Proprietary Information – Class I (Public)

DWG 001N8427 DRAWING

Proprietary in its Entirety

[[

]]

PARTS LIST 001N8428G001

[[

]]

NEDO-33866 Revision 2
Non-Proprietary Information – Class I (Public)

DWG 001N8428 DRAWING

Proprietary in its Entirety

[[

]]

PARTS LIST 101E8718

[[

]]

NEDO-33866 Revision 2
Non-Proprietary Information – Class I (Public)

DWG 101E8718 DRAWING SH1

Proprietary in its Entirety

[[

]]

NEDO-33866 Revision 2
Non-Proprietary Information – Class I (Public)

DWG 101E8718 DRAWING SH2

Proprietary in its Entirety

[[

]]

PARTS LIST 101E9520

[[

]]

NEDO-33866 Revision 2
Non-Proprietary Information – Class I (Public)

DWG 105E9520 DRAWING SH1

Proprietary in its Entirety

[[

]]

NEDO-33866 Revision 2
Non-Proprietary Information – Class I (Public)

DWG 105E9520 DRAWING SH2

Proprietary in its Entirety

[[

]]

PARTS LIST 129D4946

[[

]]

NEDO-33866 Revision 2
Non-Proprietary Information – Class I (Public)

DWG 129D4946 DRAWING

Proprietary in its Entirety

[[

]]

NEDO-33866 Revision 2
Non-Proprietary Information – Class I (Public)

PARTS LIST 101E8719

[[

]]

NEDO-33866 Revision 2
Non-Proprietary Information – Class I (Public)

DWG 101E8719 DRAWING

Proprietary in its Entirety

[[

]]

PARTS LIST 105E9521

[[

]]

NEDO-33866 Revision 2
Non-Proprietary Information – Class I (Public)

DWG 105E9521 DRAWING

Proprietary in its Entirety

[[

]]

1.3.2. Material Specifications

1.3.2.1. Seal Specifications

The Parker [[]] material specification for Parker Compound [[]] for the cask lid seal and port "O" rings is provided below. (Reference 1-2)

[[

]]

1.4 References

- 1-1 GE-Hitachi Nuclear Energy, "Quality Assurance Program for Shipping Packages for Radioactive Material (Docket 71-0170)," QAP-1, Latest Revision.
- 1-2 Parker Hannifin Corporation, "Gask-O-Seal and Integral Seal Design Handbook," CSS 5124, 2010.

2 STRUCTURAL EVALUATION

This chapter presents the structural evaluation of the Model 2000 Transport Package, and demonstrates that the design meets all applicable structural criteria. All components that comprise the Model 2000 Transport Package are evaluated to the applicable regulatory requirements that includes the NCT and HAC, in accordance with 10 CFR 71 (Reference 2-1). Detailed description of each package component is provided in in Section 2.1.1.

The decay heat limit for shipping all contents shall be conservatively limited to 1500 W. However, a decay heat of 3000 W is conservatively used as the basis for the Model 2000 Transport Package structural evaluation (analysis) in this chapter. Analyses comply with the methodology and criteria presented in Section 2.1.2. The structural design of the Model 2000 Transport Package is based on the following critical characteristics:

- Ensure the maximum payload weight does not exceed 5,450 pounds.
- Maintain structural integrity when subjected to the thermal conditions (3000 W maximum) associated with NCT and HAC in Chapter 3. This section demonstrates packaging integrity at extreme thermal conditions during NCT and HAC.
- Maintain containment integrity to remain leaktight during NCT and HAC as documented in Chapter 4. This section demonstrates cask containment integrity during NCT and HAC.
- Maintain integrity of lead and depleted uranium (DU) shielding boundaries during NCT and HAC to support Chapter 5. This section demonstrates that the shielding integrity is maintained during NCT and HAC to support the shielding analysis assumptions.

2.1 Description of Structural Design

2.1.1. Discussion

The Model 2000 Transport Package consists of a welded overpack structure containing a steel-encased, lead cask structure. The cask structure is a lead-filled SS304 weldment, cylindrical in shape, and measuring approximately 38.5 inches OD by 71 inches high. The inner cavity is 26.5 inches ID by 54 inches high. The lead shielding provided is approximately 4 inches of lead on the sides.

The cask body shell is made of 1 inch thick SS304 plate. At the bottom, the shells are welded to a 6-inch thick SS304 forging. At the upper section, the containment shell joins a 9-inch thick SS304 forging. This forging provides support and sealing surface to the cask seal. Also, it contains 15 equally spaced, internally threaded holes on a 32.25-inch diameter bolt circle. Fifteen 1¼-inch diameter ASTM A540 socket head screws attach the lid to the cask body during operation. The cask lid is SS304 encasing a lead cylinder. The lid has a lifting lug for handling.

There are three penetrations into the cask cavity. One serves as a drain for the cask cavity and another one as a vent. The drain hole goes from the center of the cavity bottom to the side of the outer surface. The vent line spirals through the cask lid around the center. These penetrations provide means to eliminate water from the cask cavity collected during underwater operations.

A ½ NPT socket head pipe plug followed by a 1¾ - 12 UN-2A cap closes both penetrations. The cap O-ring provides backup sealant to the pipe plug. The third penetration is used as a testing port for the cask seal joint. It is located in the upper forging on the side surface of the cask.

The cask lid seal and O-rings use Parker Compound No. [] material retainer. The cask lid seal retainer has a 34 inch OD and 28 inch ID. The cask lid seal and O-rings are designed for a 1500 W maximum content heat load.

The welded SS304 overpack structure is composed of two concentric cylinders, separated vertically by eight equally spaced [] sections. The external cylinder has a 48.5-inch OD. The internal cylindrical shell is 40.5-inch ID. A 24-inch [] diameter toroidal shell is attached at both ends of the external cylinder, and a circular plate is welded across the inner region of the torus. The internal cylinder is closed at each end by circular plates. All materials are 0.5 inches thick with the exception of the space [] and toroidal shells. The vertical []

[]

The toroidal shells may be fabricated using four 90° elbows (or two 180° returns). However, the Model 2000 toroidal shell wall thickness range is limited to 0.5 inches minimum to 0.76 inches maximum. The overpack structure separates near the bottom end to allow access to the lead cask. A collar 0.75 inches thick is attached in this area to provide bearing surface for the connecting bolts. A total of fifteen (15) 1-¾ inches diameter ASTM A540 shoulder screws join both portions of the overpack structure. The toroidal shell of the overpack structure acts as an energy-absorbing device during the postulated drop conditions. In addition, the overpack structure provides thermal shielding for the lead cask in the event of a fire.

A total of 20 reinforcing ribs cradle the toroidal shell to the vertical cylinder. Four of the ribs provide tie-down points for the package during transport. These ribs also provide a means for lifting and removing the overpack top section using a spreader bar. The spreader bar is not part of the transport packaging.

There is a 6-inch thick aluminum honeycomb pad attached to the top inner surface of the overpack structure. A 4-inch thick aluminum honeycomb pad covered by a ½ inch thick circular plate provides a surface base for the lead cask structure. These honeycomb pads are included in the overpack structure design to assure a uniform loading distribution on the cask surface during the postulated free-drop events.

The Model 2000 Transport Package is equipped with a high performance insert (HPI) to increase the shielding capability of the package. The HPI is [] The cavity is approximately [] The HPI body consists [] inch stainless steel concentric cylindrical shells. The annulus between the [] shells is filled with [] thick depleted uranium. The HPI body is positioned in the cask cavity by five [] (Table 2.2-3) support disks arranged axially to provide uniform support. The support disks are joined together by four [] vertical lifting arms that function as the primary lifting fixture. The HPI body assembly is completed with the addition of ASME [] at each end of the cylindrical sub-assembly.

Top and [[]] joined to the ASME [[]] provide closure of the HPI. The [[]] and a [[]] thick depleted uranium cylinder encapsulated by a [[]] shell. Holes are machined in the [[]] on the HPI body. The [[]] is attached to the bottom [[]] with eight (8) 7/8-inch socket head cap screws and four [[]] The top plug is a stepped design comprised of [[]] depleted uranium cylinder encapsulated by a [[]] shell. To facilitate lifting of the top plug, four hoist rings are recessed into the [[]] circular plate. The top plug is held in position by [[]] Attachment of the top and [[]] does not produce a pressure boundary. Grooves are cut into the surface of the plugs to allow moisture to escape during the vacuum drying process.

The material basket is a shoring device, which may be used for carrying various contents. The material basket is constructed of 18 full-length [[]], which form a [[]] pattern and are identified as Item 1 on drawing 001N8424. See for material basket details. The outer [[]] of the material basket form a composite section with the addition of stiffener plates welded to adjacent [[]] The center location of the basket is a developed cell, which is created by the surrounding [[]] To allow for the proper insertion of additional content shoring and facilitate fabrication, two partial length [[]] are inserted at the top and bottom of the developed cell and are identified as Item 2 on drawing 001N8424. Therefore, the exterior view of the basket shows [[]] Four circular [[]] evenly spaced in the axial direction facilitate loading and positioning of the material basket within the HPI cavity. In addition, dunnage (for example [[]] holders) may be used as a cask loading mechanism and to shore the contents during transport.

2.1.2. Design Criteria

This section defines the stress allowables for all the stresses resulting from the regulatory load combinations given in NRC Regulatory Guide 7.8 (Reference 2-2).

The cask is evaluated per ASME Service Levels A and D, normal and accident conditions, respectively. The analyses methods and stress criterion allowed by the ASME Code, Section III-Subsection NB is employed. Stress intensities caused by mechanical loads are combined before comparing to ASME code stress allowables, which are listed in Table 2.1-1.

Table 2.1-1. Structural Design Criteria for Model 2000 Cask

ASME CLASS 1 DESIGN	STRESS LIMITS
Normal conditions: Service Level A	$P_m \leq S$ $P_m + P_b \leq 1.5 S_m$ $P_m + P_b + Q \leq 3 S_m$ Bearing Stress $\leq S_y$ at temperature
Accident conditions: Service Level D	$P_m \leq 2.4 S_m$ or $0.7 S_u$ (whichever is less) $P_m + P_b \leq 3.6 S_m$ or $1.0 S_u$ (whichever is less)

Note: P_m = primary membrane stress intensity, P_b = primary bending stress intensity, S_m = design stress intensity, S_y = yield strength, S_u = ultimate strength, Q = secondary stress associated with thermal expansion.

The HPI is evaluated per ASME Service Levels A and D, normal and accident conditions, respectively. The analyses methods and stress criterion allowed by the ASME Code, Section III-Subsection NF is employed. Allowable stresses are based on section NF-3200. For normal conditions (Service Level A), design limits are defined in paragraph NF-3221.1. For accident conditions (Service Level D), design limits are defined in Appendix F of ASME Code, Section III (Reference 2-3). Note the evaluation of thermal stresses is not required per ASME Code III-NF (NF-3121.11). Stress intensities caused by mechanical loads are combined before comparing to ASME code stress allowables, which are listed in Table 2.1-2.

Table 2.1-2. Structural Design Criteria for HPI and Material Basket

ASME CLASS 1 DESIGN	STRESS LIMITS
Normal Conditions: Service Level A (NF-3221.1)	$P_m \leq S_m$ $P_m + P_b \leq 1.5 S_m$
Bearing Loads: Service Level A (NF-3223.1)	S_y at temperature
Pure Shear: Service Level A (NF-3223.2)	$0.6S_m$
Bearing Loads: Service Level D (Appendix F, F-1332.3)	Except for pinned and bolted joints, bearing stresses need not be evaluated for loads for which Level D Service Limits are specified.
Pure Shear: Service Level D (Appendix F, F-1332.4)	$0.42S_u$
Accident Conditions: Service Level D (Appendix F, F-1332)	$P_m > 1.2 S_y$ and $1.5 S_m < 0.7 S_u$ $P_m + P_b < 150\%$ of the limit for general primary stress intensity P_m

Note: P_m = primary membrane stress intensity, P_b = primary bending stress intensity, S_m = design stress intensity, S_y = yield strength, S_u = ultimate strength.

2.1.3. Weights and Centers of Gravity

The weights and center of gravity of the Model 2000 Transport Package and detailed contents are presented in Table 2.1-3. Refer to Section 1.3.1 for component dimensions.

Table 2.1-3. Summary of Maximum Weights

DESCRIPTION	DRAWING NUMBER	WEIGHT (LB)	C.G. (IN) ¹
Total Overpack plus Cask Weight	—	28,100	63.9
Cask Overpack	101E8719/ 105E9521	10,200	—
Cask Body	101E8718/ 105E9520	16,000	—
Closure Lid	101E8718/ 105E9520	1,900	—
Payload Weight²	—	5,450	62.3
HPI Assembly	001N8423	[[—
Material Basket	001N8424		—
Contents plus Shoring	—]] ³	—
Total Package Weight	—	33,550	63.6

- Notes:
1. Center of Gravity (C.G.) measured from component base.
 2. The HPI plus material basket plus radioactive contents (with shoring) is defined as payload for purposes of this report.
 3. If material basket is not used, contents plus shoring maximum weight is [[]] lb.

Table 2.1-4. Overpack Base Weight

Assembly ID	Component Description	Weight (lb)
2	[[
4		
5		
6		
7		
8		
12		
13		
14		
15		
16		
19		
25		
26		
27]]
	Total Overpack Base Weight =	3,633.15

2.1.4. Identification of Codes and Standards for Package Design

This section identifies the established codes and standards proposed for use in the Model 2000 Transport Package design, fabrication, assembly, testing, maintenance, and use.

The Model 2000 cask with HPI and material basket is allowed to ship a maximum of 1500 W of various radioactive contents. Per Regulatory Guide 7.11 (Reference 2-4), the package is considered Category I—Greater than 3,000 A₂ or greater than 30,000 Ci. From NUREG/CR-3854 (Reference 2-5), the fabrication code and standard is:

- The criteria for fabricating metal components of shipping containers used for transporting radioactive materials are based on the ASME Code Section III (Reference 2-3). ASME Code Section III is used for the design and fabrication of the HPI and material basket.

2.1.4.1. Category I Requirements

Acceptable criteria for the fabrication of metal components of shipping containers are contained in the ASME Code Section III, Subsection NB for containment components; Subsection NG for criticality components and Section VIII, Division I or Section III, Subsection NF for other safety components.

- The Model 2000 cask provides containment. Therefore, the cask shall be fabricated to Section III, Subsection NB.
- The HPI and material basket are relied upon for shielding, which falls under Component Safety Group "Other Safety". Therefore, the insert shall be fabricated to Section VIII, Division 1 or Section III, Subsection NF.

2.1.4.2. Component Classification According to Importance to Safety

The parts lists in Section 1.3.1 identify the Category A, B and C items for the Model 2000 cask, overpack, HPI, and material basket. The safety classification of all components is based on importance to safety criteria per NUREG/CR-6407 (Reference 2-6).

- For the Model 2000 cask, the components that comprise the cask inner shell, top forging, cask seals and lid are considered part of the containment boundary. Therefore, these items are Category A. Components such as the lead shielding, lifting and tie-down devices meet the definition of Category B items. See the parts lists in Section 1.3.1 for Drawing 101E8718 and 105E9520 for the Model 2000 cask assembly parts classification.
- See the parts list, Section 1.3.1, Drawing 001N8424, for the material basket assembly parts classification.
- The material basket is considered dunnage, and is not required to reduce impact loading on the containment boundary. However, it is required to maintain geometry during NCT to support the shielding analysis assumptions. Therefore, it is considered a Category B item. In addition, for fabrication, [[]] welds are Safety Category B. See the parts list in Section 1.3.1 for Drawing 001N8424 for the material basket assembly parts classification.

2.2 Materials

This section presents the mechanical properties of materials used to evaluate the performance of the Model 2000 cask, overpack, HPI, and material basket. Materials of construction for each component are found in Section 1.3.1, in the parts lists that accompany drawings.

2.2.1. Material Properties and Specifications

The material properties used in the structural analysis of the Model 2000 cask, HPI and material basket are presented in Tables 2.2-1 through 2.2-9. Material properties specific to the impact analysis are presented in Section 2.12.1.

Table 2.2-1. Structural Properties of Type 304 Stainless Steel

Temperature (°F)	-20	70	200	300	400	500	600	700	800	900	1000
Ultimate Tensile Strength S _u (ksi)	75.0	75.0	71.0	66.2	64.0	63.4	63.4	63.4	62.8	60.8	57.4
Yield Strength S _y (ksi)	30.0	30.0	25.0	22.4	20.7	19.4	18.4	17.6	16.9	16.2	15.5
Design Stress Intensity S _m (ksi)	20.0	20.0	20.0	20.0	18.6	17.5	16.6	15.8	15.2	—	—
Modulus of Elasticity (E+3, ksi)	28.8 ^a	28.3	27.5	27.0	26.4	25.9	25.3	24.8	24.1	23.5	22.8
Mean Coefficient of Thermal Expansion α (E-6, in/in/°F)	—	8.5	8.9	9.2	9.5	9.7	9.9	10.0	10.1	10.2	10.3
Poisson's Ratio	← 0.31 →										
Density (lb/in ³)	← 0.290 →										

References:

- Reference 2-7 Ultimate Tensile Strength: Table U, Page 493, Line 22.
- Reference 2-7 Yield Strength: Table Y-1, Page 610 & 611, Line 26.
- Reference 2-7 Design Stress Intensity: Table 2A, Page 306, Line 19.
- Reference 2-7 Modulus of Elasticity: Table TM-1, Material Group G, Page 738.
- Reference 2-7 Mean Coefficients of Thermal Expansion: Table TE-1, Group 3, Coefficient B, Page 711.
- Reference 2-7 Poisson's Ratio: Table PRD, High Alloy Steels (300 series), Page 744.
- Reference 2-7 Density: Table PRD, High Alloy Steels (300 series), Page 744.

Note:

^a This value was interpolated.

Table 2.2-3. Structural Properties of ASME Type [[**]]**

[[.....

]]

Note:
^a Interpolated.

Table 2.2-4. Structural Properties of Depleted Uranium Metal

Temperature (°F)	-20	70	200	300	400	500	600	700	800	900	1000
Yield Strength S _y (ksi)	—	47.2	43.8	40.2	36.3	33.3	30.5	23.9	15.3	9.3	5.8
Modulus of Elasticity (E+3, ksi)	—	23.6	—	—	—	—	—	—	—	—	—
Poisson's Ratio	← 0.335 →										
Density (lbm/in ³)	← 0.674 – 0.689 →										

References:
 Reference 2-8 Yield Strength: Figure 1, Page 671.
 Reference 2-8 Density: Page 670.
 Reference 2-9 Modulus of Elasticity: Table 7, Page 19.
 Reference 2-9 Poisson's Ratio: Table 7, Page 19.

Table 2.2-5. Structural Properties of Lead

Temperature (°F)	-40	-20	70	200	300	400	600
Modulus of Elasticity (E+3, ksi)	2.58	2.55 ^a	2.42	2.21	2.04	1.77	1.49
Yield Strength (psi)	795	763 ^a	620	500	400	—	—
Mean Coefficient of Thermal Expansion α (E-6, in/in/°F)	15.6 ^a	15.7 ^a	16.1 ^a	16.7 ^a	17.3 ^a	18.5 ^b	—
Poisson's Ratio	← 0.4 →						
Density (lb/in ³)	← 0.4097 →						

References:

- Reference 2-10 Modulus of Elasticity: Figure B-8.
- Reference 2-11 Yield Strength at (-40°F – 70°F).
- Reference 2-12 Yield Strength: (200°F – 300°F): Figure 12.
- Reference 2-10 Mean Coefficient of Thermal Expansion: Figure A-3.
- Reference 2-13 Poisson's Ratio: Table 6.1.9, Page 6-10.
- Reference 2-13 Density: Table 6.4.1, Page 6-47.

Notes:

- ^a Interpolated
- ^b Value for 440.33°F (500 K) used.

Table 2.2-6. Bolt – ASTM A-540 Grade B21 Class 3

Temperature (°F)	150	455
Ultimate Tensile Strength S_u (ksi)	145	
Yield Strength S_y (ksi)	127.9 ^a	117.2 ^a
Design Stress Intensity S_m (ksi)	42.6 ^a	39.1 ^a
Modulus of Elasticity (E+3, ksi)	29.2 ^a	27.7 ^a
Mean Coefficient of Thermal Expansion α (E-6, in/in/°F)	6.6	7.2
Poisson's Ratio	← 0.30 →	
Density (lb/in ³)	← 0.280 →	

References:

- Reference 2-7 Tensile Strength: Table U, Page 473, Line 11
- Reference 2-7 Yield Strength: Table Y-1, Page 562, Line 36
- Reference 2-7 Design Stress Intensity: Table 4, Page 366, Line 20
- Reference 2-7 Modulus of Elasticity: Table TM-1, Material Group C, Page 738
- Reference 2-7 Mean Coefficient of Thermal Expansion: Table TE-1, Group 1, Coefficient B, Page 708
- Reference 2-7 Poisson's Ratio: Table PRD, Low alloy steels: ½Cr to 1-¼Cr steels, Page 744
- Reference 2-7 Density: Table PRD, Low alloy steels: ½Cr to 1-¼Cr steels, Page 744

Note:

- ^a Interpolated

Table 2.2-7. Internal Thread – ASME SA-182 F304

Temperature (°F)	150	455
Ultimate Tensile Strength S_u (ksi)	73 ^a	63.7 ^a
Yield Strength S_y (ksi)	26.7	20 ^a
Design Stress Intensity S_m (ksi)	20.0	17.9 ^a
Modulus of Elasticity (E+3, ksi)	27.8 ^a	26.1 ^a
Mean Coefficient of Thermal Expansion α (E-6, in/in/°F)	8.8	9.7 ^a
Poisson's Ratio	← 0.31 →	
Density (lb/in ³)	← 0.290 →	

References:

Reference 2-7 Tensile Strength: Table U, Page 493, Line 16

Reference 2-7 Yield Strength: Table Y-1, Page 610, Line 11

Reference 2-7 Design Stress Intensity: Table 5A, Page 410, Line 25

Reference 2-7 Modulus of Elasticity: Table TM-1, Material Group G, Page 738

Reference 2-7 Mean Coefficient of Thermal Expansion: Table TE-1, Group 3, Coefficient B, Page 711

Reference 2-7 Poisson's Ratio: Table PRD, High Alloy Steels (300 series), Page 744

Reference 2-7 Density: Table PRD, High Alloy Steels (300 series), Page 744

Note:

^a Interpolated

Table 2.2-8. ASTM A-193 B6 Bolt Properties

Minimum Ultimate Tensile Strength S_u (ksi)	110
Minimum Yield Strength S_y (ksi)	85
Design Stress Intensity S_m (ksi)	26.5 ^{ab}
Modulus of Elasticity (E+3, ksi)	28.1 ^{ab}
Mean Coefficient of Thermal Expansion α (E-6, in/in/°F)	6.2 ^b
Poisson's Ratio	0.31
Density (lb/in ³)	0.280

References:

- Reference 2-7 Minimum Ultimate Tensile Strength: Table 3, Page 339, Line 17
 Reference 2-7 Minimum Yield Strength: Table 3, Page 339, Line 17
 Reference 2-7 Stress Intensity: Table 4, Page 366, Line 25
 Reference 2-7 Modulus of Elasticity: Table TM-1, Material Group F, Page 738
 Reference 2-7 Mean Coefficient of Thermal Expansion: Table TE-1; Coefficients for 12Cr, 12Cr-1Al, 13Cr, and 13Cr-4Ni Steels; Page 710.
 Reference 2-7 Poisson's Ratio: Table PRD, High alloy steels (400 series), Page 744
 Reference 2-7 Density: Table PRD, High alloy steels (400 series), Page 744

Notes:

- ^a Interpolated
^b Evaluated at 250°F

Table 2.2-9. ASTM A-540 Grade B22 Class 3 Bolt Properties

Minimum Ultimate Tensile Strength S_u (ksi)	145
Minimum Yield Strength S_y (ksi)	115.7
Design Stress Intensity S_m (ksi)	37.6 ^{a1}
Modulus of Elasticity (E+3, ksi)	27.4 ^{a1}
Mean Coefficient of Thermal Expansion α (E-6, in/in/°F)	7.3 ^a
Poisson's Ratio	0.30
Density (lb/in ³)	0.280

References:

- Reference 2-7 Minimum Ultimate Tensile Strength: Table 3, Page 335, Line 25
 Reference 2-7 Minimum Yield Strength: Table 3, Page 335, Line 25
 Reference 2-7 Design Stress Intensity: Table 4, Page 366, Line 4
 Reference 2-7 Modulus of Elasticity: Table TM-1, Group C, Page 738
 Reference 2-7 Mean Coefficient of Thermal Expansion: Table TE-1, Group 1, Column B, Page 708
 Reference 2-7 Density: Table PRD, Low alloy steels: ½-Cr to 1-¼Cr steels, Page 744

Notes:

- ^a Evaluated at 500°F
¹ B21 Bolt properties used because data for B22 Bolts could not be found

2.2.2. Chemical, Galvanic, or Other Reactions

The Model 2000 cask is fabricated from SS304, SS316, and lead. The lead is completely encased in the SS. This construction excludes moisture at the stainless boundary, thus assuring no galvanic or deleterious reactions could occur. The cask contents contact the stainless cavity surface. The radioactive material contents are in solid form and typically are placed in supplemental shoring. GEH's experiences in operating other transport packages with similar arrangements show that chemical, galvanic or other reactions between the cask cavity surface and the radioactive material shoring, or between the shoring and their solid contents, do not occur.

The structural components of the HPI and material basket are fabricated from SS304, [[]] steels, which are chemically compatible. These materials are selected because of their strength, ductility, and high resistance to corrosion and brittle fracture over a broad temperature range and high levels of radiation. Therefore, no chemical or galvanic reaction is anticipated. The primary function of the HPI body, including top and [[]], is to encapsulate the depleted uranium shield. Depleted uranium is cast and machined to precise tolerance to form the required shield geometry. To prevent potential oxidation, assembly of the shield is performed in an inert atmosphere. Once encapsulated, oxidation and galvanic reactions with stainless steel does not occur.

The cask containment features have no indication of chemical or galvanic reactions between [[]] compounds and stainless interfaces of the cask. This has been confirmed in the qualification of the cask containment.

2.2.3. Effects of Radiation on Materials

Gamma radiation has no significant effect on metal and therefore, the radiation produced by the contents does not cause any measurable damage to the packaging metallic components (stainless steel, aluminum, depleted uranium, and lead). Seals are inspected prior to each use. The Parker O-ring Handbook (Reference 2-14) states that when experiencing radiation levels 1×10^6 rads the effects on all compounds are minor. The maximum absorbed dose rates that these [[]] seals could be exposed to through a year of continuous use, with the cask loaded and maximum cobalt-60 activity, are on the order of 10^2 to 10^4 rad. As the Model 2000 is not a storage cask, overall exposure time for the seals is significantly shorter than an entire year. With a 1-year replacement period on the [[]] seals and O-rings, there is no significant degradation of the seals due to irradiation.

2.3 Fabrication and Examination

2.3.1. Fabrication

Fabrication and examination of the Model 2000 Transport Package (i.e., overpack and cask) conform to the requirements of ASME Section, III, Subsection NB for Category A and B components. Components of the HPI assembly and material basket assembly that are Category B items are fabricated in accordance with ASME Section III, Subsection NF. Fabrication of package components follows the guidelines presented in NUREG/CR-3854, Fabrication Criteria for Shipping Containers (Reference 2-5). All package components are fabricated in accordance with an NRC approved quality assurance program.

2.3.2. Examination

Examination of the Model 2000 Transport Package (i.e., overpack and cask) conforms to the requirements of ASME Section, III, Subsection NB for Category A and B components. Components of the HPI assembly and material basket assembly that are Category B items are examined in accordance with ASME Section III, Subsection NF. All package components are examined in accordance with an NRC approved quality assurance program.

2.4 General Requirements for All Packages

This section addresses the requirements of 10 CFR 71.43, “General Standards for All Packages.”

2.4.1. Minimum Package Size

The smallest overall dimension of the Model 2000 Transport Package is 131.5 inches. The cask overall dimensions are 71.0 inches high and 38.5 inches OD.

2.4.2. Tamper-Indicating Feature

A lock wire and seal of the type that must be broken is installed across the overpack joint section. This seal while intact, would be evidence that unauthorized persons have not opened the package.

2.4.3. Positive Closure

The Model 2000 Transport Package is an assembly of components for shipping radioactive material contents inside of a cask with a design pressure of 30 psia. The cask is sealed using a gasket and fifteen 1¼-inch socket head screws. In turn, the cask is contained by the overpack structure, which is bolted closed during transport by 15 shoulder bolts. With this double closure, overpack and cask, inadvertent opening of the cask cannot occur. The vent and drain ports on the cask each are plugged and sealed by pipe plugs and straight thread caps with O-rings.

The evaluation of the closure bolts is presented in Section 2.12.4. Review of the closure bolt evaluation at 3000 W shows that the bolt preload does not change as a result of the increase in thermal load. The closure bolt calculation shows that the controlling loads for the bolt preload are the internal pressure and the pin puncture loads. Further review of the temperatures presented in Chapter 3 show that because of the thermal modeling methodology, the heat load is concentrated

in the HPI and material basket. As a result, the temperature distribution in the closure bolt and flange are more uniform resulting in a smaller temperature delta and lower thermal stresses. To maintain positive closure during normal and hypothetical accident conditions, the closure bolts are torqued to 720 ± 30 ft-lb.

2.5 Lifting and Tie-Down Standards for All Packages

The regulations require that lifting devices which are a structural part of the package shall be capable of supporting three times the weight of the loaded package without generating stress in any material of the package in excess of its yield stress. The following sections provide a summary of the lifting and tie-down evaluation, which is presented in Section 2.12.3.

2.5.1. Lifting Devices

The Model 2000 Transport Package lifting components are evaluated structurally in the following sections. The lifting and tie-down requirements are as specified in 10 CFR 71.45(a).

2.5.1.1. Lifting Ear Evaluation

As shown in Figure 2.5.1-1, there are two types of lifting ear designs employed during the handling of the Model 2000 cask, standard and auxiliary. The ears are removed from the cask during transport and are shipped separately. The ear design identified as Standard is used for crane and fork truck lifting, and only one pair is required for these operations. The Auxiliary ear is used in crane lifting only, and 2 pairs or 4 ears are required. The user may combine the different types of ears as necessary including, 2 Standard/2 Auxiliary, 4 Auxiliary or 2 Standard.

Both ear designs are attached to the cask outer shell by means of four ASTM A193-B6 1-8 UNC-2-1/2 bolts. For this evaluation, the following loading conditions are considered:

- Load rating of $W = 23,630$ pounds, which includes the dead weight of the cask, lifting ears and the cask maximum payload.
- The two pairs of auxiliary ears are to support $3W$ such that the lifting cable does not make an angle of more than $+30^\circ$ measured from the vertical.
- The pair of standard ears is to support $3W$.

Three load cases are considered for this evaluation: Case I – vertical lift by crane; Case II – angular lift 30° from vertical by crane; and Case III – fork truck lift at two different points on the standard ears only. Figure 2.5.1-1 provides a free-body diagram for Cases I and II. Case III is similar to Case I and is not shown.

The magnitude and direction of loading in the ear analysis is shown in Figure 2.5.1-2. The analysis of each type of ear is presented in Section 2.12.3.

Material properties are based upon 250°F for the outer cask. The 249°F temperature is the maximum temperature under normal conditions for the cask outer surface (Section 3.3.1). Both standard and auxiliary ears and the cask outer shell are ASTM A240, Type 304 stainless steel. The attaching bolt material is ASTM A193-B6.

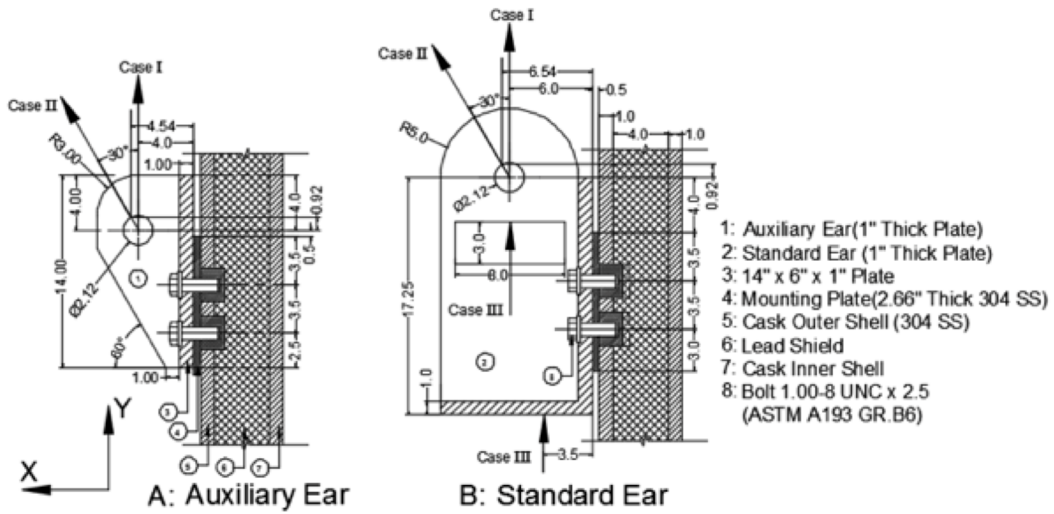


Figure 2.5.1-1. Lifting Ear Details

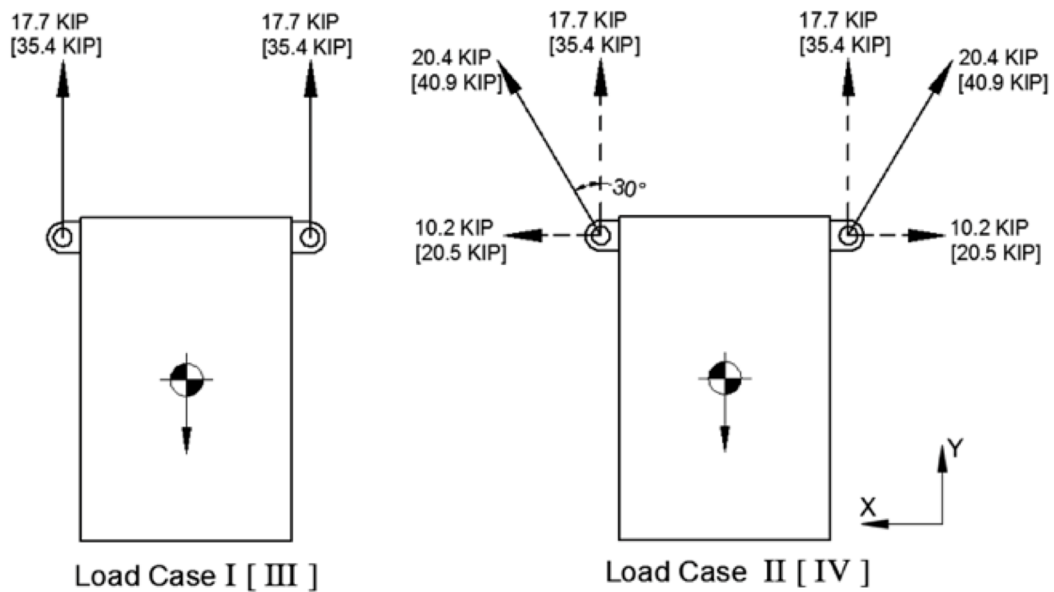


Figure 2.5.1-2. Magnitude and Direction of Loading in Ear Analysis

Table 2.5.1-1 provides a summary of the stress evaluation presented in Section 2.12.3. As the table shows, the margin of safety for all components and cases are positive. Therefore, the cask lifting device meets the requirements of 10 CFR 71.45.

Table 2.5.1-1. Summary of Cask Lifting Device Stresses

Condition	Allowable Yield (ksi)	Allowable Ultimate (ksi)	Case I			Case II			Case III		
			Stress (ksi)	*MS (y)	*MS (U)	Stress (ksi)	MS (y)	MS (U)	Stress (ksi)	MS (y)	MS (U)
Shear tearout of lifting hole - Auxiliary	14.00	26.18	6.02	1.33	3.35	---	---	---	---	---	---
Shear tearout of lifting hole - Standard	14.00	26.18	8.98	0.56	1.92	---	---	---	---	---	---
Tensile failure of lifting ear plate - Auxiliary	23.70	68.60	4.82	3.92	13.23	---	---	---	---	---	---
Tensile failure of lifting ear plate - Standard	23.70	68.60	17.70	0.34	2.88	---	---	---	---	---	---
Bearing of shackle pin on ear - Auxiliary	23.70	68.60	10.20	1.32	5.73	---	---	---	---	---	---
Bearing of shackle pin on ear - Standard	23.70	68.60	17.70	0.34	2.88	---	---	---	4.72	4.02	13.53
Tensile stress on weld joint - Auxiliary	23.70	68.60	6.50	2.65	9.55	---	---	---	---	---	---
Tensile stress on base metal - Auxiliary	23.70	68.60	9.19	1.58	6.46	9.20	1.58	6.46	---	---	---
Tensile stress on weld joint - Standard	23.70	68.60	8.16	1.90	7.41	---	---	---	---	---	---
Tensile stress on base metal - Standard	23.70	68.60	5.77	3.11	10.89	4.85	3.89	13.14	---	---	---
Tensile stress on mounting bolt-Standard	85.00	110.00	61.42	0.38	0.79	---	---	---	---	---	---
Shearing of bolt - Standard	51.00	---	14.60	2.49	---	---	---	---	---	---	---
Shearing of bolt threads-Standard	51.00	---	11.76	3.34	---	---	---	---	---	---	---
Shearing of tapered threads-Standard	14.00	26.18	9.18	0.53	1.85	---	---	---	---	---	---
Tensile stress on cask outer shell - Standard	23.70	68.60	10.95	1.16	5.26	---	---	---	---	---	---

*Note:

MS(y): Margin of safety based on yield strength.

MS(U): Margin of safety based on ultimate strength.

2.5.1.2. Cask Lifting Ear Mounting Bolt Fatigue Evaluation

The fatigue evaluation of the lifting ear mounting bolts per ASME Section III NB indicates that the bolts have an expected life of 11 years based on 12 usages per year. Bolts are inspected during the installation of the lifting ears. Damaged or defective bolts are replaced as needed.

2.5.1.3. Excessive Load Failure

The lifting devices must be designed such that their failure under excessive load would not impair the ability of the package to meet other requirements of 10 CFR 71.45(a). A review of the above margin of safety from Table 2.5.1-1 indicates that, under excessive loading, the ear attaching bolts will fail before the ear plates, ear welds or cask shell. Failure of the bolts assures that the ability of the package to meet any other regulatory requirements is not impaired.

2.5.1.4. Model 2000 Lid Lifting Lug Analysis

The lid is lifted by a single lifting lug that is composed of a 1-inch diameter stainless steel rod located at the center of the lid top. It is shown by analysis that this lifting device complies with requirements of 10 CFR 71.45(a). The lifting lug is able to support three times the weight of the lid without yielding.

The weakest part of the lifting lug is determined to have a factor of safety of 1.76 when analyzed for lifting three times the weight of the lid. Details of the analysis are documented in Section 2.12.3.

Because the lid lifting lug is covered by the cask overpack during transport the device is rendered inoperable. Therefore, no further evaluation is required.

2.5.2. Tie-Down Devices

The Model 2000 Transport Package tie-down components are evaluated structurally in the following sections. The lifting and tie-down requirements are as specified in 10 CFR 71.45(b).

2.5.2.1. Tie-Down Evaluation

The Model 2000 Transport Package is normally shipped by truck. Figure 2.5.2-1 shows the overall plan for tying the package to the vehicle. Eight wire ropes or chains tie the package to the vehicle: four connect to the upper [] tie-down ribs of the overpack, and the other four connect to the overpack base [] tie-down ribs. In addition, the base of the package is wedged to the truck bed to prevent sliding. Evaluation of the tie-down stresses is presented in Table 2.5.2-1. As the table shows all components exhibit a positive margin of safety.

Table 2.5.2-1. Tie-Down System Stress Analysis Results

Condition	Stress (ksi)	Allowable based on Yield (ksi)	MS	Allowable Based on Ultimate Strength (ksi)	MS
Shear tear-out of rib hole	20.99	$0.6 \times 45.2 = 27.12$	0.29	$96.8 / (2 \times 1.31) = 36.95$	0.76
Bearing of shackle pin	42.46	45.2	0.06	96.8	1.28
Shear stress in weld joints	20.99	$0.6 \times 45.2 = 27.12$	0.29	$96.8 / (2 \times 1.31) = 36.95$	0.76

2.5.2.2. Excessive Load Failure

Tie-down devices must be designed such that their failure under excessive load would not impair the ability of the package to meet other requirements of 10 CFR 71.45(b)(3). A review of the above margin of safety from Table 2.5.2-1 indicates that, under excessive loading, either the rib hole will tear out or the connecting weld will fail in shear. Failure of the rib or connecting weld does not impair the ability of the overpack or other package components from meeting other regulatory requirements.

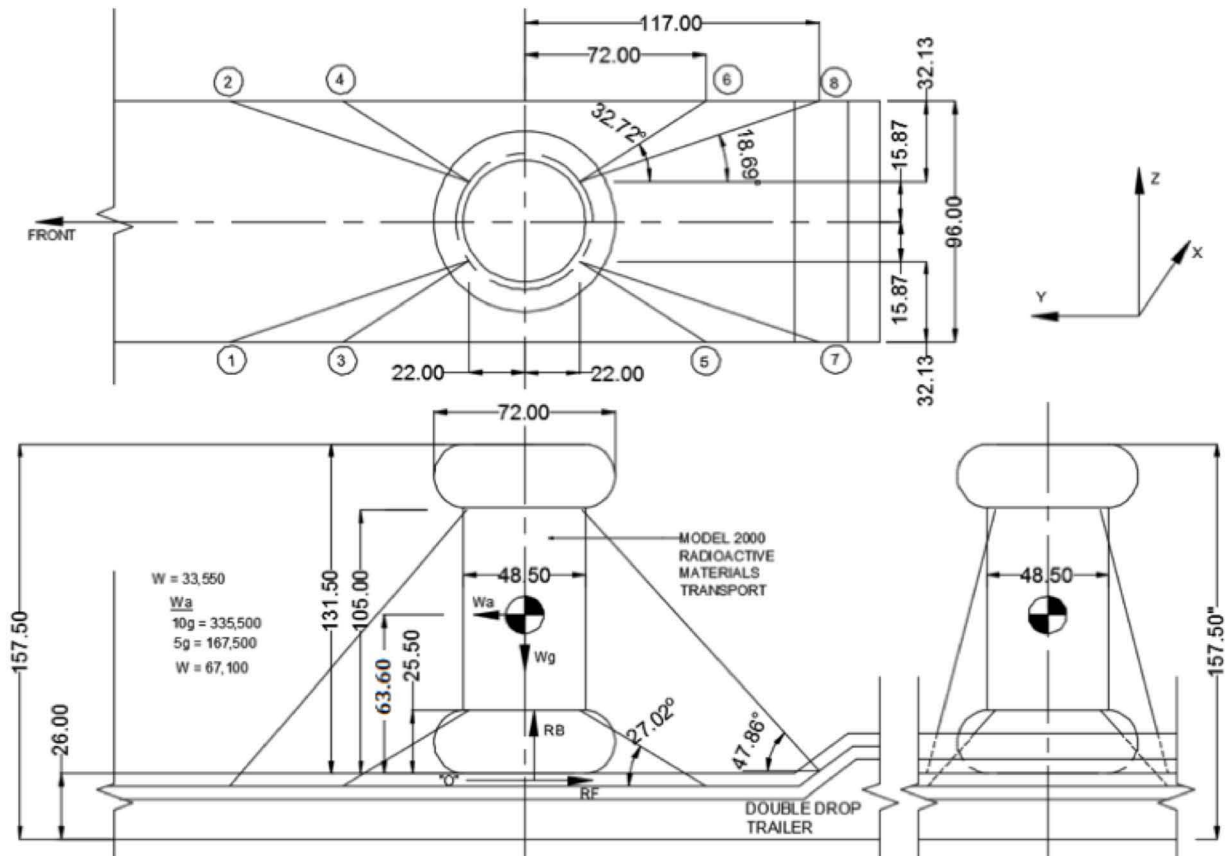


Figure 2.5.2-1. Tie-Down of Transport Package to Vehicle

2.6 Normal Conditions of Transport

This section provides the evaluation that shows the Model 2000 Transport Package, with HPI and material basket, meets the standards specified in 10 CFR 71.43 and 71.51, when subjected to the tests and conditions specified in 10 CFR 71.71 (Normal Conditions of Transport). The package is evaluated against each condition individually.

2.6.1. Heat

The thermal evaluation for the NCT heat conditions is presented in Section 3.3. The NCT heat condition consists of exposing the cask to direct sunlight and 100°F still air. For routine conditions, solar insolation is neglected. For NCT, solar insolation is applied to the package surface. For both cases, an initial temperature of 100°F and an internal power generation of 3000 W are used for the evaluation.

2.6.1.1. Summary of Pressures and Temperatures

Table 2.6.1-1 provides a summary of temperatures for the 3000 W thermal evaluation which thermally bounds 1500 W presented in Chapter 3 of this application. Additionally, internal gases in the cask and HPI are explicitly modeled in Chapter 3. Evaluation of the maximum pressure at the calculated average gas temperatures, presented in Section 3.1.4, shows that the 3000 W heat decay does not exceed the design pressure of 30 psia.

2.6.1.2. Differential Thermal Expansion

The differential thermal expansion of the Model 2000 cask is evaluated as part of the ASME Section III NB stress analysis included in Section 2.6.7 of this application to show compliance with the design criteria presented in Section 2.1.2. Review of the NCT heat conditions shows that a bounding thermal expansion model is possible by applying a 300°F temperature differential from the outside surface to the inside surface of the cask. To maximize thermal expansion, a temperature of 300°F is applied to the outer surface of the cask and 600°F to the inside surface of the cask. For the HPI and material basket thermal expansion and fit during worst-case thermal conditions assuming an initial temperature of 70°F.

Radial Thermal Expansion

Figure 2.6.1-1 through Figure 2.6.1-3 shows the HPI support disk, material basket, and HPI [] and cask inner shell diameters. Using the bounding temperature for each component, the change in diameter is calculated as:

$$d_{\text{final}} = d_0 (1 + \alpha \Delta T)$$

Where, the initial diameter, d_0 , is multiplied by the product of the coefficient of thermal expansion, α , and change in temperature, ΔT , plus one. Table 2.6.1-2 shows the results of the evaluation. The minimum worst case difference in diameters is calculated to be [] between the HPI [], which results in no radial interference. Therefore, the HPI and material basket can be removed from the cask following shipment.

Axial Thermal Expansion

Axial thermal expansion occurs when the material basket is heated by the source material from ambient conditions to NCT steady-state temperatures. Axial thermal expansion also occurs as the HPI heat reaches steady state and the inner shell of the cask expands. Using the bounding temperature for each component, the change in length is calculated as:

$$L_{\text{final}} = L_0 (1 + \alpha\Delta T)$$

Where, the initial length, L_0 , is multiplied by the product of the coefficient of thermal expansion, α , and change in temperature, ΔT . Table 2.6.1-3 shows the results of the evaluation. The minimum worst case difference in lengths is calculated to be 0.13 inches between the material basket and HPI inner cavity, which results in no axial interference.

2.6.1.3. Stress Calculations

Regulatory Guide 7.8 stress combination results are presented in Section 2.6.7. Individual thermal stresses are summarized in Table 2.6.1-4. For the HPI and material basket, the evaluation of thermal stresses is not required per ASME Code III-NF (NF-3121.11).

2.6.1.4. Comparison with Allowable Stresses

This section presents the stress combinations based upon the design criteria presented in Section 2.1.2 for NCT. The cask stresses resulting from NCT are presented in Table 2.6.1-5. Comparison of the calculated stresses to the allowable stresses presented in Section 2.1.2 demonstrates that the Model 2000 cask meets the performance requirements. In addition, the condition of the overpack during NCT is evaluated in Section 2.12.1, Cases 4, 5, and 6.

Evaluation of the HPI for end and side drop orientations calculated stresses in key components including the inner and outer [[]] and support disks. The results show that in all cases the calculated margin of safety is greater than +1. Therefore, the HPI meets the performance requirements specified in Section 2.1.2. The material basket was also evaluated for NCT drop conditions using classic methods. The results of the analysis show that the margin of safety is greater than +1. Therefore, the material basket meets the performance requirements specified in Section 2.1.2.

The NCT analysis results show that the overpack, cask, HPI and material basket meet all performance requirements, which include maintaining containment and geometry.

[[

]]

Figure 2.6.1-1. HPI Support Disk Details

[[

]]

Figure 2.6.1-2. Material Basket Detail

[[

]]

Figure 2.6.1-3. HPI Inside Diameter

Table 2.6.1-1. Temperature Results, NCT (in Shade and with Insolation)

Component	100°F Ambient Temperature, in Shade			100°F Ambient Temperature, with Insolation		
	Max	Min	Avg	Max	Min	Avg
Material Basket	989	465	801	1,001	490	815
HPI	581	360	---	604	388	---
HPI Shielding (top)	517	506	513	539	529	535
HPI Shielding (sides)	581	435	544	601	460	565
HPI Shielding (bottom)	477	427	451	501	452	475
Cask (bottom, shells, top, lid)	430	309	---	455	338	---
Cask Shielding (lid)	424	408	414	449	433	440
Cask Shielding (sides)	405	341	385	431	370	412
Cask Lid Seal	406	383	---	432	409	---
Cask Drain Port (bottom)	342	309	---	370	338	---
Cask Test Port (top)	400	383	---	426	409	---
Cask Vent Port (lid)	416	410	---	442	435	---
Overpack Base	335	159	---	364	184	---
Overpack Cover	272	108	---	308	174	---
Overpack Toroidal Shell (top)	159	110	125	207	165	179
Overpack Toroidal Shell (bottom)	215	114	139	249	136	176
Overpack Honeycomb Impact Limiter (top)	220	205	215	263	249	258
Overpack Honeycomb Impact Limiter (bottom)	330	275	304	359	305	334
HPI Fill Gas	971	460	672	983	485	689
Cask Fill Gas	574	346	462	594	374	486
HPI and Cask Fill Gas, Combined	971	346	481	983	374	505

Note: Data taken from Table 3.3.1-1

Table 2.6.1-2. Radial Thermal Expansion Evaluation for HPI and Material Basket

[[
]]

Table 2.6.1-3. Axial Thermal Expansion Evaluation for HPI and Material Basket

[[
]]

Table 2.6.1-4. NCT Thermal Stress Results (psi)

Case	Section Number	Thermal Stress (psi)
NCT End Drop	1	15110
NCT End Drop	2	6404
NCT Side Drop	3	9649
NCT Side Drop	4	15110
NCT Side Drop	5	7039

Table 2.6.1-5. Model 2000 Cask NCT Stress Analysis Summary (psi)

Case	Stress Component	Stress Combination	Stress Intensity	Allowable	Margin of Safety
1	P _m	5411	20000	20000	2.7
	P _m + P _b	17510	20000	30000	0.7
	P _m + P _b + Q	40690	20000	60000	0.5
2	P _m	14500	20000	20000	0.4
	P _m + P _b	25000	20000	30000	0.2
	P _m + P _b + Q	42864	20000	60000	0.4
3	P _m	2906	19300	19300	5.6
	P _m + P _b	9699	19300	28950	2.0
	P _m + P _b + Q	19355	19300	57900	2.0
4	P _m	6023	19300	19300	2.2
	P _m + P _b	17910	19300	28950	0.6
	P _m + P _b + Q	41280	19300	57900	0.4
5	P _m	16090	19300	19300	0.2
	P _m + P _b	25950	19300	28950	0.1
	P _m + P _b + Q	44469	19300	57900	0.3

2.6.2. Cold

The Model 2000 Transport Package is analyzed for structural adequacy in accordance with the thermal evaluation of the Model 2000 Transport Package for the temperatures specified in 10 CFR 71.71(c)(2) is presented in Chapter 3. The thermal evaluation demonstrates that the Model 2000 Transport Package component temperatures are maintained within their safe operating ranges for all normal conditions of transport. The bounding methodology for evaluating the thermal stress in the Model 2000 Transport Package is presented in Section 2.6.1 and individual thermal stresses are summarized in Table 2.6.1-4. Thermal stresses are combined with mechanical stresses in Section 2.6.7 and compared to the appropriate ASME Code allowables.

2.6.3. Reduced External Pressure

The drop in atmospheric pressure to 24 kPa (3.5 psia) is specified in 10 CFR 71.71(c)(3). This additional differential pressure has a negligible effect on the Model 2000 cask because, in Section 2.6.7, the cask is analyzed for a normal transport conditions internal pressure of 15.3 psig (30 psia). Maximum internal pressure is included in combination with internal loads. Because the margins of safety are all positive, this satisfies the requirements of 10 CFR 71.71(c)(3) for reduced external pressure.

2.6.4. Increased External Pressure

An increased external pressure of 20 psia (5.3 psig external pressure), as specified in 10 CFR 71.71(c)(4), has a negligible effect on the Model 2000 cask because of the thick outer shell and end closures. Section 2.6.7 addresses many different loading cases, which exceed these prescribed external pressure requirements. Therefore, the requirements of 10 CFR 71.71(c)(4) are satisfied.

2.6.5. Vibration

The Model 2000 Transport Package is evaluated for effects of vibrations that are normally incident to transport, as specified in 10 CFR 71.71(c)(5). The effects of shock and vibration loads associated with this road on transportation on the Model 2000 are negligible as determined in this section. For this evaluation, rather than determining the frequency of vibration of the package to establish the maximum acceleration, the cask has been structurally analyzed using the accelerations associated with NCT. Table 2.6.7-1 provides a summary of the accelerations used to evaluate the cask. The accelerations are applied statically to the ANSYS model described in detail in Section 2.6.7 to produce the maximum stress intensity in the package components. The results of the cask body, HPI and material basket analyses show that the package is capable of experiencing continuous NCT accelerations without degrading the ability of the package to meet the other parts of the regulations. Additionally, the closure system is designed in accordance with NUREG/CR-6007, which determines the bolt preload based on the impact loads experienced during HAC, which bounds the loads experienced during transport (Reference 2-15). Further, a fatigue analysis is performed in accordance with ASME Code, Section III, NB-3232.3, which concluded that after 190 transports, all bolts shall be replaced. Therefore, the requirements of 10 CFR 71.71(c)(5) are satisfied.

2.6.6. Water Spray

Water causes negligible corrosion of the stainless shell of the Model 2000 Transport Package. The cask housed in the overpack and the contents are protected in the sealed cask cavity. A water spray as specified in 10 CFR 71.71(c)(6) has no adverse effect on the package. Therefore, the requirements of 10 CFR 71.71(c)(6) are satisfied.

2.6.7. Free Drop

The free drop scenario outlined by 10 CFR 71.71(c)(7) requires a demonstration of the structural adequacy of the Model 2000 cask for a 1-ft drop onto a flat, essentially unyielding horizontal surface in the orientation that inflicts the maximum damage to the cask. The Model 2000 Transport Package is shown to meet the free drop requirements through a combination of classic calculations, impact analyses, and static finite element. The evaluations include the qualification of the Model 2000 cask lid bolt design for the combined effects of free drop impact force, internal pressures, thermal stress, O-ring compression force, and bolt preload following the methodology of NUREG/CR-6007 (Reference 2-15) (Section 2.12.4). The combined effects of inertial loads, internal pressures, and thermal stress are considered for packaging components. The impact analysis of the package is presented in Section 2.12.1. Section 2.6.7.1 presents the evaluation of the cask body and Section 2.6.7.2 presents the structural evaluation of the HPI and material basket during free drop conditions. The cask body and HPI structural analyses are performed using the finite element program ANSYS (Reference 2-16) and the material basket is analyzed using classic methods.

2.6.7.1. Cask Body Stress Analysis

This section evaluates the structural performances of the Model 2000 cask body analyses and shows that the design meets the requirements of 10 CFR 71.71. Specifically, the evaluation addresses the loads associated with the NCT. The results of the analyses for various load cases are presented pictorially in stress intensity contour plots as well as in table form, with the corresponding safety factors in critical components of the cask body.

2.6.7.1.1. Model Description

Finite element analysis methods are used to perform the stress evaluation of the Model 2000 cask for normal free drop conditions. Each drop condition is analyzed using a three-dimensional finite element model using the computational modeling software ANSYS that were developed in accordance with the certification drawings. Figure 2.6.7-1 shows the major components of the cask represented in the model including the inner and outer shells, flange, top and bottom forgings, lid, and closure bolts.

As shown in Figure 2.6.7-1, the finite element model, which corresponds to half (180°) of the cask body, is generated by de-features the AutoDesk Inventor solid model and exporting the model to a .STEP file format. The .STEP file is imported directly into ANSYS where the finite element model is developed. The solid portion of the model is constructed using ANSYS solid (SOLID185) elements. Surface-to-surface contact elements are used to simulate the interaction between adjacent components. Specifically, contact between the cask shells and lead shielding is

modeled using CONTAC174/TARGE170 surface-to-surface contact elements with zero friction, which allows the lead to float between the inner and outer shells. Contact elements are also used to bond dissimilarly meshed components. Nodal displacements are used to simulate the interaction between the cask and overpack. Weak springs elements (COMBIN14) are inserted automatically during the solution to help stabilize the model. ANSYS assigns low spring stiffness so their presence will not adversely affect the accuracy of the solution.

Boundary conditions are applied to the model simulating the loading conditions the Model 2000 cask experiences during NCT. The categories of cask loading considered in the free drop event are closure lid bolt preload, internal pressure load, thermal load, inertial body load and displacement. ANSYS input files are used to apply boundary conditions and loads to the cask model.

Closure Lid Bolt Preload

The closure lid bolt preload for 750 ft-lb maximum torque is 48,000 lb (Section 2.12.4). To apply the bolt preload ANSYS pre-tension elements (PRETS179) are used to define the 3D pre-tension section within the meshed bolt. The PRETS179 element uses a single translation degree of freedom to define pretension direction. The pretension section is modeled by a set of pretension elements defined by the bolt shaft. Figure 2.6.7-2 shows the bolt pretension values and locations. As the figure shows, the bolt divided by the symmetry plane of the model is half of the other values presented.

Internal Pressure Loading

A pressure of 30 psia is used to envelope the maximum design pressure for all NCT impact loadings considered.

Inertial Loads

To evaluate the impact performance of the cask, an LS-DYNA analysis was performed (Section 2.12.1) to determine the maximum acceleration during hot/cold and heavy/light environmental conditions and varying impact limiter shell thicknesses. Table 2.6.7-1 provides a summary of the maximum accelerations that occur during cold/light conditions.

Table 2.6.7-1. LS-DYNA Results

DESCRIPTION	DROP ANGLE (DEGREE)	APPLICABLE BOUNDARY CONDITION						ACCELERATION (g)
		Temperature			Payload			
		*Amb.	Hot	Cold	*Nom.	Heavy	Light	
NCT, End Drop, Cold	90	—	—	✓	—	—	✓	15.5
NCT, Side Drop, Cold	0	—	—	✓	—	—	✓	55.1
NCT, C.G.-Over-Corner Drop, Cold	22	—	—	✓	—	—	✓	14.6

*Note: Amb. = Ambient; Nom. = Nominal.

Cask Contents Loading - End Drop

For the end drop analyses, the contents weight is assumed to be uniformly distributed on the cask top end, over an area determined by the inside diameter of the cask lid. Therefore, one half the payload weight of 5,450 lb (see Table 2.1-3) is applied to the cask inner shell bottom plate as nodal forces. The contents load is multiplied by the appropriate g-load to accurately represent the 1-foot and 30-foot end drop.

Cask Contents Loading - Side Drop

For side drop conditions, the contact area between the contents and the cask cavity is approximately 120° (60° on each side of the drop centerline). The inertial load produced by the 5,450 lb payload weight is represented as nodal forces applied on the interior surface of the cask. The force is applied at the HPI [] and is varied in the circumferential direction as a cosine distribution. The maximum pressure occurs at the impact centerline; the load decreases to zero at locations that are approximately 60° either side of the impact centerline, as illustrated in Figure 2.6.7-3. The actual location is dependent on the actual nodal position. The following formula is used to determine the contents forces for the side drop analyses. This method uses a summation scheme to approximate the integration of the cosine-shaped pressure distribution:

$$F_{total} = \sum_{i=1}^4 F_{max} \cos(\theta_i) \cos(\theta'_i)$$

$$F_{total} = 5,450/2 \text{ lb} \times G$$

where

F_{max} = maximum pressure (at impact centerline)

θ_i = average angle of subtended arc of i^{th} element measured from centerline at point of impact, to obtain vertical component of pressure

i = i^{th} circumferential sector

θ'_i = normalized angle to peak at 0° and to be zero at 61.2°

G = impact acceleration

Figure 2.6.7-4 shows the applied nodal forces in the four regions for HAC based on the cosine distribution.

Nodal Displacement

With the absence of the overpack, nodal displacements are used to simulate the interaction between the overpack and cask body, which treats the cask body as a beam. For the side the nodes are constrained radially at the location where the cask body contacts the overpack. For the end drop, the nodal locations are visible in Figure 2.6.7-2 as a radial band at the top end of the cask. For the side drop, an additional smaller band of nodes located at the bottom end of the cask is used to represent the bottom impact limiter. Nodal displacements are also applied at the center plane of the cask to simulate symmetry. This is accomplished by fixing the out of plane displacement (Y) and the rotations about the other axes (X and Z).

Thermal

According to Regulatory Guide 7.8 (Reference 2-2), four credible thermal conditions must be considered.

Condition 1 – Hot Case 1:

- a. Ambient temperature, 100°F
- b. Initial temperature, 100°F
- c. Heat transfer to ambient by natural convection, still air
- d. Heat transfer to ambient by radiation
- e. Solar insolation as a periodic heat flux applied as 12-hr on and 12-hr off
- f. Internal heat load of 3000 W

Condition 2 – Hot Case 2:

- a. Ambient temperature, 100°F
- b. Initial temperature, 100°F
- c. Heat transfer to ambient by natural convection, still air
- d. Heat transfer to ambient by radiation
- e. No solar insolation, in shade
- f. Internal heat load of 3000 W

Condition 3 – Cold Case 1:

- a. Ambient temperature, -40°F
- b. Initial temperature, -40°F
- c. Heat transfer to ambient by natural convection, still air
- d. Heat transfer to ambient by radiation
- e. No solar insolation, in shade
- f. Internal heat load of 500 W (minimum payload case)

Condition 4 – Cold Case 2:

- a. Ambient temperature, -20°F
- b. Initial temperature, -20°F
- c. Heat transfer to ambient by natural convection, still air
- d. Heat transfer to ambient by radiation
- e. No solar insolation
- f. Internal heat load of 3000 W

Review of the four heat conditions shows that a bounding thermal expansion model is possible by applying a 300°F temperature differential from the outside surface to the inside surface of the cask. For the thermal stress evaluation, a temperature of 300°F is applied to the outer surface of the cask and 600°F to the inside surface of the cask. Using the higher temperatures maximizes the thermal expansion of the materials. The temperatures for the structural analysis are obtained from the results file and database file of the thermal analysis by writing the results to an ASCII file using the ANSYS BFINT command. Nodes for the structural model are transferred to the same coordinate system as used by the thermal run and the thermal results are interpolated for each thermal condition. The temperatures are applied as a boundary condition static structural model using the ANSYS BF command. Figure 2.6.7-5 shows the temperature distribution that is imported into the static structural model to solve for the thermal stresses. The resulting thermal stresses (Q) are combined with the inertial and pressure stresses ($P_m + P_b$) to meet the stress requirements presented in Section 2.1.2.

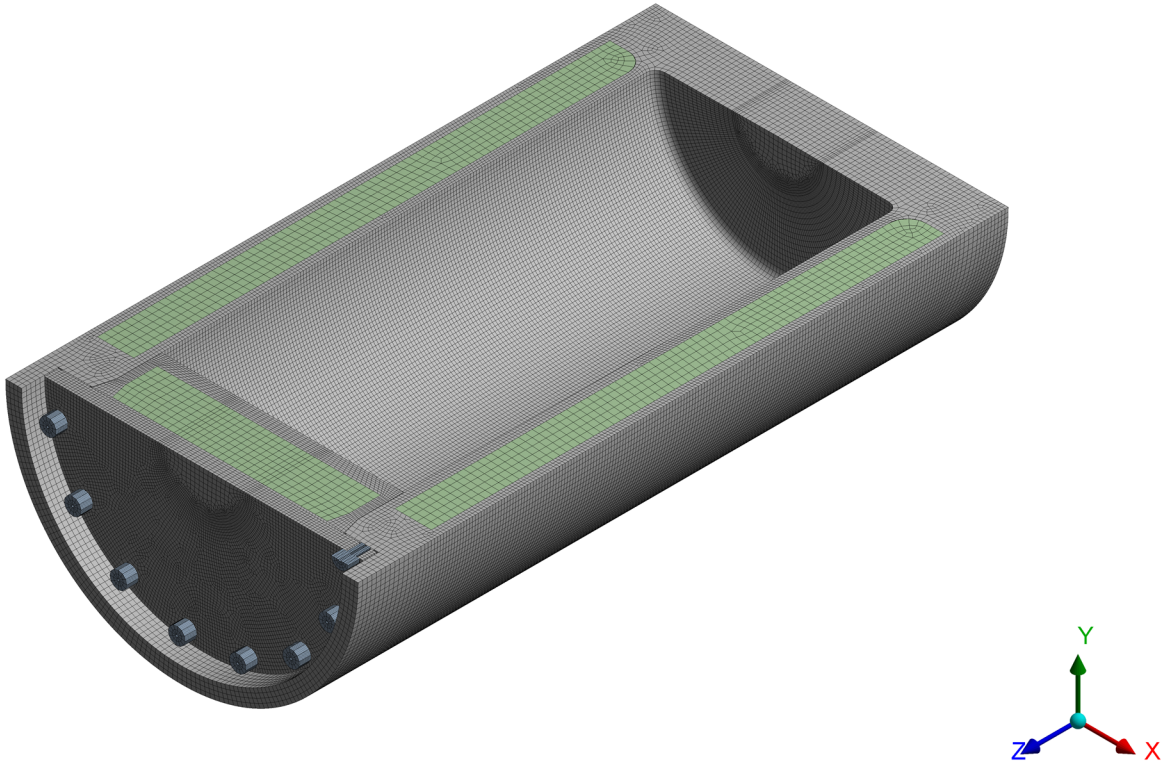


Figure 2.6.7-1. ANSYS Finite Element Model of the Cask Body

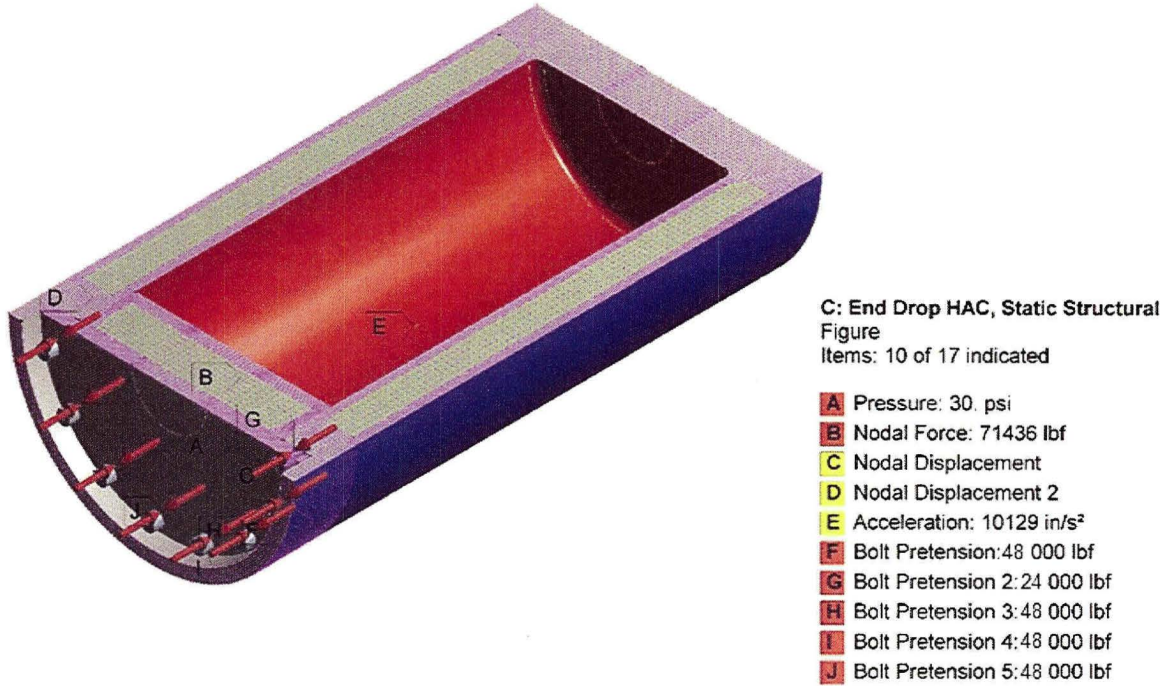


Figure 2.6.7-2. Applied Boundary Conditions for End Drop Model

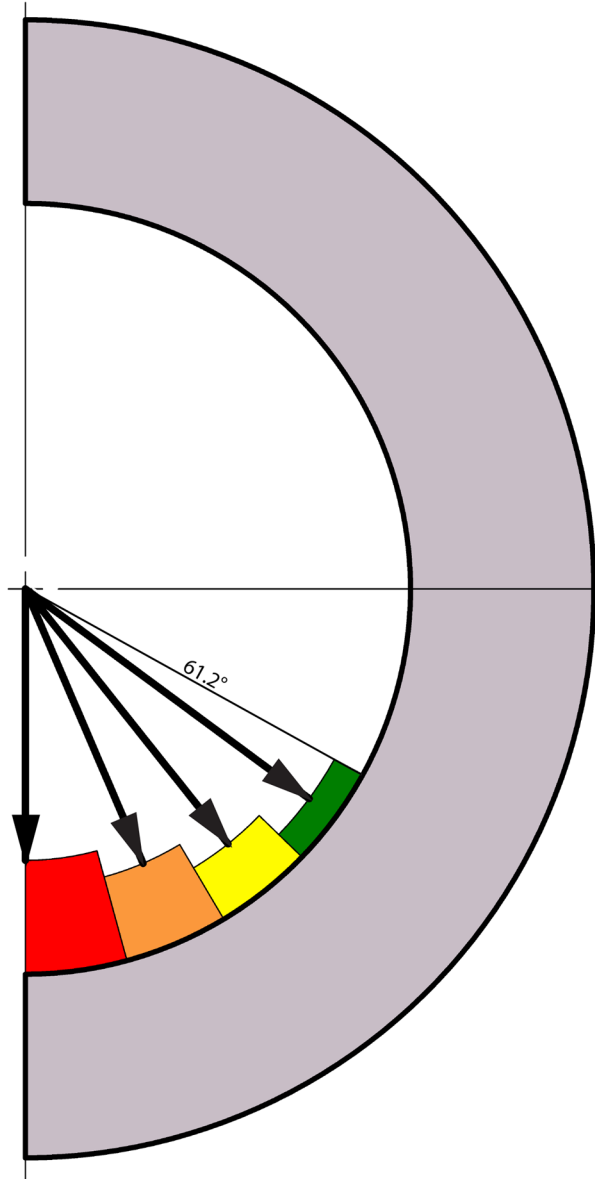


Figure 2.6.7-3. Cosine Distribution to Simulate Contents Loading During Side Drop

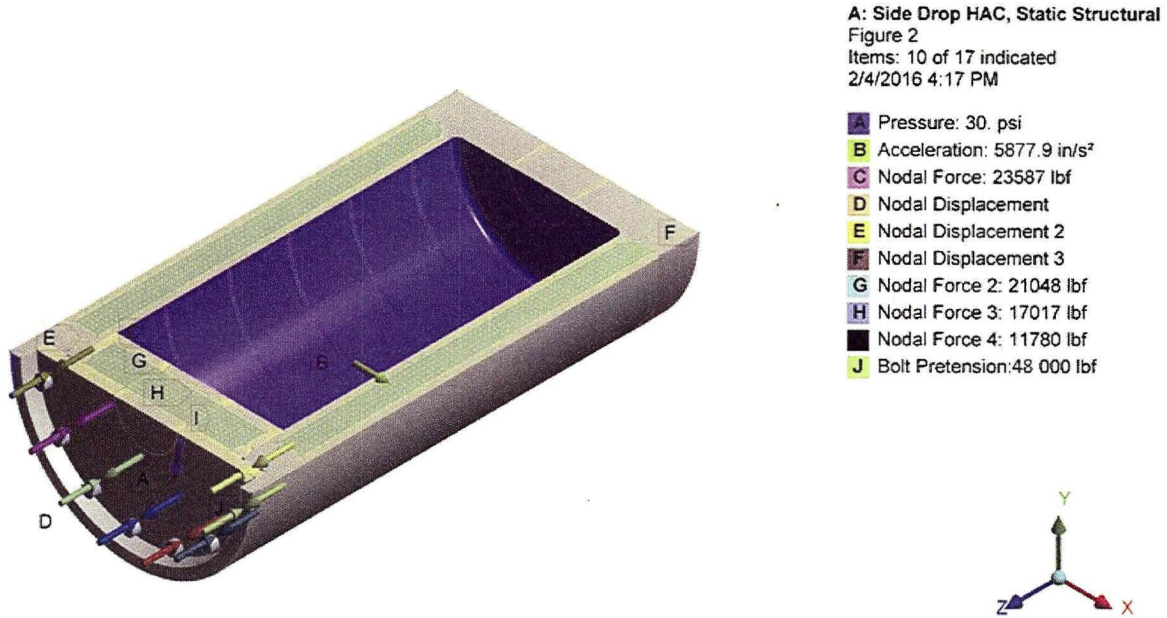


Figure 2.6.7-4. Applied Boundary Conditions for Side Drop Model

G: Steady-State Thermal
Temperature
Type: Temperature
Unit: °F
Time: 1
Custom
Max: 600
Min: 299.02
2/18/2016 11:15 AM

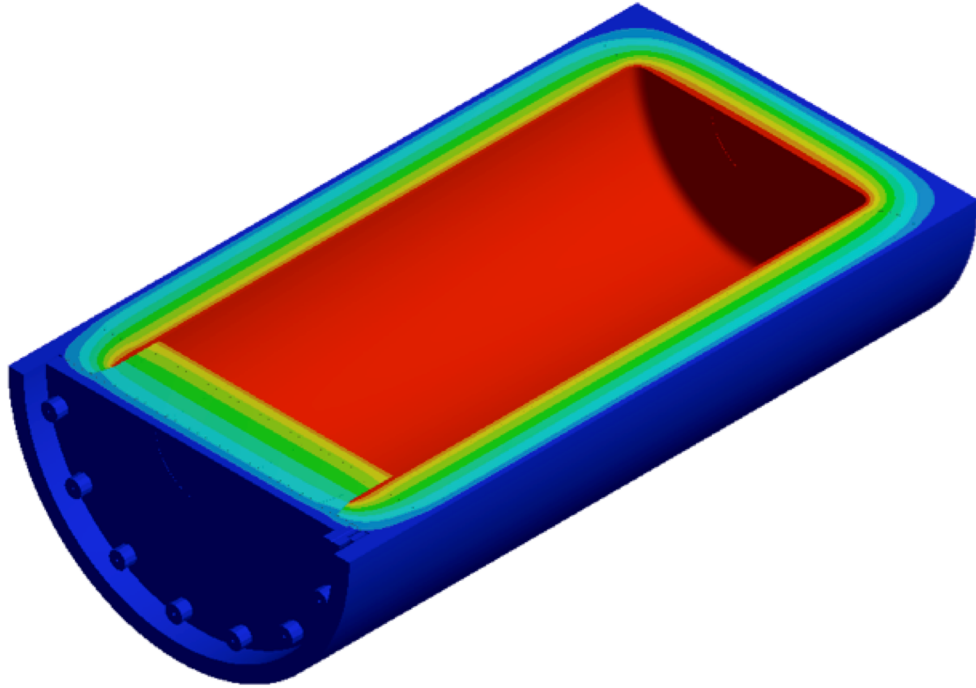
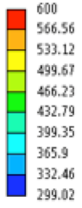


Figure 2.6.7-5. Temperature Profile for Thermal Stress Evaluation

2.6.7.1.2. NCT End Drop

In accordance with the requirements of 10 CFR 71.71, the Model 2000 cask is structurally evaluated for the normal condition of transport 1-foot end-drop. In this event, the cask (equipped with an impact limiter over each end) falls a distance of 1-foot onto a flat, unyielding, horizontal surface. The cask strikes the surface in a vertical position; consequently, an end impact on the bottom end or top end of the cask occurs. Because the cask bottom is fabricated from a solid stainless steel forging, the top drop orientation was chosen to maximize damage to the cask containment boundary. Closure bolts are evaluated separately (Section 2.12.4).

The most critically stressed component in the system is the cask flange region, which is due to bending of the flange from the inertial load imposed by the cask lid. The second region of interest is in the cask lid in the closure bolt contact region. To evaluate the stresses in these regions linearized stress are calculated across the thickness of the plate. For the top flange, Figure 2.6.7-6 shows the location of the maximum total stress intensity and Figure 2.6.7-7 indicates the path (Section 1) location where the stresses are calculated. Table 2.6.7-2 is a listing of the Section 1 stresses. Table 2.6.7-3 documents the primary membrane (P_m), primary membrane plus primary bending (P_m+P_b), primary membrane plus primary bending plus secondary stress (P_m+P_b+Q) in accordance with the criteria presented in Regulatory Guide 7.6 (Reference 2-17). Stresses are compared to the allowable at a bounding temperature of 300°F. The minimum margin of safety is found to be +2.7 for primary membrane, +0.7 for primary membrane plus bending and +0.5 for primary membrane plus bending plus secondary stress intensity.

Figure 2.6.7-8 shows the location of the maximum total stress intensity in the lid and Figure 2.6.7-9 indicates the path (Section 2). Table 2.6.7-4 presents a listing of the Section 2 stresses and Table 2.6.7-5 provides the stress combinations in accordance with the Regulatory Guide 7.6 criteria. The minimum margin of safety is found to be +0.4 for primary membrane, +0.2 for primary membrane plus bending and 0.4 for primary membrane plus bending plus secondary stress intensity. Because all of the margins of safety are positive, the Model 2000 cask meets the end drop requirement of 10 CFR 71.71(c)(7).

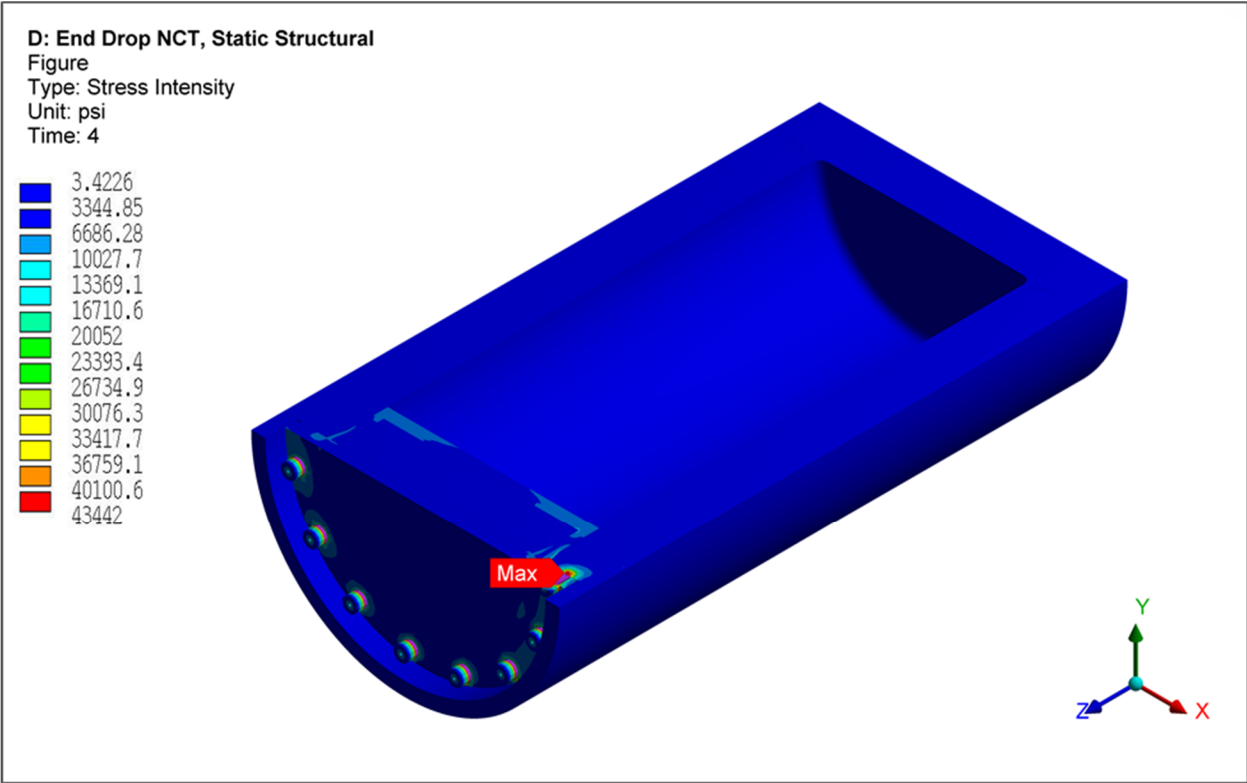


Figure 2.6.7-6. NCT End Drop Cask Body Stress Intensity (total stress psi)

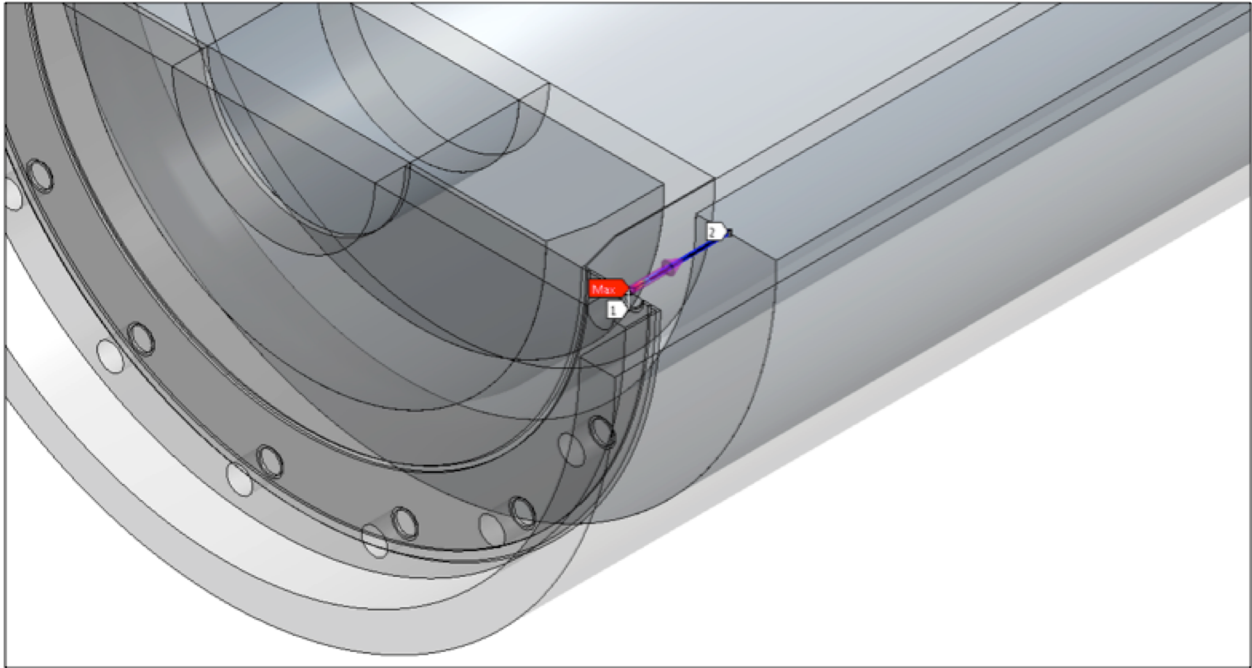


Figure 2.6.7-7. NCT End Drop Linearized Stress Location (Section 1)

Table 2.6.7-2. NCT End Drop Section 1 Stress Results (psi)

Stress State	Location	S1	S2	S3	SINT
MEMBRANE (P_m)	—	5846	902	435	5411
BENDING (P_b)	Inside	14100	2053	1685	12420
	Center	0	0	0	0
	Outside	-1685	-2053	-14100	12420
MEMBRANE + BENDING	Inside	19920	2688	2411	17510
	Center	5846	902	435	5411
	Outside	-748	-1599	-8309	7561
PEAK	Inside	23120	13060	9779	13340
	Center	-626	-827	-5431	4805
	Outside	7948	1290	966	6982
TOTAL	Inside	42540	15680	12760	29781
	Center	962	-224	-438	1401
	Outside	366	-369	-449	815

Table 2.6.7-3. NCT End Drop Section 1 Stress Results (psi)

Stress Component	Stress Combination	Stress Intensity	Allowable	Margin of Safety
P_m	5411	20000	20000	2.7
$P_m + P_b$	17510	20000	30000	0.7
$P_m + P_b + Q$	40690	20000	60000	0.5

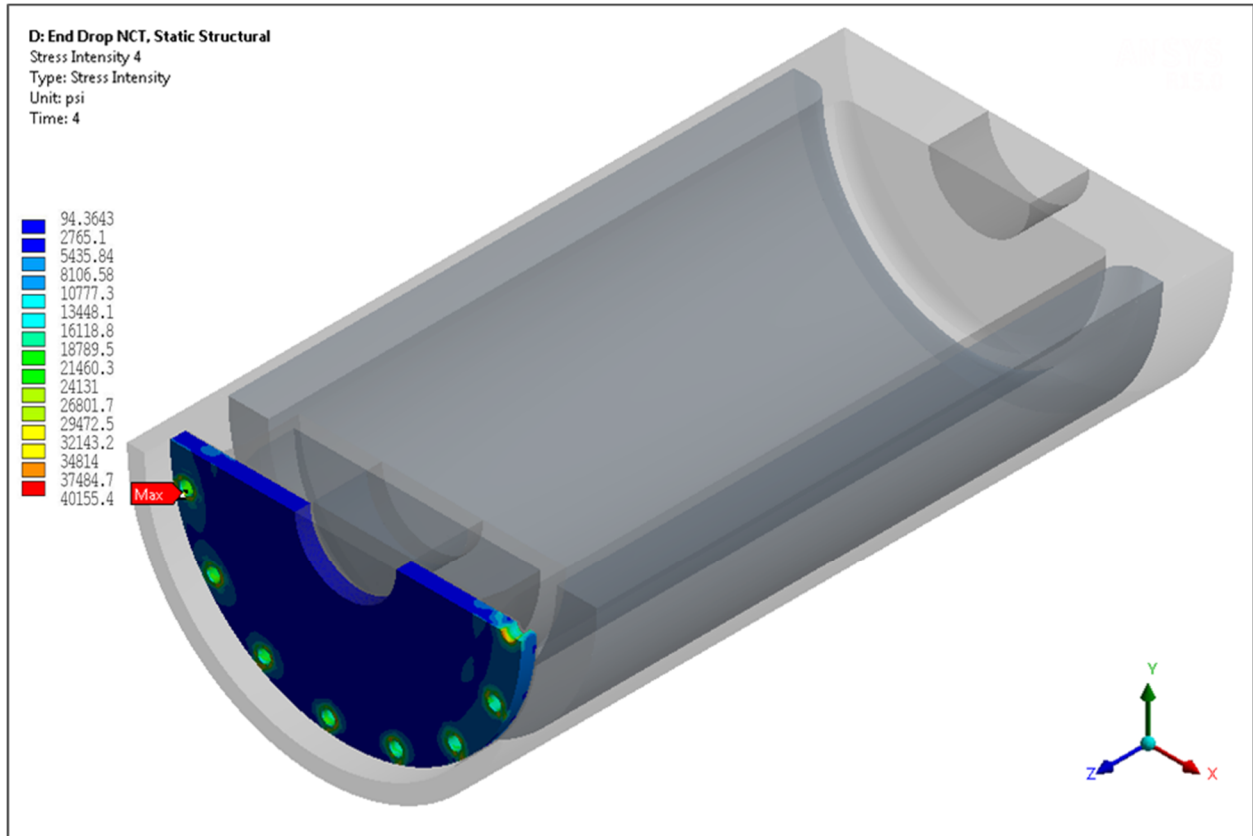


Figure 2.6.7-8. NCT End Drop Lid Stress Intensity (total stress psi)

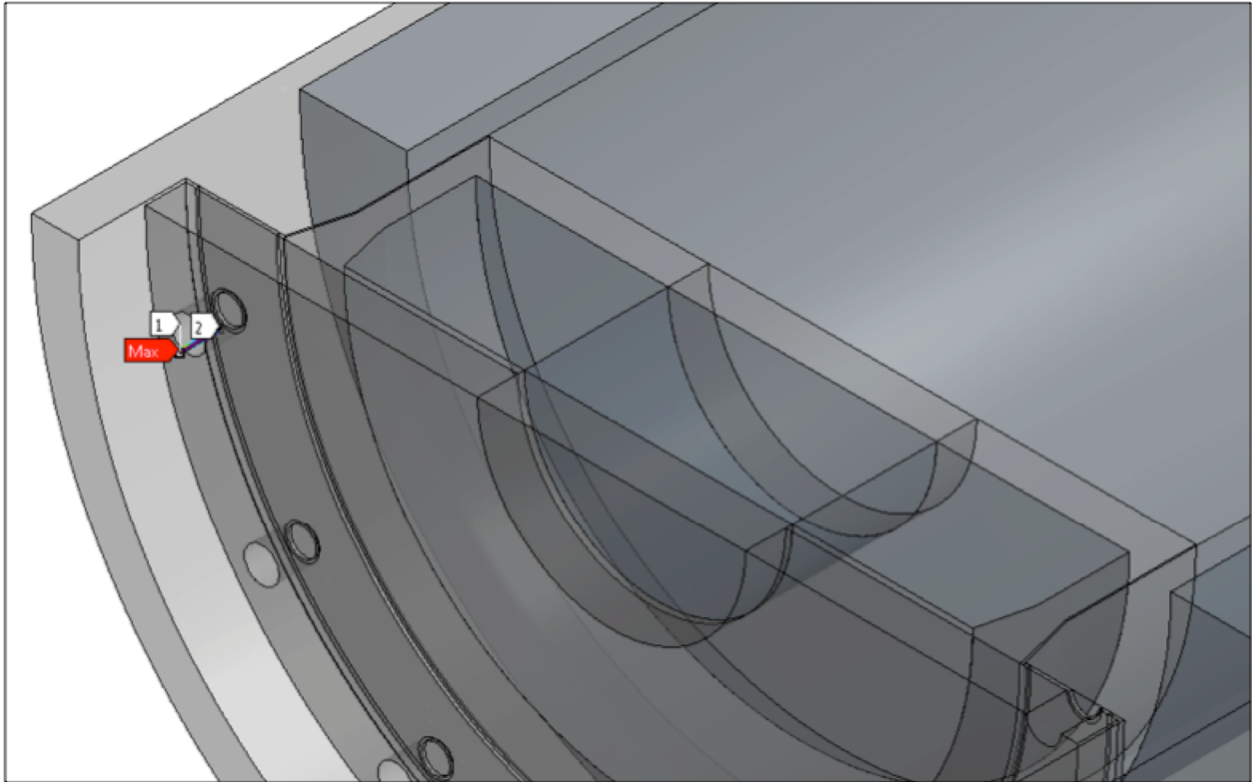


Figure 2.6.7-9. NCT End Drop Linearized Stress Location (Section 2)

Table 2.6.7-4. NCT End Drop Section 2 Stress Results (psi)

Stress State	Location	S1	S2	S3	SINT
MEMBRANE (P_m)	—	285	-189	-14210	14500
BENDING (P_b)	Inside	-2024	-5455	-13050	11030
	Center	0	0	0	0
	Outside	13050	5455	2024	11030
MEMBRANE + BENDING	Inside	-2239	-5170	-27240	25000
	Center	285	-189	-14210	14500
	Outside	5740	2036	-1360	7100
PEAK	Inside	-9130	-10750	-14340	5215
	Center	4992	2307	395	4597
	Outside	235	-3380	-6623	6858
TOTAL	Inside	-13380	-14350	-41140	27760
	Center	2592	294	-9308	11900
	Outside	2789	1800	-7942	10730

Table 2.6.7-5. NCT End Drop Section 2 Stress Results (psi)

Stress Component	Stress Combination	Stress Intensity	Allowable	Margin of Safety
P_m	14500	20000	20000	0.4
$P_m + P_b$	25000	20000	30000	0.2
$P_m + P_b + Q$	42864	20000	60000	0.4

2.6.7.1.3. NCT Side Drop

In accordance with the requirements of 10 CFR 71.71, the Model 2000 cask is structurally evaluated for the normal condition of transport 1-foot side-drop. In this event, the cask (equipped with an impact limiter over each end) falls a distance of 1-foot onto a flat, unyielding, horizontal surface. The cask strikes the surface in a horizontal position. Closure bolts are evaluated separately Section 2.12.4.

The most critically stressed component in the system is the cask inner shell at the interface with the bottom forging, the cask flange region, and the cask lid. To evaluate the stresses in these

regions linearized stress are calculated across the thickness of the plate. For the cask inner shell, Figure 2.6.7-10 shows the location of the maximum total stress intensity and Figure 2.6.7-11 indicates the path (Section 3) location where the stresses are calculated. Table 2.6.7-6 is a listing of the Section 3 stresses. Table 2.6.7-7 documents the primary membrane (P_m), primary membrane plus primary bending (P_m+P_b), primary membrane plus primary bending plus secondary stress (P_m+P_b+Q) in accordance with the criteria presented in Regulatory Guide 7.6. Stresses are compared to the allowable at a bounding temperature of 350°F. The minimum margin of safety is found to be +5.6 for primary membrane, +2.0 for primary membrane plus bending and +2.0 for primary membrane plus bending plus secondary stress intensity.

For the top flange, Figure 2.6.7-12 shows the location of the maximum total stress intensity and Figure 2.6.7-13 indicates the path (Section 4) location where the stresses are calculated. Table 2.6.7-8 is a listing of the Section 4 stresses. Table 2.6.7-9 documents the primary membrane (P_m), primary membrane plus primary bending (P_m+P_b), primary membrane plus primary bending plus secondary stress (P_m+P_b+Q) in accordance with the criteria presented in Regulatory Guide 7.6. The minimum margin of safety is found to be +2.2 for primary membrane, +0.6 for primary membrane plus bending and +0.4 for primary membrane plus bending plus secondary stress intensity.

Figure 2.6.7-14 shows the location of the maximum total stress intensity in the lid and Figure 2.6.7-15 indicates the path (Section 5). Table 2.6.7-10 presents a listing of the Section 5 stresses and Table 2.6.7-11 provides the stress combinations in accordance with the Regulatory Guide 7.6 criteria. The minimum margin of safety is found to be +0.2 for primary membrane, +0.1 for primary membrane plus bending and +0.3 for primary membrane plus bending plus secondary stress intensity. Because all of the margins of safety are positive, the Model 2000 cask meets the end drop requirement of 10 CFR 71.71.

For NCT bearing stresses are also considered in the region where the HPI contacts the cask inner shell. Bearing stress is the total applied load divided by the contact area. Because contact with the HPI is explicitly modeled by applying nodal force at the location of the HPI support disk, the bearing stress can be represented as the normal stress in ANSYS. Figure 2.6.7-16 presents the normal stress distribution. As predicted the compressive stress with the largest magnitude, -10,009 psi, occurs at the centerline of the cask. Comparing the absolute value of the compressive stress to the yield strength of the 304 stainless steel at 600°F, 18,400 psi, the margin of safety is +0.84. Therefore, the bearing stress meets the stress criteria presented in Section 2.1.2.

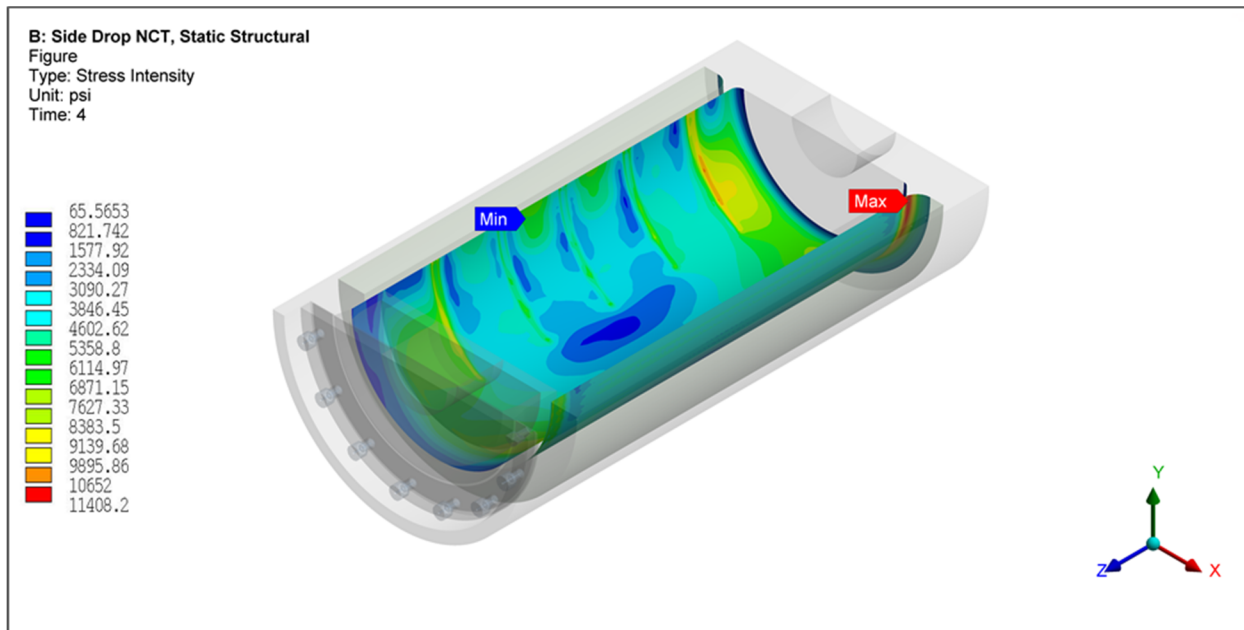


Figure 2.6.7-10. NCT Side Drop Cask Inner Shell Stress Intensity (total stress psi)

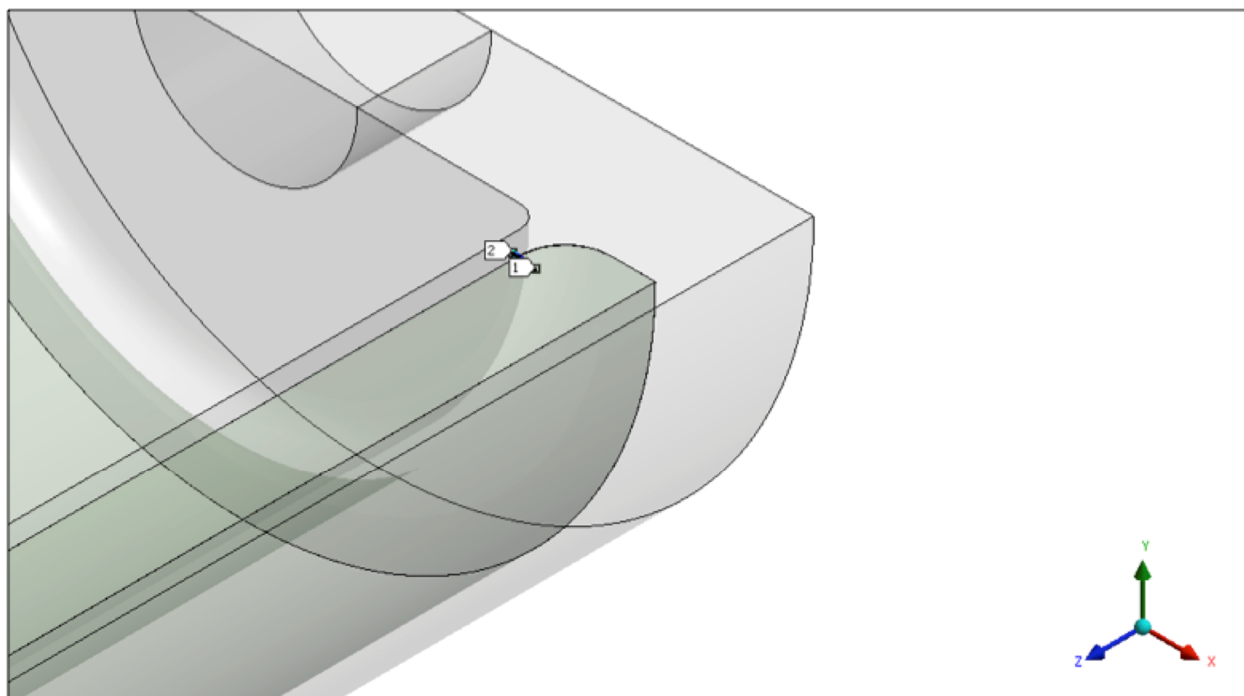


Figure 2.6.7-11. NCT Side Drop Linearized Stress Location (Section 3)

Table 2.6.7-6. NCT Side Drop Section 3 Stress Results (psi)

Stress State	Location	S1	S2	S3	SINT
MEMBRANE (P_m)	—	2685	1199	-221	2906
BENDING (P_b)	Inside	7757	2447	384	7373
	Center	0	0	0	0
	Outside	-384	-2447	-7757	7373
MEMBRANE + BENDING	Inside	10150	3660	447	9699
	Center	2685	1199	-221	2906
	Outside	-50	-1218	-5656	5606
PEAK	Inside	1466	320	-257	1723
	Center	118	-40	-328	446
	Outside	379	-33	-363	742
TOTAL	Inside	11600	3980	200	11401
	Center	2363	1155	-104	2468
	Outside	41	-1251	-5731	5772

Table 2.6.7-7. NCT Side Drop Section 3 Stress Results (psi)

Stress Component	Stress Combination	Stress Intensity	Allowable	Margin of Safety
P_m	2906	19300	19300	5.6
$P_m + P_b$	9699	19300	28950	2.0
$P_m + P_b + Q$	19355	19300	57900	2.0

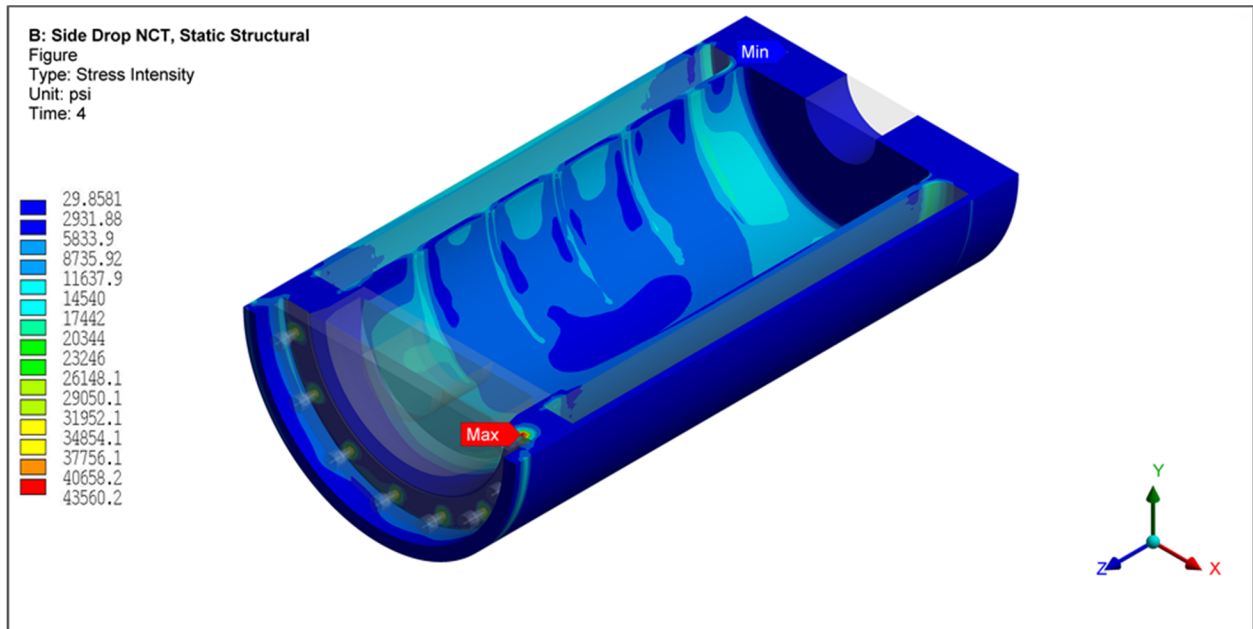


Figure 2.6.7-12. NCT Side Drop Cask Flange Stress Intensity (total stress psi)

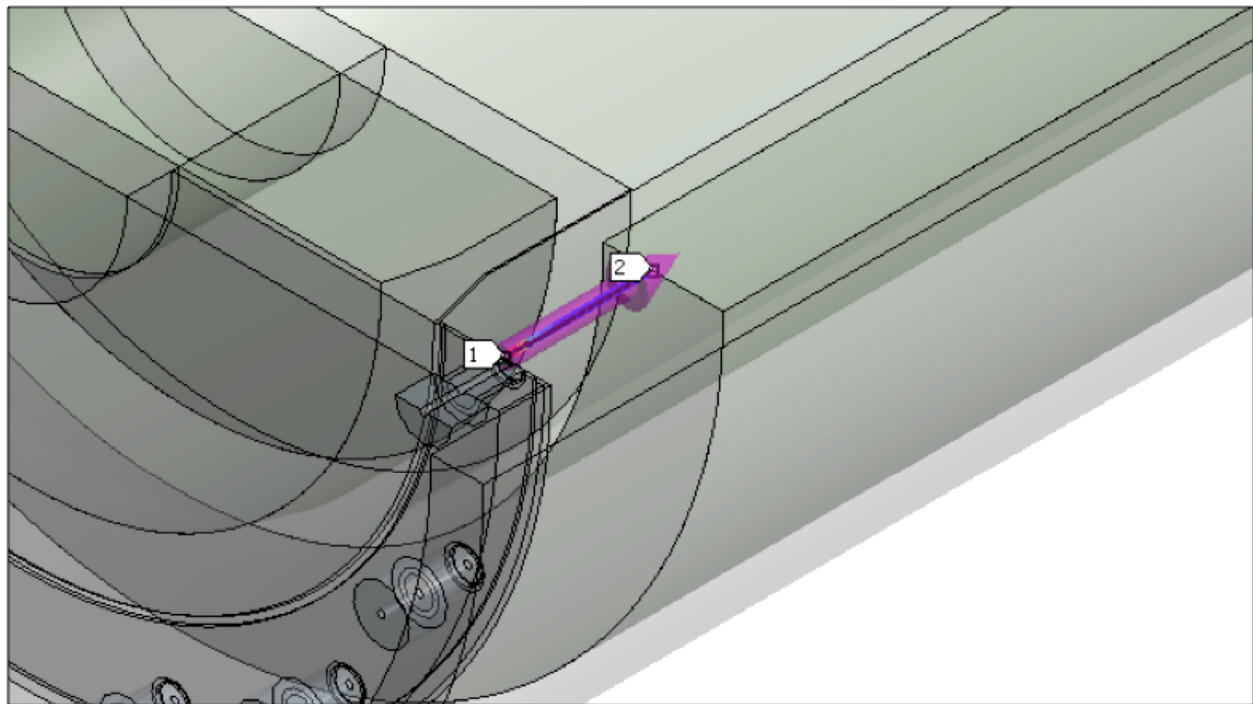


Figure 2.6.7-13. NCT Side Drop Linearized Stress Location (Section 4)

Table 2.6.7-8. NCT Side Drop Section 4 Stress Results (psi)

Stress State	Location	S1	S2	S3	SINT
MEMBRANE (P_m)	—	6412	939	389	6023
BENDING (P_b)	Inside	13800	2527	1895	11900
	Center	0	0	0	0
	Outside	-1895	-2527	-13800	11900
MEMBRANE + BENDING	Inside	20200	3478	2287	17910
	Center	6412	939	389	6023
	Outside	-1476	-1576	-7429	5952
PEAK	Inside	22380	12760	10030	12350
	Center	-681	-1027	-5044	4363
	Outside	7436	1432	1107	6329
TOTAL	Inside	42240	16060	12840	29400
	Center	1480	-190	-302	1782
	Outside	45	-120	-431	477

Table 2.6.7-9. NCT Side Drop Section 4 Stress Results (psi)

Stress Component	Stress Combination	Stress Intensity	Allowable	Margin of Safety
P_m	6023	19300	19300	2.2
$P_m + P_b$	17910	19300	28950	0.6
$P_m + P_b + Q$	41280	19300	57900	0.4

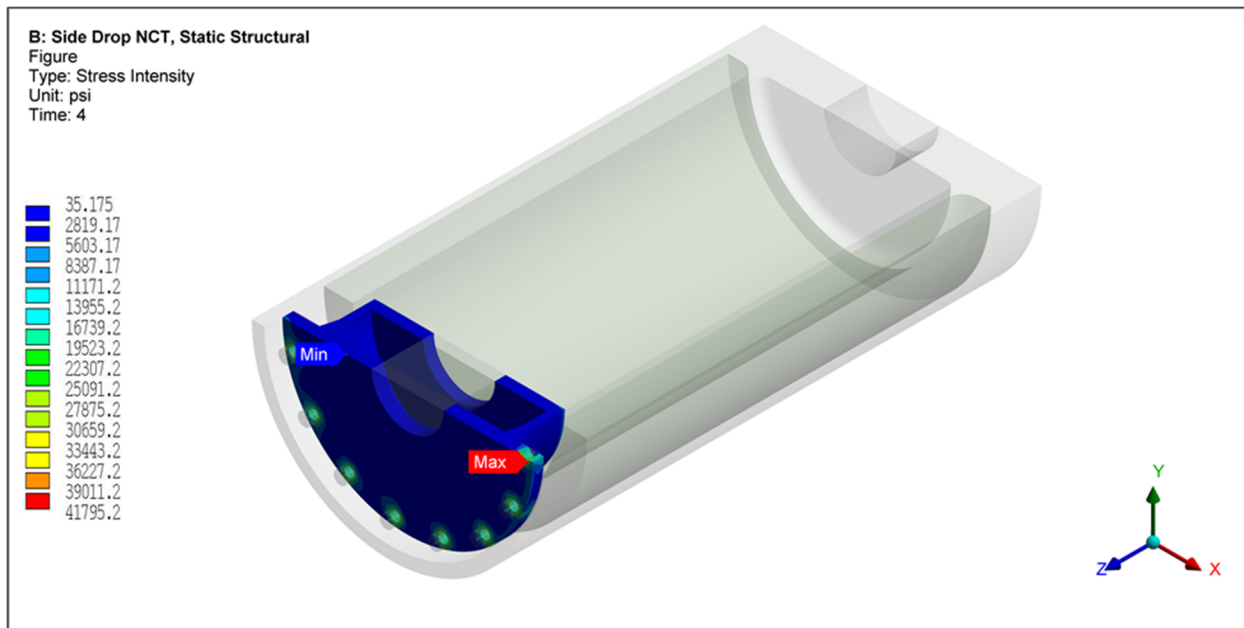


Figure 2.6.7-14. NCT Side Drop Cask Lid Stress Intensity (total stress psi)

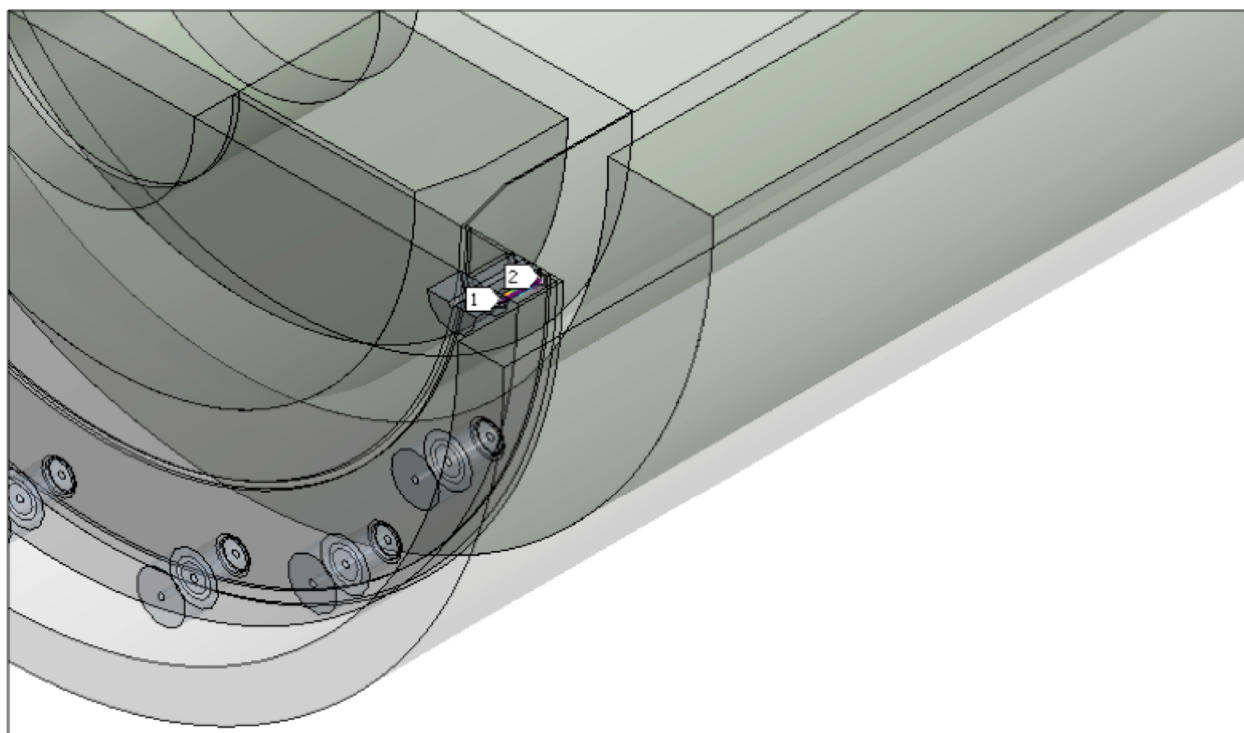


Figure 2.6.7-15. NCT Side Drop Linearized Stress Location (Section 5)

Table 2.6.7-10. NCT Side Drop Section 5 Stress Results (psi)

Stress State	Location	S1	S2	S3	SINT
MEMBRANE (P_m)	—	-684	-4079	-16770	16090
BENDING (P_b)	Inside	-343	-5757	-10400	10060
	Center	0	0	0	0
	Outside	10400	5757	343	10060
MEMBRANE + BENDING	Inside	-1106	-9877	-27050	25950
	Center	-684	-4079	-16770	16090
	Outside	1773	-30	-6771	8544
PEAK	Inside	117	-4066	-6171	6288
	Center	3818	2746	408	3410
	Outside	640	-4755	-5971	6611
TOTAL	Inside	-1541	-15960	-30660	29120
	Center	10	-1488	-13080	13090
	Outside	726	-3232	-12610	13330

Table 2.6.7-11. NCT Side Drop Section 5 Stress Results (psi)

Stress Component	Stress Combination	Stress Intensity	Allowable	Margin of Safety
P_m	16090	19300	19300	0.2
$P_m + P_b$	25950	19300	28950	0.1
$P_m + P_b + Q$	44469	19300	57900	0.3

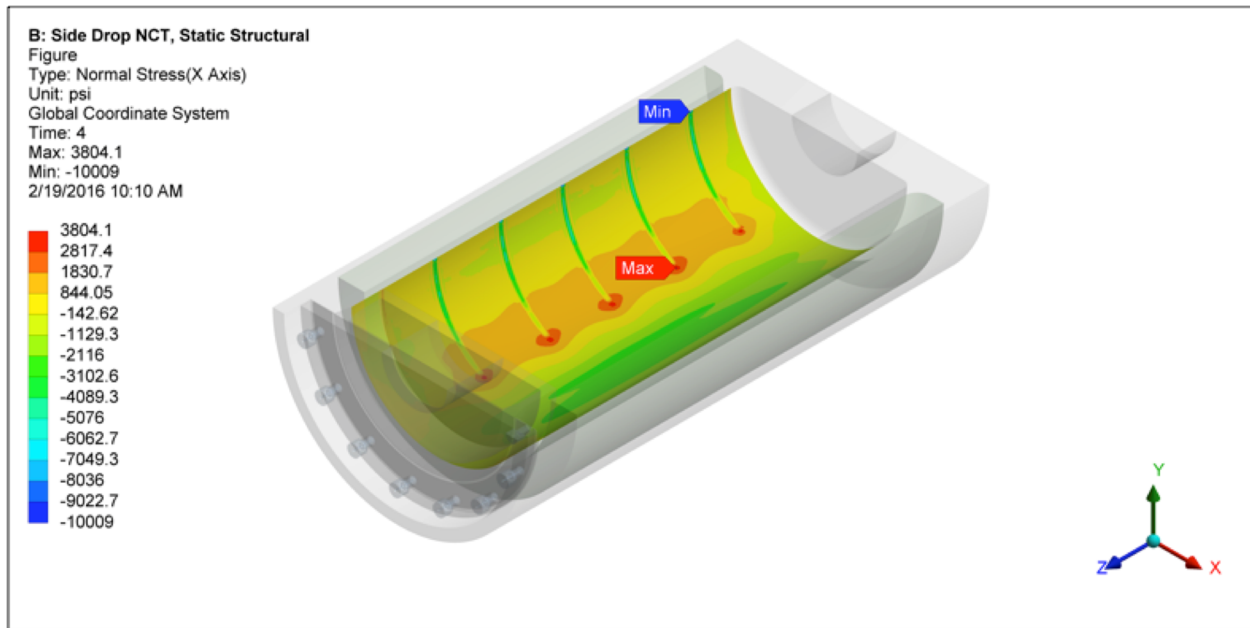


Figure 2.6.7-16. NCT Side Drop Normal Stress Distribution (psi)

2.6.7.1.4. NCT Corner Drop

The Model 2000 cask is composed of materials other than fiberboard or wood. Also, the weight of the Model 2000 cask exceeds 220 lb. According to 10 CFR 71.71(c)(8), the corner drop test is not applicable to the Model 2000 cask.

2.6.7.1.5. Penetration

According to 10 CFR 71.71(c)(10), a penetration test involving a 13-lb penetration cylinder dropped from a height of 40 inches is required for evaluation of packages during normal conditions of transport. However, Regulatory Guide 7.8 states “the penetration test of 10 CFR 71.71 is not considered by the NRC staff to have structural significance for large shipping casks (except for unprotected valves and rupture disks) and is not considered as a general requirement.” A penetration evaluation is not performed because the Model 2000 cask has no unprotected valves or rupture disks that could be affected by normal conditions of transport.

2.6.7.1.6. Cask Overpack Bolt Evaluation

During normal use, the overpack bolt is subjected to two stresses. One is the stress due to preload and acts on the reduced cross sectional area between the threaded region and the shoulder. The other stress is due to the shear from lifting the package by the top part of the overpack. Fatigue life for each stress case is evaluated to determine the limiting value.

Preload Stress:

Because the bolt is loaded in shear, preloading is only required to prevent its loosening during transport. To further ensure that the bolt will not come loose during transport, an adhesive/sealant compound is applied to the bolt threads prior to installation. The required torque for the overpack bolts is 100±5 ft-lb dry per 101E8719 and 105E9521.

The cask overpack uses 15 equally spaced 7/8-9 UNC-2A, ASTM A540 Grade B22, Class 3 bolts:

Proof Strength = Minimum Yield Strength x 85% = 115700 (0.85) = 98345 psi (Table 2.2-9)

Temperature = 192°F (Figure 3.5.1-2(b), Average of 175.0°F and 209.8°F)

The maximum preload on the bolt is:

$$P = 5T_{\text{Max}} / D_{\text{Nom}} = 7200 \text{ lb}$$

where:

$$T_{\text{Max}} = 100 + 5 = 105 \text{ ft-lb} = 1260 \text{ in-lb}$$

$$D_{\text{Nom}} = \text{Nominal thread size} = 7/8 \text{ in} = 0.875 \text{ in}$$

The area of the reduced cross section between the threads and the shoulder is

$A = 0.25 \pi (0.726)^2 = 0.414 \text{ in}^2$ The tensile stress in this region is:

$$\sigma_T = P/A = 7200/0.414 = 17391 \text{ psi} \ll \text{Proof Strength} = 98345 \text{ psi}$$

From ASME NB 3232.3 (Reference 2-18), the fatigue strength reduction factor is 4.0. The modulus of elasticity at 192°F is $29.04(10)^6$ psi (Reference 2-7, Table TM-1, Material Group C, Page 785). Because the fatigue curve (ASME Section III, Figure I-9.4, Page 12) is based on a modulus of elasticity of $30(10)^6$ psi, the stress range is given by:

$$S_r = 17391 (4.0) [30(10)^6/29.04(10)^6] = 71864 \text{ psi}$$

The alternating component is one-half of the range:

$$S_a = S_r/2 = 71864/2 = 35932 \text{ psi}$$

The number of cycles to fatigue failure is determined from Reference 2-18, Table I-9.0, Figure I-9.4: $MNS \leq 2.7S_m$. The number of cycles to failure is calculated using the procedure defined in Table I-9.0, general note (b):

$$\text{Fatigue Limit} = 5000 (10,000/5,000)^{\text{Log}(45/35.9)/\text{Log}(45/34)} = 5000 (2)^{0.806} \text{ cycles}$$

$$\text{Fatigue Limit} \approx 8700 \text{ cycles}$$

Assuming an average of 2 cycles/usage and 12 usages per year, the expected life of the bolts is:

$$\text{Bolt life} = 8700/[2(12)] = 362 \text{ years}$$

Lifting Shear Stress:

The weight transferred through the bolts during lifting of the assembled package is equal to the combined weight of the cask, HPI, material basket, contents, and overpack base. This total combined weight is:

$$\begin{aligned} W_T &= (W_{\text{cask body}} + W_{\text{cask lid}}) + W_{\text{HPI}} + (W_{\text{material basket}} + W_{\text{contents}}) + W_{\text{overpack base}} \\ &= (16000 + 1900) + 5,133 + (114 + 203) + 3633 = 26983 \text{ lb} \end{aligned}$$

The above component weights are obtained from Table 2.1-3 and Table 2.1-4.

The area of the 15 bolts loaded in double shear is:

$$A_T = \text{Total area of bolt shoulders} = (2)(15)(0.25)\pi(1.375)^2 = 44.55 \text{ in}^2$$

The bolt shearing stress associated with a vertical lift of the package and contents is:

$$\tau = W_T / A_T = 26983 / 44.55 = 606 \text{ psi}$$

Correcting for fatigue strength and modulus of elasticity gives a stress range of:

$$\tau_r = 606 (4.0) [30(10)^6 / 29.04(10)^6] = 2504 \text{ psi}$$

The alternating component is:

$$\tau_a = \tau_r / 2 = 2,504 / 2 = 1,252 \text{ psi}$$

The fatigue limit is $> 10^6$ cycles (ASME Section III, Figure I-9.4, Page 12)

2.6.7.2. HPI Stress Analysis

The purpose of this section is to document the Model 2000 HPI and material basket analyses that shows the design meets the requirements of 10 CFR 71. Specifically, the evaluation addresses the mechanical loads associated with the NCT.

The results of the analyses for various load cases are presented pictorially as stress intensity contour plots as well as in table form, with the corresponding margin of safety in each component of the cask body.

2.6.7.2.1. HPI Model Description

The HPI design was developed using Autodesk Inventor. To generate the ANSYS compatible solid model, the Inventor model of the HPI is divided in half (180°) along the center plane. The final solid model is exported as a .STEP file and is imported directly into ANSYS where the finite element model is meshed. The solid model of the HPI is shown in Figure 2.6.7-17.

The solid portion of the model is constructed using ANSYS solid (SOLID185) elements. Surface-to-surface contact elements are used to simulate the interaction between adjacent components. Specifically, contact between the HPI shells and depleted uranium shielding is modeled using CONTACT174/TARGE170 surface-to-surface contact elements with zero friction, which allows the DU to float between the inner and outer shells. Contact elements are also used to bond dissimilarly meshed components. Spring elements (COMBIN14) are inserted automatically during the solution to help stabilize the model. ANSYS assigns low spring stiffness so their presence will not adversely affect the accuracy of the solution. Welds are modeled using ANSYS contact elements.

2.6.7.2.2. HPI Side Drop Model

The HPI side drop model evaluates the stresses in the support disks and HPI assembly to ensure the HPI maintains structural integrity during NCT. Using the base model, refinements are made in the support disk mesh to ensure accurate results. Figure 2.6.7-18 shows the finite element model of the HPI.

To simulate contact with the cask, the interaction between the HPI and cask inner shell is modeled using CONTACT52 gap elements, which acts as a compression only element. The size of the CONTACT52 gaps is determined from nominal dimensions between the impact limiter and cask body. Figure 2.6.7-19 shows the distribution of the contact elements used to simulate contact between the HPI and cask inner shell.

2.6.7.2.3. HPI End Drop Model

Of primary concern during a top or bottom end impact event is the inertial loading of the depleted uranium filled plug. For this case, a top impact is assumed because the HPI [[
]] of depleted uranium. To evaluate the [[
]] subassembly is treated as a separate component. Figure 2.6.7-20 shows the solid model of the [[
]] is bolted to the HPI as a means of lifting the HPI from the cask without the need to remove the material basket. However, no credit is taken for the bolt. Therefore, only the lid assembly is evaluated using a highly-refined mesh to accurately predict stresses at the weld seam. Figure 2.6.7-21 shows the finite element model of the [[
]]

]]

Figure 2.6.7-17. HPI Solid Model

[[

]]

Figure 2.6.7-18. HPI Side Drop Finite Element Model

[[

]]

Figure 2.6.7-19. Contact Elements Between HPI and Cask Inner Shell

[[

]]

Figure 2.6.7-20. Solid Model of HPI [[]]

[[

]]

Figure 2.6.7-21. Finite Element Model of HPI [[]]

2.6.7.2.4. Boundary Conditions

Boundary conditions are applied to the model simulating the loading conditions the HPI will experience during NCT. The five categories of cask loading considered in the free drop event are pressure loaded to simulate side drop contents, discrete mass to simulate end drop, thermal conditions, inertial body load and displacement. ANSYS input files are used to apply boundary conditions and loads to the cask model.

Inertial Load

To evaluate the impact performance of the HPI, an LS-DYNA analysis was performed (Section 2.12.1) to determine the maximum acceleration during hot/cold and heavy/light environmental conditions and varying impact limiter shell thicknesses. Table 2.6.7-12 provides a summary of the maximum accelerations that occur during cold conditions. With the exception of corner drop case, the accelerations listed in Table 2.6.7-12 are applied to the HPI model using the ANSYS ACEL command equivalent to NCT accelerations corresponding to the 0.3-meter drop case. Equivalent static forces, in accordance with D’Alembert’s principle, represent the applied accelerations.

Pressure Loading Contents - Side Drop

Two cases are presented to evaluate the performance of the HPI during the side drop. Case 1 is a concentrated pressure distribution at the four [[]] Case 2 is a uniform pressure distribution (“area load”). The contact area between the material basket and the HPI inner shell is approximately 180° (90° on each side of the drop centerline). The inertial load produced by the 317-lb. content weight is represented as an equivalent static pressure applied on the interior surface of the cask. The pressure is uniformly distributed along the cavity length and is varied in the circumferential direction as a cosine distribution. The maximum pressure occurs at the impact centerline; the pressure decreases to zero at locations that are 90° from either side of the impact centerline. The pressure loading simulating the Case 1 (line load) is illustrated in Figure 2.6.7-22 and Figure 2.6.7-23 shows the pressure loading for Case 2 (area load). The following formula is used to determine the contents pressures for the side drop analyses, which vary around the circumference. This method uses a summation scheme to approximate the integration of the cosine-shaped pressure distribution:

$$F_{total} = \sum_{i=1}^{180} P_{max} A_i \cos(\theta_i) \cos(\theta'_i)$$

$$F_{total} = 317/2 \text{ kg} \times G$$

where

- P_{max} = maximum pressure (at impact centerline)
- θ_i = average angle of subtended arc of i^{th} element measured from centerline at point of impact, to obtain vertical component of pressure
- i = i^{th} circumferential sector
- θ'_i = normalized angle to peak at 0° and to be zero at 90°
- A_i = i^{th} circumferential area over which the pressure is applied
- G = side acceleration

Gap elements are defined at both ends of the cask to simulate the pressure applied by the cask inner shell during side drop conditions (see Figure 2.6.7-19). This is accomplished by defining the gap stiffness as a cosine function from a maximum value 1×10^6 lb/in at the centerline to 87,156 lb/in at 85° from the centerline of impact, and a value 50,000 lb/in from 90° to 180°.

Table 2.6.7-12. LS-DYNA NCT Impact Results Summary

DESCRIPTION	DROP ANGLE (DEGREE)	APPLICABLE BOUNDARY CONDITION						ACCELERATION (g)
		Temperature			Payload			
		Amb.	Hot	Cold	Nom.	Heavy	Light	
NCT, Cold, End Drop	90	—	—	X	—	—	X	15.5
NCT, Cold, Side Drop	0	—	—	X	—	—	X	55.1
NCT, Cold, Corner Drop	68 (=90-22)	—	—	X	—	—	X	14.6

[[

]]

Figure 2.6.7-22. Cosine Pressure Distribution Simulating Material Basket [[
]]

[[

]]

Figure 2.6.7-23. Cosine Pressure Distribution Assuming Uniform Contact

2.6.7.2.5. HPI NCT Side Drop Results

To evaluate the stresses in the HPI body, with a concentrated pressure load at the material basket [[]] linearized section stresses are evaluated at the intersection of plates, weld joints and anywhere a stress riser is observed. Stresses are evaluated using the ANSYS Parametric Design Language (APDL) macro language to cycle through each location of interest. To provide a thorough understanding of the stress profile, 684 individual sections are evaluated at axial and radial increments. At each section location, the primary membrane (P_m) and primary membrane plus primary bending (P_m+P_b) are calculated and compared to the stress criteria in accordance with the criteria presented in ASME Section III-NF (Reference 2-3). Figure 2.6.7-24 provides a visual representation of the section stress locations. Because of the total number of sections and close proximity, the section numbers are not legible. Separately, an additional seven sections are evaluated in the worst-case support disk. Figure 2.6.7-25 provides a visual representation of the section stress locations for the support disk.

2.6.7.2.6. NCT Case 1 Stress Results

The top 30 stress results for the Case 1 NCT HPI body results are presented in Table 2.6.7-13. Figure 2.6.7-26 and Table 2.6.7-14 present the Case 1 NCT support disk stress results. As shown in the tables, the margins of safety when compared to the stress intensity for each category are greater than one.

Bearing loads, per ASME III-NF-3223.1 for Service Level A (NCT) events, are compared to the yield stress at temperature. From the ANSYS output, the maximum bearing stress that results from the total force applied by the material basket [[]] to the HPI inner shell is 1690.2 psi. Assuming a maximum temperature of 1000°F the yield stress is 17,000 psi. Therefore, the margin of safety is 9.1.

[[

]]

Figure 2.6.7-24. Linearized Section Locations for the HPI Body Evaluation

[[

Figure 2.6.7-25. Linearized Section Locations for the Support Disk Evaluation

]]

[[

]]

Figure 2.6.7-26. Case 1, NCT, Stress Intensity Result (psi)

Table 2.6.7-14. NCT Support Disk Case 1 Results

[[
]]

2.6.7.2.7. NCT Case 2 Stress Results

The top 30 stress results for the Case 2 NCT HPI body results are presented in Table 2.6.7-15. Figure 2.6.7-27 and Table 2.6.7-16 present the Case 2 NCT support disk stress results. Review of the stress results shows that there is sufficient positive margin of safety of all cases.

Bearing loads per ASME III-NF-3223.1 for Service Level A (NCT) events are compared to the yield stress at temperature. From the ANSYS output the maximum bearing stress that results from the total force applied by the material basket to the HPI inner shell is 60.0 psi. Assuming a maximum temperature of 1000°F the yield stress is 17,000 psi. Therefore, the margin of safety is +Large.

2.6.7.2.8. HPI NCT End Drop Results

Stress results for the NCT end drop discussed previously are documented in Table 2.6.7-17. The table presents the primary membrane (P_m) and primary membrane plus primary bending (P_m+P_b) in accordance with the criteria presented in ASME Section III-NF (Reference 2-3).

As shown in the table, the margins of safety when compared to the stress intensity for each category are positive. The most critically stressed component in the system is the [[

]] The minimum margin of safety is found to be large. The locations of the critical sections corresponding to the maximum stress location and axial displacement are shown in Figure 2.6.7-28.

Table 2.6.7-17. NCT End Drop Stress Summary

[[.....
.....	
]]

[[

]]

Figure 2.6.7-28. HPI NCT End Drop Results – Peak Stress Intensity (psi) and Displacement (inches)

2.6.7.3. Material Basket Evaluation

This section evaluates the material basket for NCT. Factors of safety for the basket are calculated based on the criteria for Service Level ‘A’ limits from ASME Section III-NF (NF-3221).

End Drop Case

During the end drop the material basket is loaded by inertia loads acting on the end of the [[]]. Depending on the orientation of the outer cask when dropped, the basket contents will either load the material basket or the lid of the high performance insert (HPI). There is a washer welded to the bottom of the basket [[]] that holds the rod holders. Nothing prevents the rod holders from exiting the top of the material basket. If the outer cask is dropped while in the upright position, the material basket will be loaded by the contents. The worst-case condition of upright end drop is evaluated. The inertial loading will load the [[]] bundle in compression. There is no bending or shear stress present. For this evaluation, all 18 full length [[]] are loaded.

Stresses at bottom of [[]]:

$$\sigma_{\text{membrane}} = \frac{P}{A} = 837 \text{ psi compression}$$

$$\sigma_{\text{bending}} = 0 \text{ psi}$$

$$\tau_{\text{shear}} = 0 \text{ psi}$$

where $P = W \times G = 4913.5 \text{ lbs}$ inertial load on 18 [[]] bundle

$W = [[]] \text{ lbs}$ basket plus contents weight

$G = 15.5$ NCT end drop acceleration

$A = [[]] \text{ in}^2$ Cross section area of [[]], Table 2.6.7-18)

$S_y = 16900 \text{ psi}$ Yield Strength, 316 stainless steel, 800°F (Table 2.2-1)

Minimum Margin of Safety:

The minimum margin of safety for the NCT end drop case is:

$$MS = \frac{S_y}{\sigma_m} - 1 = \frac{16900}{837} - 1 = +19.2$$

Side Drop Case

During the side drop the steel [[]] provides a close fit with the high performance insert inner shell, which distributes the inertial load as three beam segments along the length of the basket assembly. The basket is assembled using short [[]] at each end of the basket starting at the center location. To provide strength to the basket assembly, [[]] are added between the [[]] at the outside of the assembly forming a [[]] shape. For this evaluation it is assumed that only the outer [[]] carry the load. Additionally, no credit is taken for the [[]], which is significantly stiffer than the individual [[]]. The basket is analyzed using classical hand calculations for a 55.1 g side drop inertia load and a bounding weight of [[]] pounds. Assuming one-third of the inertial load is carried by one of the equivalent beam segments, the bending stress in the basket is:

The margin of safety is

$$MS = \frac{1.5S_m}{\sigma} - 1 = \frac{23850}{1641.0} - 1 = +\text{Large}$$

[[]] hold the basket together using [[]] (ASME III-NF, Class 1). The [[]] and welds are equivalent in thickness and strength to the adjoining [[]]. Therefore, the previous analysis bounds the stresses generated in the welds.

2.6.8. Corner Drop

The Model 2000 cask is composed of materials other than fiberboard or wood. Also, the weight of the Model 2000 cask exceeds 220 lb. According to 10 CFR 71.71(c)(8), the corner drop test is not applicable to the Model 2000 cask. Additionally, as can be seen in Table 2.6.7-12, the end drop and side drop NCT accelerations bound the corner drop. Therefore, a stress analysis of the corner drop scenario is not required.

2.6.9. Compression

This test does not apply to the Model 2000 Transport Package, because the package weight is in excess of 11,000 lb (5,000 kg).

2.6.10. Penetration

According to 10 CFR 71.71(c)(10), a penetration test involving a 13-lb penetration cylinder dropped from a height of 40 inches is required for evaluation of packages during NCT. However, Regulatory Guide 7.8 states “the penetration test of 10 CFR 71.71 is not considered by the NRC staff to have structural significance for large shipping casks (except for unprotected valves and rupture disks) and is not considered as a general requirement.” A penetration evaluation is not performed because the Model 2000 cask has no unprotected valves or rupture disks that could be affected by normal conditions of transport.

2.7 Hypothetical Accident Conditions

The Model 2000 Transport Package has been demonstrated to meet the performance requirements specified in Subpart E of 10 CFR 71, when subjected to hypothetical accident conditions as specified in 10 CFR 71.73. According to the Regulatory Guide 7.6 (Reference 2-17), for the hypothetical accident conditions the stress intensities resulting from primary membrane and primary bending stresses are to be investigated. The stress intensities from the thermal stresses are presented in this section.

2.7.1. Free Drop

The free drop scenario outlined by 10 CFR 71.73(c)(1) requires a demonstration of the structural adequacy of the Model 2000 cask for a 30-ft drop onto a flat, essentially unyielding horizontal surface in the orientation that inflicts the maximum damage to the cask. The Model 2000 Transport Package is shown to meet the free drop requirements through a combination of classic calculations,

impact analyses, and static finite element. The evaluations include the qualification of the Model 2000 cask lid bolt design for the combined effects of free drop impact force, internal pressures, thermal stress, O-ring compression force, and bolt preload following the methodology of NUREG/CR-6007 (Reference 2-15) (Section 2.12.4). The combined effects of inertial loads, and internal pressures are considered for packaging components. The impact analysis of the package is presented in Section 2.12.1. Section 2.7.1.1 presents the evaluation of the cask body and Section 2.7.1.2 presents the structural evaluation of the HPI and material basket during free drop conditions. The cask body and HPI structural analyses are performed using the finite element program ANSYS (Reference 2-16) and the material basket is analyzed using classic methods. Table 2.7.1-1 provides a summary of the HAC accelerations predicted by the LS-DYNA analysis presented in Section 2.12.1. A lead slump analysis is provided in Section 2.12.2.

Table 2.7.1-1. LS-DYNA Results

DESCRIPTION	DROP ANGLE (DEGREE)	APPLICABLE BOUNDARY CONDITION						ACCELERATION (g)
		Temperature			Payload			
		Amb.	Hot	Cold	Nom.	Heavy	Light	
HAC, End Drop, Hot	90	—	✓	—	—	✓	—	157.5
HAC, Side Drop, Cold	0	—	—	✓	—	—	✓	161.9
HAC, Corner Drop, Cold	68 (90-22)	—	—	✓	—	—	✓	80.3
HAC, Slap Down	5	✓	—	—	✓	—	—	114.4
HAC, Slap Down	10	✓	—	—	✓	—	—	118.0

2.7.1.1. Cask Body Stress Analysis

This section evaluates the structural results of the Model 2000 cask body analyses and shows that the design meets the requirements of 10 CFR 71.71. Specifically, the evaluation addresses the loads associated with the HAC. The results of the analyses for various load cases are presented pictorially in stress intensity contour plots as well as in table form, with the corresponding safety factors in critical components of the cask body.

2.7.1.1.1. End Drop

In accordance with the requirements of 10 CFR 71.73(c)(1), the Model 2000 Transport Package is structurally evaluated for the 30-foot end-drop condition. In this hypothetical accident, the cask including the payload and the impact limiters falls 30 feet onto a flat, unyielding, horizontal surface. The cask strikes the surface in a vertical upright position. For the Model 2000 cask, the bottom end drop is bounding. In the bottom down position, the prying load on the closure bolts is maximized. Closure bolts are evaluated separately in Section 2.12.4.

The most critically stressed component in the system is the cask flange region, which is due to bending of the flange from the inertial load imposed by the cask lid. The second region of interest is in the cask lid in the closure bolt contact region. To evaluate the stresses in these regions

linearized stress are calculated across the thickness of the plate. For the top flange, Figure 2.7.1-1 shows the location of the maximum total stress intensity and Figure 2.7.1-2 indicates the path (Section 6) location where the stresses are calculated. Table 2.7.1-2 is a listing of the Section 6 stresses. Table 2.7.1-3 documents the primary membrane (P_m) and primary membrane plus primary bending (P_m+P_b) in accordance with the criteria presented in Regulatory Guide 7.6. Stresses are compared to the allowable at a bounding temperature of 300°F. The minimum margin of safety is found to be +3.7 for primary membrane, and +1.8 for primary membrane plus bending.

Figure 2.7.1-3 shows the location of the maximum total stress intensity in the lid and Figure 2.7.1-4 indicates the path (Section 7). Table 2.7.1-4 presents a listing of the Section 2 stresses and Table 2.7.1-5 provides the stress combinations in accordance with the Regulatory Guide 7.6 criteria. The minimum margin of safety is found to be +1.4 for primary membrane and +0.8 for primary membrane plus bending. Because all of the margins of safety are positive, the Model 2000 cask meets the end drop requirement of 10 CFR 71.73.

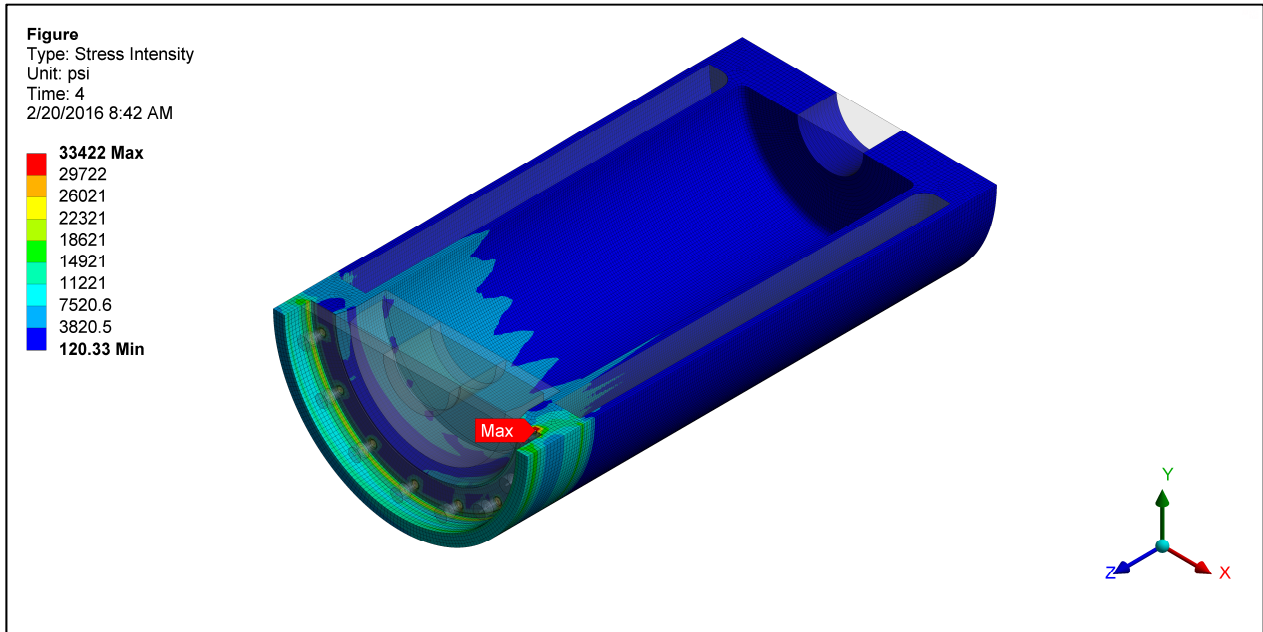


Figure 2.7.1-1. HAC End Drop Cask Body Stress Intensity (total stress psi)

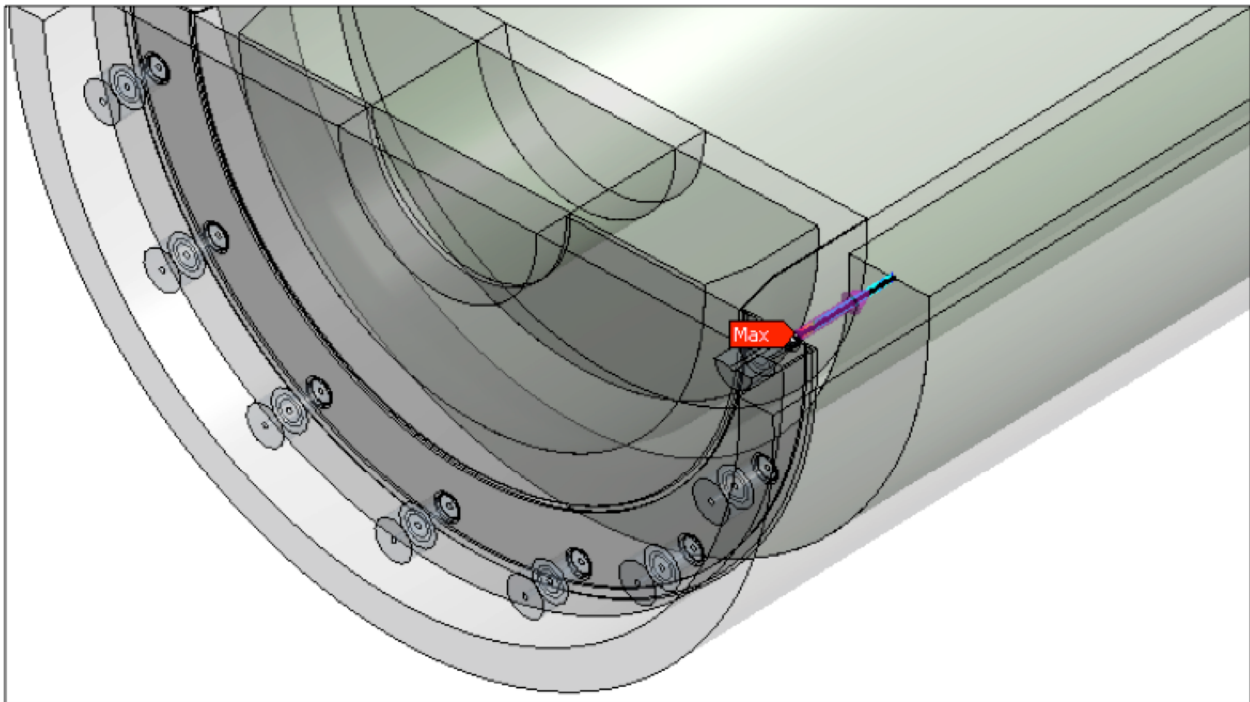


Figure 2.7.1-2. HAC End Drop Linearized Stress Location (Section 6)

Table 2.7.1-2. HAC End Drop Section 6 Stress Results (psi)

Stress State	Location	S1	S2	S3	SINT
MEMBRANE (P_m)	—	6581	-895	-3558	10140
BENDING (P_b)	Inside	14700	1514	-5075	19770
	Center	0	0	0	0
	Outside	5075	-1514	-14700	19770
MEMBRANE + BENDING	Inside	19290	500	-6531	25830
	Center	6581	-895	-3558	10140
	Outside	5773	-2708	-12070	17840
PEAK	Inside	23680	14560	11820	11860
	Center	-301	-939	-5909	5608
	Outside	7995	1326	524	7471
TOTAL	Inside	41600	13550	8174	33422
	Center	4518	-1942	-7597	12120
	Outside	6665	-1547	-4280	10940

Table 2.7.1-3. HAC End Drop Section 6 Stress Results (psi)

Stress Component	Stress Combination	Stress Intensity	Allowable	Margin of Safety
P_m	10140	20000	48000	3.7
$P_m + P_b$	25830	20000	72000	1.8

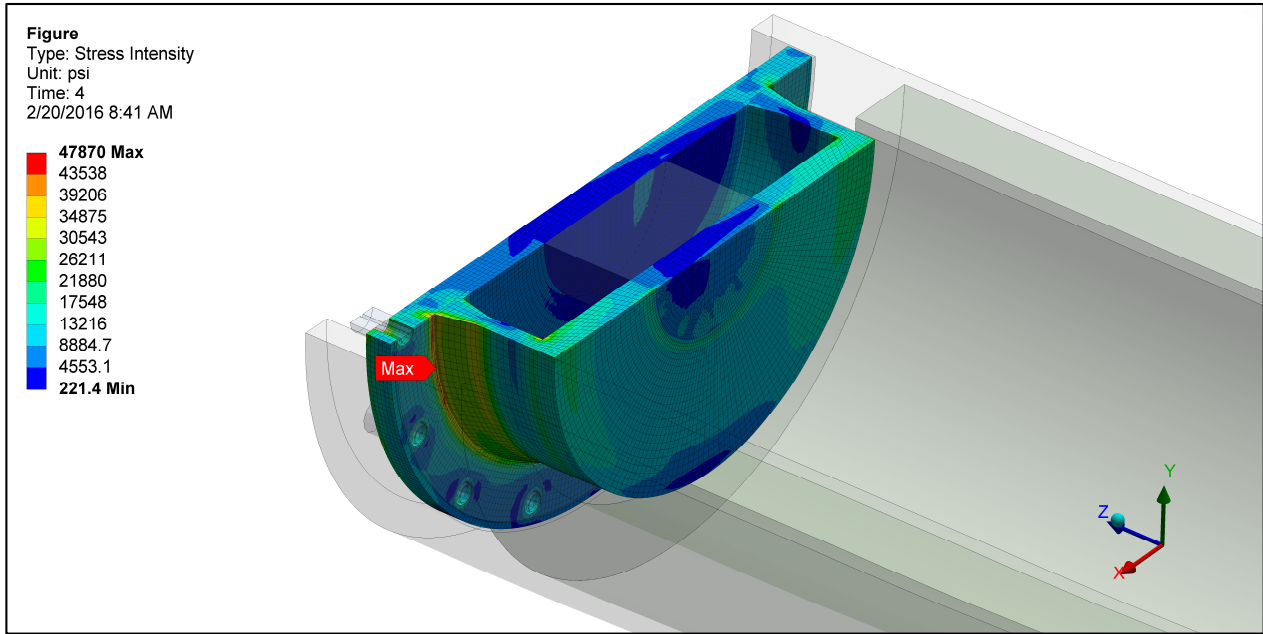


Figure 2.7.1-3. HAC End Drop Lid Stress Intensity (total stress psi)

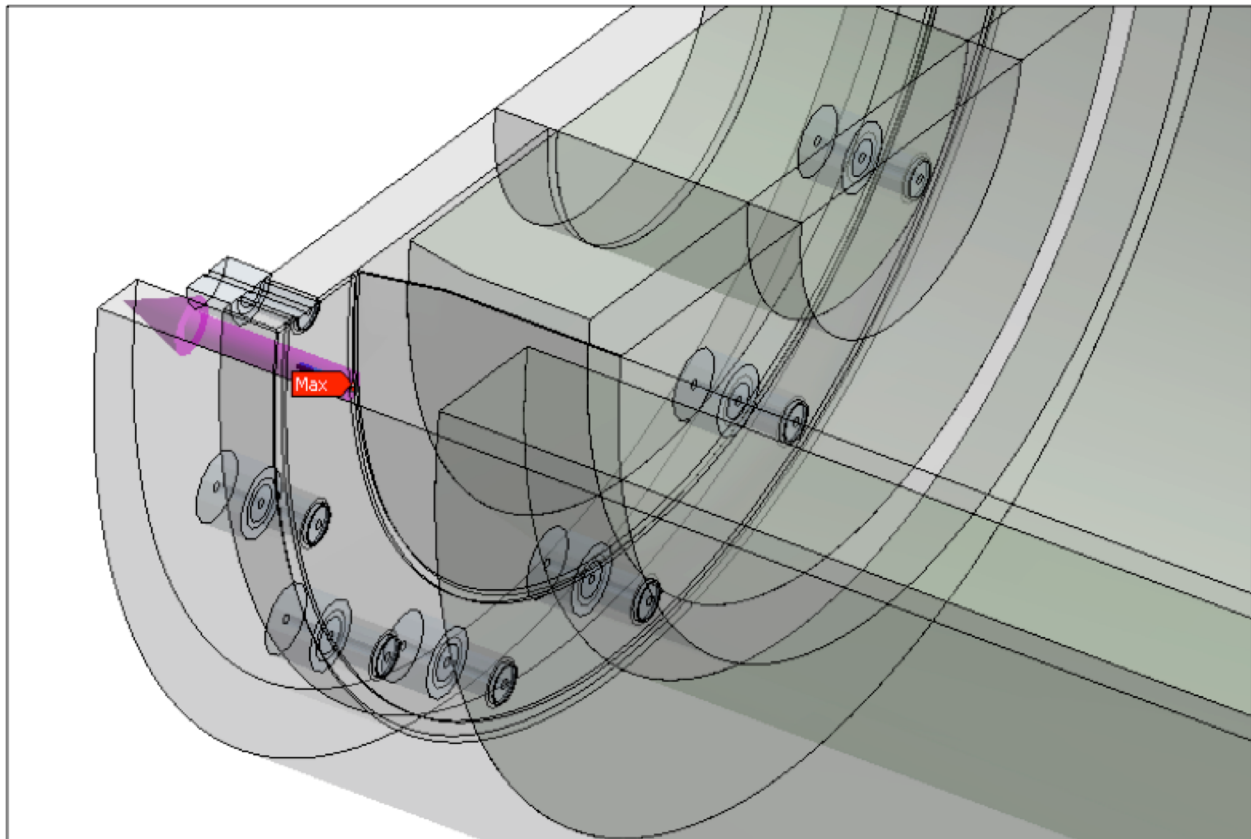


Figure 2.7.1-4. HAC End Drop Linearized Stress Location (Section 7)

Table 2.7.1-4. HAC End Drop Section 7 Stress Results (psi)

Stress State	Location	S1	S2	S3	SINT
MEMBRANE (P _m)	—	4664	-9598	-15170	19830
BENDING (P _b)	Inside	6095	-5767	-15640	21730
	Center	0	0	0	0
	Outside	15640	5767	-6095	21730
MEMBRANE + BENDING	Inside	10350	-15400	-30370	40720
	Center	4664	-9598	-15170	19830
	Outside	3790	-4026	-4558	8348
PEAK	Inside	6105	805	-4285	10390
	Center	1161	-449	-3088	4249
	Outside	3340	607	-925	4265
TOTAL	Inside	14800	-14510	-33070	47870
	Center	3087	-10080	-15480	18570
	Outside	3323	-1612	-3483	6806

Table 2.7.1-5. HAC End Drop Section 7 Stress Results (psi)

Stress Component	Stress Combination	Stress Intensity	Allowable	Margin of Safety
P _m	19830	20000	48000	1.4
P _m + P _b	40720	20000	72000	0.8

2.7.1.1.2. Side Drop

In accordance with the requirements of 10 CFR 71.73(c)(1), the Model 2000 cask is structurally evaluated for the hypothetical accident 30-foot side drop condition. In this event, the cask including the payload and impact limiters falls 30 feet onto a flat, unyielding, horizontal surface. The package strikes the surface in a horizontal position resulting in a side impact. The types of loading involved in a side drop accident are closure lid bolt preload, internal pressure, and inertial body load. Closure bolts are evaluated separately in Section 2.12.4.

The most critically stressed component in the system is the cask inner shell at the interface with the bottom forging, the cask flange region, and the cask lid. To evaluate the stresses in these regions linearized stress are calculated across the thickness of the plate. For the cask inner shell, Figure 2.7.1-5 shows the location of the maximum total stress intensity and Figure 2.7.1-6 indicates the path (Section 8) location where the stresses are calculated. Table 2.7.1-6 is a listing of the Section 8 stresses. Table 2.7.1-7 documents the primary membrane (P_m) and primary membrane plus primary bending (P_m+P_b) in accordance with the criteria presented in Regulatory Guide 7.6. Stresses are compared to the allowable at a bounding temperature of 350°F. The minimum margin of safety is found to be +4.5 for primary membrane and +1.5 for primary membrane plus.

Figure 2.7.1-7 shows the location of the maximum total stress intensity in the lid and Figure 2.7.1-8 indicates the path (Section 9). Table 2.7.1-8 presents a listing of the Section 9 stresses and Table 2.7.1-9 provides the stress combinations in accordance with the Regulatory Guide 7.6 criteria. The minimum margin of safety is found to be +1.6 for primary membrane and +1.2 for primary membrane plus bending. Because all of the margins of safety are positive, the Model 2000 cask meets the end drop requirement of 10 CFR 71.71.

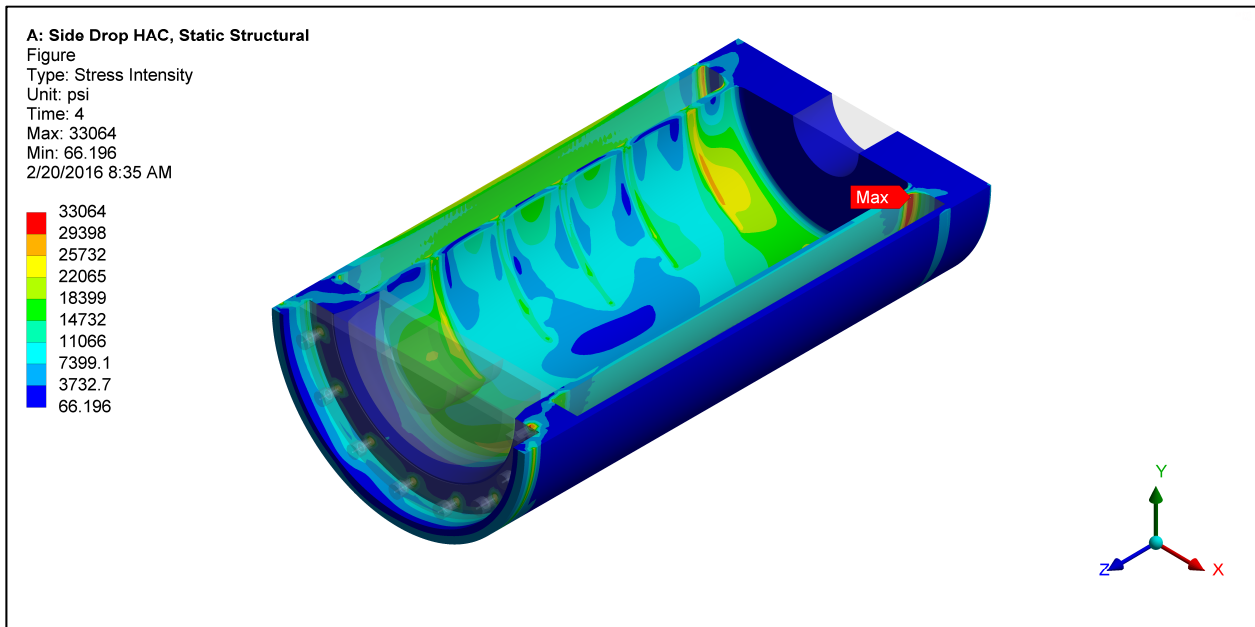


Figure 2.7.1-5. HAC Side Drop Cask Body Stress Intensity (total stress psi)

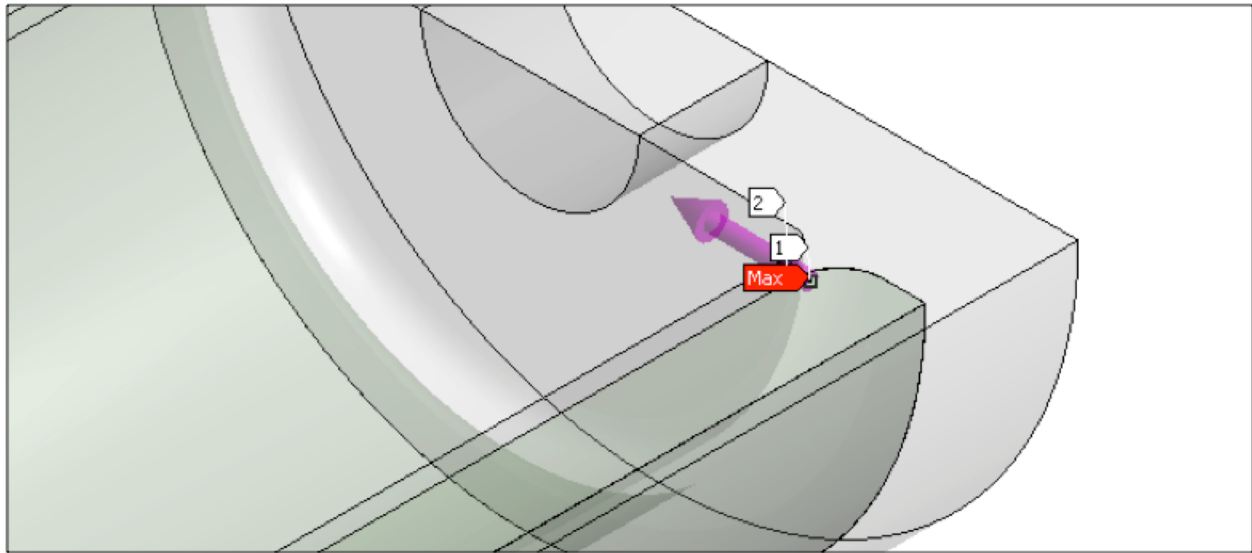


Figure 2.7.1-6. HAC Side Drop Linearized Stress Location (Section 8)

Table 2.7.1-6. HAC Side Drop Section 8 Stress Results (psi)

Stress State	Location	S1	S2	S3	SINT
MEMBRANE (P_m)	—	7919	3810	-536	8455
BENDING (P_b)	Inside	22400	7025	1106	21300
	Center	0	0	0	0
	Outside	-1106	-7025	-22400	21300
MEMBRANE + BENDING	Inside	29540	10850	1339	28200
	Center	7919	3810	-536	8455
	Outside	-98	-3191	-16050	15950
PEAK	Inside	4194	930	-743	4937
	Center	335	-133	-962	1297
	Outside	1120	-76	-1042	2162
TOTAL	Inside	33700	11780	633	33060
	Center	6962	3673	-204	7167
	Outside	175	-3267	-16250	16420

Table 2.7.1-7. HAC Side Drop Section 8 Stress Results (psi)

Stress Component	Stress Combination	Stress Intensity	Allowable	Margin of Safety
P_m	8455	19300	46320	4.5
$P_m + P_b$	28200	19300	69480	1.5

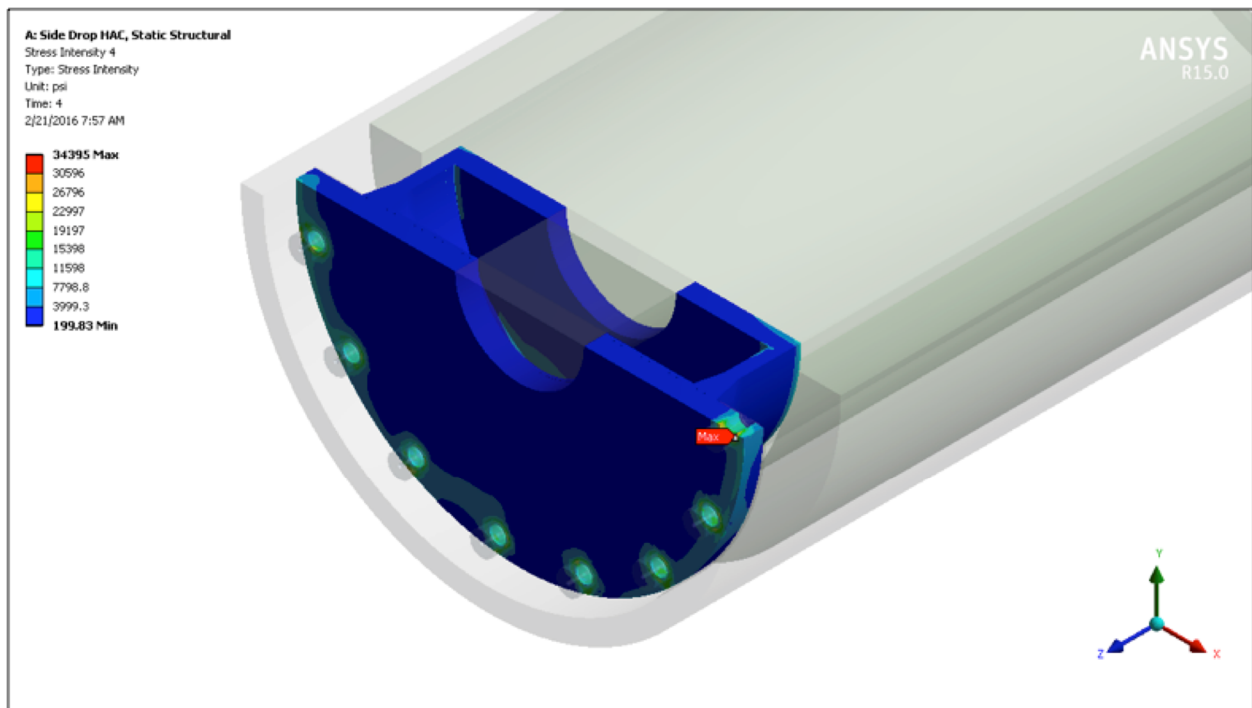


Figure 2.7.1-7. HAC Side Drop Lid Stress Intensity (total stress psi)

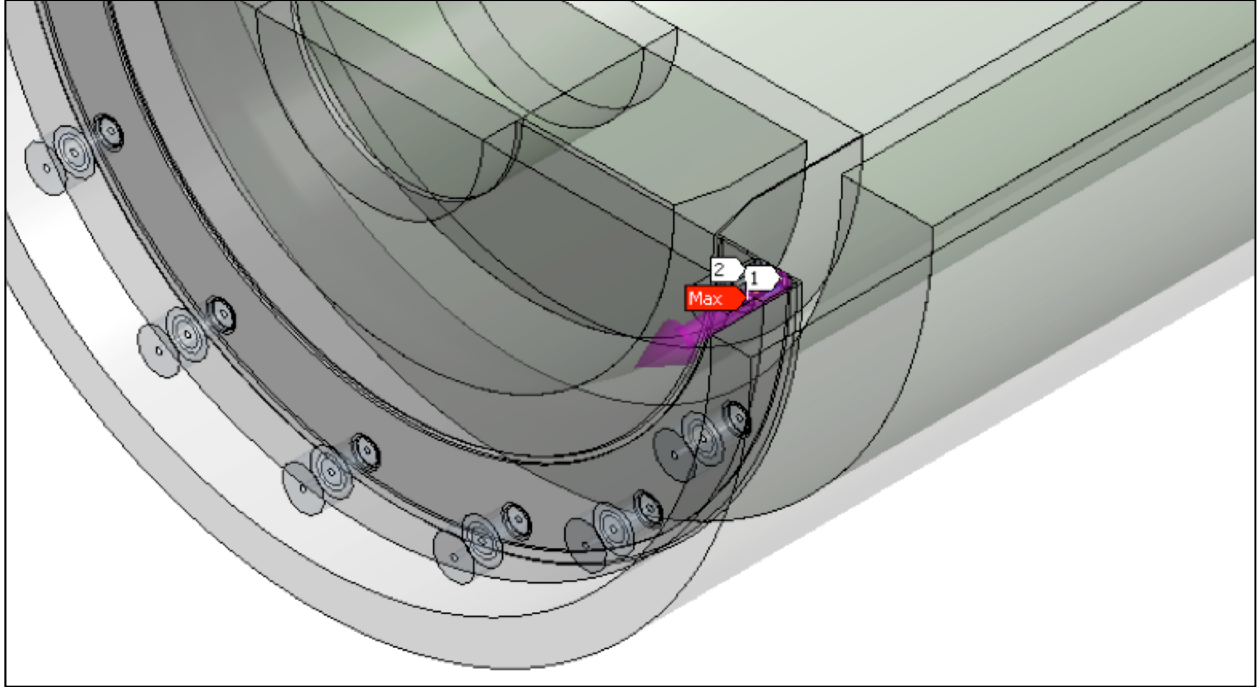


Figure 2.7.1-8. HAC Side Drop Linearized Stress Location (Section 9)

Table 2.7.1-8. HAC Side Drop Section 9 Stress Results (psi)

Stress State	Location	S1	S2	S3	SINT
MEMBRANE (P_m)	—	191	-4176	-17400	17590
BENDING (P_b)	Inside	13120	4683	-811	13930
	Center	0	0	0	0
	Outside	811	-4683	-13120	13930
MEMBRANE + BENDING	Inside	1165	-624	-4936	6102
	Center	191	-4176	-17400	17590
	Outside	993	-9012	-30360	31350
PEAK	Inside	945	-4458	-6602	7547
	Center	4003	2423	215	3787
	Outside	1120	-3506	-6124	7244
TOTAL	Inside	379	-4426	-10460	10840
	Center	1337	-1978	-14100	15440
	Outside	1005	-14500	-33390	34400

Table 2.7.1-9. HAC Side Drop Section 9 Stress Results (psi)

Stress Component	Stress Combination	Stress Intensity	Allowable	Margin of Safety
P_m	17590	19300	46320	1.6
$P_m + P_b$	31350	19300	69480	1.2

2.7.1.1.3. Corner Drop

In accordance with the requirements of 10 CFR 71.73(c)(1), the Model 2000 cask is structurally evaluated for the hypothetical accident 30-foot corner drop condition. The impact analysis presented in Section 2.12.1 and the summary of accelerations provided in Table 2.7.1-1 shows that the end and side drop accelerations bound the C.G. over corner drop acceleration. Therefore, the corner drop requirement is satisfied.

2.7.1.1.4. Oblique Drops

In accordance with the requirements of 10 CFR 71.73(c)(1), the Model 2000 cask is structurally evaluated for the hypothetical accident 30-foot oblique drop condition. The impact analysis presented in Section 2.12.1 and the summary of accelerations provided in Table 2.7.1-1 shows that the end and side drop accelerations bound the slap-down/oblique angle drops. Therefore, the oblique drop requirement is satisfied.

2.7.1.2. HPI Stress Analysis

The purpose of this section is to document the Model 2000 HPI and material basket analyses that shows the design meets the requirements of 10 CFR 71. Specifically, the evaluation addresses the mechanical loads associated with the HAC.

The results of the analyses for various load cases are presented pictorially as stress intensity contour plots as well as in table form, with the corresponding margin of safety in each component of the cask body.

2.7.1.2.1. End Drop

The HPI is evaluated using the ANSYS finite element model presented in Section 2.6.7. Stress results for the HAC end drop discussed previously are documented in Table 2.7.1-10. The table presents the primary membrane (P_m) and primary membrane plus primary bending (P_m+P_b) in accordance with the criteria presented in ASME Section III, Appendix F (Reference 2-18).

As shown in Table 2.7.1-10, the margins of safety when compared to the stress intensity for each category are positive. The most critically stressed component in the system is the interface between the [[]] that surrounds and supports the depleted uranium shield. The minimum margin of safety is +8.0 for primary membrane stress intensity. The locations of the critical sections correspond to the maximum stress location and axial displacement is shown in Figure 2.7.1-9.

[[

]]

Figure 2.7.1-9. HPI HAC End Drop Results – Peak Stress Intensity (psi) and Displacement (in)

Table 2.7.1-10. HAC End Drop Stress Summary

[[.....]]
.....
]]

2.7.1.2.2. Side Drop

The HPI is evaluated using the ANSYS finite element model presented in Section 2.6.7. Table 2.7.1-1 provides a summary of the HAC accelerations predicted by the LS-DYNA analysis presented in Section 2.12.1. As with the NCT evaluation, two cases are presented to evaluate the performance of the HPI during the side drop. Case 1 is concentrated pressure distribution at the four [[.....]] locations (“line load”). Case 2 is a uniform pressure distribution (“area load”).

Stress results for Case 1 are presented in Tables 2.7.1-11 and 2.7.1-12. Stress results for Case 2 are presented in Table 2.7.1-13 and 2.7.1-14. Figures 2.7.1-10 and 2.7.1-11 illustrate the stresses in the support disk for Case 1 and Case 2, respectively. The tables present the primary membrane (P_m) and primary membrane plus primary bending (P_m+P_b) in accordance with the criteria presented in ASME Section III, Appendix F (Reference 2-18).

As Tables 2.7.1-11 through 2.1.7-14 show, the margins of safety for the HPI body and support disk when compared to the stress intensity for each category are positive. The minimum margin of safety in the HPI body is found to be +0.8 for primary membrane plus bending stress intensity for both Cases 1 and 2.

[[

]]

Figure 2.7.1-10. Case 1, HAC, Stress Intensity Result (psi)

Table 2.7.1-12. HAC Support Disk Case 1 Results

[[

]]

[[

Figure 2.7.1-11. Case 2, HAC, Stress Intensity Result (psi)

Table 2.7.1-14. HAC Support Disk Case 2 Results

[[.....

]]

|

]]

2.7.1.2.3. Corner Drop

Results of the LS-DYNA analysis presented in Section 2.12.1 shows that the side drop accelerations bound the corner drop.

2.7.1.2.4. Oblique Drops

Results of the LS-DYNA analysis presented in Section 2.12.1 shows that the side drop accelerations bound the oblique drop angles.

2.7.1.2.5. Cask Overpack Bolt Evaluation

Bolt Torque

Per Model 2000 cask overpack drawings 1018719 and 105E9521 (Table 1.3.-1), the overpack bolt torque is 100±5 lb-ft dry. The following overpack evaluation assumes a maximum torque of 105 lb-ft.

Bolt Evaluation Procedure

This analysis is based on the procedure outlined in NEDE-31581, Subsection 2.10.7, which was developed to account for the overpack fastener failure during the quarter-scale model side drop test. Once the procedure was satisfactorily developed to explain the fastener failure, it was used to redesign the fastening system. This section presents the steps and results of this analysis as applied to the Model 2000 with the HPI.

Bolt Stresses – HAC Side Drop

The Model 2000 transport package overpack is fastened together with 15 equally spaced ASTM A-540 Grade B22, Class 3 or equivalent 7/8-9 UNC socket head shoulder bolts. The adequacy of these fasteners is determined by comparing the service loads (from the HAC) to the allowable loads, using the criteria given in the ASME Code, Section III, Division 1, Appendix F.

Bolts: 7/8-9 UNC-2A, ASTM A540 Grade B22, Class 3, 15 equally spaced

Tensile area of threaded portion = 0.462 in²

Proof Strength = Minimum Yield Strength x 85% = 115700 (0.85) = 98345 psi

Loading: The highest stresses for the overpack fasteners occur during the HAC side drop accident condition. The maximum load is calculated for an impact acceleration of 161.9 g's.

For the side drop case, the load is applied to the overpack junction as shown in Figure 2.7.1-12. The overpack is modeled as a simple beam with the force of the cask and contents as a distributed load and the neutral axis at the side of the overpack opposite the side of impact.

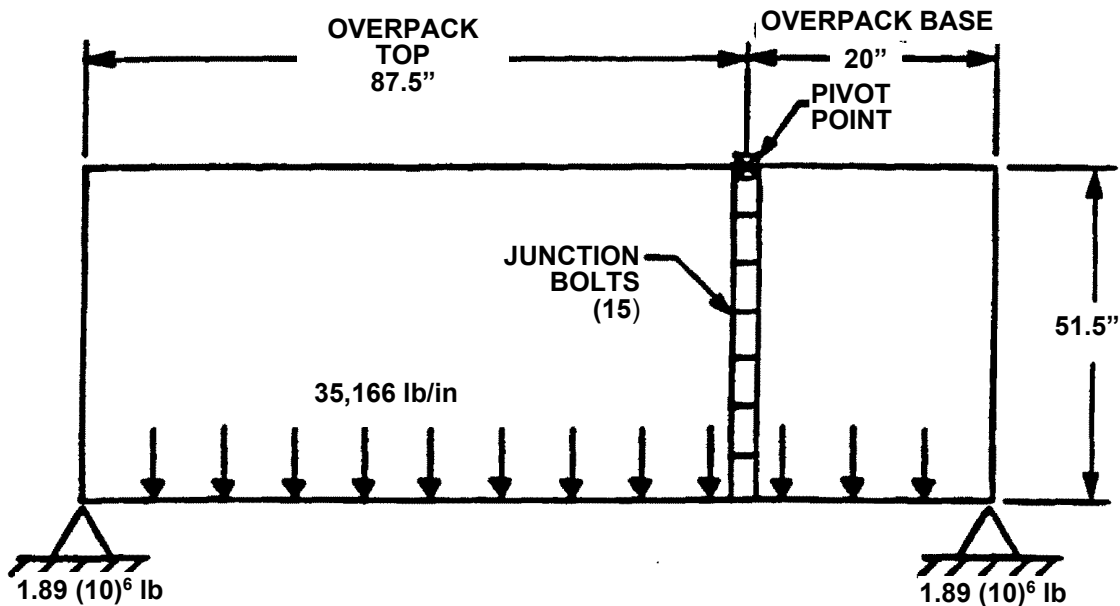


Figure 2.7.1-12. Overpack Loading, HAC Side Drop

The distributed load equals the weight of the cask (cask body and closure lid) and contents (HPI assembly + material basket + content) times the acceleration, divided by the length between toroidal reaction points:

$$\text{Distributed Load} = WG/L = 35,166 \text{ lb/in}$$

Where:

$$W = (16,000 + 1,900) + [\quad] = 23,350 \text{ lb}$$

$$G = 161.9 \text{ g} \quad \text{HAC Side Drop Cold}$$

$$L = \text{Overpack vertical length} - \text{toroid diameter} \\ = 131.50 - 24 = 107.5 \text{ in}$$

The total load to be reacted is:

$$F_T = WG = 3.780(10)^6 \text{ lb}$$

The force at each reaction point is:

$$F_R = 0.5F_T = 1.890(10)^6 \text{ lb}$$

Figure 2.7.1-13 shows a free body diagram of the overpack top. The distributed load from the cask is applied as a point load so that the moments can be calculated and the bolt loads determined.

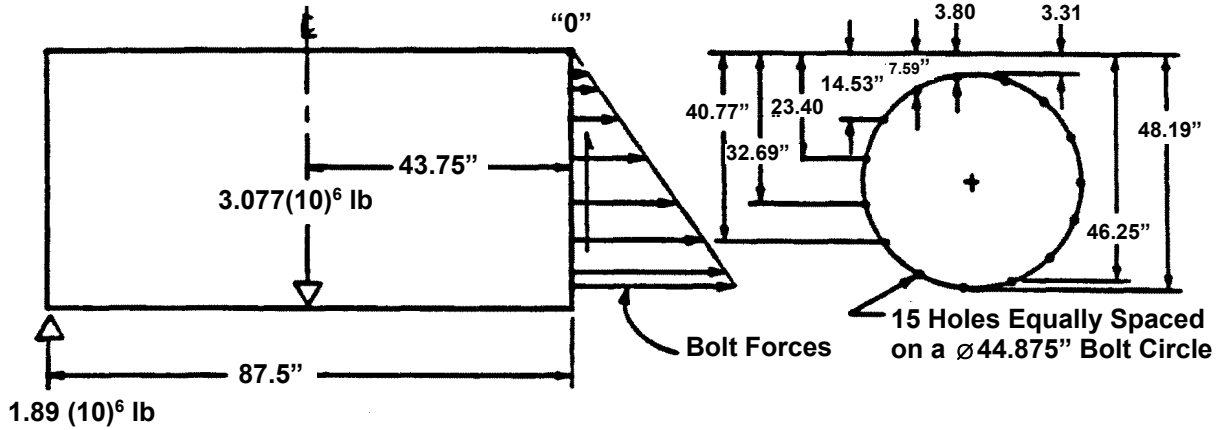


Figure 2.7.1-13. Free Body Diagram of Overpack Top

Summing the moments about the pivot point "0" yields the following equation:

$$\begin{aligned} \Sigma M_0 = 0 = & -1.89(10)^6 (87.5) + 3.077(10)^6 (43.75) + k (48.19)^2 + \\ & 2k (46.25)^2 + 2k (40.77)^2 + 2k (32.69)^2 + 2k (23.40)^2 + \\ & 2k (14.53)^2 + 2k (7.59)^2 + 2k (3.80)^2 \end{aligned}$$

Solving for k yields:

$$\begin{aligned} k = & 3.0756(10)^7 / [48.19^2 + 2(46.25^2 + 40.77^2 + 32.69^2 + 23.40^2 + 14.53^2 + 7.59^2 + 3.80^2)] \\ k = & 2,241 \text{ lb/in} \end{aligned}$$

The maximum shear force on a bolt occurs at the point farthest from the pivot point, so the maximum bolt load is:

$$F_{S \text{ Max}} = (2,241) 48.19 = 10,7994 \text{ lb}$$

Because the bolts are loaded in double shear on the shoulder (see Figure 2.7.1-14), the maximum shear stress in the bolt material is:

$$\tau_{\text{Max}} = F_{S \text{ Max}} / (2A_s) = 36,362 \text{ psi}$$

where:

$$A_s = \text{Area of bolt shoulder} = 0.25\pi D_s^2 = 1.485 \text{ in}^2$$

$$D_s = \text{Diameter of bolt shoulder} = 1.375 \text{ in}$$

The allowable shear stress in the bolt for HAC conditions is $0.42S_U$.

where:

$$S_U = \text{Ultimate strength for the bolts} = 14,5000 \text{ psi}$$

$$\tau_{\text{All}} = 0.42S_U = 60900 \text{ psi} > \tau_{\text{Max}} = 36,362 \text{ psi}$$

$$MS = (.42S_U / \tau_{\text{Max}}) - 1 = 0.67$$

The results indicate that the cask overpack bolts are sufficient for HAC side drop loading.

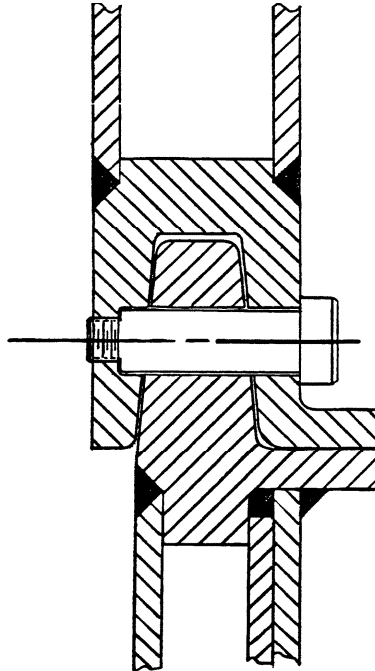


Figure 2.7.1-14. Overpack Junction

2.7.1.3. Material Basket Evaluation

This section evaluates the material basket for HAC. Factors of safety for the basket are calculated based on the criteria for Service Level ‘D’ limits from ASME Section III, Appendix F (F-1332).

HAC End Drop

The worst-case condition of upright end drop is evaluated. The inertial loading will load the [] in compression. There is no bending or shear stress present. For this evaluation, all 18 [] are loaded. The compression stress on the bottom of the [] is:

$$\sigma_{\text{membrane}} = \frac{P}{A} = 8,505.5 \text{ psi compression}$$

$$\sigma_{\text{bending}} = 0 \text{ psi}$$

$$\tau_{\text{shear}} = 0 \text{ psi}$$

where $P = W \times G = [] \text{ lbs}$ Inertial load on 18 [] sections

$W = [] \text{ lbs}$ Basket plus contents weight

$G = 157.5 \text{ G}$ HAC end drop acceleration (Table 2.7.1-1)

$A = []$ Cross section area of [] x 1.5)

Per Table 2.1-2, except for pinned and bolted joints, the bearing stress margin of safety need not be evaluated for which Level D service limits are specified.

The basket elastic stability is evaluated at HAC end drop conditions. The basket [[]] are modeled as a column with pinned ends. The bottom third of the 18 [[]] bundle is located between the HPI bottom and the material package center of gravity and is therefore evaluated using the Euler equation for buckling of a column with pinned ends:

$$P_{cr} = \frac{\pi^2 EI_{cc}}{L^2} = 5.553 \times 10^7 \text{ lbs}$$

where $E = 24.1 \times 10^6$ psi

Modulus of 316 stainless steel, 800°F
 (Table 2.2-2)

$L =$ [[]]

Length of lower 3rd of basket between [[]]
 (Drawing 001N1824)

$I_{cc} = 51.76 \text{ in}^4$

Moment of inertia (18 [[]])

For the HAC end drop elastic stability evaluation, the moment of inertia for the 18 [[]] is determined from Table 2.6.7-18, as follows:

[[]]	[]	[]
]]

Comparing the critical load to the load applied to the 18-[[]] basket during the HAC end drop, the factor of safety is:

$$FS = \frac{P_{cr}}{P} = \frac{5.553 \times 10^7}{49927.5} = +1112.2$$

HAC Side Drop

Assuming one-third of the inertial load is carried by one of the segments, the bending stress in the basket is:

$$\sigma_b = \frac{Mc}{I_{cc}} = 2022.7 \text{ psi}$$

where	P = W × G = [[]]	lb	Load on [[]]	section
	W = [[]]	lb	Bounding basket weight	
	G = 161.9 g		HAC side drop acceleration	
	M = $\frac{W_a \times l^2}{12}$ = 21227.5 lb-in		Bending moment	
	l = [[]]		Length of beam section	
	W _a = 1148.92 lb/in		Uniformly distributed load	
	c = 3.73 in		Neutral axis to outer fiber	
	I _{cc} = 39.09 in ⁴		Moment of inertia [[]]]]

The moment of inertia calculation is shown in Table 2.7.1-15.

Table 2.7.1-15. Moment of Inertia Calculation

[[

]]

The pure shear stress, ASME Appendix F (F-1332.4), which develops across the section during the side drop is

$$\tau = \frac{P}{2A} \approx 2188.5 \text{ psi} < 0.42S_u = 0.42 \times 70800 = 29736 \text{ psi}$$

where

P	= 17107.4 lb	
A	= 3.91 in ²	Cross-sectional area (12 [[]])
d _o	= [[] in	Outside diameter of [[]]
d _i	= [[] in	Inside diameter of [[]]

The stress intensity in the basket that results from the combination of the bending and shear stresses is

$$\sigma = \sqrt{\sigma_b^2 + 4\tau^2} = 4821.8 \text{ psi}$$

The margin of safety is per ASME Appendix F (F-1332) is

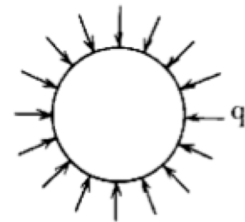
$$MS = \frac{1.5 \times (1.5S_m)}{\sigma} - 1 = \frac{35775}{4821.8} - 1 = +6.4$$

[[]] hold the basket together using [[]] (ASME III-NF, Class 1). The [[]] are equivalent in thickness and strength to the adjoining [[]]. Therefore, the previous analysis bounds the stresses generated in the [[]].

Because the [[]] form a composite section with the addition of [[]] is distributed along the face of the disk. Therefore, [[]] wall permanent deformation is unlikely to occur. However, assuming the basket [[]] are unsupported and uniformly loaded, a lateral external pressure load may be applied along the length of the [[]]. Treating the [[]] as a thin shell, the elastic stability can be evaluated during HAC side drop event. From Roark's, Table 15.2, Case 19 (Reference 2-19), the elastic stability of a single basket [[]] is evaluated by applying the total payload weight times the side drop acceleration that is then applied as an exterior pressure load, q. The critical external pressure, q', is:

$$q' = \frac{1}{4} \frac{E}{1-\nu^2} \frac{t^3}{r^3} = 3180 \text{ psi}$$

E	= 24.1 × 10 ⁶ psi	Modulus at 800°F
v	= 0.3	Poisson's ratio
t	= [[] in	Wall thickness
r	= [[] in	[[]] outside radius



Applying the total contents weight during the HAC side drop to a single [[]], the external pressure is:

$$q = \frac{P}{A} = 208.5 \text{ psi}$$

$G = 161.9 \text{ g}$		Side drop acceleration
$W = [[] \text{ lb}$		Bounding loaded basket weight
$P = W \times G = 51322.3 \text{ lb}$		Total load
$l = [[] \text{ in}$		Basket length
$A = 2\pi r l = 246.1 \text{ in}^2$		Surface area of single [[]]

Comparing the critical external pressure to the external pressure applied to a single [[]] during the HAC side drop event, the factor of safety is:

$$FS = \frac{q_c}{q} = 15.2$$

Therefore, unsupported basket [[]] sections will not collapse during HAC side drop conditions and the Subsection NF, Level A stress acceptance criteria still applies.

2.7.1.4. Summary of Results

Structural analyses are performed for the Model 2000 cask, HPI and material basket for hypothetical accident conditions free drop conditions. To evaluate the Model 2000 Transport Package, ANSYS finite element models and classic calculations are used to analyze the governing drop cases. All structural members have a positive margin of safety under worst case loading conditions. It is concluded that the Model 2000 Transport Package is structurally adequate for the HAC free drop conditions. Therefore, the requirements of 10 CFR 71.73(c)(1) have been satisfied.

2.7.2. Crush

In accordance with the requirements of 10 CFR 71.73(c)(2), the Model 2000 Transport Package is to be subjected to a dynamic crush test by evaluating the package on essentially unyielding horizontal surface so as to suffer maximum damage by the drop of an 1,100 pound mass from 30 feet onto the package. The mass must consist of a solid mild steel plate 40 inches × 40 inches and must fall in a horizontal attitude. The crush test is required only when the specimen has a mass not greater than 1,100 pounds, and overall density not greater than 1000 kg/m³ (62.4 lb/ft³) based on external dimension. The crush condition is not applicable because the Model 2000 Transport Package weighs more than 500 kg (1,100 lb.) and overall density is greater than 62.4 lb/ft³.

2.7.3. Puncture

This section addresses the second event in the accident design sequence outlined in 10 CFR 71.73(c)(3), the 40-inch drop of the Model 2000 Transport Package onto a mild steel cylindrical punch. The evaluation of this condition is conducted for the package structure and the containment vessel. The demonstration of the puncture capability of the package is presented in Section 2.12.1 to predict the accumulated damage in support of the thermal analysis. The

maximum strain in the outer shell of the cask is 31% and limited to the puncture area. Therefore, no gross deformations of the cask are predicted.

2.7.4. Thermal

The fire condition is analyzed in Section 3.4. In this section, maximum values of temperatures and pressures are provided.

2.7.4.1. Summary of Pressures and Temperatures

Table 2.7.1-16 provides summary temperatures for the Model 2000 Transport Package for HAC. During HAC, the average temperature of the cask fill gas (including the gas within the HPI) peaks at 585°F 11 hours after the end of the 30-minute fire. Using the ideal gas law, the cask internal pressure from gas expansion is 29.0 psia, which is less than the design pressure of 30 psia.

Table 2.7.1-16. Summary Temperatures for HAC

Item	Peak Temperature (°F)
Material basket	1,045
HPI shielding (side)	670
HPI shielding (top)	599
HPI shielding (bottom)	618
Cask lid seal	508
Cask shielding (side)	570
Cask shielding (top)	529
Cask shell, puncture location	782
Cask shell, opposite side to puncture location	512
Overpack outer shell, puncture location	1,103
Overpack outer shell, opposite side to puncture location	1,337
Cask drain port (bottom)	612
Cask test port (top)	608
Cask vent port (lid)	520
HPI fill gas (average)	740
Cask fill gas (average)	571
HPI and cask fill gas, combined (average)	585

(Note: Data taken from Table 3.4.3-1)

2.7.4.2. Differential Thermal Expansion

Differential thermal expansion resulting from the fire transient has minimal consequence to the Model 2000 Transport Package. All stresses are classified ASME Section III Subsection NB as secondary displacement-limited stresses. Heat conditions that bound both NCT and HAC are presented in Section 2.6.7, which evaluates the thermal expansion of the Model 2000 cask by applying a temperature differential 300°F from the outside surface to the inside surface of the cask. Thermal expansion of the closure bolts are evaluated using the temperatures associated with the HAC fire in Section 2.12.4.

2.7.4.3. Stress Calculations

In accordance with the requirements of 10 CFR 71.73(c)(4), the Model 2000 Transport Package is structurally evaluated when subjected to the design pressure of 30 psia. The design pressure is applied in combination with the mechanical loads defined in Section 2.7.1. To obtain stress results, a uniform internal pressure of 30 psia is applied to the ANSYS finite element in combination with the mechanical loading conditions of Section 2.7.1.

2.7.4.4. Comparison with Allowable Stresses

The combined HAC pressure and mechanical stresses are presented in Table 2.7.4-1, which documents the primary membrane (P_m), primary membrane and plus primary bending (P_m+P_b) stresses in accordance with the criteria presented in Regulatory Guide 7.6. As Table 2.7.4-1 shows, the margins of safety are positive when the allowable is compared to the stress intensity for each category. Therefore, the requirement of 10 CFR 71.73(c)(4) is satisfied.

Table 2.7.4-1. Summary of HAC Stress Results

Case	Component	Stress Component	Stress Combination	Stress Intensity	Allowable	Margin of Safety
End Drop	Cask body	P_m	10140	20000	48000	+3.7
		$P_m + P_b$	25830	20000	72000	+1.8
	Cask Lid	P_m	19830	20000	48000	+1.4
		$P_m + P_b$	40720	20000	72000	+0.8
Side Drop	Cask body	P_m	8455	19300	46320	+4.5
		$P_m + P_b$	28200	19300	69480	+1.5
	Cask Lid	P_m	17590	19300	46320	+1.6
		$P_m + P_b$	31350	19300	69480	+1.2

2.7.5. Immersion - Fissile Material

The Model 2000 Transport Package is not licensed for the transport of fissile material. See Chapter 1 for further discussion.

2.7.6. Immersion - All Packages

According to the requirements of 10 CFR 71.73(c)(6), a package must be subjected to water pressure equivalent to immersion under a head of water of at least 15 meters (50 feet) for a period of 8 hours, which is equivalent to 21.7 psig. The cask closure including the lid and bolts are designed to survive puncture loads, which exceed the load experienced during immersion (Sections 2.12.1 and 2.12.4). From ASME Section III-NB, A-2221, when subjected to 21.7 psig the 1.0-inch thick outer shell of the cask with a mean radius of 18.75 inches, produces a primary membrane stress intensity 418 psi that is much less than the material yield strength. Therefore, the Model 2000 Transport Package satisfies all of the immersion requirements for a package that is used for the international shipment of radioactive materials.

2.7.7. Deep Water Immersion Test (for Type B Packages Containing More than 10^5 A₂)

The contents specified in this application is less than 10^5 A₂. Therefore, this is not applicable for the Model 2000 Transport Package with HPI and material basket.

2.7.8. Summary of Damage

The analytical results reported in Sections 2.7.1 through 2.7.7 indicate that the damage incurred by the Model 2000 Transport Package during the hypothetical accident is minimal, and such damage does not diminish the cask ability to maintain the containment boundary. A 30-foot side drop followed by the 40-inch pin puncture accident may damage the overpack and inflict local damage on the outer shell of the cask. However, the shielding remains intact and satisfies the accident shielding criteria. Additionally, the HPI and material baskets maintain structural integrity during all postulated HAC events, which supports the criticality analysis assumptions. Based on the analyses of Sections 2.7.1 through 2.7.7, the Model 2000 Transport Package fulfills the structural and shielding requirements of 10 CFR 71.73 for all of the hypothetical accident conditions.

2.8 Accident Conditions for Air Transport of Plutonium

This section does not apply for the Model 2000 Transport Package with HPI and material basket.

2.9 Accident Conditions for Fissile Material Packages for Air Transport

This section does not apply for the Model 2000 Transport Package with HPI and material basket.

2.10 Special Form

Special form capsules specifically designed for carrying isotope source materials are permitted in the Model 2000 Transport Package. Each special form capsule shall show compliance with the requirements of 10 CFR 71.75 when subjected to the applicable test conditions of 10 CFR 71.77 and independently certified. Special form capsules are not a requirement of this application, because containment is provided by the cask.

2.11 Fuel Rods

This section does not apply for the Model 2000 Transport Package, because containment is provided by the cask.

2.12 Appendix

2.12.1. LS-DYNA Evaluation of the Model 2000 Transport Package

This section summarizes the results of impact evaluation of the Model 2000 Transport Package during NCT of 10 CFR 71.71 and HAC of 10 CFR 71.73 (Reference 2-1) and supplements the test data documented in Section 2.12.5. The primary purpose of this section is to report accelerations for the HPI cask contents and provide realistic damage predictions for the thermal evaluation presented in Chapter 3.

2.12.1.1. Introduction

The NCT and HAC impact analyses presented in this section evaluate the performance of the Model 2000 Transport Package using LS-DYNA Version 971 finite element code (Reference 2-20). Benchmarks of the analysis methodology are first performed using 3-drop orientations to compare with the actual drop tests of a quarter-scale model (see Section 2.12.5). The benchmark results are presented in detail in Section 2.12.1.11.1 through Section 2.12.1.11.3 as Drop Cases 1 through 3, respectively. The benchmark performed confirmed that the LS-DYNA program and dynamic analysis methodology are conservative and bounding.

The accident conditions are conservatively simulated using material properties corresponding to temperatures ranging from -40°F to 300°F for stainless steel and 400°F for aluminum honeycomb. Also considered are variations of the payload weight that is up to 10% of the maximum weight. The overpack toroidal shell thickness is also varied between two thicknesses of 0.50 inches and 0.76 inches. The overall variations include the following configurations,

1. NCT and HAC (2 variations of initial velocities)
2. Hot and cold temperature conditions. (2 variations of material properties)
3. Payload weight of $\pm 10\%$ of the maximum weight. (3 variations of payload weights)
4. Two different toroidal shell thicknesses of 0.50 inches and 0.76 inches. (2 variations of shell thicknesses)
5. Four-drop orientations including two end drops, side drop, and C.G. over corner drops. (4 variations of drop geometries)

There are 96 ($=2 \times 2 \times 3 \times 2 \times 4$) possible drop configurations. Evaluating the bounding cases reduces the total number of drop configurations. This simplification resulted in performing nine (9) bounding drop configurations. The bounding drop configurations are designated as Drop Cases 4 through 12. The summary of results for the 9 bounding drop cases is presented in Table 2.12.1-1. The worst-case HAC accelerations occur during the cold/thick/light side drop and the hot/thin/heavy bottom end drop. For the bottom end drop, the acceleration trend showed that the accelerations dropped until the honeycomb temperature was increased to 400°F and the honeycomb fully compresses. Because the average temperature of the honeycomb is less than 350°F, the honeycomb has sufficient capacity to protect the package during hot conditions.

Two shallow angle drop simulations are also performed. The drop configurations include nominal payload at ambient temperature with thick toroidal shell thickness ($t=0.76$ inches) to compare with the side-drop test performed for the benchmarking test. The results for the two shallow angle drop cases are presented in Table 2.12.1-1. The two shallow angles are 5° and 10° slapdown drops that are designated as Drop Case 13 and 14. The results of shallow angle drops for the 0° (Drop Case 2, side drop), 5° (Drop Case 13) and 10° (Drop Case 14) conclude that the side drop bounds the shallow angle cases with an acceleration of 157 g.

Besides the 30-foot drop configurations, two HAC drop configurations (side drop and end drop) are selected to perform the code-required pin puncture test, where the cask is dropped 30 feet and then followed by a drop height of 40 inches onto a rigid pin 6 inches in diameter. The maximum strain in the cask outer shell is 31% and limited to the puncture location. No gross deformations of the cask are predicted and the structural integrity of the containment boundary is maintained. Additionally, results for the combined 30-foot impact and pin puncture are used as input for the HAC thermal evaluation.

NEDO-33866 Revision 2
Non-Proprietary Information – Class I (Public)

Table 2.12.1-1. Summary of Drop Cases and Results

Case No.	Description	Drop Angle degree	Drop Height (ft)	Shell thickness	Applicable Boundary Condition						Acceleration Results (g)
					Temperature			Payload			
					Amb	Hot	Cold	Normal	Heavy	light	
1	Benchmark HAC End Drop	90	30	Thick	X			X			130.0
2	Benchmark HAC Side Drop	0	30	Thick	X			X			157.0
3	Benchmark HAC Corner Drop	68 (=90-22)	30	Thick	X			X			73.8
4	NCT, Cold, End Drop	90	1	Thick			X			X	15.5
5	NCT, Cold, Side Drop	0	1	Thick			X			X	55.1
6	NCT, Cold, Corner Drop	68 (=90-22)	1	Thick			X			X	14.6
7	HAC, Cold, End Drop	90	30	Thick			X			X	129.8
8	HAC, Hot, End Drop	90	30	Thin		X			X		157.5
9	HAC, Cold, Side Drop	0	30	Thick			X			X	161.9
10	HAC, Hot, Side Drop	0	30	Thin		X			X		110.7
11	HAC, Cold, Corner Drop	68 (=90-22)	30	Thick			X			X	80.3
12	HAC, Hot, Corner Drop,	68 (=90-22)	30	Thin		X			X		52.8
13	HAC, Ambient, Slap down	5	30	Thick	X			X			114.4
14	HAC, Ambient, Slap down	10	30	Thick	X			X			118.0
15	HAC, Hot, End Drop + Puncture	90	30 ft + 40 in.	Thin		X			X		Same as Case No. 8
16	HAC, Hot, Side Drop + Puncture	0	30 ft + 40 in.	Thin		X			X		Same as Case No. 10

Multiple LS-DYNA dynamic finite element analyses are performed to determine the structural response of the Model 2000 cask during the impacts onto unyielding surface following NCT and HAC accident events. For each drop case the acceleration of the payload and inner containment enclosure is calculated. Three full 3D half-symmetry models are used to account for the asymmetry of the cask configuration. The three finite element models consist of the same node numbers, elements, material properties and control cards. The only differences are the nodal geometry and the direction of initial velocity. A representative finite element solid model is shown in Figure 2.12.1-1.

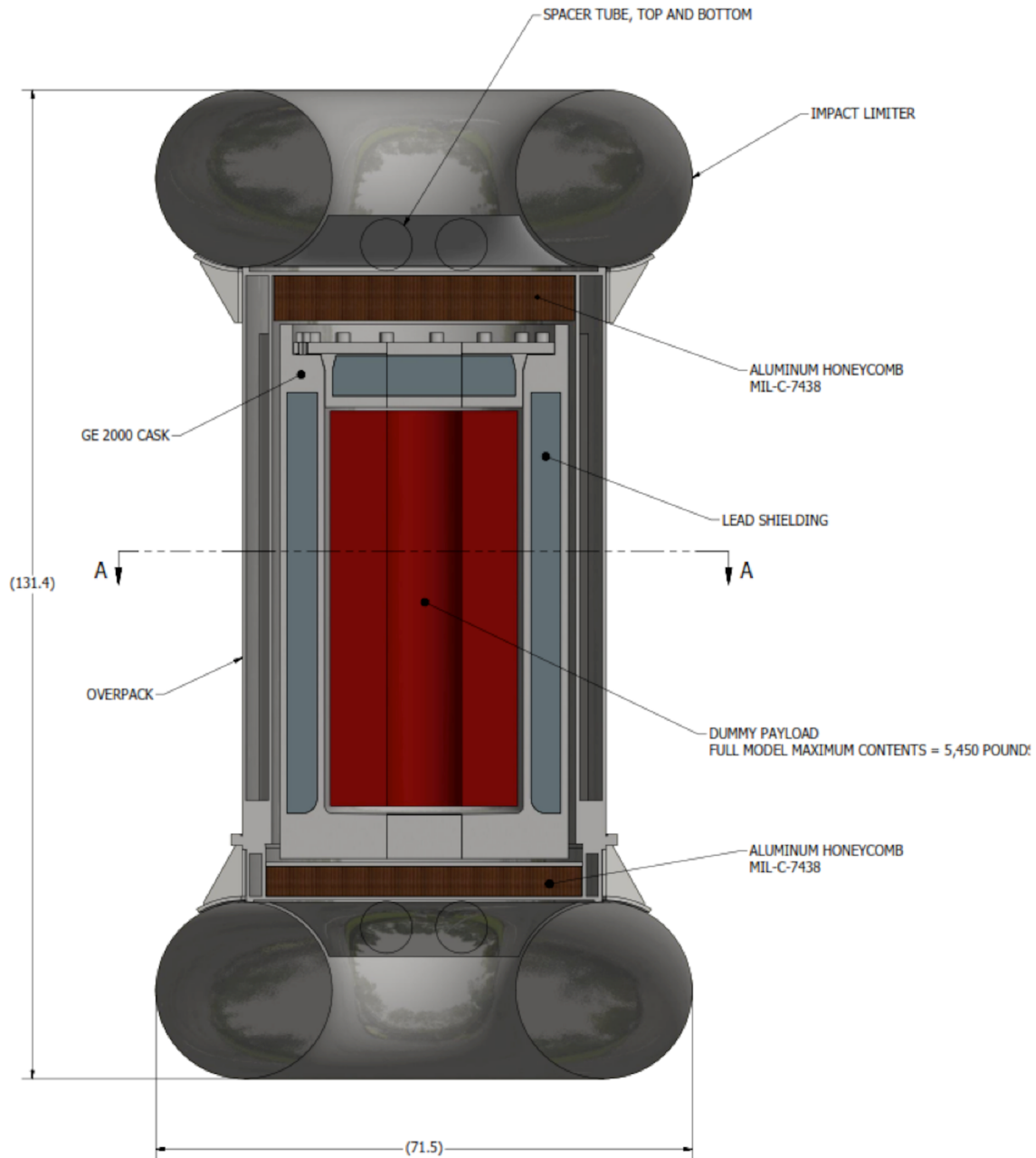


Figure 2.12.1-1. Model 2000 Solid Model

The three drop orientations are shown in Figure 2.12.1-2.

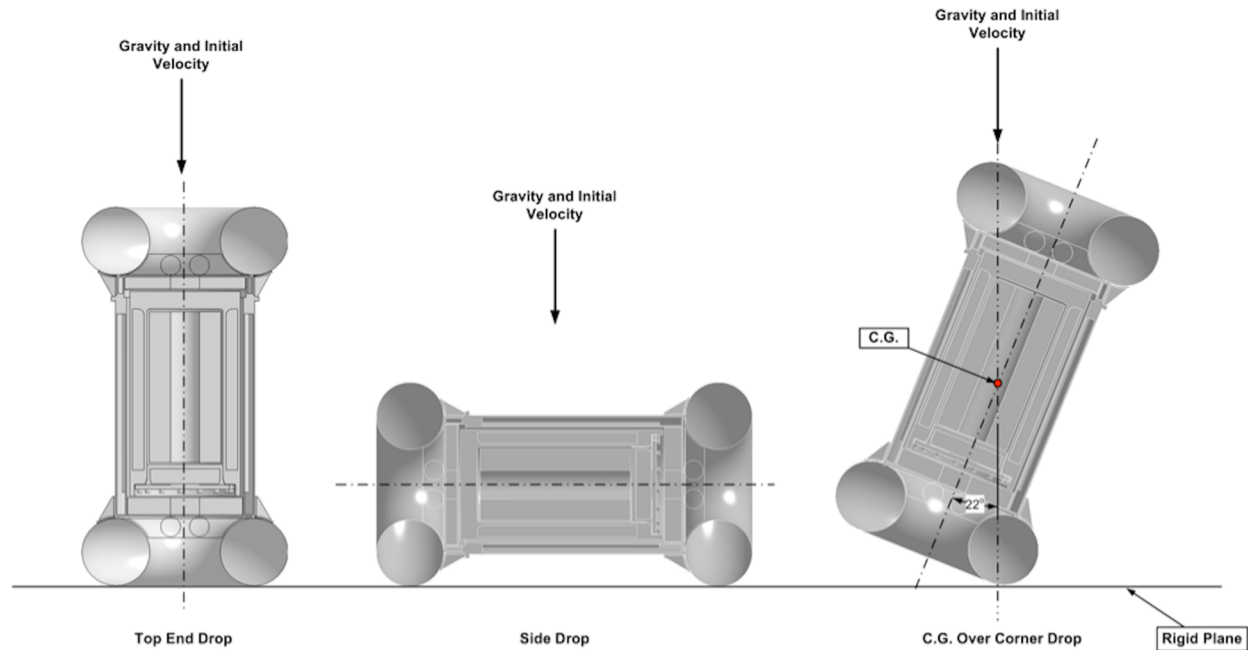


Figure 2.12.1-2. Drop Orientations

2.12.1.2. Benchmarking Runs

The selection of the drop cases is described in this section. Section 2.12.1.2.1 contains the benchmark results. Benchmarks of the analysis methodology are performed using the 3-drop orientations shown in Figure 2.12.1-2 to compare with the actual drop tests performed on a quarter-scale model. The benchmark runs are designated as Drop Cases 1 through 3. The actual drop tests were performed under at ambient temperature. The nominal payload weight is 5,450 pounds. The thickness in the toroidal shell is 0.76 inches. The drop height is 30 feet. The parameters of the benchmarking runs are listed in Table 2.12.1-2.

Table 2.12.1-2. Benchmark Runs and the Drop Parameters

Case No.	Description	Drop Angle degree	Drop Height, (ft)	Toroid Thickness (in)	Applicable Boundary Condition					
					Temperature			Payload		
					Amb.	Hot	Cold	Normal	Heavy	light
1	End Drop	90	30	0.76	X	—	—	X	—	—
2	Side Drop	0	30	0.76	X	—	—	X	—	—
3	C.G. Over Corner Drop	22	30	0.76	X	—	—	X	—	—

2.12.1.3. Normal Condition of Transport

The purpose of the drop simulation is to determine the peak acceleration of the payload and contents during the drop. The bounding acceleration occurs when the toroidal shell is thick so a stiffer response will result. At cold temperature, the material properties have greater elasticity and

yield strength, therefore results in a stiffer response. Finally, a lighter payload will result in lower total cask weight, which in turn causes greater acceleration during impact. The bounding three drops are simulated with thick toroidal shell, reduced-weight payload, and material properties at cold temperature. The drop cases are designated as Drop Case 4 through Drop Case 6, as listed in Table 2.12.1-3.

Table 2.12.1-3. Normal Condition of Transport Runs and the Drop Parameters

Case No.	Description	Drop Angle degree	Drop Height, (ft)	Shell Thickness (in)	Applicable Boundary Condition					
					Temperature			Payload		
					Amb.	Hot	Cold	Normal	Heavy	light
4	NCT Cold, End Drop	90	1.0	0.76	—	—	X	—	—	X
5	NCT Cold, Side Drop	0	1.0	0.76	—	—	X	—	—	X
6	NCT Cold, Corner Drop	68 (=90-22)	1.0	0.76	—	—	X	—	—	X

2.12.1.4. Hypothetical Accident Condition

The purpose of the drop simulation is to determine the peak acceleration of the payload and/or the maximum damage during the drop.

The bounding acceleration occurs when the toroidal shell is thick so a stiffer response will result. At cold temperatures, the material properties have greater elasticity and yield strength, which results in a stiffer response. Finally, a lighter payload will result in lowered total cask weight, which in turn causes greater acceleration during impact. The three drops with bounding accelerations are simulated with thick toroidal shell, reduced payload, and material properties at cold temperature. For the end drop, the maximum force on the closure lid bolts occurs when the container lid is oriented towards to the rigid plane. The drop cases are designated as Drop Cases 7, 9, and 11 for the end drop, side drop and C.G. over corner drop, respectively.

The maximum damage of the cask occurs when the toroidal shell is thin and has less structural strength. At warmer temperature, comparing with the material strength at ambient temperature, the material has lower elasticity and yield strength therefore resulted in greater damage to the cask. The heavier payload will also result in greater deformation of the toroidal shell. The drop cases with the bounding damage are designated as Drop Cases 8, 10, and 12 for the end drop, side drop and C.G. over corner drop, respectively. The six bounding drop cases for the HAC are listed in Table 2.12.1-4.

Table 2.12.1-4. Hypothetical Accident Condition of Transport Runs and the Drop Parameters

Case No.	Description	Drop Angle degree	Drop Height, (ft)	Shell Thickness (in)	Applicable Boundary Condition					
					Temperature			Payload		
					Amb.	Hot	Cold	Normal	Heavy	light
7	HAC, Cold, End Drop	90	30.0	0.76	—	—	X	—	—	X
8	HAC, Hot, End Drop	90	30.0	0.50	—	X	—	—	X	—
9	HAC, Cold, Side Drop	0	30.0	0.76	—	—	X	—	—	X
10	HAC, Hot, Side Drop	0	30.0	0.5	—	X	—	—	X	—
11	HAC, Cold, Corner Drop	68 (=90-22)	30.0	0.76	—	—	X	—	—	X
12	HAC, Hot, Corner Drop	68 (=90-22)	30.0	0.50	—	X	—	—	X	—

2.12.1.5. Shallow Angle Drops

Two shallow angle drops (5° and 10° from horizontal) with the drop configuration shown in Figure 2.12.1.5-1 are performed to compare the acceleration with the result of the side drop benchmark run. With the same material parameters as the benchmark run, the shallow angle drop parameters consist of the nominal payload weight, material properties at ambient temperature, and thick toroidal shell thickness. The drop cases are designated as Drop Cases 13 and 14 as listed in Table 2.12.1-5.

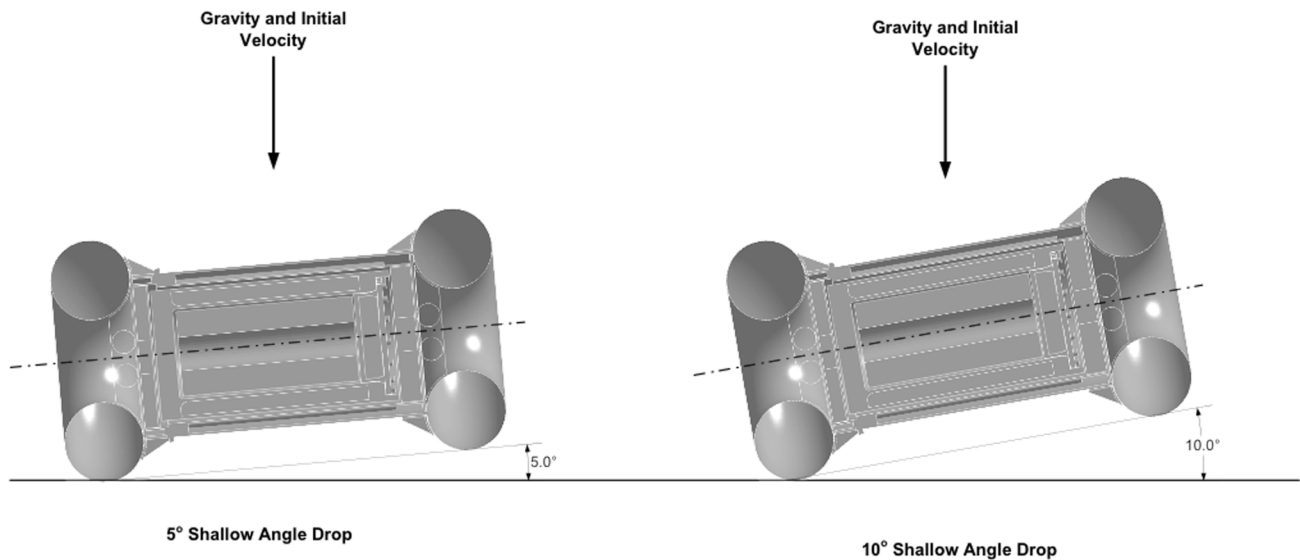


Figure 2.12.1.5-1. Shallow Angle Drops

Table 2.12.1-5. Shallow Angle Drop Runs and the Drop Parameters

Case No.	Description	Drop Angle degree	Drop Height, (ft)	Shell Thickness (in)	Applicable Boundary Condition					
					Temperature			Payload		
					Amb.	Hot	Cold	Normal	Heavy	light
13	HAC, Ambient, Slap Down	5	30.0	0.76	X	—	—	X	—	—
14	HAC, Ambient, Slap Down	10	30.0	0.76	X	—	—	X	—	—

2.12.1.6. Pin Puncture

10 CFR 71.73 requires that a free drop of the specimen through a distance of 1 meter (40 inches) in a position for which maximum damage is expected, onto the upper end of a solid, vertical, cylindrical, mild steel bar mounted on an essentially unyielding, horizontal surface. The bar must be 15 cm (6 inches) in diameter, with the top horizontal and its edge rounded to a radius of not more than 6 mm (0.25 inches), and of a length as to cause maximum damage to the package, but not less than 20 cm (8 inches) long. The long axis of the bar must be vertical.

To simulate the sequential drops, a rigid plane and a rigid pin 6 inches in diameter and 8 inches long are created, for the end drop and side drop respectively. During the pin puncture, the model is allowed to pass through the rigid plane; therefore, the puncture is independent of the pin length. Two-drop configurations are selected, that will be subjected to maximum damage. The drop configurations selected for the pin puncture drop are listed in Table 2.12.1-6. The drop cases are designated as Drop Cases 15 and 16 as listed in Table 2.12.1-6.

Table 2.12.1-6. HAC Drop Cases with Pin Puncture

Case No.	Description	Drop Angle degree	Drop Height (ft)	Pin Puncture Height in)	Shell Thickness (in)	Applicable Boundary Condition					
						Temperature			Payload		
						Amb.	Hot	Cold	Normal	Heavy	light
15	HAC, Hot, End Drop + Pin Puncture	90	30.0	40	0.50	—	X	—	—	X	—
16	HAC, Hot, Side Drop + Pin Puncture	0	30.0	40	0.50	—	X	—	—	X	—

2.12.1.7. Material Properties

2.12.1.7.1. 304 Stainless Steel

This material is used in the cask inner shell, over pack outer shell, gussets, and toroidal shell (impact limiter). The mechanical properties of the 304 SS at three different temperatures of interest in this calculation are tabulated in Table 2.12.1-7.

Table 2.12.1-7. Mechanical Properties of SS304 at Temperature of Interest

Temperature	-40°F	70°F	300°F
Ultimate Tensile Strength, ksi	75.0	75.0	66.2
Yield Strength, ksi	30.0	30.0	22.4
Modulus of Elasticity, E (10 ⁶ psi)	28.8	28.3	27.0
Poisson's Ratio	0.31	0.31	0.31
Density, lb/in ³	0.29	0.29	0.29

The stress strain curves for SS304, taken from References 2-7 and 2-21, and are presented in Tables 2.12.1-8 through 2.12.1-10. The graphical representations of the stress strain curves of the SS304 are displayed in Figures 2.12.1.7-1 through 2.12.1.7-3.

Table 2.12.1-8. Stress Strain Curve of SS304 at -40°F

Strain	Stress, psi
0.0020	27,000
0.0034	30,000
0.0074	34,868
0.0182	39,736
0.0395	44,604
0.0625	49,472
0.0816	54,340
0.0998	59,208
0.1189	64,076
0.1398	68,944
0.1624	73,812
0.1870	78,680
0.2134	83,548
0.2418	88,416
0.2722	93,284
0.3045	98,152
0.3389	103,020
0.3753	107,888
0.4137	112,755
0.4542	117,623
0.5542	117,623
0.6542	117,623
0.7542	117,623

Table 2.12.1-9. Stress Strain Curve of SS304 at Ambient Temperature

Strain	Stress, psi
0.0020	27,000
0.0035	30,000
0.0075	34,868
0.0183	39,736
0.0396	44,604
0.0626	49,472
0.0817	54,340
0.0999	59,208
0.1191	64,076
0.1399	68,944
0.1626	73,812
0.1871	78,680
0.2136	83,548
0.2420	88,416
0.2723	93,284
0.3047	98,152
0.3391	103,020
0.3755	107,888
0.4139	112,755
0.4544	117,623
0.5544	117,623
0.6544	117,623
0.7544	117,623

Table 2.12.1-10. Stress Strain Curve of SS304 at 300°F

Strain	Stress, psi
0.0022	22,500
0.0033	25,000
0.0076	29,477
0.0198	33,953
0.0431	38,430
0.0659	42,906
0.0849	47,383
0.1036	51,859
0.1236	56,336
0.1454	60,812
0.1691	65,289
0.1947	69,765
0.2223	74,242
0.2518	78,719
0.2832	83,195
0.3167	87,672
0.3522	92,148
0.3896	96,625
0.4291	101,101
0.4707	105,578
0.5707	105,578
0.6707	105,578

Stress Strain curve for SS304 per ASME VIII, Div 2, Annex 3.D

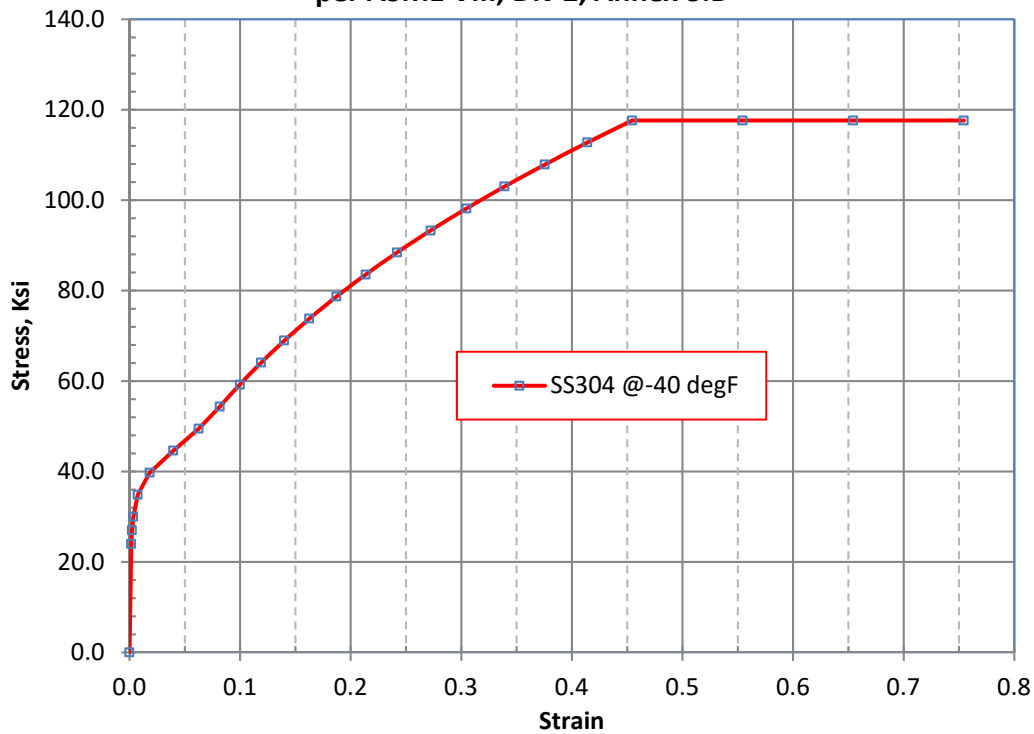


Figure 2.12.1.7-1. Stress-Strain Curve of SS304 at -40°F

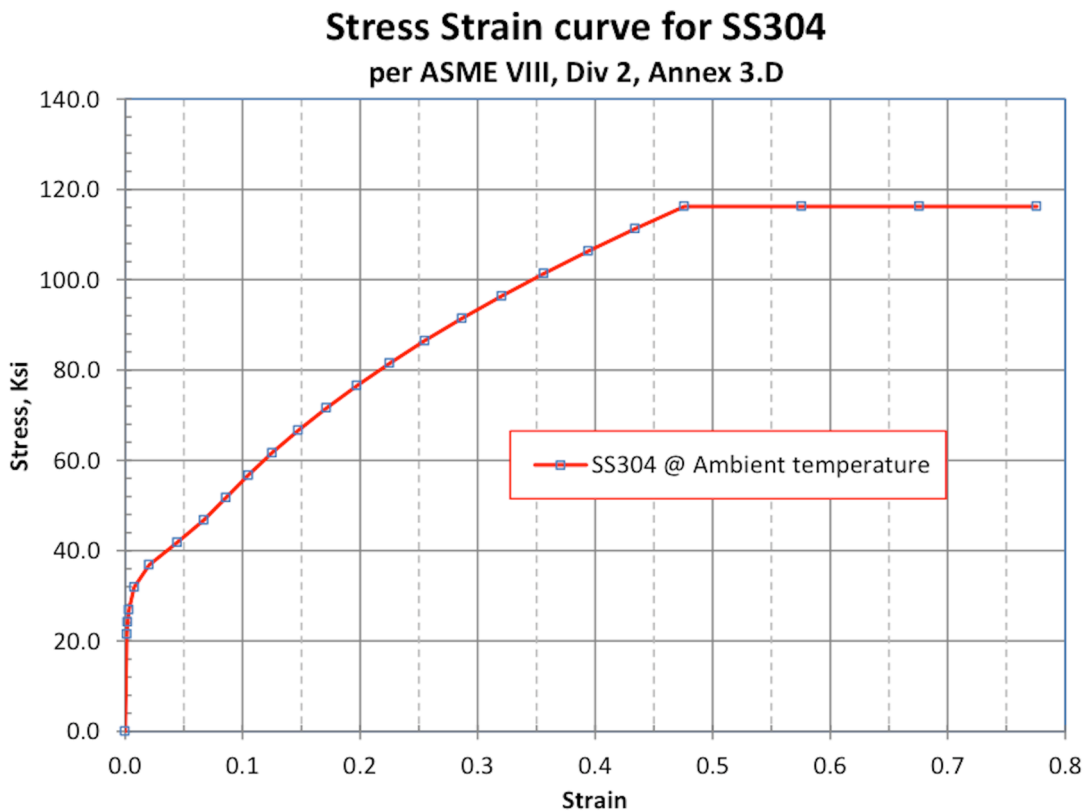


Figure 2.12.1.7-2. Stress-Strain Curve of SS304 at Ambient Temperature

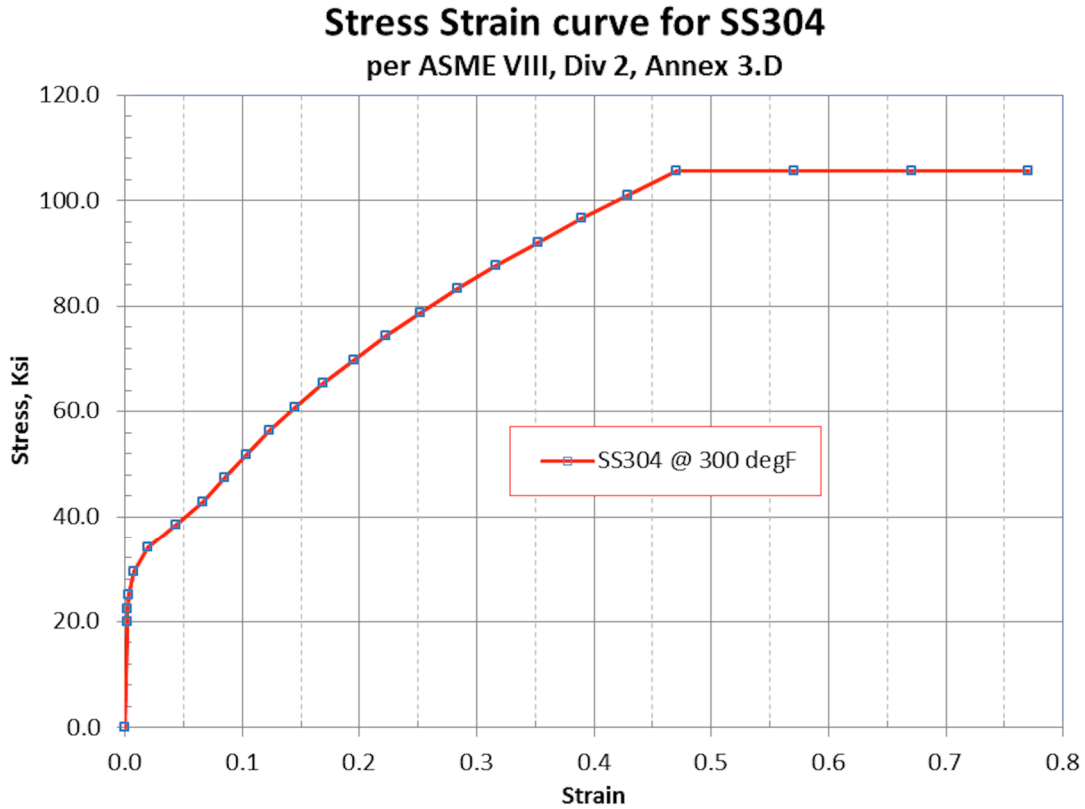


Figure 2.12.1.7-3. Stress-Strain Curve of SS304 at 300°F

2.12.1.7.2. Lead

Chemical lead is used in the cask as shielding material. The mechanical property of the chemical lead is presented in Table 2.12.1-11.

Table 2.12.1-11. Lead Temperature Dependent Properties

Temperature, (°F)	Modulus of Elasticity, $\times 10^6$ (psi)	Density (lb _m /in ³)	Yield Strength, (psi)
-40	2.58	0.41	795
75	2.41	0.41	620
100	2.38	0.41	580
150	2.30	0.41	550
300	2.04	0.41	390

2.12.1.7.3. Strain-Rate Sensitive Material Properties of SS304

The factors that elevate true stress-strain curves for SS304 at various strain rates and temperatures were generated by Reference 2-22 (pp. 84-87) and reproduced in Table 2.12.1-12.

Table 2.12.1-12. Strain-Rate Factors that elevated the Stress-Strain Curves of SS304

Strain Rate (in/in/sec)	-20°F	70°F	300°F	600°F
5	1.333	1.235	1.166	1.043
10	1.361	1.278	1.210	1.094
22	1.428	1.381	1.316	1.217
25	1.445	1.407	1.342	1.247

The data from the above table are used to generate the strain-rate multiplication factors for the current analyses at temperatures of -40°F, ambient temperature and 300°F.

2.12.1.7.4. Honeycomb Material Property

The crush strength of the honeycomb material is 750 psi. The material property at temperature of -20°F is assigned a value of 10% greater to account for the increase of rigidity due to cold temperature. Based on the HPI thermal analyses presented in Section 3, the temperature of the honeycomb material is bounded by 400°F. For the crush strength of honeycomb material at 400°F, a reduction of the crush strength of 40% is conservatively assigned. This is based on the thermal tests from Reference 2-23, p. 9. The temperature test result is presented in Figure 2.12.1.7-4.

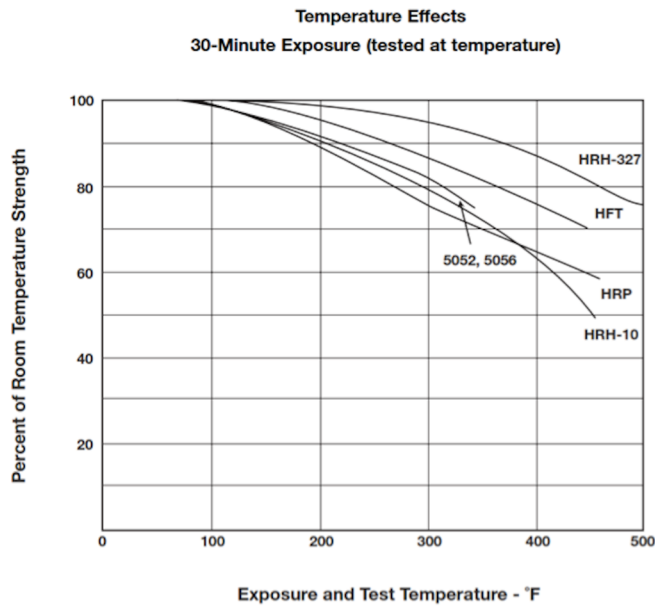


Figure 2.12.1.7-4. Temperature Effect of Honeycomb Material

2.12.1.7.5. Temperature Range for Material Properties

The component temperature range and justification for the applied temperature is discussed in Table 2.12.1-13.

Table 2.12.1-13. Component Temperature Range and Justification

Component, Material	Predicted Temperature Range	Applied Temperature	Justification for Use of Non-Bounding Peak Temperature
Overpack Toroids, 304 SS	-20 to 110-250	-20 to 300	Bounding. Provides primary impact protection
Cask Shell, 304 SS	-20 to 300-460	-20 to 300	Cask does not provide primary impact protection. Temperature range selected to best represent the performance of the cask during impact.
Cask Shielding, Lead	-20 to 330-450	-20 to 300	Lead does not provide primary impact protection. Therefore, temperature range considered acceptable for analyses.
Overpack Cover and Base, 304 SS	-20 to 170-370	-20 to 300	Overpack cover not included in model. The base does not provide primary impact protection. Therefore, range considered acceptable for analyses.
Overpack Honeycomb, Aluminum	-20 to 200-360	-20 to 400	40% compressive strength reduction bounds temperature of 400F. 10% compressive strength increase bounds temperature of -20F.

2.12.1.8. LS-DYNA Model Description

2.12.1.8.1. Finite Element Model

In accordance with the Model 2000 licensing drawings, an LS-DYNA finite element model was generated to evaluate the structural performance of the cask when loaded with the maximum content weight. The model includes the overpack and the Model 2000 cask body with lead shield and lid. The contents of the cask are modeled as a rigid body.

The 3D (half-symmetry) solid model of the Model 2000 cask and overpack was generated using Autodesk Inventor, which was imported into ANSYS Workbench Design Modeler (Reference 2-16). The finite element mesh was generated using the ANSYS Workbench Mechanical interface. The completed FEA model was then saved as a text input file to perform the analyses. Figure 2.12.1.8-1 shows the finite element model.

The finite element model is comprised of 3D brick elements (fully integrated selective-reduced solid) that represent the main body of cask components. Contact between components is modeled as surfaces using contact pairs. Boundary conditions such as symmetry are applied to the symmetry plane of the model. The final model includes 790,526 elements and 1,355,593 nodes.

[[

]]

Figure 2.12.1.8-1. Model 2000 Overpack and Cask Finite Element Model

2.12.1.8.2. Pin Puncture Analysis Methodology

The accident sequence presented in 10 CFR 71.73 requires that the cask, after a 30-foot drop, be dropped onto 6-inch diameter pin. To simulate the sequential drops, a rigid plane and a rigid pin with a 6-inch diameter and 8-inch length are created as shown in Figures 2.12.1.8-2 and 2.12.1.8-3 for the end drop and side drop, respectively.

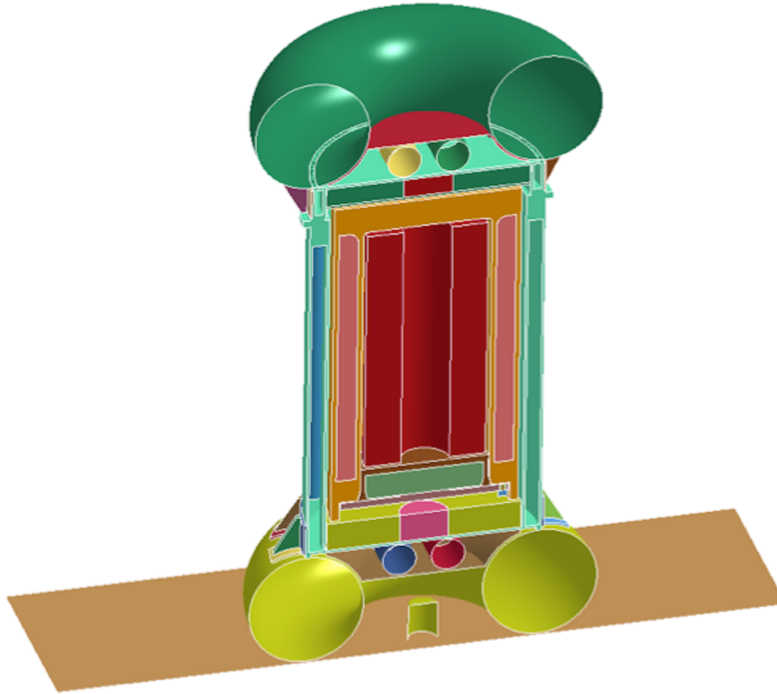


Figure 2.12.1.8-2. Rigid Plane and Pin Model for the End Drop Configuration

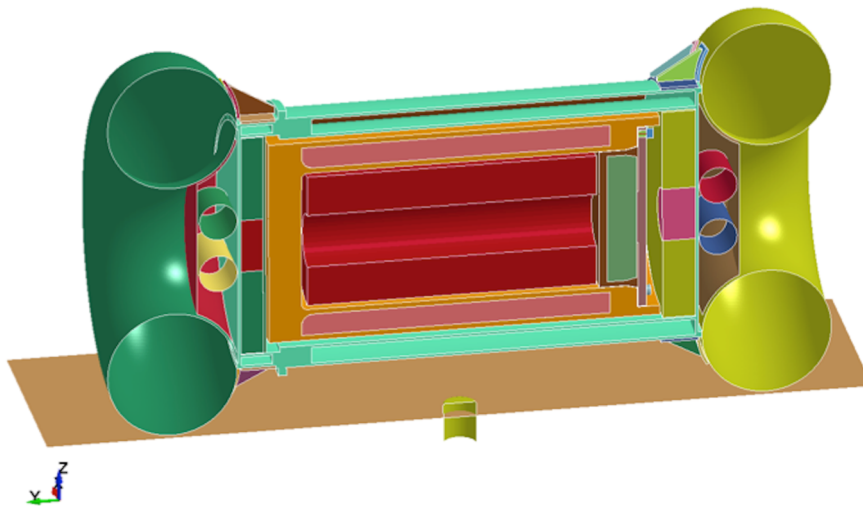


Figure 2.12.1.8-3. Rigid Plane and Pin Model for the Side Drop Configuration

The dynamic simulation for this 30-foot drop onto an unyielding surface followed by a 40-inch drop onto a pin is performed using a two steps drop sequence. For the first sequence, the impact velocity of the 30-foot drop is 527.5 in/sec. For the second sequence, the initial velocity for a 40-inch drop is 175.8 in/sec.

During the first drop sequence at the beginning of the 30-foot drop accident, the cask travels in the downward direction with an initial velocity of 703.3 in/sec ($=527.5+175.8$). The rigid plane and the pin travel at an initial velocity of 175.8 in/sec and the contact interface is activated between the cask and the rigid plane while the contact interface between the cask and the pin is not activated. Therefore, the relative velocity between the cask and the rigid plane is 527.5 in/sec, which is equivalent to a drop height of 30 feet. During this sequence, the distance between the cask the pin is reduced as time progresses. The kinetic energy of the cask dissipates to zero at time = 35 milliseconds. This is the time at which the puncture impact starts.

At the beginning of the second sequence, the distance between the pin and the cask is reduced to a minimum gap but not touching. At this point, the absolute velocity of the cask and pin is 175.8 in/sec. At this time, the contact interface between the pin and the cask is activated while the contact interface between the rigid plane and the cask is deactivated, which allows the damaged impact limiters to pass through the rigid plane. Additionally, the velocity of the pin is set to zero, which results in relative velocity between the cask and the pin of 175.8 in/sec. Figure 2.12.1.8-4 shows the cumulative damage following the 30-foot top end drop and 40-inch pin puncture.

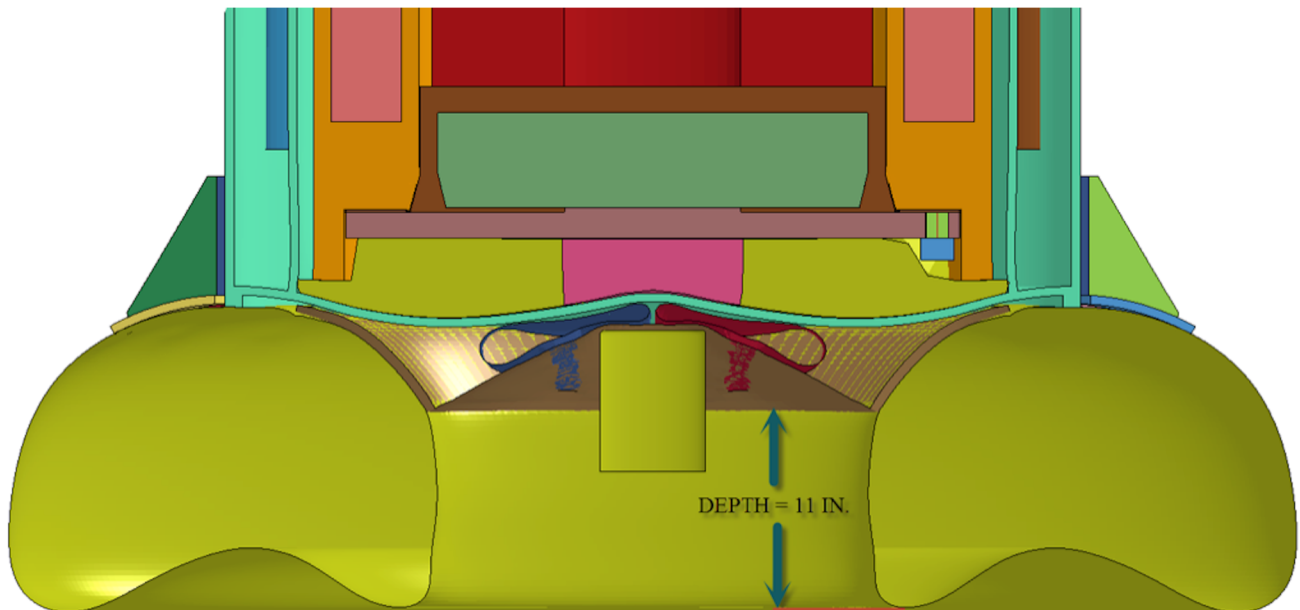


Figure 2.12.1.8-4. Deformed Geometry of the Overpack after a 30 foot End Drop

Figure 2.12.1.8-5 shows the cumulative damage for the side drop and pin puncture sequence. For the side drop, the depth of the unexposed cavity below the toroidal shell is less than 2.3 inches (taken from the result of Drop Case 10). Therefore, the modeled pin length of 8 inches is sufficient to sustain maximum damage.

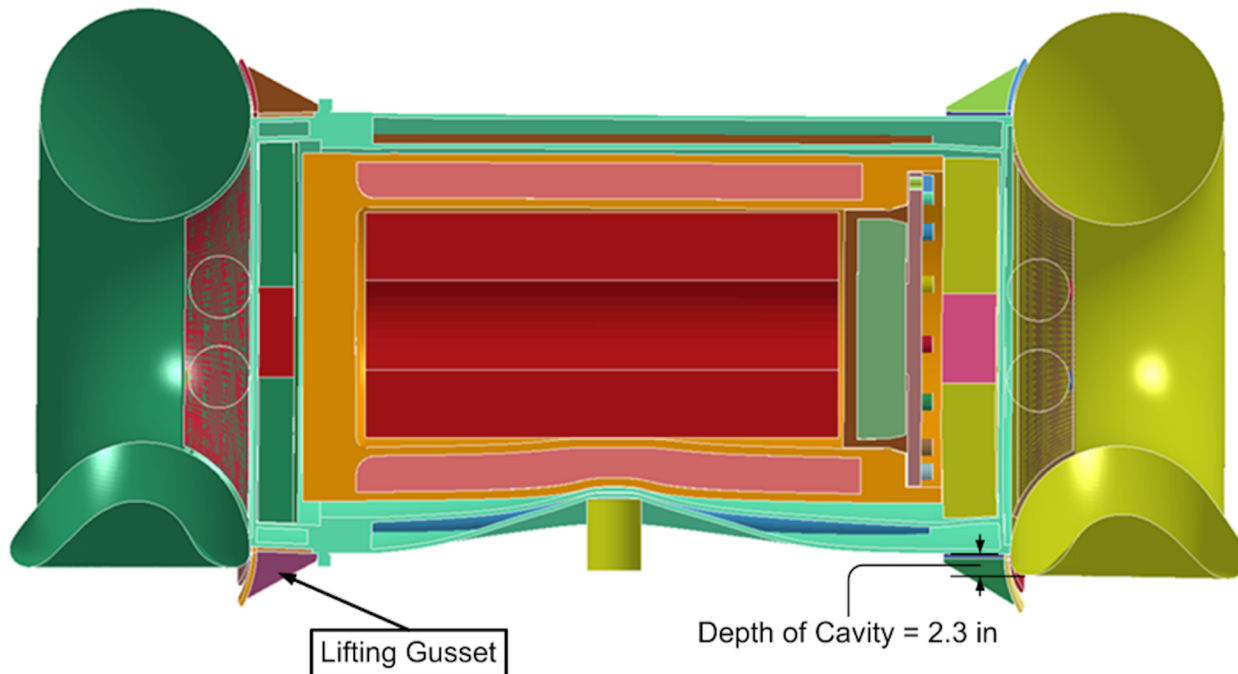


Figure 2.12.1.8-5. Deformed Geometry of the Overpack after a 30 foot Side Drop

2.12.1.9. Weight

The Model 2000 Transport Package components consist of the closure lid, cask body and overpack. The dimensions used in the calculations are taken from the Model 2000 Transport Package fabrication drawings. The total weight of the Model 2000 Transport Package empty is calculated to be 28,100 lb. From the finite element model, the center of gravity is located 1.5 inches below the centerline of the overpack, 64.25 inches from the bottom line. Table 2.1-3 presents the breakdown of the components weights used for the dynamic analyses.

2.12.1.9.1. Material Model

The LS-DYNA material models used in the analyses are described below:

- The stainless steel shells are modeled using *MAT_PIECEWISE_LINEAR_PLASTICITY.
- The honeycomb impact limiters are modeled using *MAT_CRUSHABLE_FOAM.
- The payload is modeled as *MAT_RIGID.
- The closure lid bolts of the inner shell are modeled as *MAT_ELASTIC.

2.12.1.9.2. Contact Interfaces

The control card *CONTACT_TIED_SURFACE_TO_SURFACE is used to fasten the welded components. For the components within the cask and the overpack, the control card *CONTACT_AUTOMATIC_SINGLE_SURFACE is used to provide global contact control. The honeycomb material has significant stiffness difference between the adjacent part, therefore the control card *CONTACT_AUTOMATIC_SURFACE_TO_SURFACE is used to control and prevent penetration between parts.

2.12.1.10. Boundary Conditions

2.12.1.10.1. Symmetry Plane

The half-symmetry finite element model utilizes symmetry boundary conditions that are applied to the cut plane of the half-model in the Z-direction.

2.12.1.10.2. Initial Velocity

The drop height, H, is converted to kinetic energy using the formula below.

$$V = \sqrt{2 \times g \times H}$$

where

V = the initial velocity at the threshold of impact, in/s

g = gravity constant = 386.4 in/s².

H = drop height, in

Therefore, the drop height of H=30 ft is converted to initial velocity, V360-in, as

$$V_{360\text{-in}} = \sqrt{2 \times g \times 360} = 527.45 \text{ in/s}$$

And the drop height of H=40-in is converted to initial velocity, V40-in, as

$$V_{40\text{-in}} = \sqrt{2 \times g \times 40} = 175.8 \text{ in/s}$$

2.12.1.10.3. Gravity

The gravity of 386.4 in/s is applied to all components in the global Z-direction with an initial ramp up period of 0.05 seconds.

2.12.1.11. Dynamic Analysis Results HAC 30-foot Drops

The results of the impact analyses of the Model 2000 cask model in the forms of acceleration of the payload and plastic strain of the toroid shell are presented in Sections 2.12.1.11.1 through 2.12.1.11.14. Further, each section contains four plots, which include a plot for the deformed overpack shape, the cask acceleration time history, energy time histories and interface sliding energy time history (Figures 2.12.1.11-1 through 2.12.1.11-58). Section 2.12.1.11.15 presents the results of the 30-foot drop followed by pin puncture drop. The significance of the accelerations and energy time histories (kinetic energy, internal energy, hourglass energy, and sliding energy) of the simulations are described below.

Accelerations – Accelerations are extracted from the LS-DYNA MATSUM file. Using the MATSUM data allows for the reporting of the maximum acceleration in any part and at any point in the model.

Kinetic Energy - The kinetic energy time history is used to confirm that the kinetic energy of the cask assembly is completely dissipated during the impact and the acceleration has peaked. For a normal and completed drop impact scenario, the kinetic energy must be decreasing to a minimum value as close to zero as possible and starts to increase (due to gravity loading). At the moment of minimum kinetic energy, the primary impact event is over.

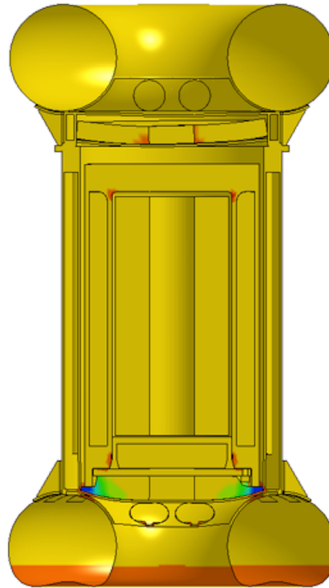
Internal Energy - The internal energy plot is a measure of how much of the kinetic energy is converted into strain energy, either elastic or inelastic. Most likely, the internal energy is a measure of inelastic strain energy corresponding to the permanent deformation of the energy absorber material. The accumulated internal energy is a measure of how well the impact limiter is working as designed. Internal energy that is significantly smaller than the initial kinetic energy is an indication that the impact limiter is not dissipating the impact energy.

Hourglass Energy - The hourglass energy and the sliding energy are numerical terms that are produced by the mathematic solver but not derived from kinetic energy. The hourglass energy is strain energy numerically produced and proportional to the energy used to control the distortion of brick finite elements (solid element). As recommended by the LS-DYNA user manual, the brick elements perform best during the solution when the hourglass energy is limited to less than 10% of the internal energy.

Sliding Energy - The sliding energy plots represent the efficiency of the contact interface and the level of penetration between adjacent parts. A negative sliding energy indicates that the contact interface is not working well with a high degree of part penetrations. The contact interface control parameters must be revised to allow the use of different contact algorithms to prevent parts penetrations and pass-through. A positive sliding energy indicates the contact interface is working well and no penetrations are present.

2.12.1.11.1. Case 1 End Drop Benchmark

GE-2000 CASK AND OVERPACK MODEL
 Time = 0.035
 Contours of Effective Plastic Strain
 max IP. value
 min=-1.63975, at elem# 388422
 max=0.429583, at elem# 296895



Fringe Levels
 4.296e-01
 2.227e-01
 1.572e-02
 -1.912e-01
 -3.981e-01
 -6.051e-01
 -8.120e-01
 -1.019e+00
 -1.226e+00
 -1.433e+00
 -1.640e+00

Figure 2.12.1.11-1. Case 1 Deformed Overpack Shape (Effective Plastic Strain)

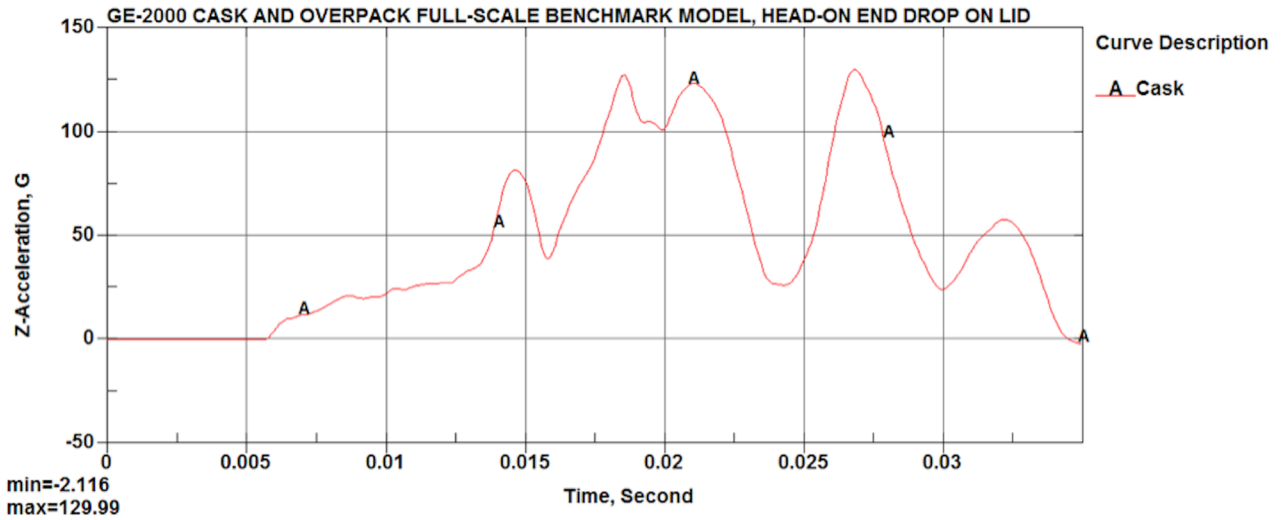
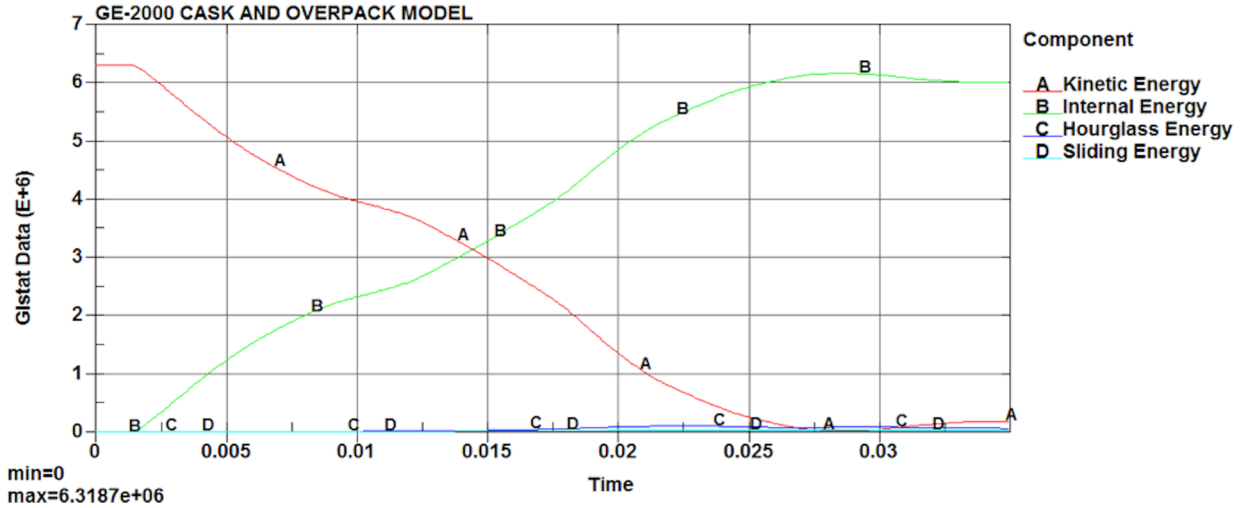
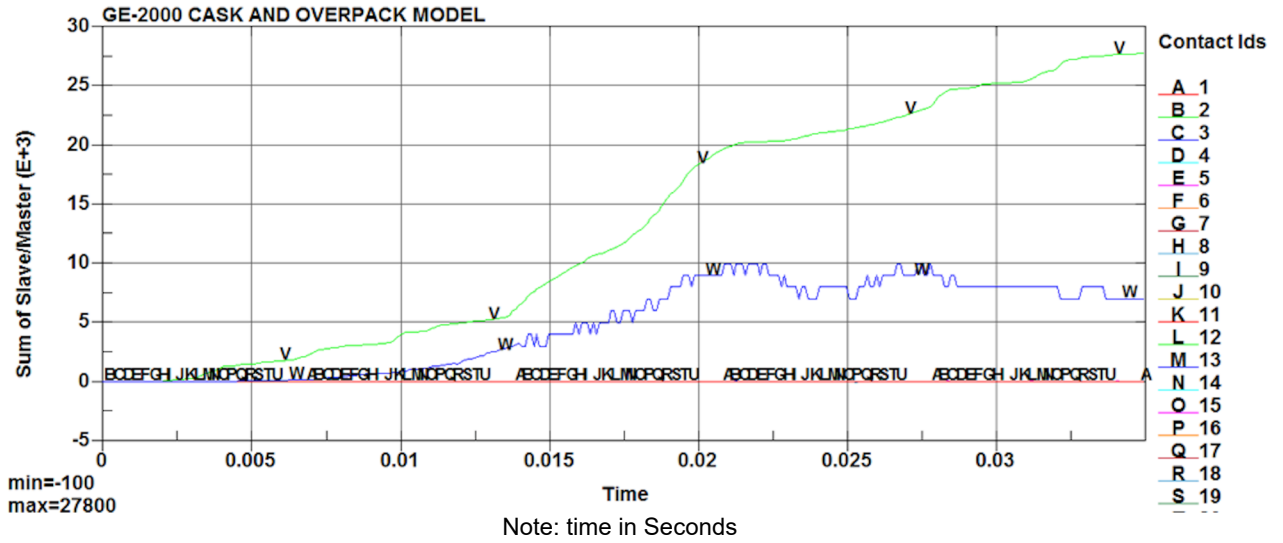


Figure 2.12.1.11-2. Case 1 Payload Acceleration Time History



Note: time in Seconds

Figure 2.12.1.11-3. Case 1 Impact Energy Plot



Note: time in Seconds

Figure 2.12.1.11-4. Case 1 Interface Sliding Energy Time History

2.12.1.11.2. Case 2 Side Drop Benchmark

GE-2000 CASK AND OVERPACK MODEL
 Time = 0.025
 Contours of Effective Plastic Strain
 max IP. value
 min=-0.0581017, at elem# 388099
 max=0.442052, at elem# 420824

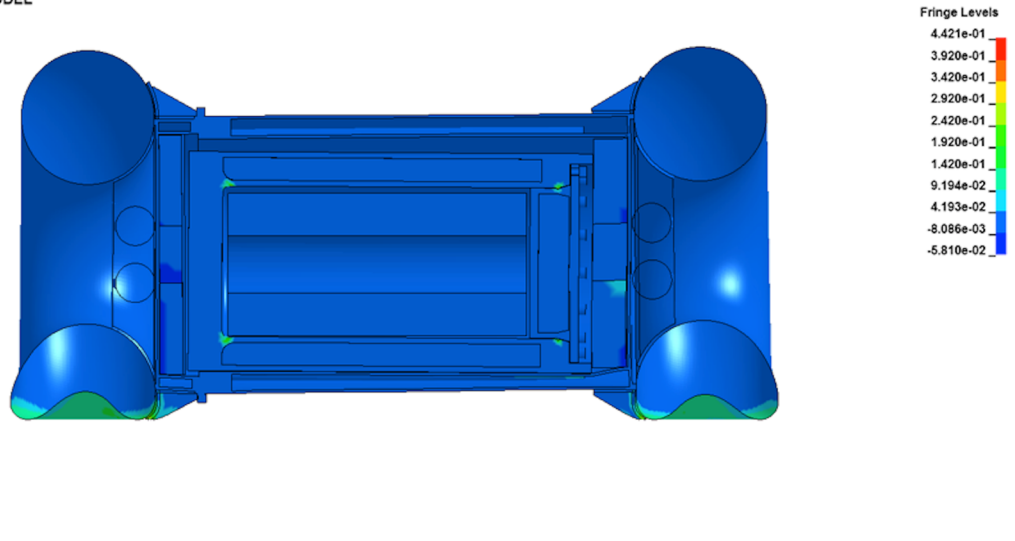


Figure 2.12.1.11-5. Case 2 Deformed Overpack Shape (Effective Plastic Strain)

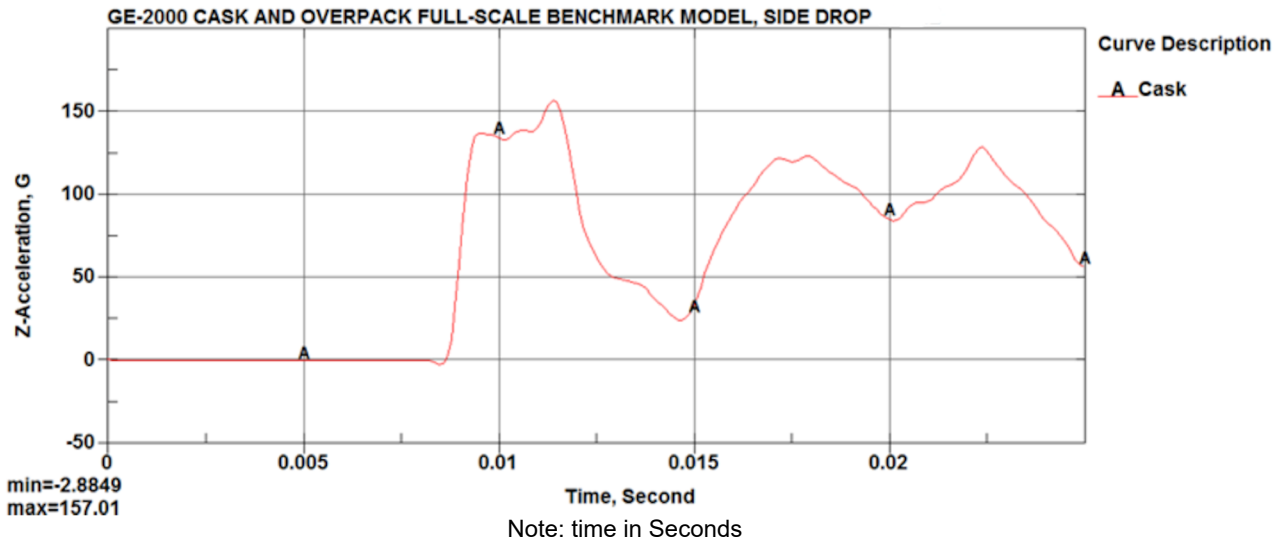


Figure 2.12.1.11-6. Case 2 Payload Acceleration Time History

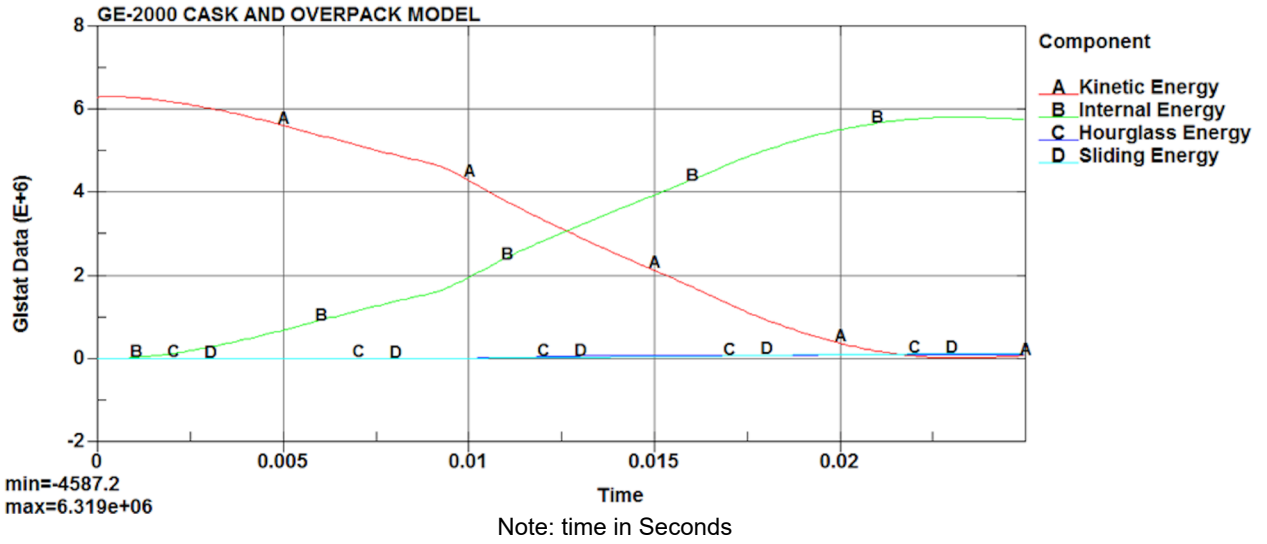


Figure 2.12.1.11-7. Case 2 Impact Energy Plot

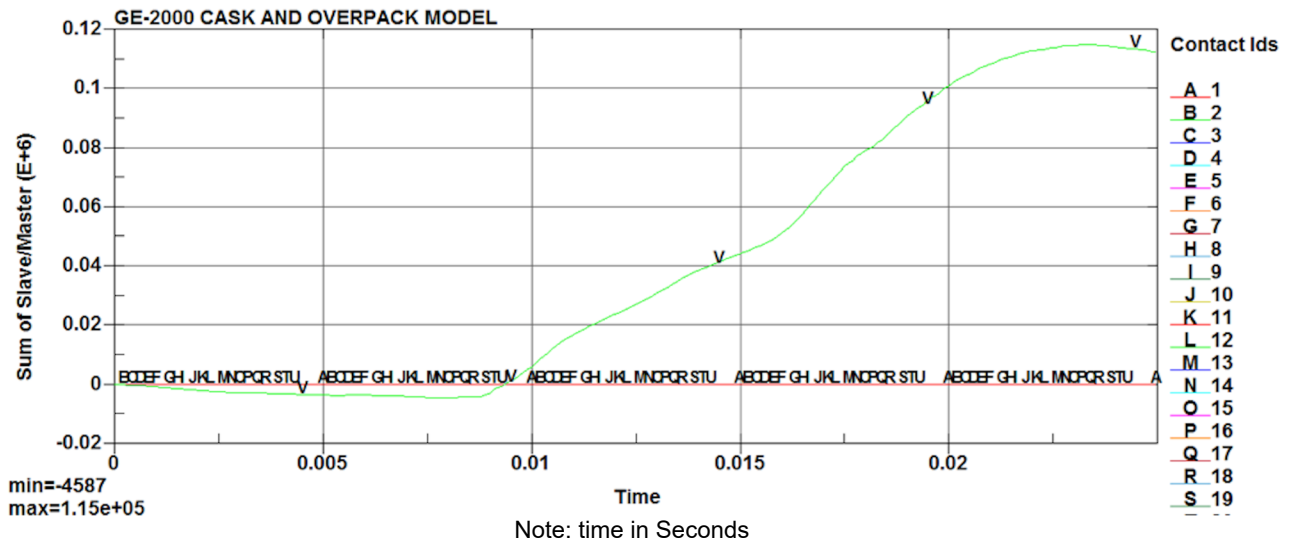


Figure 2.12.1.11-8. Case 2 Interface Sliding Energy Time History

2.12.1.11.3. Case 3 C.G. over Corner Drop Benchmark

GE-2000 CASK AND OVERPACK MODEL
 Time = 0.045001
 Contours of Effective Plastic Strain
 max IP. Value
 min=-1.47019, at elem# 398962
 max=0.402424, at elem# 296780

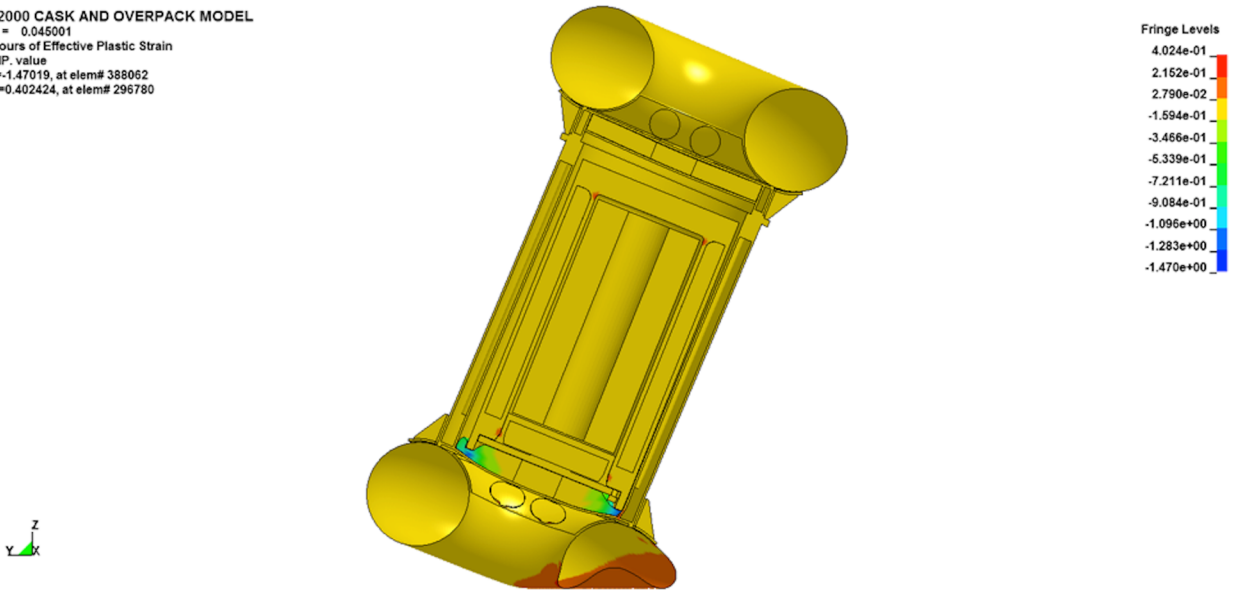
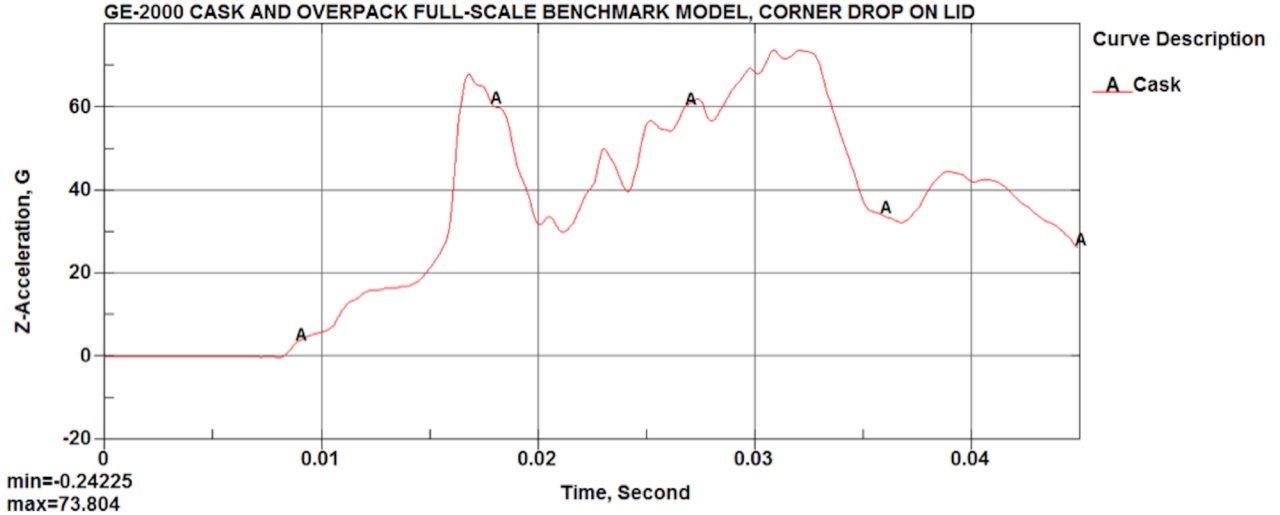


Figure 2.12.1.11-9. Case 3 Deformed Overpack Shape (Effective Plastic Strain)



Note: time in Seconds

Figure 2.12.1.11-10. Case 3 Payload Acceleration Time History

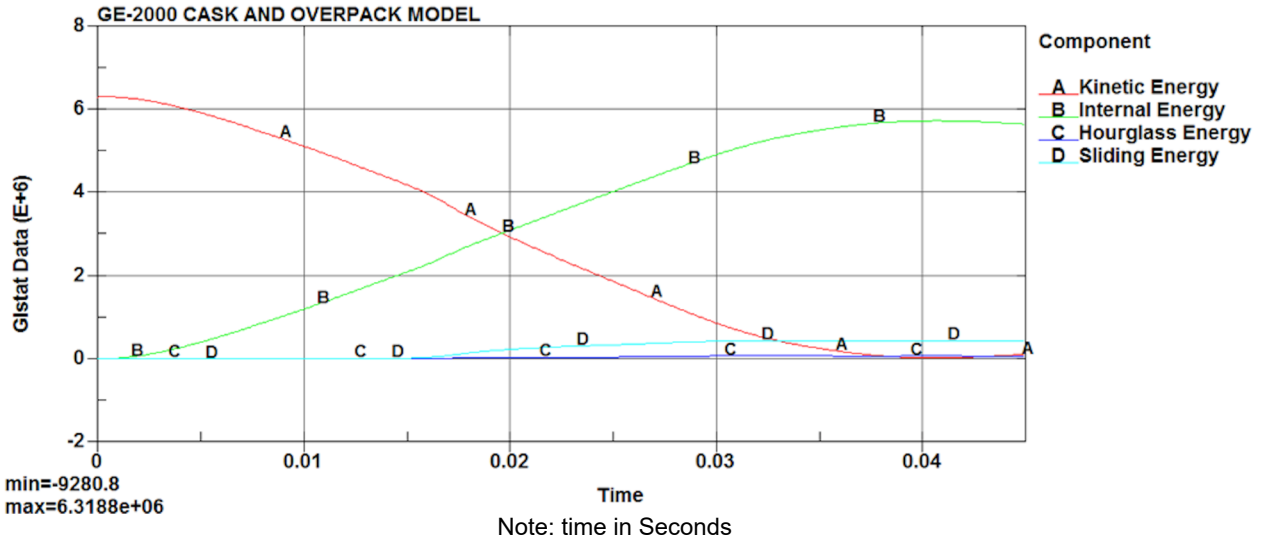


Figure 2.12.1.11-11. Case 3 Impact Energy Plot

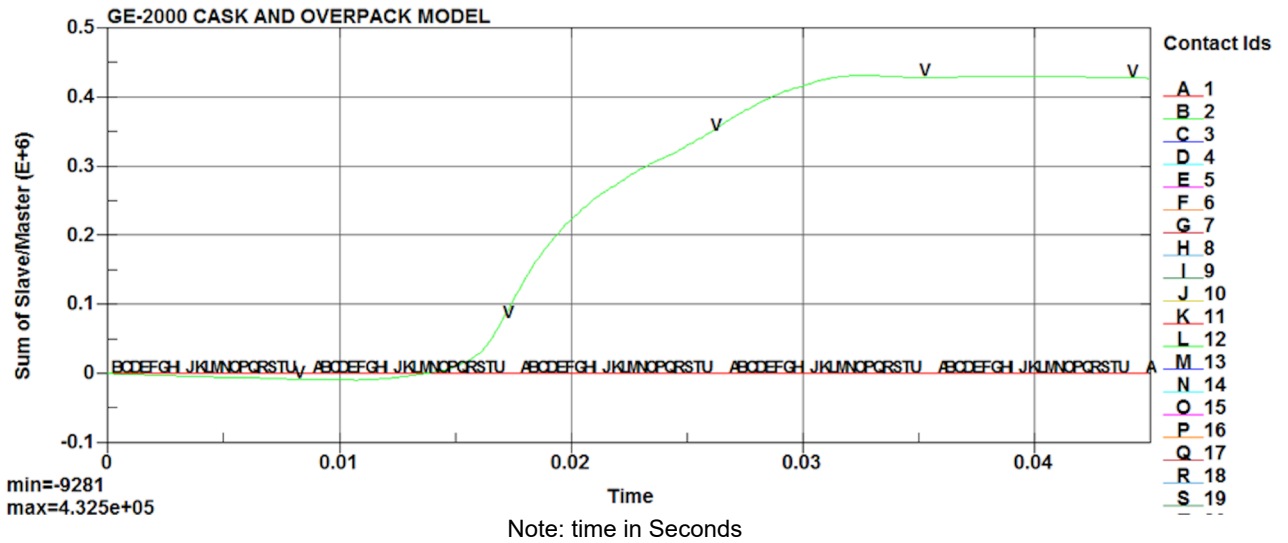


Figure 2.12.1.11-12. Case 3 Interface Sliding Energy Time History

2.12.1.11.4. Case 4 NCT End Drop with Thick Shell, Cold Condition and Light Payload

Case_4_Thick_Cold_Light_EndDrop
 Time = 0.035
 Contours of Effective Plastic Strain
 max IP, value
 min=-0.290278, at elem# 388265
 max=0.0441127, at elem# 388087

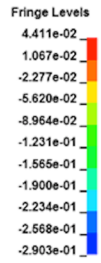
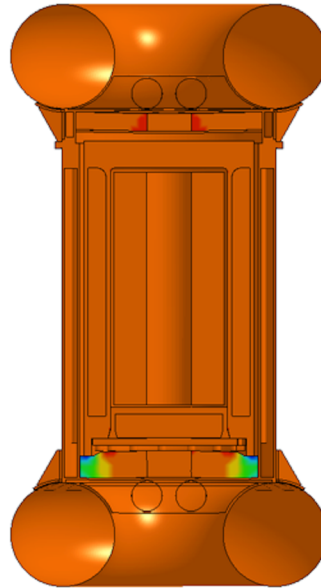


Figure 2.12.1.11-13. Case 4 Deformed Overpack Shape (Effective Plastic Strain)

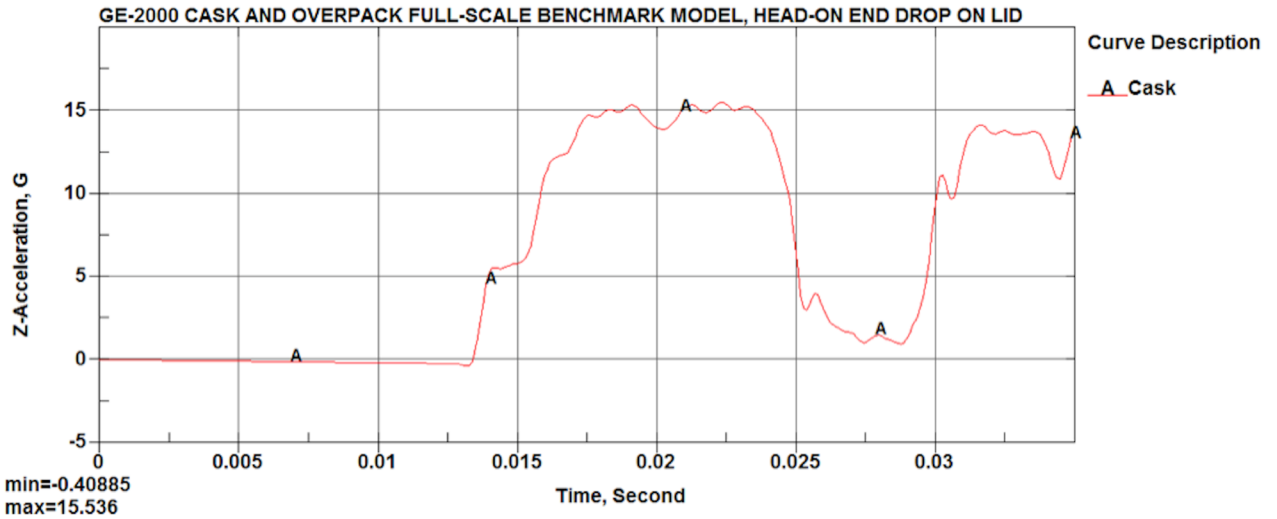


Figure 2.12.1.11-14. Case 4 Payload Acceleration Time History

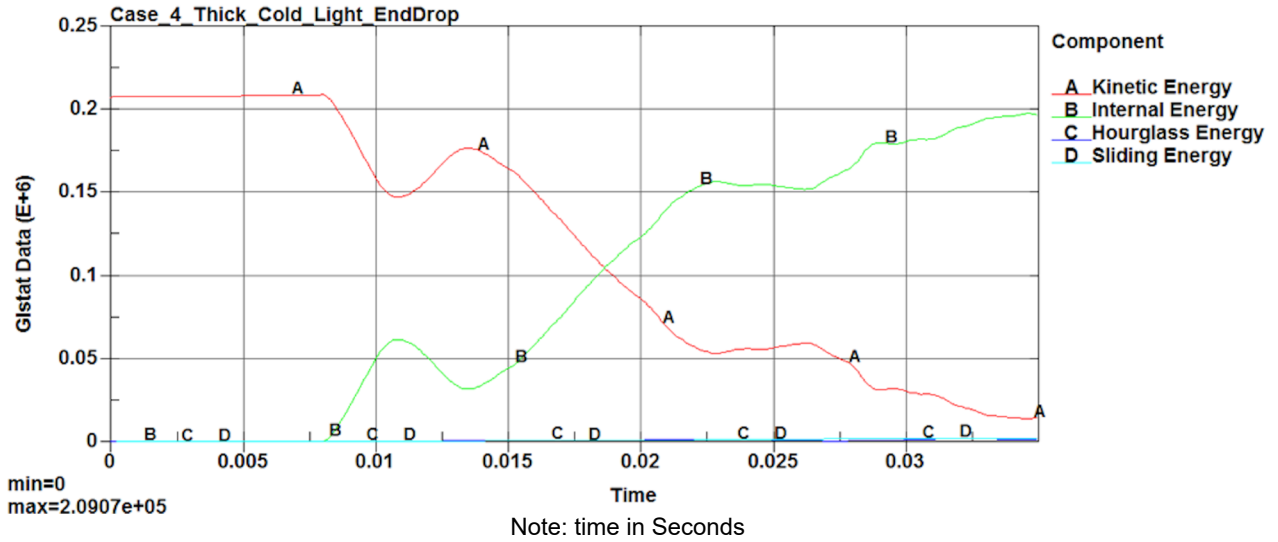


Figure 2.12.1.11-15. Case 4 Impact Energy Plot

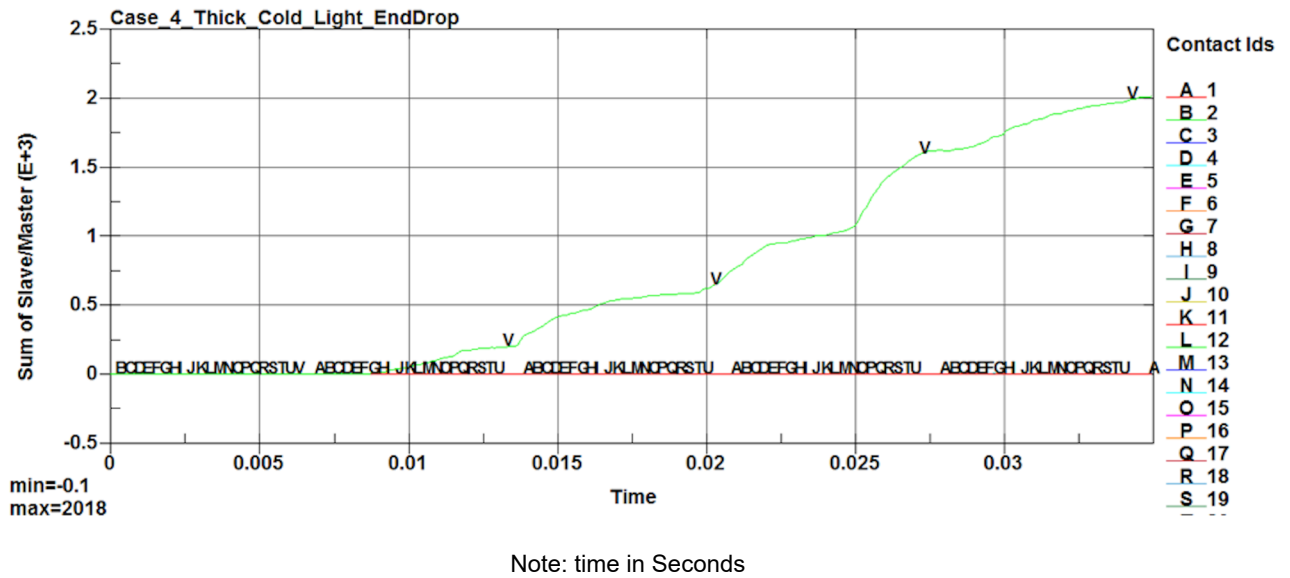
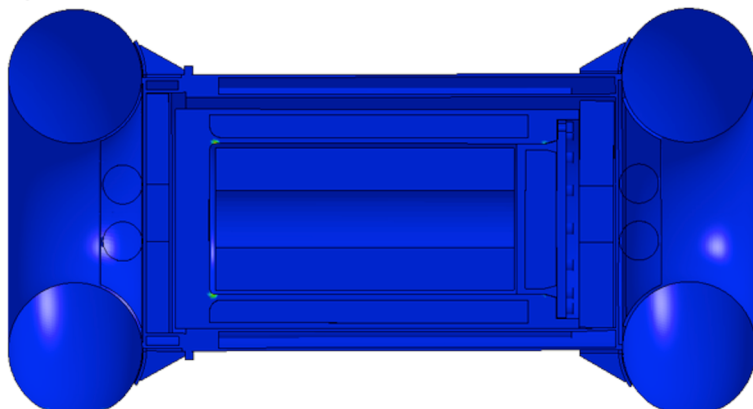


Figure 2.12.1.11-16. Case 4 Interface Sliding Energy Time History

2.12.1.11.5. Case 5 NCT Side Drop with Thick Shell, Cold Condition and Light Payload

Case_5_thick_thick_Cold_Light_SideDrop
Time = 0.04
Contours of Effective Plastic Strain
max IP. value
min=-0.0123294, at elem# 387939
max=0.368119, at elem# 296779



Fringe Levels
3.681e-01
3.301e-01
2.920e-01
2.540e-01
2.159e-01
1.779e-01
1.398e-01
1.018e-01
6.376e-02
2.572e-02
-1.233e-02



Figure 2.12.1.11-17. Case 5 Deformed Overpack Shape (Effective Plastic Strain)

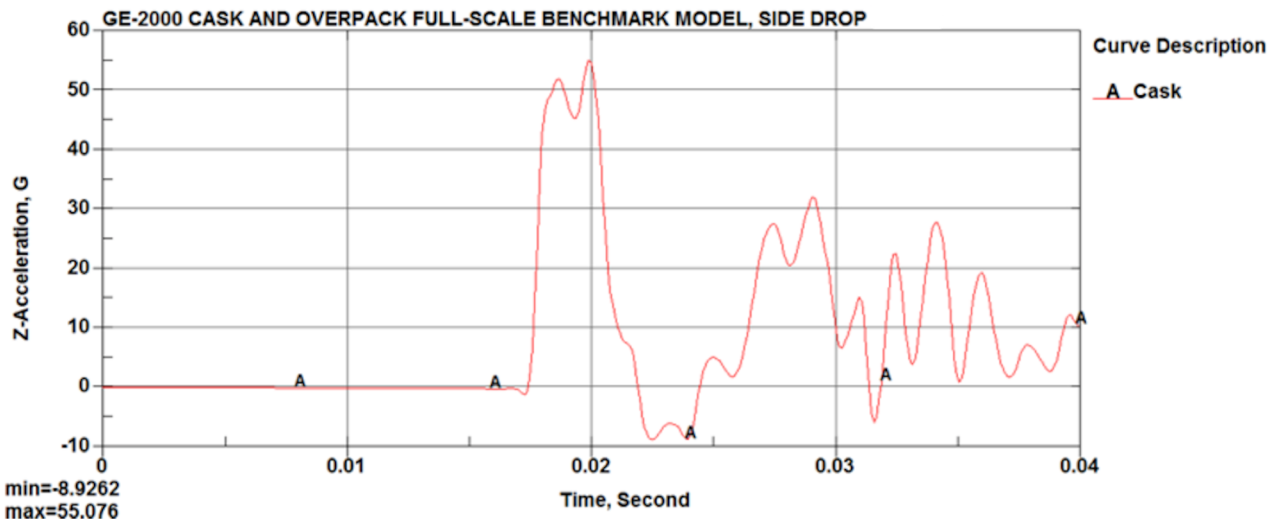


Figure 2.12.1.11-18. Case 5 Payload Acceleration Time History

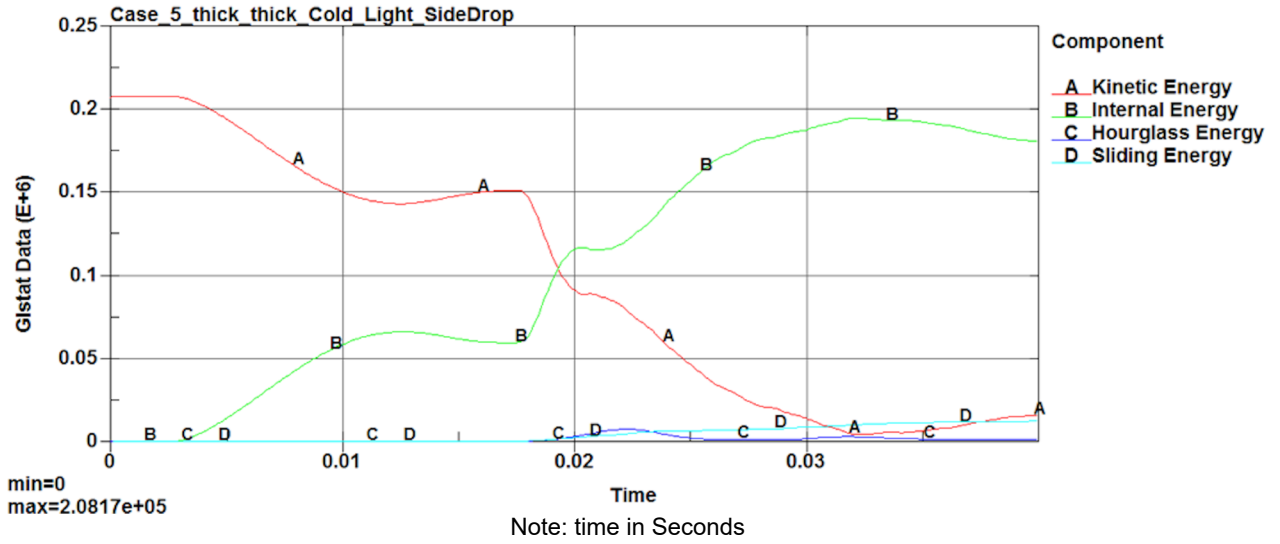


Figure 2.12.1.11-19. Case 5 Impact Energy Plot

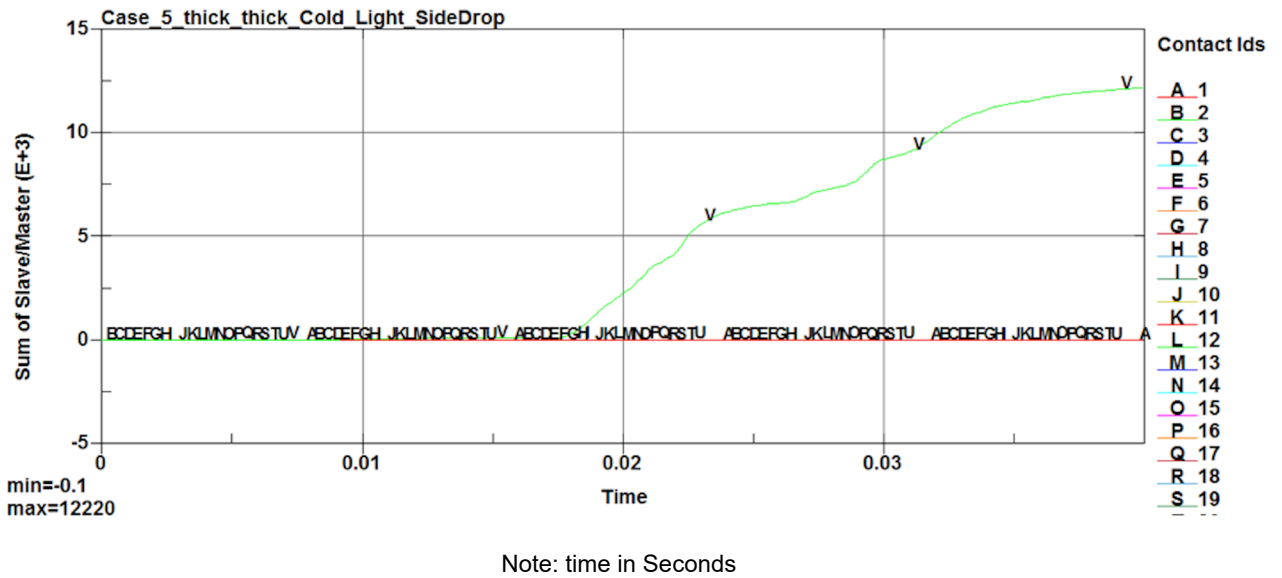


Figure 2.12.1.11-20. Case 5 Interface Sliding Energy Time History

2.12.1.11.6. Case 6 NCT Corner Drop with Thick Shell, Cold Condition and Light Payload

Case_6_Thick_Cold_Light_Corner_Drop
 Time = 0.045001
 Contours of Effective Plastic Strain
 max IP value
 min=-0.222077, at elem# 388419
 max=0.174147, at elem# 296780

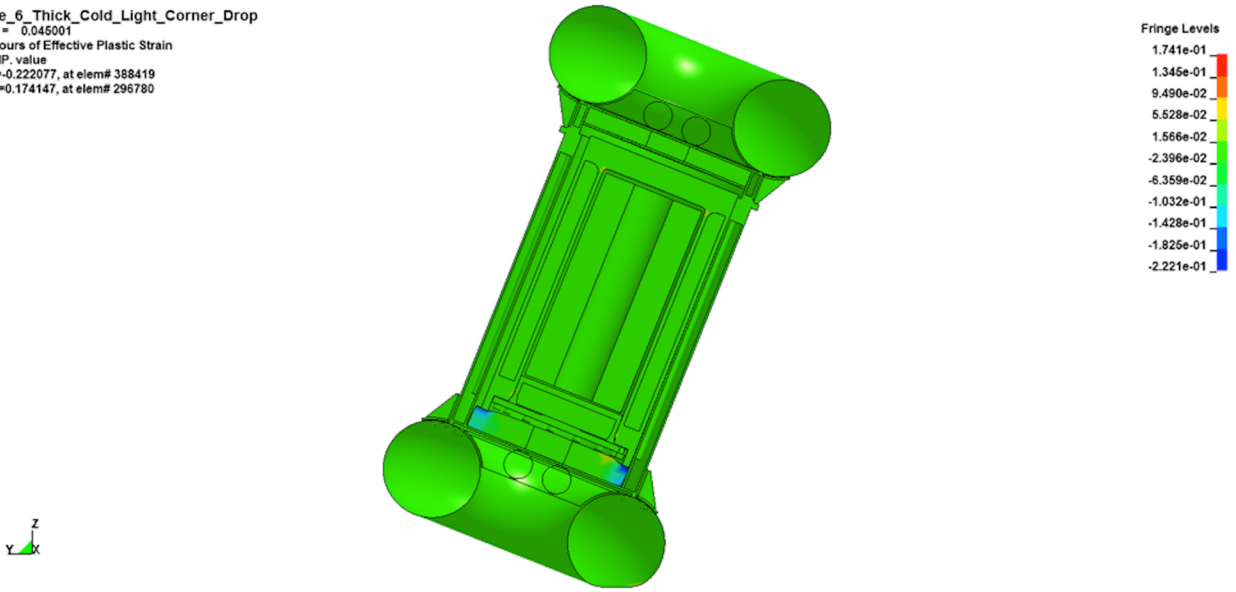


Figure 2.12.1.11-21. Case 6 Deformed Overpack Shape (Effective Plastic Strain)

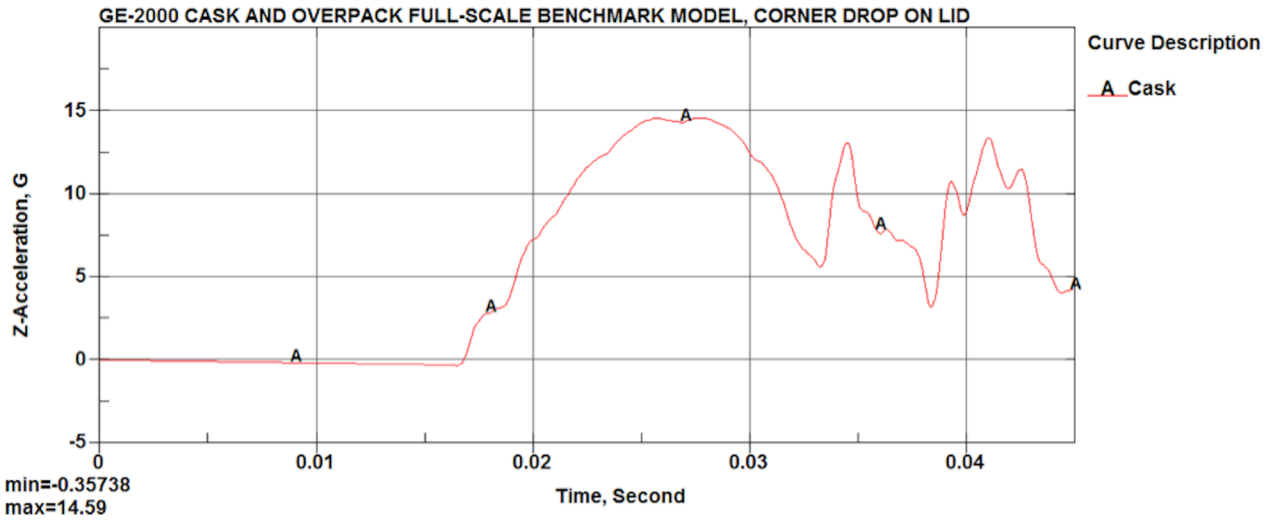


Figure 2.12.1.11-22. Case 6 Payload Acceleration Time History

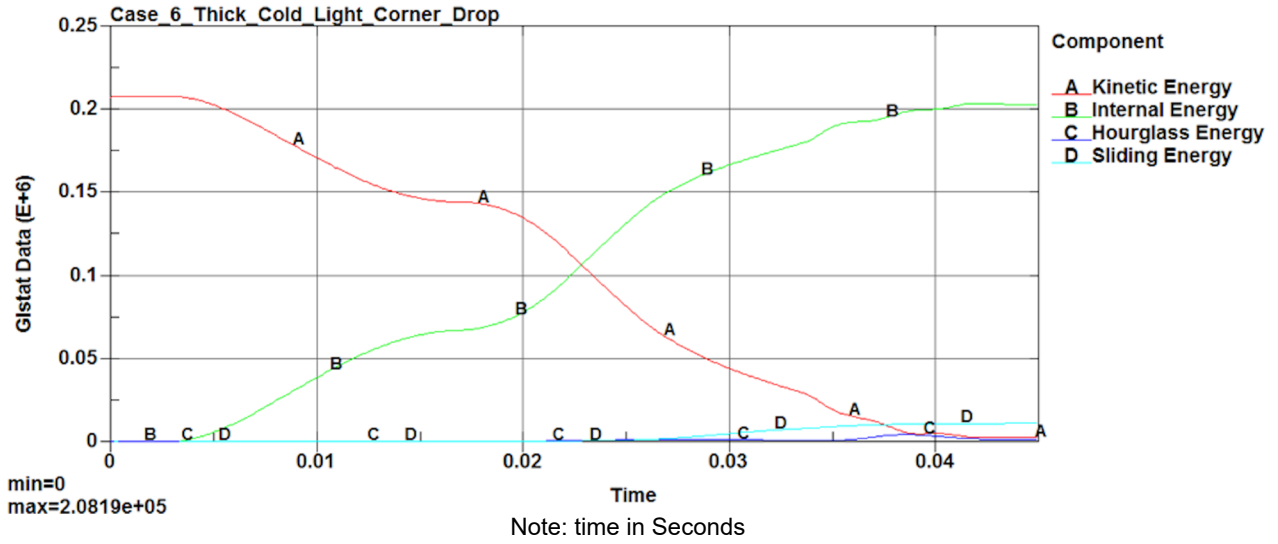


Figure 2.12.1.11-23. Case 6 Impact Energy Plot

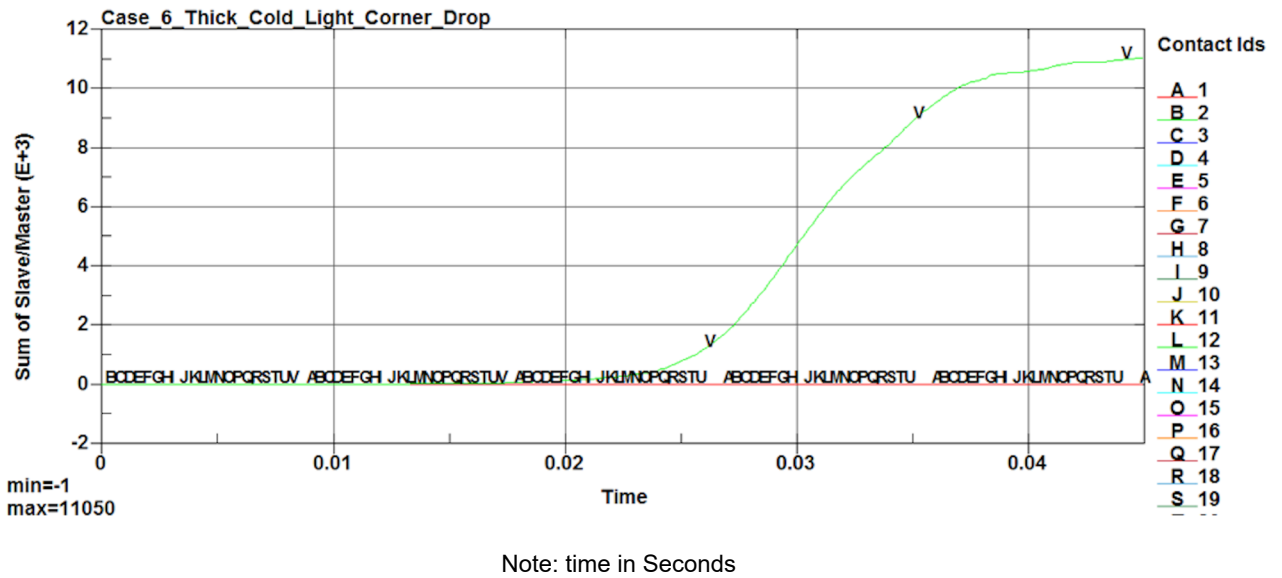


Figure 2.12.1.11-24. Case 6 Interface Sliding Energy Time History

2.12.1.11.7. Case 7 HAC End Drop with Thick Shell, Cold Condition and Light Payload

Case_7A_EndDrop_thick_cold_Light
 Time = 0.035
 Contours of Effective Plastic Strain
 max IP. value
 min=-1.63149, at elem# 388422
 max=0.386009, at elem# 296895

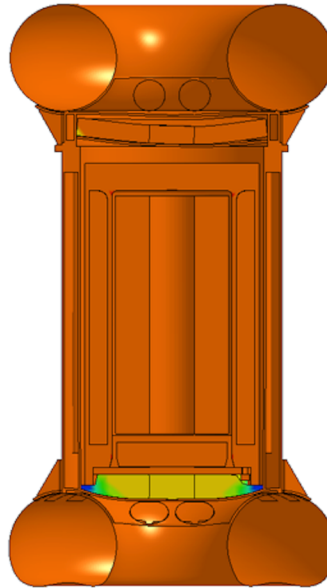


Figure 2.12.1.11-25. Case 7 Deformed Overpack Shape (Effective Plastic Strain)

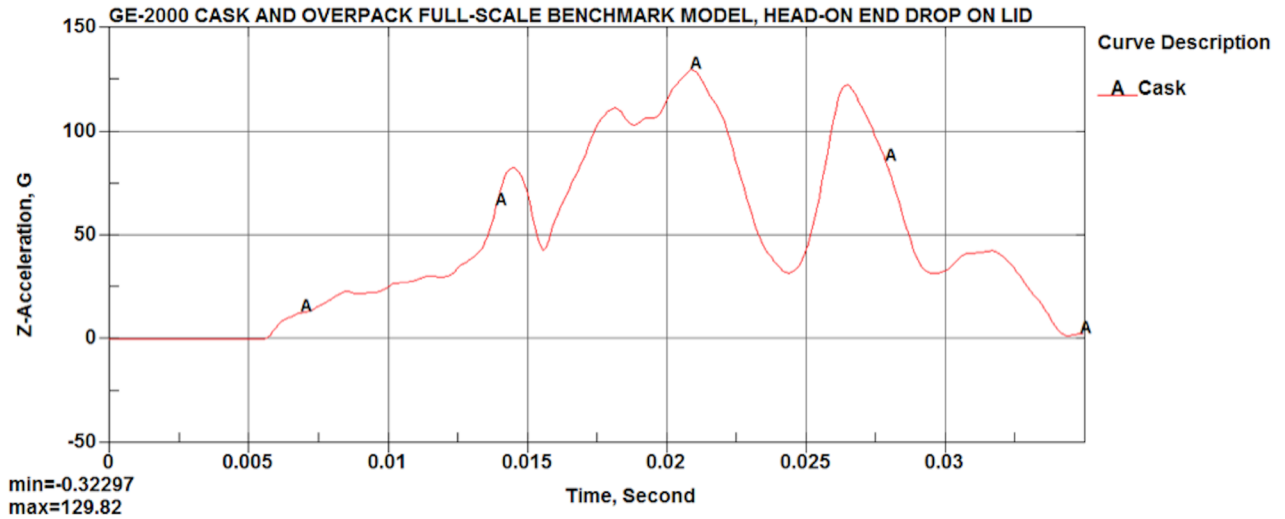


Figure 2.12.1.11-26. Case 7 Payload Acceleration Time History

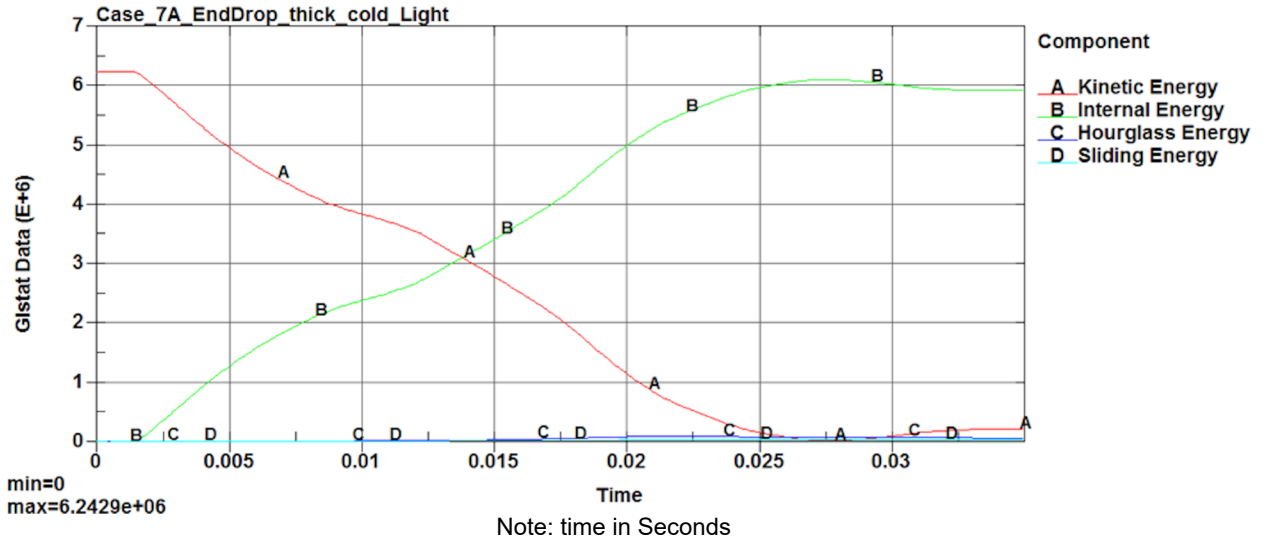


Figure 2.12.1.11-27. Case 7 Impact Energy Plot

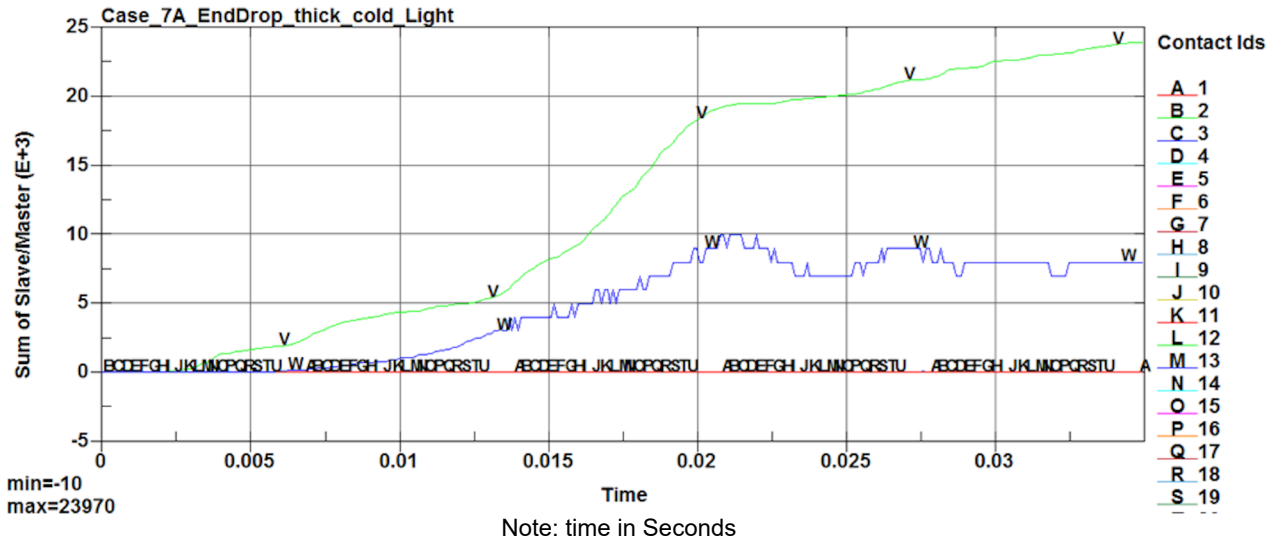


Figure 2.12.1.11-28. Case 7 Interface Sliding Energy Time History

2.12.1.11.8. Case 8 HAC End Drop with Thick Shell, Hot Condition and Heavy Payload

Case_8C_EndDrop_thin_hot_heavy
 Time = 0.035
 Contours of Effective Plastic Strain
 max IP. value
 min=-1.72667, at elem# 388419
 max=0.414946, at elem# 275552



Fringe Levels
 4.149e-01
 2.008e-01
 -1.338e-02
 -2.275e-01
 -4.417e-01
 -6.559e-01
 -8.700e-01
 -1.084e+00
 -1.298e+00
 -1.513e+00
 -1.727e+00

Figure 2.12.1.11-29. Case 8 Deformed Overpack Shape (Effective Plastic Strain)

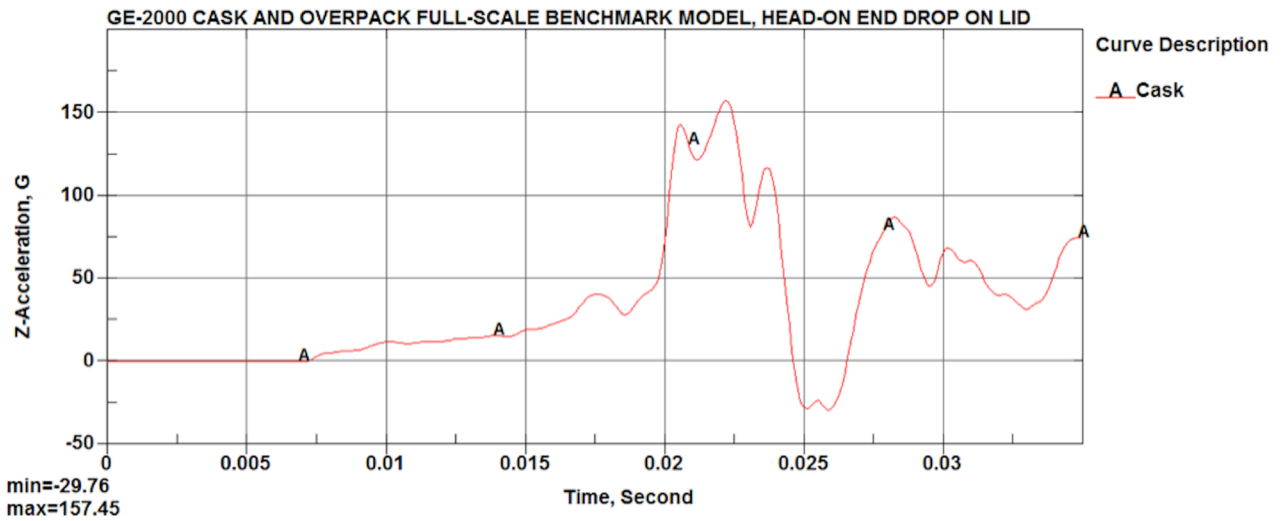


Figure 2.12.1.11-30. Case 8 Payload Acceleration Time History

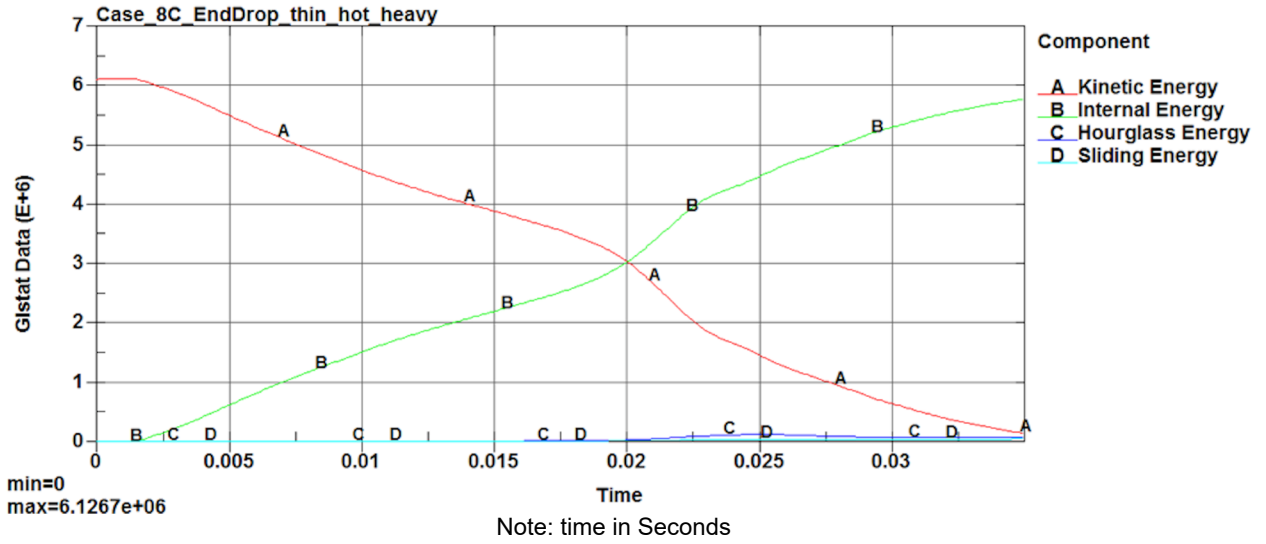


Figure 2.12.1.11-31. Case 8 Impact Energy Plot

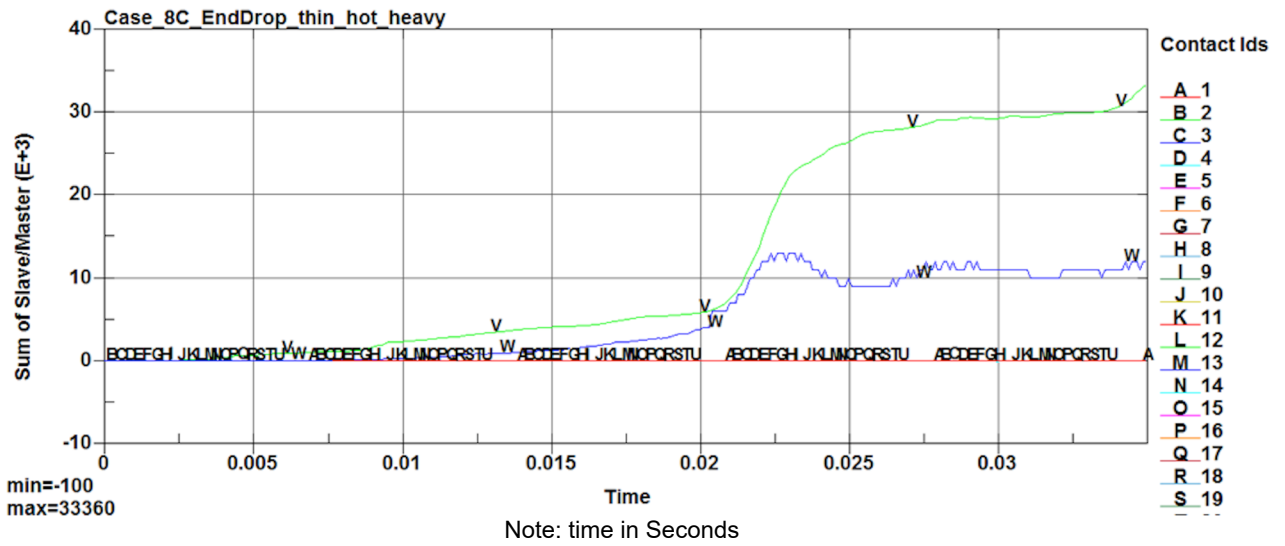


Figure 2.12.1.11-32. Case 8 Interface Sliding Energy Time History

2.12.1.11.9. Case 9 Side Drop with Thick Shell, Cold Condition and Light Payload

Case_9_SideDrop_thick_cold_light
 Time = 0.025
 Contours of Effective Plastic Strain
 max IP. value
 min=-0.0578508, at elem# 398099
 max=0.427268, at elem# 398569

Fringe Levels
 4.273e-01
 3.788e-01
 3.302e-01
 2.817e-01
 2.332e-01
 1.847e-01
 1.362e-01
 8.768e-02
 3.917e-02
 -9.339e-03
 -5.785e-02

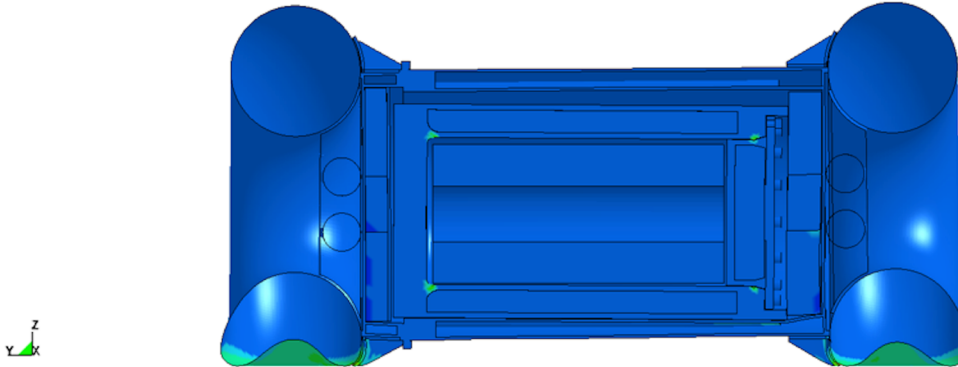


Figure 2.12.1.11-33. Case 9 Deformed Overpack Shape (Effective Plastic Strain)

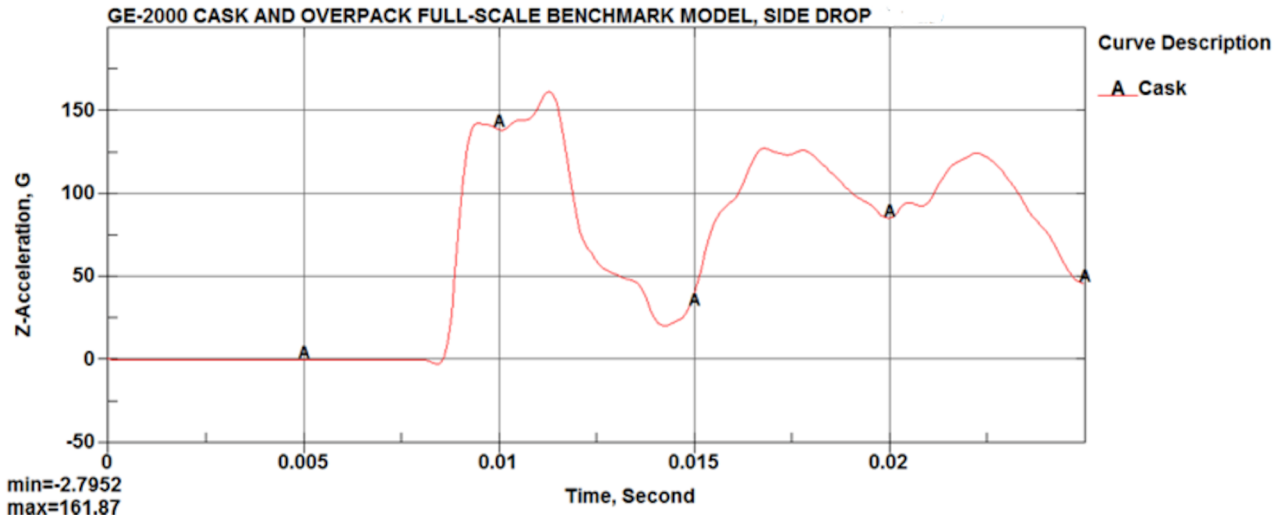


Figure 2.12.1.11-34. Case 9 Payload Acceleration Time History

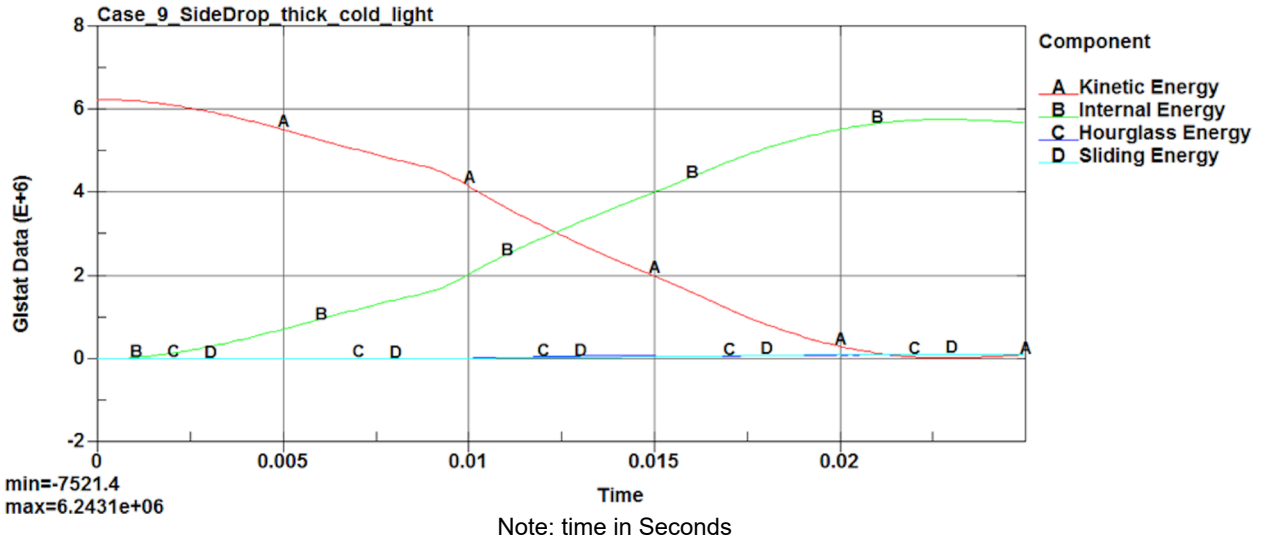


Figure 2.12.11-35. Case 9 Impact Energy Plot

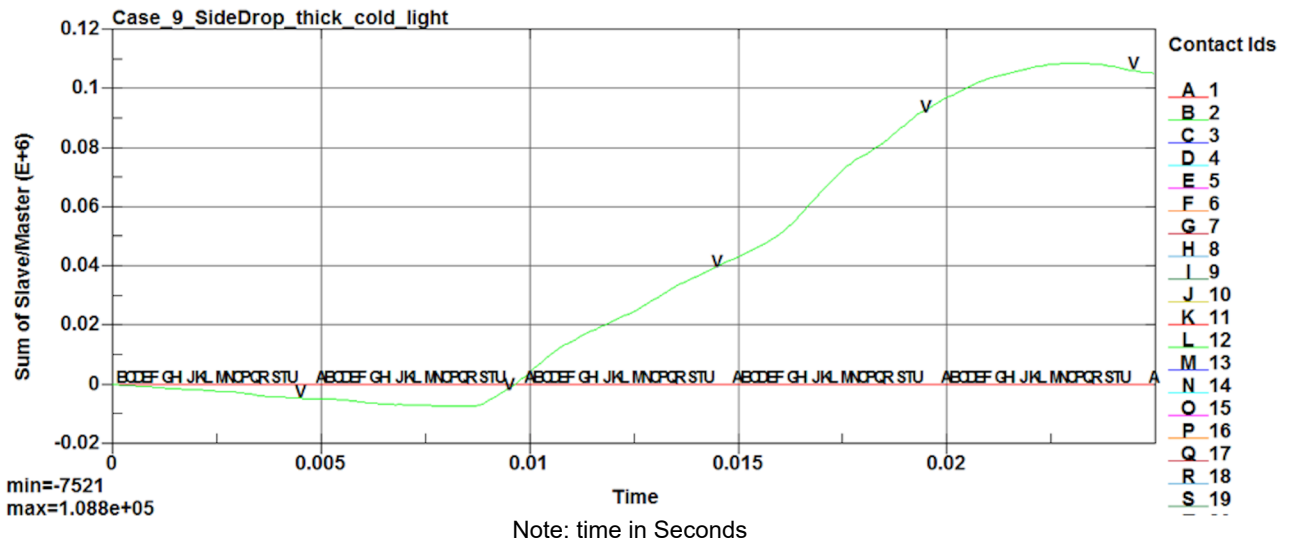


Figure 2.12.11-36. Case 9 Interface Sliding Energy Time History

2.12.1.11.10. Case 10 Side Drop with Thin Shell, Hot Condition and Heavy Payload

Case_10_SideDrop_thin_hot_heavy
Time = 0.035
Contours of Effective Plastic Strain
max IP. value
min=-0.0438089, at elem# 388059
max=0.469419, at elem# 398124

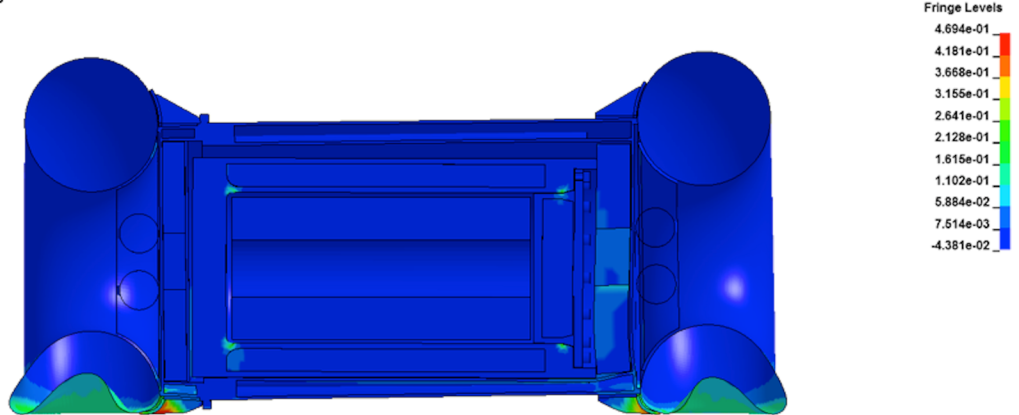


Figure 2.12.1.11-37. Case 10 Deformed Overpack Shape (Effective Plastic Strain)

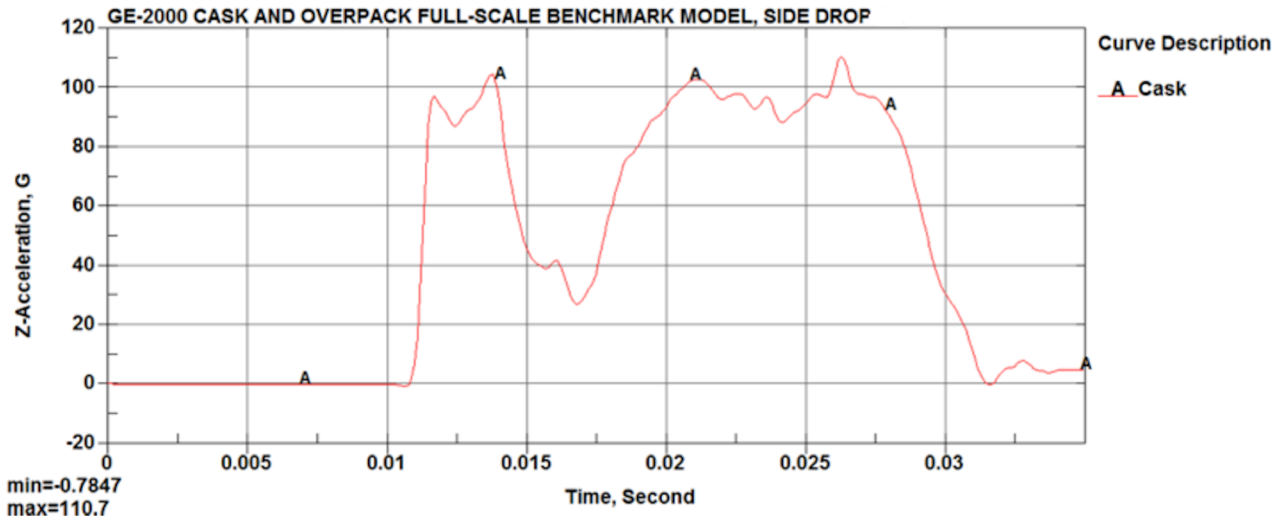


Figure 2.12.1.11-38. Case 10 Payload Acceleration Time History

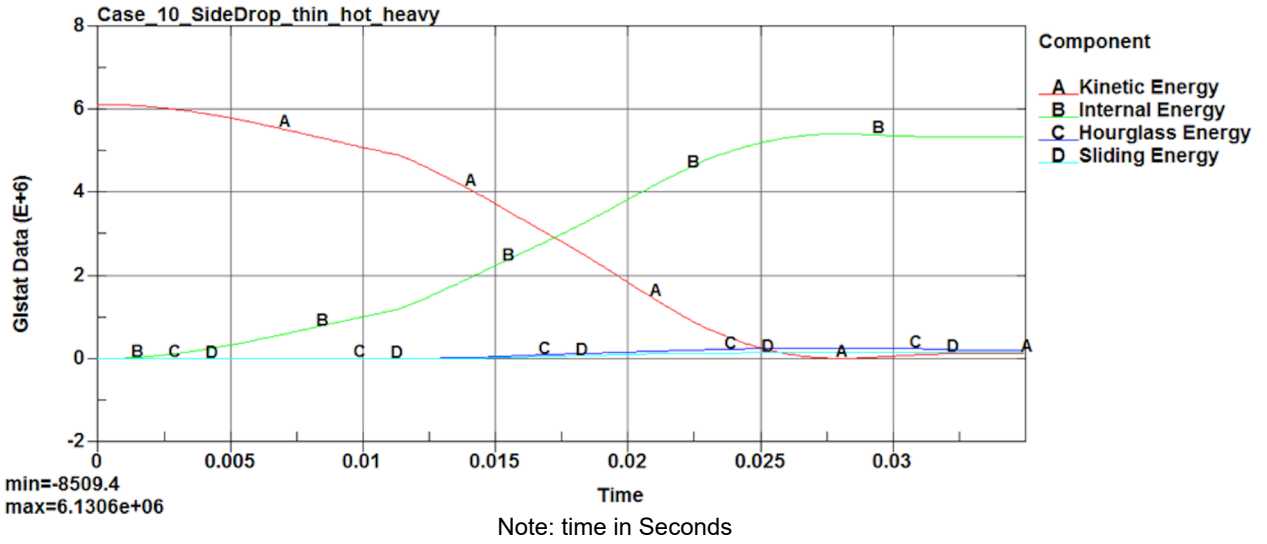


Figure 2.12.1.11-39. Case 10 Impact Energy Plot

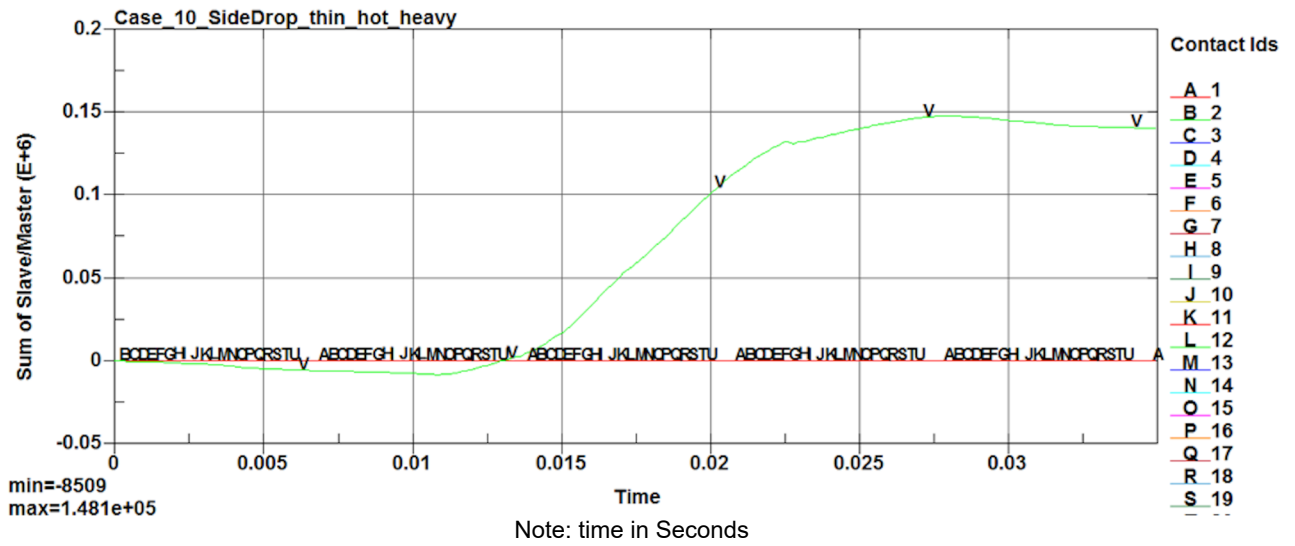


Figure 2.12.1.11-40. Case 10 Interface Sliding Energy Time History

2.12.1.11.11. Case 11 Corner Drop with Thick Shell, Cold Condition and Light Payload

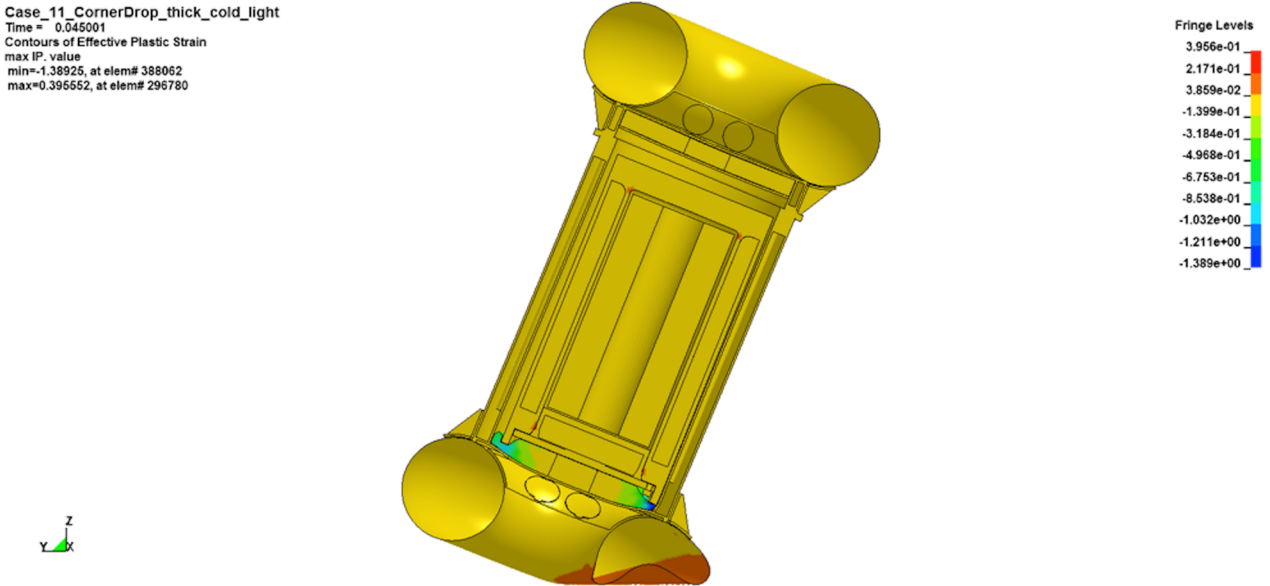


Figure 2.12.1.11-41. Case 11 Deformed Overpack Shape (Effective Plastic Strain)

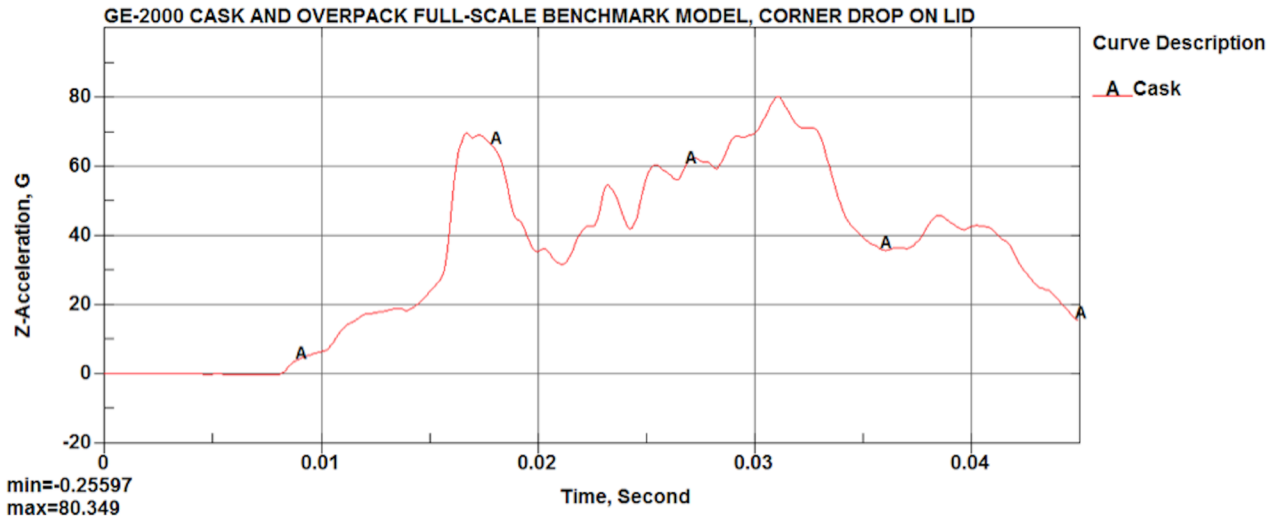


Figure 2.12.1.11-42. Case 11 Payload Acceleration Time History

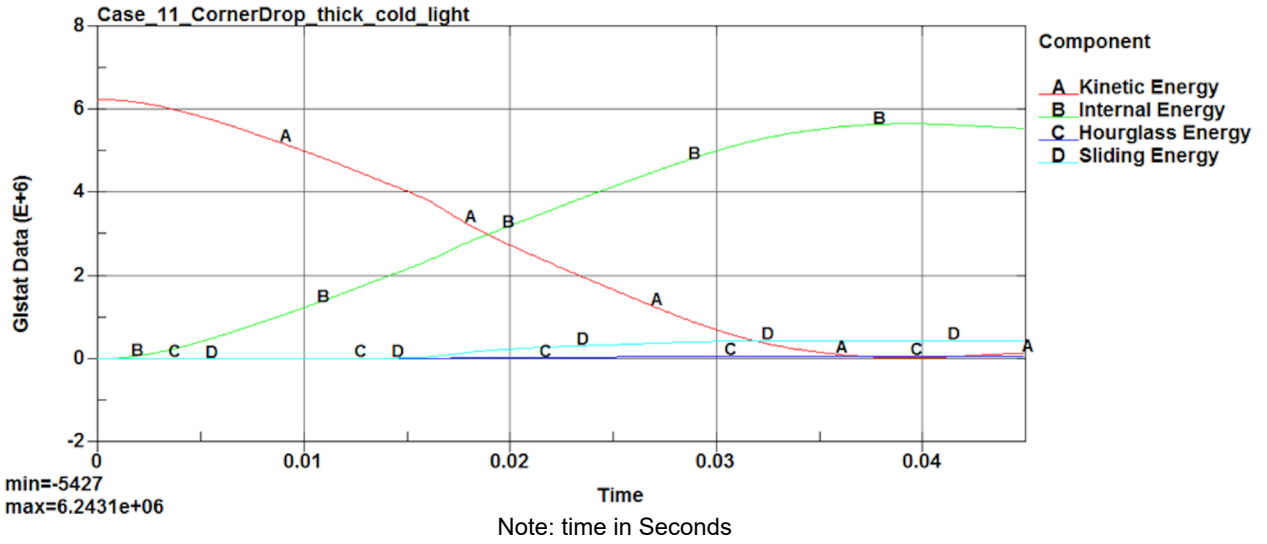


Figure 2.12.1.11-43. Case 11 Impact Energy Plot

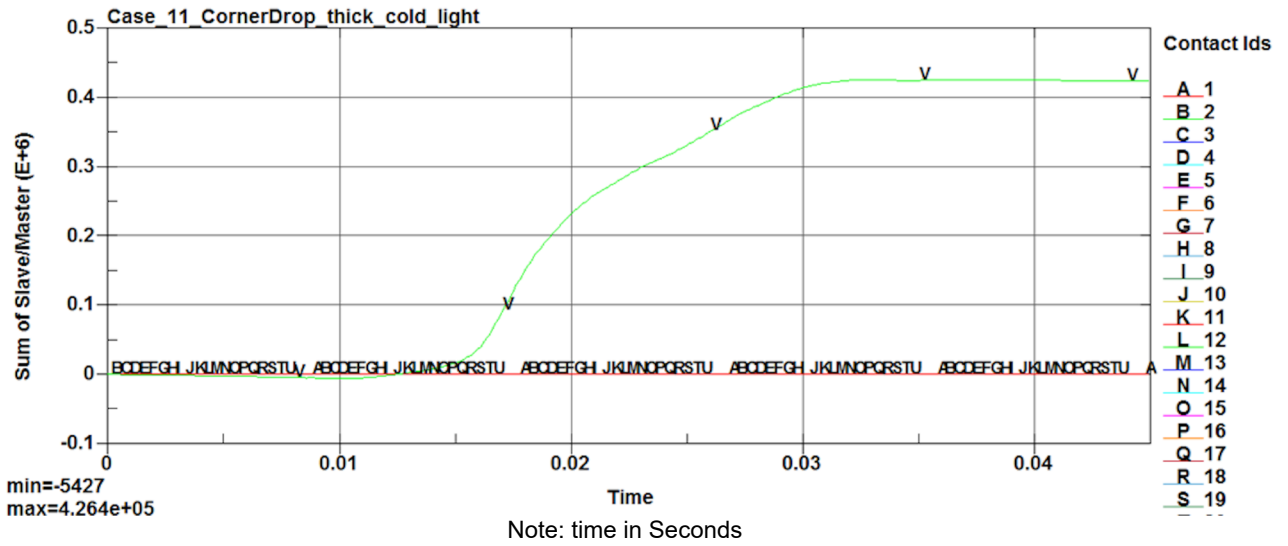


Figure 2.12.1.11-44. Case 11 Interface Sliding Energy Time History

2.12.1.11.12. Case 12 Corner Drop with Thin Shell, Hot Condition and Heavy Payload

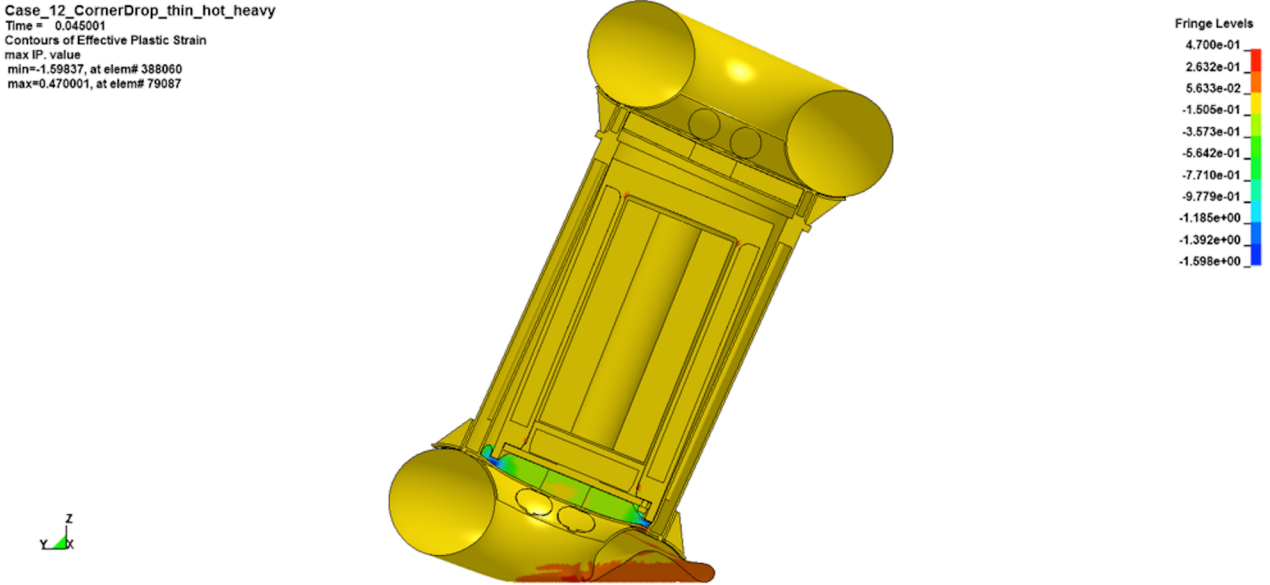


Figure 2.12.1.11-45. Case 12 Deformed Overpack Shape (Effective Plastic Strain)

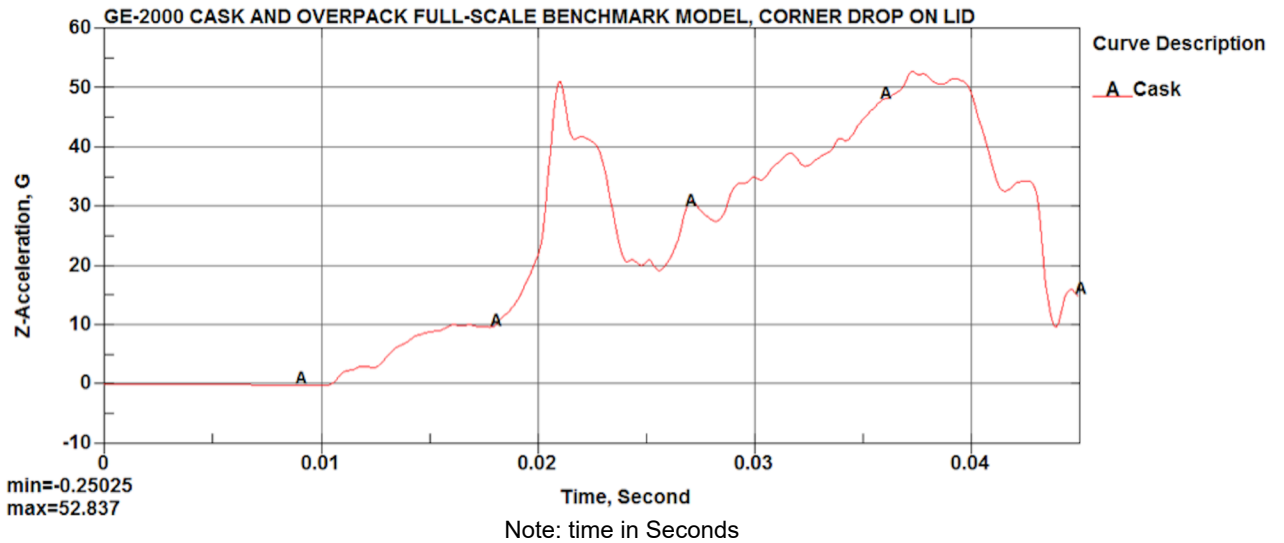


Figure 2.12.1.11-46. Case 12 Payload Acceleration Time History

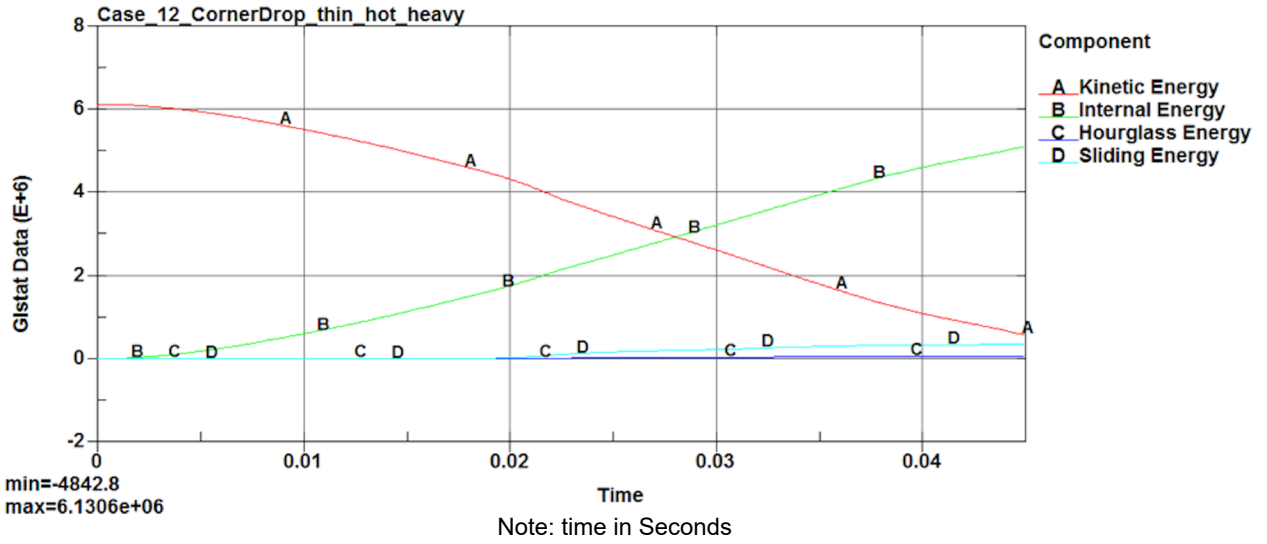


Figure 2.12.1.11-47. Case 12 Impact Energy Plot

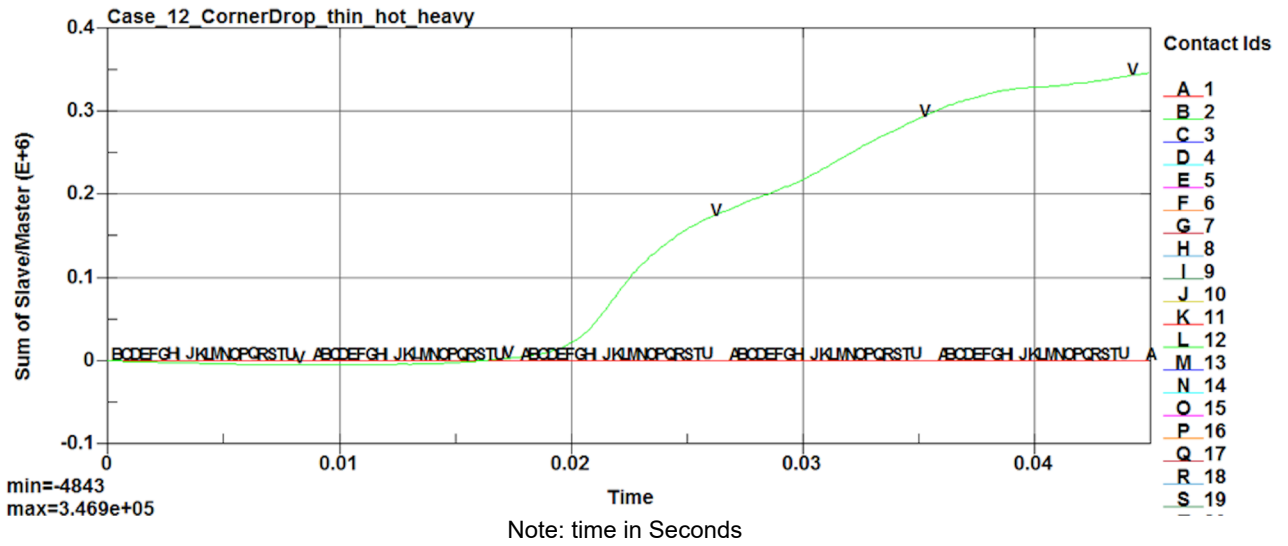


Figure 2.12.1.11-48. Case 12 Interface Sliding Energy Time History

2.12.1.11.13. Case 13 Slapdown Drop (5°), Thick Shell, Ambient Condition and Nominal Payload

Case_13_SlapDown_Thick_ambient_normal
 Time = 0.035
 Contours of Effective Plastic Strain
 max IP. value
 min=-0.192596, at elem# 387736
 max=0.453218, at elem# 398568

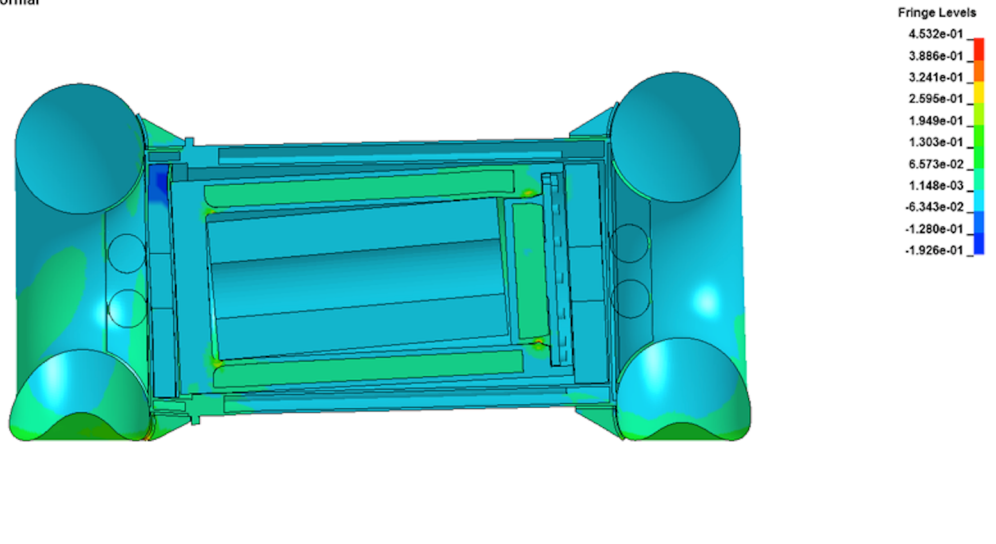


Figure 2.12.1.11-49. Case 13 Deformed Overpack Shape (Effective Plastic Strain)

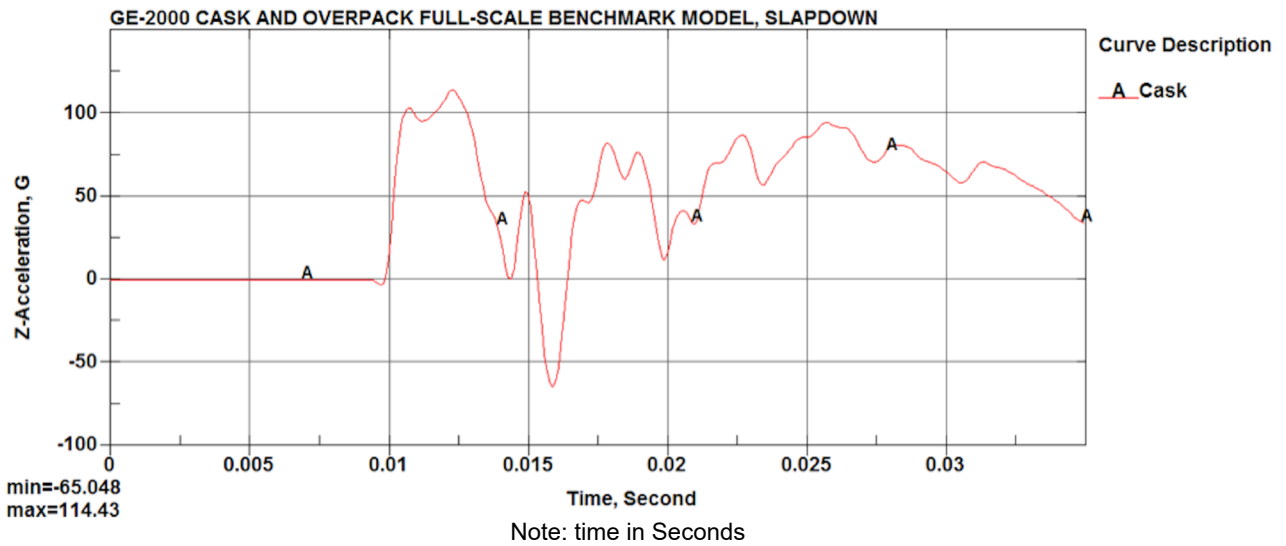


Figure 2.12.1.11-50. Case 13 Payload Acceleration Time History

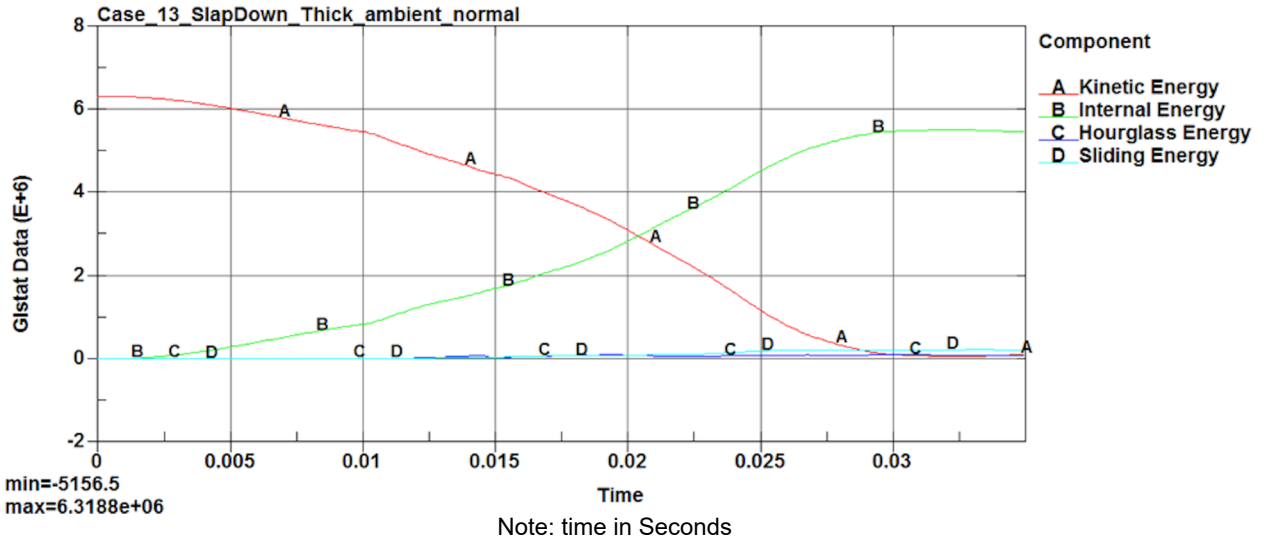


Figure 2.12.1.11-51. Case 13 Impact Energy Plot

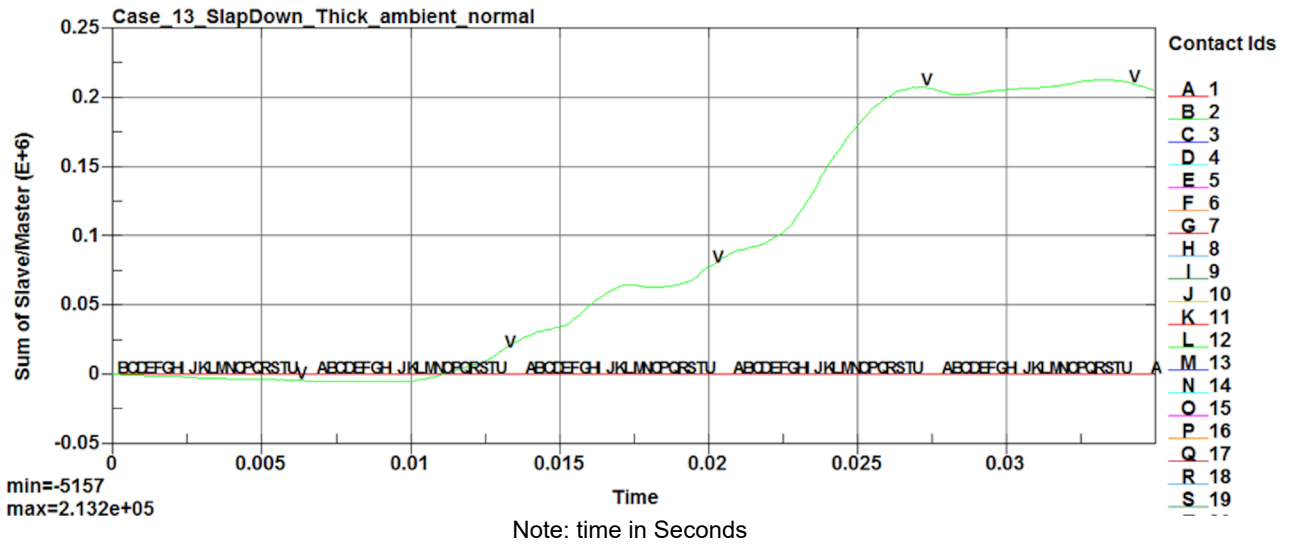


Figure 2.12.1.11-52. Case 13 Interface Sliding Energy Time History

2.12.1.11.14. Case 14 Slapdown Drop (10°), Thick Shell, Ambient Condition and Nominal Payload

Case_14_SlapDown_thick_ambient_normal
 Time = 0.05
 Contours of Effective Plastic Strain
 max IP. value
 min=-0.582812, at elem# 387736
 max=0.446691, at elem# 777857

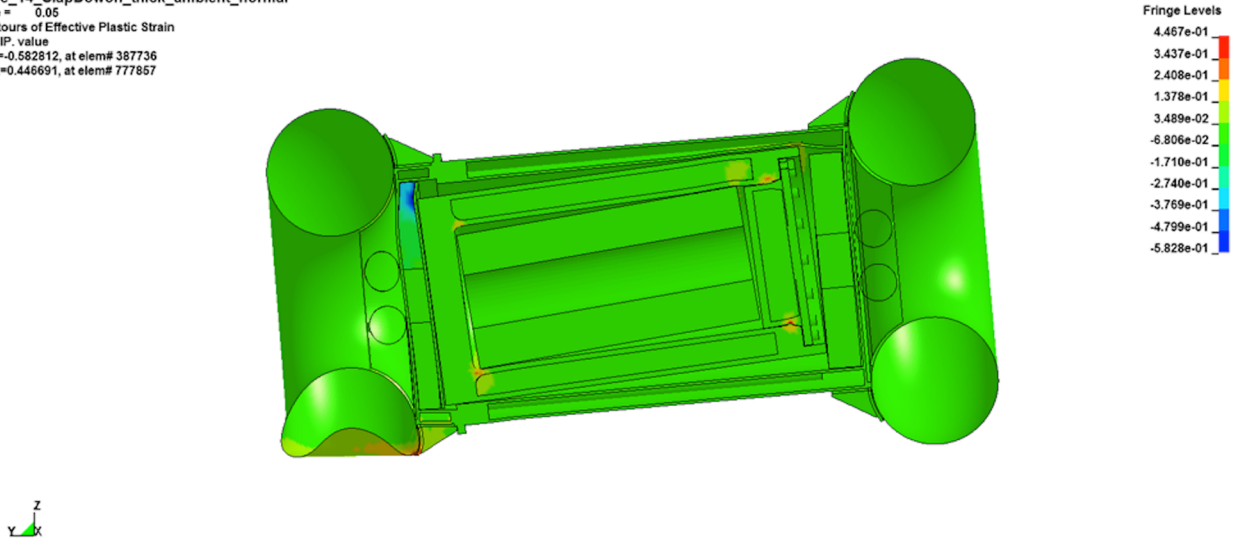


Figure 2.12.1.11-53. Case 14 Deformed Overpack Shape (Effective Plastic Strain)

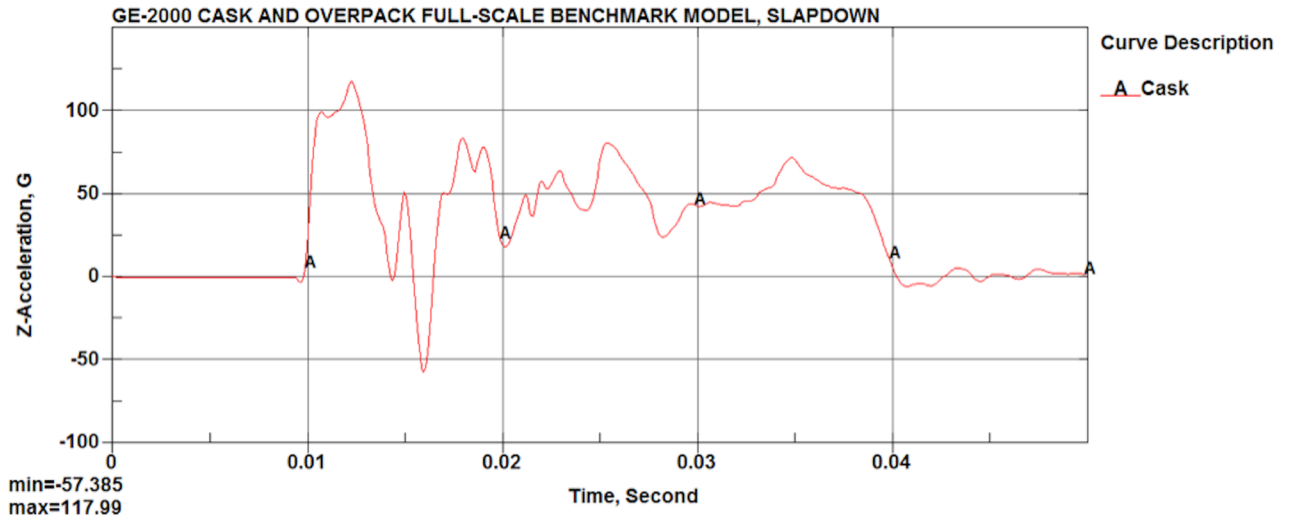


Figure 2.12.1.11-54. Case 14 Payload Acceleration Time History

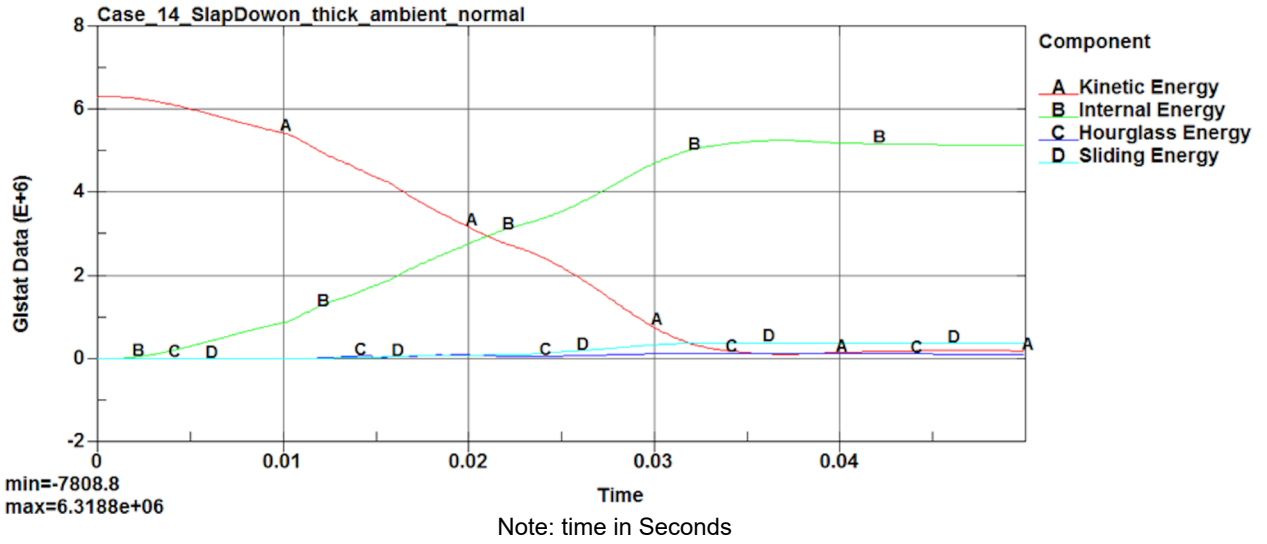


Figure 2.12.1.11-55. Case 14 Impact Energy Plot

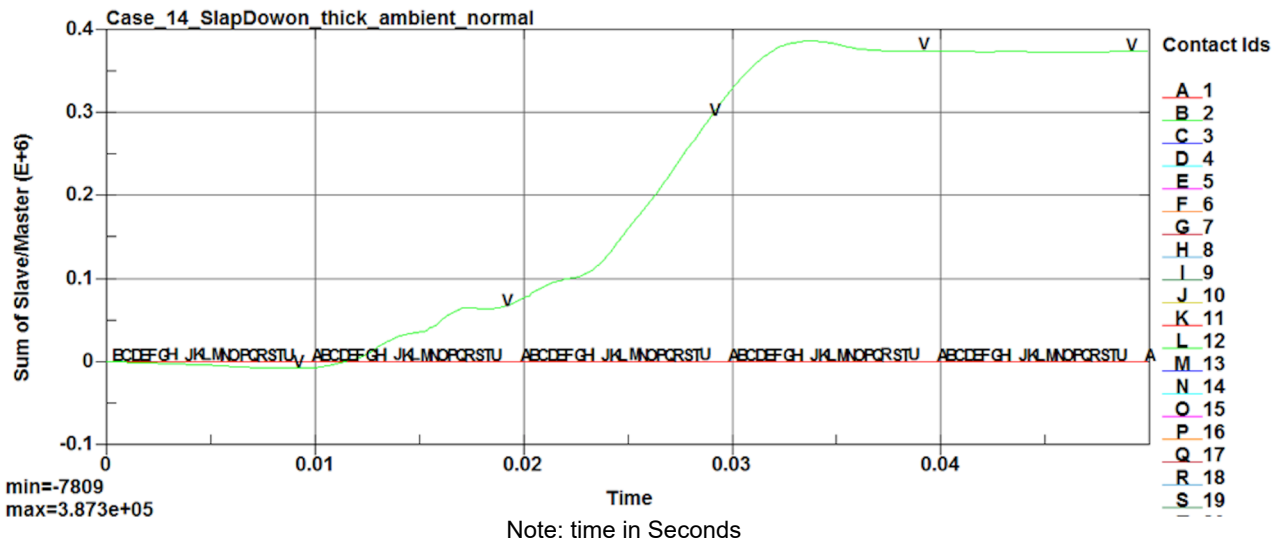


Figure 2.12.1.11-56. Case 14 Interface Sliding Energy Time History

2.12.1.11.15. Results for 30 ft Drop Followed and 40 in Pin Puncture Drop Sequence

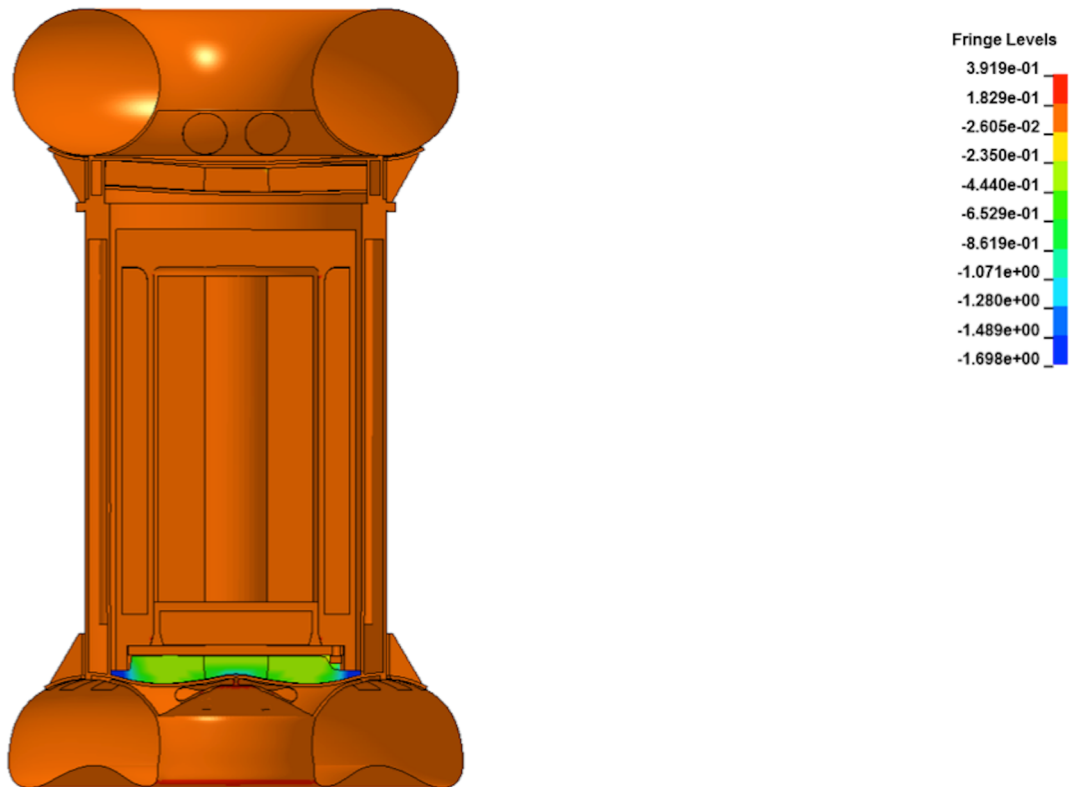


Figure 2.12.1.11-57. Strain Contour of Package after 30 ft End Drop and Pin Puncture Sequence

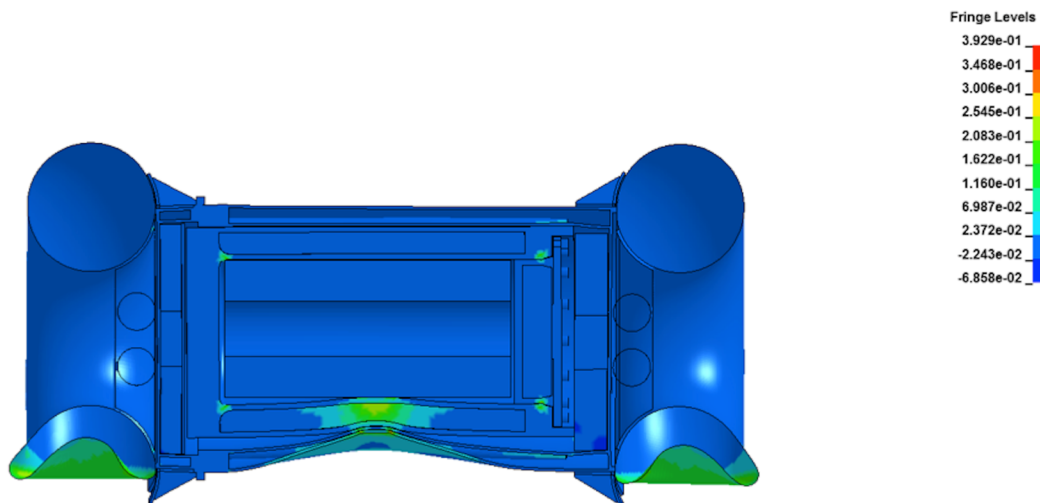


Figure 2.12.1.11-58. Strain Contour of Package after 30 ft Side Drop and Pin Puncture Sequence

2.12.1.12. Summary of Impact Analysis Results

Conservative impact analyses of the Model 2000 cask during the NCT and HAC impact events were performed to evaluate the performance of impact limiter design. This report summarizes the results of structural analyses of the Model 2000 Transport Package during NCT per 10 CFR 71.71 and HAC per 10 CFR 71.73. The summary of results for the bounding drop cases are presented in Table 2.12.1-1.

The worst-case HAC accelerations occur during the cold/thick/light side drop and the hot/thin/heavy bottom end drop. For the bottom end drop, the acceleration trend showed that the accelerations dropped until the honeycomb temperature was increased to 400°F and the honeycomb fully compresses. Because the average temperature of the honeycomb is less than 350°F, the honeycomb has sufficient capacity to protect the package during hot conditions.

The results of the evaluations presented in this section show that the Model 2000 overpack provides sufficient protection of the cask and contents.

2.12.1.12.1. Benchmark Tests

The peak accelerations of the benchmark analysis results from Drop Cases 1 through 3 are compared with the drop test results from Section 2.12.5 in Table 2.12.1-14.

Table 2.12.1-14. Comparison of Benchmark Simulations and Drop Tests Acceleration

Drop Case No.	Drop Configuration	LS-DYNA Analysis	Drop Test ¹ Measurements	Notes
1	30-ft End Drop	130.0 g	408/4 = 102 g	Quarter-scale model
2	30-ft Side Drop	157.0 g	Not available	Instrument failure, No result
3	30-ft Corner Drop	70.9 g	156/4 = 39 g	Quarter-scale model

Note: 1. Section 2.12.5.

The comparison of ¼-scale drop test deformation results and the LS-DYNA benchmark simulation is provided in Table 2.12.1-15.

Table 2.12.1-15. Comparison of Benchmark Simulations and Drop Tests Deformations

Drop Case No.	Drop Configuration	LS-DYNA Analysis	Drop Test ¹ Measurements
1	30-ft End Drop	3.5 in	2.255×4 = 9.0 in
2	30-ft Side Drop	9.4 in	3.18×4 = 12.7 in
3	30-ft Corner Drop	11.8 in	5.3×4 = 21.2 in

Note: 1. Section 2.12.5.

The comparison of measured accelerations and deformations with LS-DYNA analysis results for each drop orientation shows that the LS-DYNA model is stiffer, which results in higher accelerations.

2.12.1.12.2. Shallow Angle Drops—Slap Down

Two shallow angle drop simulations are also performed. The drop configurations include nominal payload at ambient temperature with thick toroidal shell thickness (t=0.76 inches) to compare with the side-drop test performed for the benchmarking test. The two shallow angles are 5° and 10° slapdown drops that are designated as Drop Cases 13 and 14. The results of shallow angle drops for the 0° (Drop Case 2, side drop), 5° (Drop Case 13) and 10° (Drop Case 14) conclude that the side drop (Drop Case 2) bounds the shallow angle cases with an acceleration of 157 g. Table 2.12.1-16 provides a summary of results for the shallow angle analyses.

Table 2.12.1-16. Comparison of Shallow Angle Drop Analyses

Drop Case No.	Shallow Angle Drop Angle	Peak Acceleration
2	0°	157.0 g
13	5°	115.0 g
14	10°	118.0 g

2.12.1.12.3. Pin Puncture

Besides the 30-foot drop configurations, two HAC drop configurations (side drop and end drop) are selected to perform the code-required pin puncture test, where the cask is dropped 30-feet and then followed by a drop height of 40 inches onto a rigid pin 6 inches in diameter. Evaluation of the pin puncture results shows that the maximum strain is limited to local area and will not result in the degradation of the containment boundary. As the figures show, the maximum strain is 39%. However, review of results show the maximum strain is limited to local deformation of the overpack. The maximum strain in the outer shell of the cask is 31% and limited to the puncture area. Therefore, no gross deformations of the cask are predicted. Additionally, results for the combined 30-foot impact and pin puncture are used as input for the HAC thermal evaluation.

2.12.1.12.4. Containment Integrity

Based on the analyses presented in the calculation, there are no gross structural deformations of the cask body or containment boundary. Therefore, the containment integrity of the cask is maintained.

2.12.2. Lead Slump Calculation

The following sections provide a detailed analysis for lead slump. Section 2.12.2.1 assesses the thermal expansion of the lead at the operating temperature of the lead shielding. Subsequently, in Sections 2.12.2.2 and 2.12.2.3, the shielding capability of the Model 2000 cask is evaluated for the potential of lead slump during a bottom end drop using classic methods to support the shielding analysis assumptions. Further, Sections 2.12.2.4 through 2.12.2.6 assess the thermal contraction of the lead and the lead deformation that results at the NCT extreme cold ambient temperature of -40°F (-40°C).

2.12.2.1. Thermal Expansion of Lead Shielding at Operating Temperature

It is possible that during fabrication an air gap will develop between the lead and the outer steel shell of the cask (Reference 2-24), which could potentially result in a lead slump condition, meanwhile noting that the lead is inspected during fabrication. However, during NCT the operating temperature of the lead is taken at 500°F (260°C) (see Section 3.3.1.1) to envelope all conditions. The change in the outer radius of the lead shield due to thermal expansion is calculated as follows:

$$r_{\text{final}} = r_0 (1 + \alpha\Delta T) = 18.40 \text{ in (467.4 mm)}$$

where

$$\begin{aligned} r_0 &= 18.25 \text{ in} \\ &= \text{Outside radius of lead shield} \\ \alpha &= 1.90 \times 10^{-5} \text{ in/in/}^\circ\text{F} \\ &= \text{Coefficient of thermal expansion at } 500^\circ\text{F} \\ \Delta T &= 500^\circ\text{F} - 70^\circ\text{F} = 430^\circ\text{F} \\ &= \text{Temperature difference} \end{aligned}$$

NOTE: Coefficient of thermal expansion for lead extrapolated from data provided in Section 2.2.1.

For the outer steel shell the thermal expansion for the inside radius is:

$$r_{\text{final}} = r_i (1 + \alpha\Delta T) = 18.33 \text{ in (465.6 mm)}$$

where

$$\begin{aligned} r_i &= 18.25 \text{ in} \\ &= \text{Inside radius of steel shell} \\ \alpha &= 9.70 \times 10^{-6} \text{ in/in/}^\circ\text{F} \\ &= \text{Coefficient of thermal expansion at } 500^\circ\text{F} \\ \Delta T &= 500^\circ\text{F} - 70^\circ\text{F} = 430^\circ\text{F} \\ &= \text{Temperature difference} \end{aligned}$$

Comparing the final outside radius of the lead shield to the inner radius of the outer shell, the difference is -0.07000 inches (1.800 mm), which indicates that the lead expands more than the steel shell during NCT. Further, this demonstrates the temperature sensitivity of lead and steel at high temperatures. Relative expansion of the lead exceeds the expansion of the steel. Therefore, any existing gap that may have formed during fabrication will close, minimizing the potential for lead slump.

2.12.2.2. Compressive Stress in Lead Slump During Bottom End Drop

The previous section shows that the relative change in thermal expansion does not create a void. However, if the lead shield column did not bond to the mating steel shells during the fabrication process, compressive stress will develop in the column. The maximum stress occurs at the bottom of the column and progressively decreases as the elevation increases. The maximum compressive stress is

$$\sigma_{\max} = \frac{P}{A} = 3,613.6 \text{ psi}$$

where

- P = Total load
- = $W \times G = 1.476 \times 10^6 \text{ lb}$
- = Weight of lead shield
- W = $V \times \rho = 9370.2 \text{ lb}$
- V = Volume of lead shield
- = $A \times h = 22870.8 \text{ in}^3$
- A = Cross-sectional area of lead shield
- = $\pi(r_o^2 - r_i^2) = 408.4 \text{ in}^2$
- r_o = Outside radius of lead shield
- = 18.25 in
- r_i = Inside radius of lead shield
- = 14.25 in
- h = Height of lead column
- = 56 in
- ρ = Density of lead
- = 0.4097 lb/in³
- G = End drop acceleration
- = 157.5 g

NOTE: Value for the height of the lead column is rounded up to the nearest integer for conservatism.

Table 2.12.2-1 shows the stresses varying along the length of the lead column. The yield strength at 500°F is 189 psi. However, lead is sensitive to the strain-rate effects of the material. During the end drop, the estimated strain-rate is 12 in/in/sec (see Section 2.12.1). The yield strength varies from 823 psi at 0.002 in/in to 6,279 psi at 0.30 in/in. Therefore, during the end drop if yielding of the lead occurs it is localized to a small region near the bottom of the column.

NOTE: Yield strength of lead shielding at 500°F is extrapolated from data provided in Section 2.2.1.

2.12.2.3. Elastic Deformation During Bottom Impact

The elastic deformation is calculated assuming the cask lead shield column is unsupported by the steel inner and outer shells during an end drop event. The response of the lead shield is determined by multiplying the shield weight by the HAC end drop acceleration of 1,57.5 g. Therefore, an estimate of lead slump during HAC free drop conditions is (Reference 2-19):

$$y_{\max} = \frac{P}{k} = 0.075 \text{ in (1.91 mm)}$$

where

- k = Effective stiffness of the lead shield
 = $\frac{A \times G}{h} = 1.98 \times 10^7 \text{ lb/in}$
- G = Bulk modulus of lead
 = $\frac{E}{3(1-2\nu)} = 2.72 \times 10^6 \text{ psi}$
- A = Cross-sectional area of lead shield
 = $\pi(r_o^2 - r_i^2) = 408.4 \text{ in}^2$
- W = Weight of lead shield
 = 9370.2 lb
- P = Total load
 = $W \times g = 1.476 \times 10^6 \text{ lb}$
- g = End drop acceleration
 = 157.5 g
- h = Height of lead column
 = 56 in
- E = $1.63 \times 10^6 \text{ psi}$
 = Modulus of elasticity of lead at 500°F
- ν = Poisson’s ratio for lead
 = 0.4

The calculation shows that this estimate of lead slump is small for an unsupported lead shield. With the lead fully supported by the inner and outer shells of the cask, the actual lead slump is even smaller.

Table 2.12.2-1. Compressive Stress in Lead Shield

Column Height from Bottom	Compressive Stress / G (psi)	Compressive Stress (psi)
55.0	0.4	64.5
50.0	2.5	387.2
45.0	4.5	709.8
40.0	6.6	1032.4
35.0	8.6	1355.1
30.0	10.7	1677.7
25.0	12.7	2000.4
20.0	14.7	2323.0

2.12.2.4. Axial Thermal Expansion at NCT Extreme Cold Ambient Temperature

A small gap occurs at the top of the lead column when the cask is exposed to the extreme cold temperature of -40°F (-40°C) per the NRC requirements of 10 CFR 71.71 (c)(2). This is due to changes at the molecular level that cause the materials to contract. This reduction in the height of the lead shield is represented by the following equation:

$$h_{\text{lead}} = h_{0\text{-lead}} (1 + \alpha_{\text{lead}} \Delta T) = 55.904 \text{ in (1420.0 mm)}$$

where

$$\begin{aligned} h_{0\text{-lead}} &= \text{Initial lead shield height} \\ &= 56 \text{ in} \\ \alpha_{\text{lead}} &= \text{Lead coefficient of thermal expansion at } -40^{\circ}\text{F} \\ &= 1.56\text{E-}05 \text{ in/in/}^{\circ}\text{F} \\ \Delta T &= \text{Temperature difference} \\ &= -40^{\circ}\text{F} - 70^{\circ}\text{F} = -110^{\circ}\text{F} \end{aligned}$$

The same calculation can be made to determine the reduction in the height of the steel shells:

$$h_{\text{steel}} = h_{0\text{-steel}} (1 + \alpha_{\text{steel}} \Delta T) = 55.95 \text{ in (1421.1 mm)}$$

where

$$\begin{aligned} h_{0\text{-steel}} &= \text{Initial steel shell height} \\ &= 56 \text{ in} \\ \alpha_{\text{steel}} &= \text{Steel coefficient of thermal expansion at } -40^{\circ}\text{F} \\ &= 8.09\text{E-}06 \text{ in/in/}^{\circ}\text{F} \\ \Delta T &= \text{Temperature difference} \\ &= -40^{\circ}\text{F} - 70^{\circ}\text{F} = -110^{\circ}\text{F} \end{aligned}$$

2.12.2.5. Radial Thermal Expansion at NCT Extreme Cold Ambient Temperature

The radial gaps that occur during exposure to NCT extreme cold conditions can also be calculated in a similar manner by taking the initial radius prior to exposure and then adding the change in radius due to thermal expansion. The outside radius of the lead shield at -40°F is:

$$r_o = r_{0\text{-outer}}(1 + \alpha_{\text{lead}} \Delta T) = 18.22 \text{ in (462.8 mm)}$$

where

$$\begin{aligned} r_{0\text{-outer}} &= \text{Initial outside radius of the lead shield} \\ &= 18.25 \text{ in (463.6 mm)} \end{aligned}$$

Accordingly, the inside radius of the lead shield at -40°F is:

$$r_i = r_{0\text{-inner}}(1 + \alpha_{\text{lead}} \Delta T) = 14.23 \text{ in (361.3 mm)}$$

where

$$\begin{aligned} r_{0\text{-inner}} &= \text{Initial inside radius of the lead shield} \\ &= 14.25 \text{ in (362 mm)} \end{aligned}$$

Now the decrease in radius is evaluated for the steel shells starting with the inside radius of the outer steel shell at -40°F:

$$R_o = R_{0\text{-outer}} (1 + \alpha_{\text{steel}} \Delta T) = 18.23 \text{ in (463.1 mm)}$$

where

$$\begin{aligned} R_{0\text{-outer}} &= \text{Initial inside radius of the outer steel shell} \\ &= 18.25 \text{ in (463.6 mm)} \end{aligned}$$

The decrease in the outside radius of the inner steel shell at -40°F is:

$$R_i = R_{0\text{-inner}} (1 + \alpha_{\text{steel}} \Delta T) = 14.24 \text{ in (361.6 mm)}$$

where

$$\begin{aligned} R_{0\text{-inner}} &= \text{Initial outside radius of the inner steel shell} \\ &= 14.25 \text{ in (362 mm)} \end{aligned}$$

2.12.2.6. Lead Slump Due to Impact After NCT Extreme Cold Ambient Temperature

A small gap occurs during extreme cold exposure due to the contraction of components in relation to each other as determined by the calculations in the previous section. In order to determine the magnitude of lead slump, the reduced height of the lead column based on the net gap is calculated and then the difference between the reduced height of the lead column and the height of the annular region is taken. The volume of the lead column at the extreme cold conditions (-40°F) is:

$$\begin{aligned} V_{f\text{-lead}} &= A_{f\text{-lead}} \times h_{\text{lead}} \\ &= (407.011 \text{ in}^2 \times 55.904 \text{ in}) = 22,753.59 \text{ in}^3 \text{ (3.73E+08 mm}^3\text{)} \end{aligned}$$

where

$$\begin{aligned} A_{f\text{-lead}} &= \pi(r_o^2 - r_i^2) \\ &= \pi[(18.22 \text{ in})^2 - (14.23 \text{ in})^2] = 407.011 \text{ in}^2 \text{ (262,587.22 mm}^2\text{)} \end{aligned}$$

The cross-sectional area of the annulus between the outer and inner steel shells at -40°F is:

$$\begin{aligned} A_{\text{annulus}} &= \pi(R_o^2 - R_i^2) \\ &= \pi[(18.23 \text{ in})^2 - (14.24)^2] = 407.68 \text{ in}^2 \text{ (263,018.83 mm}^2\text{)} \end{aligned}$$

The reduced height of the lead column when taking into account impact after contraction of components is:

$$\begin{aligned} h_{\text{final}} &= \frac{V_f}{A_{\text{annulus}}} \\ &= \frac{22,753.59 \text{ in}^3}{407.68 \text{ in}^2} = 55.81 \text{ in (1417.57 mm)} \end{aligned}$$

Taking the difference between the reduced height of the lead shielding and the height of the annular region, the lead deformation due to impact after NCT extreme cold (-40°F) is:

$$\begin{aligned} h_{\text{slump}} &= h_{\text{steel}} - h_{\text{final}} \\ &= 55.95 \text{ in} - 55.81 \text{ in} = 0.14 \text{ in (3.56 mm)} \end{aligned}$$

2.12.3. Lifting and Tie-Down Analysis

2.12.3.1. Model 2000 Transport Package Lifting Analysis

The purpose and scope of this analysis is to demonstrate the structural integrity of the lifting ears and lid-lifting lug on the Series 2000 shielded shipping casks.

There are two types of ear designs employed during the handling of the Model 2000 cask, standard and auxiliary (see Figure 2.12.3-1). The ear design identified as standard is used for crane and fork truck lifting, and only one pair is required for these operations. The auxiliary ear is used in crane lifting only, and two pairs or four ears are required. The user may combine the different types of ears as follows:

1. 2 Standard/2 Auxiliary
2. 4 Auxiliary
3. 2 Standard

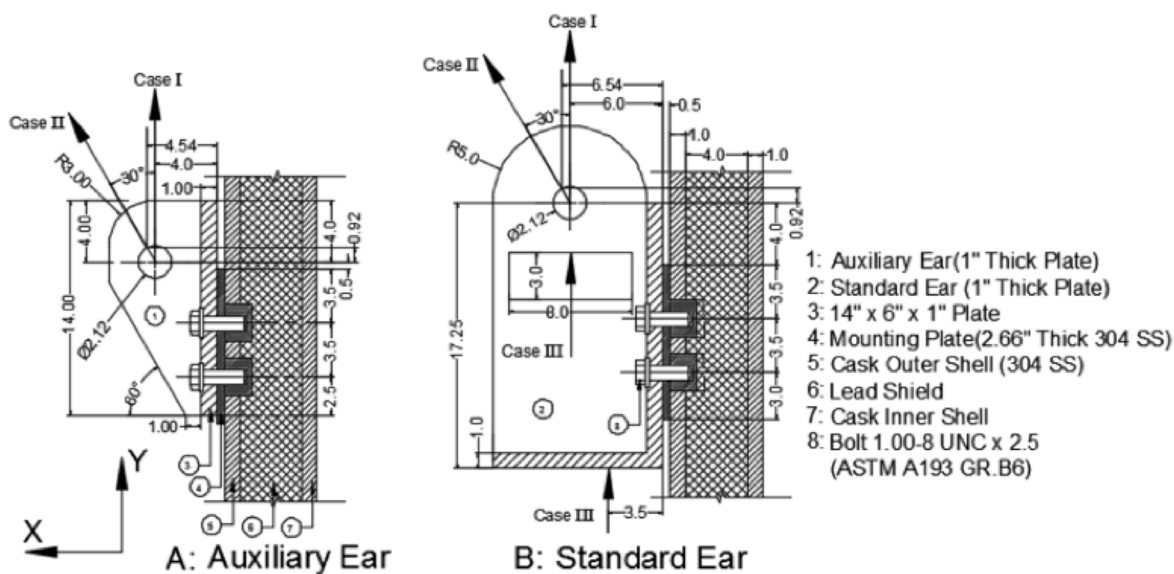


Figure 2.12.3-1. Structural Locations for Ear Analysis

Both ear designs (Auxiliary and Standard) are attached to the cask outer shell by means of four ASTM A193-B6 1-8 UNC-2-1/2 attaching bolts; only two bolts are shown. Also on this figure, the line of action of the different lifting forces is drawn. The different lifting forces are: Case I, straight up by crane; Case II, angular lift 30° from vertical, also by crane; and Case III, fork truck lift at two different points on the standard ear only. This analysis mainly considers Case II and I. The loading conditions are the following:

- The design rated load, W, shall be 23,630 pounds. This includes the dead weight of the cask (1 body, lid, 2 standard ears, and 2 auxiliary ears) and the cask payload including the liner.
- The two pairs of auxiliary ears (Auxiliary) are to support 3W such that the lifting cable does not make an angle of more than +30° measured from the vertical.

- The pair of standard ears (Standard) is to support 3W.
- These ears are removed from the cask during transport and are shipped separately.

Material properties are based upon 250°F for the outer cask. The 249°F temperature is the maximum temperature under normal conditions for the cask outer surface. Both types of ears, standard and auxiliary, and the cask outer shell are ASTM A240, Type 304 stainless steel. The attaching bolt material is ASTM A193-B6.

The standard ear individual load is obtained by dividing the weight of the cask and content (23,630 lbs.) by 2 (only two standard ears are used), and multiplying the resulting value by 3. The auxiliary ear load is obtained in a similar manner with the weight divided by 4 instead of 2 because 4 ears are used when this design is employed. Case III represents the fork truck loading condition on the standard ear, and it has a magnitude equal to that of Case I for the standard ear. Case III loading is not shown in Figure 2.12.3-2.

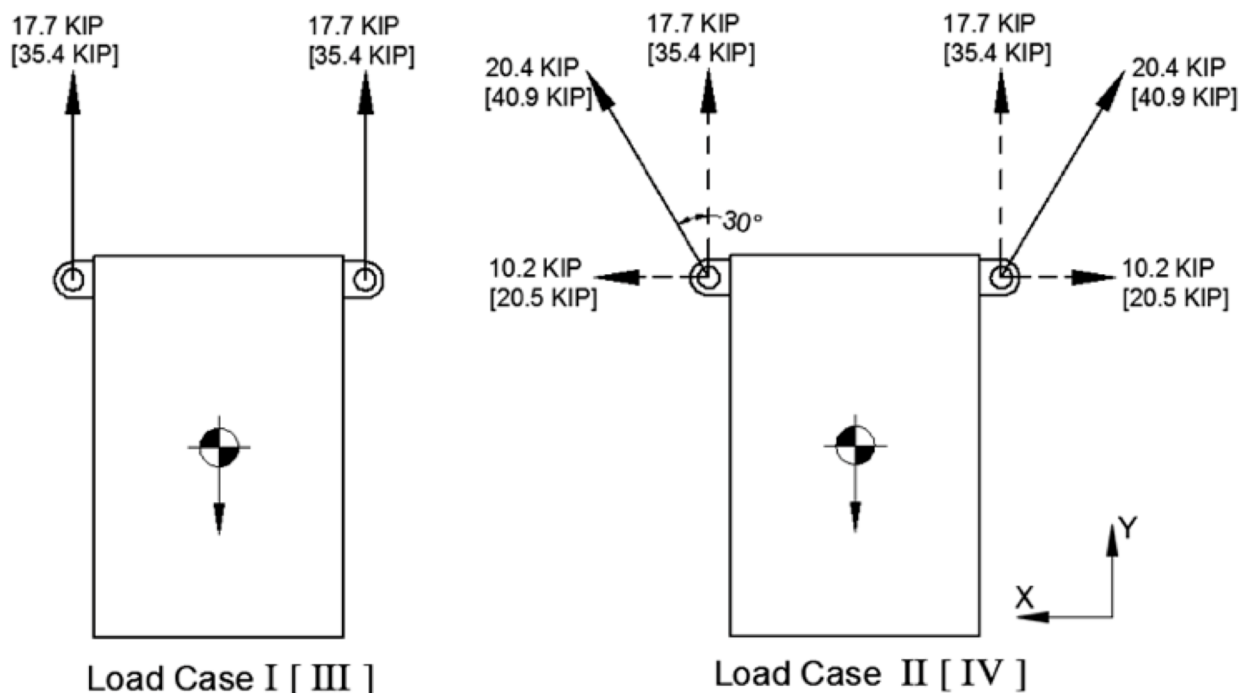


Figure 2.12.3-2. Magnitude and Direction of Loading in Model 2000 Cask

The following modes of failure are investigated for both ear designs:

- Shear tearout of lifting hole
- Tensile failure of ear plate
- Bearing of shackle pin on ear
- Yielding of weld joint
- Yielding of attaching bolt
- Shearing of bolt threads
- Shearing of tapped threads
- Yielding of cask outer shell

- SHEAR TEAR-OUT OF LIFTING HOLE-AUXILIARY AND STANDARD DESIGNS

Auxiliary Ear Design

For Load Case I, the shear tearout stress is computed as follows:

$$\tau = \frac{F}{A} \quad \text{Reference 2-25 page 89.}$$

where

$$F = 17.7 \text{ kip (see Figure 2.12.3-2) and}$$

$$A = \text{cross sectional area along the force line of action}$$

$$= \left(4 - \frac{2.12}{2}\right) \times 1 \quad (\text{see Figure 2.12.3-1}) = 2.94 \text{ in}^2$$

$$\tau = \frac{F}{A} = \frac{17.7}{2.94} = 6.02 \text{ ksi} < 15 \text{ ksi}$$

Standard Ear Design

For Load Case I, the shear tearout stress is:

$$\tau = \frac{F}{A} = \frac{35.4}{\left(5 - \frac{2.12}{2}\right) \times 1} = 8.98 \text{ ksi} < 15 \text{ ksi}$$

• TENSILE FAILURE OF EAR PLATE

Auxiliary Ear Design

In order to compute tensile failure for Load Case II, the internal forces that react to the lifting force are resolved into planes containing the minimum ligament cross-sectional area, as illustrated in Figure 2.12.3-3.

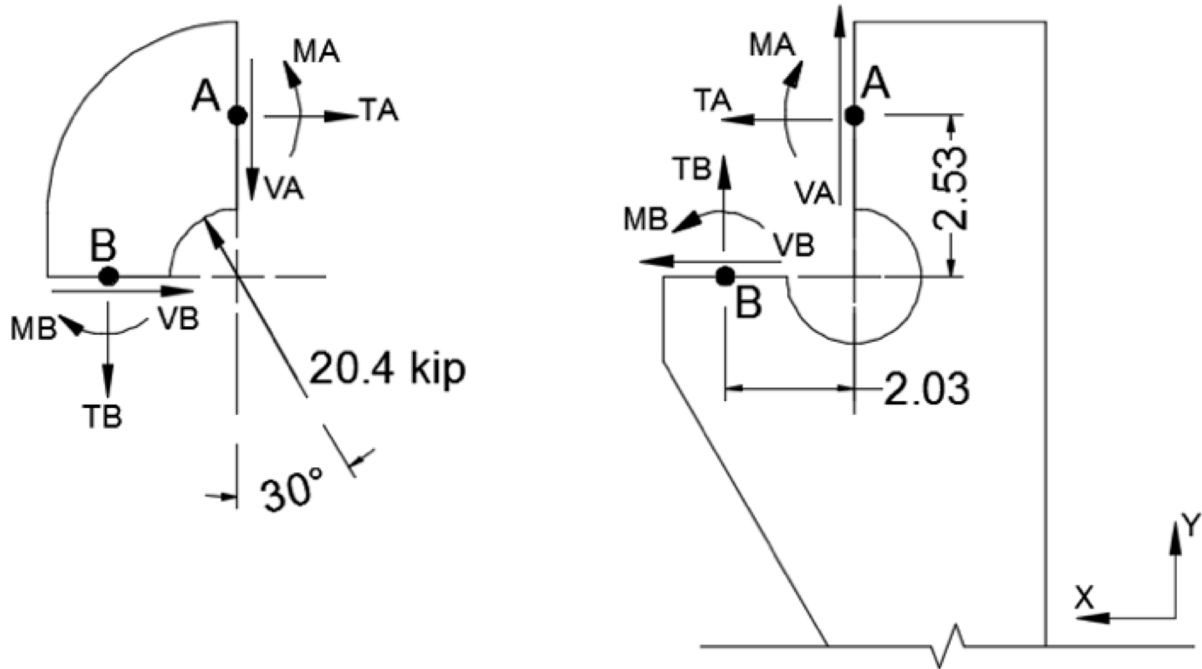


Figure 2.12.3-3. Ear Hole Cross Section

$$\begin{aligned} FH &= 20.4 (\sin 30^\circ) = 10.2 \text{ kip} \\ FV &= 20.4 (\cos 30^\circ) = 17.7 \text{ kip} \end{aligned}$$

Equilibrium:

$$\text{Eq. I} \quad \sum M_o = 0 = MA - MB - 2.53 TA + 2.03TB$$

$$\text{Eq. II} \quad \sum FV = 0 = 17.7 - VA - TB$$

$$\text{Eq. III} \quad \sum FH = 0 = 10.2 - TA - VB$$

This is a statically indeterminate problem; however, by making some conservative simplifying assumptions, a solution may be obtained without resorting to indeterminate analysis methods. For the evaluation of primary stresses, we may conservatively assume $MA = MB = 0$. Also, on the basis of relative stiffness, $TA > VB$; consequently, it may be conservatively assumed that $TA = VB$. Therefore, we may write the following:

From Eq. III,

$$TA = VB = \frac{10.2}{2} = 5.1 \text{ kip}$$

From Eq. I,

$$TB = \frac{2.53}{2.03} TA = 6.35 \text{ kip}$$

From Eq. II,
$$VA = 17.7 - TB = 11.35 \text{ kip}$$

The principal stresses will now be calculated at point A.

From Reference 2-25, page 81, the principal stresses are calculated using:

$$\sigma_1, \sigma_2 = \frac{\sigma}{2} \pm \sqrt{\left(\frac{\sigma}{2}\right)^2 + \tau^2}$$
$$\sigma = \frac{TA}{A} = \frac{5.1}{2.94} = 1.735 \text{ ksi}$$
$$\tau = \frac{VA}{A} = \frac{11.35}{2.94} = 3.86 \text{ ksi}$$
$$\sigma_1 = \frac{1.735}{2} + \sqrt{\left(\frac{1.735}{2}\right)^2 + 3.86^2} = 4.82 < 23.7 \text{ ksi}$$

Standard Ear Design

Load Case I or III

Standard ear dimensions and loading are shown in Figure 2.12.3-4. The critical tensile section is at Section X-X, see Figure 2.12.3-4. The exact force distribution cannot be determined without a detailed analysis that would include all of the stiffness characteristics (e.g., a finite element analysis). However, it can be deduced that the limiting load at the critical section (i.e., point “A”) will not exceed P/2. Then the tensile stress is:

$$\sigma_T = \frac{P/2}{A} = \frac{35.4/2}{1 \times 1} = 17.7 \text{ ksi} < 23.7 \text{ ksi}$$

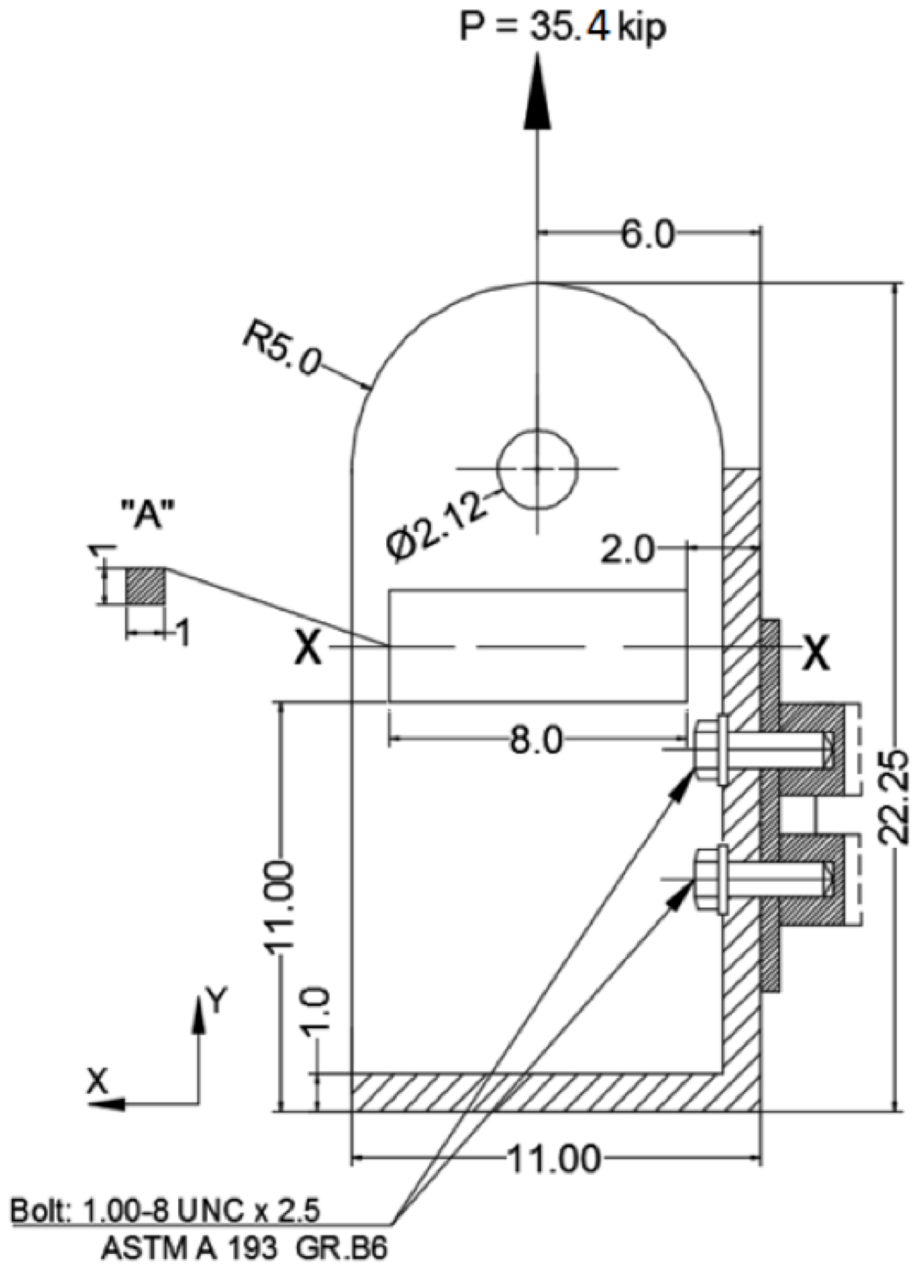


Figure 2.12.3-4. Standard Ear Load Case I or III

- BEARING OF SHACKLE PIN ON EAR

Auxiliary Ear Design

The bearing stress is computed assuming that the force is uniformly distributed over the projected contact area of the pin. This gives a stress:

$$\sigma = \frac{F}{A}$$

Where the projected area for the pin is $A = t \times d$. Here, t is the thickness of the ear plate (1") and d is the pin diameter (2").

$$\sigma = \frac{20.4}{1 \times 2} = 10.2 \text{ ksi} < 23.7 \text{ ksi}$$

Standard Ear Design

Case I

$$\sigma = \frac{35.4}{1 \times 2} = 17.7 \text{ ksi} < 23.7 \text{ ksi}$$

Case III

$$\sigma = \frac{35.4}{1 \times 7.5} = 4.72 \text{ ksi} < 23.7 \text{ ksi}$$

- YIELDING OF WELD JOINTS

Auxiliary Ear Design

Figure 2.12.3-5 shows a free-body diagram of the ear with the lifting force acting through the center of the hole for Load Case I and Case II. The center of gravity of the weld group and of the bottom of the bracket point A is G. The force F_G is the force of the weld group acting on the ear. Because F_G has a different line of action than the lifting force, there is also a moment M .

Load Case I

The moment M produces a bending stress in the welds. The force F_G produces shear throughout the weld. These effects are:

$$M = 17.7 \times 3 = 53.10 \text{ k-in}$$

$$F_G = 17.7 \text{ kip}$$

- WELD GEOMETRY AND CROSS SECTION PROPERTIES

Weld throat area (A_w)

$$A_w = 1.414 (0.375)(6.75 + 2.0 + 2.25) = 5.833 \text{ in}^2$$

Centroid of weld group (G)

$$\bar{Y} = \frac{\sum_1^3 (\bar{Y}_i A_i)}{\sum_1^3 A_i} = \frac{((1.125 \times 2.25 \times 0.375) + (4.75 \times 2 \times 0.375) + (10.625 \times 6.75 \times 0.375))}{(2.25 \times 0.375 + 2 \times 0.375 + 6.75 \times 0.375)} = 7.614 \text{ in}$$

Unit moment of inertia (I_u):

$$\begin{aligned} I_u &= \sum(I_o + A_i d_i^2) \\ &= 2 \times \left\{ \left(\frac{2.25^3}{12} + 2.25 \times 6.488^2 \right) + \left(\frac{2^3}{12} + 2 \times 2.863^2 \right) + \left(\frac{6.75^3}{12} + 6.75 \times 3.012^2 \right) \right\} \\ &= 399.17 \text{ in}^3 \end{aligned}$$

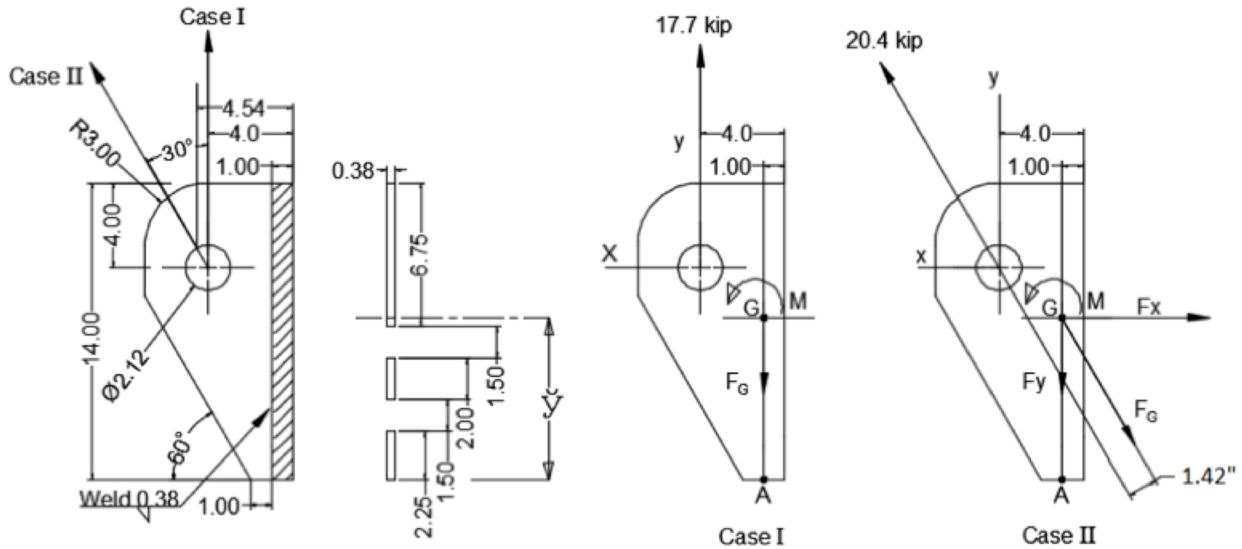


Figure 2.12.3-5. Auxiliary Ear, Case I and Case II Weld Stresses

Then the moment of inertia about an area through G parallel to area Z is:

$$I = 0.707 h I_u = 0.707 (0.375) (399.17) = 105.83 \text{ in}^4$$

For the weld metal the normal stress at point A:

$$\sigma_x = \frac{M c}{I} = \frac{53.10(7.614)}{105.83} = 3.82 \text{ ksi}$$

The shear stress is:

$$\tau_{xy} = \frac{F}{A} = \frac{17.7}{5.833} = 3.03 \text{ ksi}$$

The resulting Von Mises stress in the weld metal is:

$$\sigma' = \sqrt{\sigma_x^2 + 3\tau_{xy}^2} = \sqrt{3.82^2 + 3(3.03)^2} = 6.5 \text{ ksi} < 75 \text{ ksi}$$

CALCULATION OF STRESS IN THE PARENT METAL:

The area subject to shear is :

$$A = 0.375 (6.75 + 2.0 + 2.25) = 4.125 \text{ in}^2$$

$$\tau_{xy} = \frac{17.7}{4.125} = 4.29 \text{ ksi}$$

The section modulus of the ear at the weld interface is:

$$\frac{I}{C} = \frac{hI_u}{C} = \frac{0.375 \times 0.5 \times 399.17}{7.614} = 9.83 \text{ in}^3$$

Thus, the tensile stress at A in the parent metal is:

$$\sigma_x = \frac{M}{I/C} = \frac{53.10}{9.83} = 5.4 \text{ ksi}$$

$$\sigma' = \sqrt{\sigma_x^2 + 3\tau_{xy}^2} = \sqrt{5.4^2 + 3(4.29)^2} = 9.19 \text{ ksi} < 23.7 \text{ ksi}$$

Load Case II

Figure 2.12.3-5 (Case II) shows a free body diagram of the ear for the Load Case II.

The moment M produces a bending stress in the welds.

The force component Fx produces tension throughout the weld.

The force component Fy produces shear throughout the weld.

These effects are:

$$M = 20.4 (1.42) = 28.97 \text{ k-in.}$$

$$F_x = 10.2 \text{ kip}$$

$$F_y = 17.7 \text{ kip}$$

$$A_w = [(2.25 + 2 + 6.75) \times 0.375 \times 0.707] \times 2 = 5.833 \text{ in}^2$$

At the point A the bending stress and tensile stress due to Fx add. For the weld metal the total normal stress is:

$$\sigma_x = \frac{F_x}{A} + \frac{M_C}{I} = \frac{10.2}{5.83} + \frac{28.97(7.614)}{105.84} = 3.83 \text{ ksi}$$

The shear stress is:

$$\tau_{xy} = \frac{F_y}{A} = \frac{17.7}{5.83} = 3.03 \text{ ksi}$$

Thus, the Von Mises stress in the weld is:

$$\sigma' = \sqrt{\sigma_x^2 + 3\tau_{xy}^2} = \sqrt{3.83^2 + 3(3.03)^2} = 6.51 \text{ ksi} < 23.7 \text{ ksi}$$

The stresses in the parent metal are:

$$A_{pm} = (2.25 + 2 + 6.75) \times 0.375 = 4.125$$

$$\tau_{xy} = \frac{F_y}{A} = \frac{17.7}{4.125} = 4.29 \text{ ksi}$$

$$\sigma_x = \frac{F_x}{A} + \frac{M}{I/C} = \frac{10.2}{4.125} + \frac{28.97}{9.83} = 5.42 \text{ ksi}$$

$$\sigma' = \sqrt{\sigma_x^2 + 3\tau_{xy}^2} = \sqrt{5.42^2 + 3(4.29)^2} = 9.2 \text{ ksi} < 23.7 \text{ ksi}$$

Standard Ear Design

Figure 2.12.3-6 shows a detailed sketch of the standard ear design. It includes dimensions, weld lines identification diagram, and a free body diagram of the ear plate for load conditions Case I and Case II. The investigation of stress on the welds is conducted conservatively by considering only welds A and B are active, in this part the welds are analyzed for both load conditions Case I and Case II. Case III was not analyzed because the resultant force in this case acts along the same line of action as the force in Case I.

Load case I

Figure 2.12.3-6 (Case I) shows a free body diagram of the standard ear for Load Case I.

Centroid of weld group (\bar{Y})

$$\bar{Y} = \frac{\sum_1^2 (\bar{Y}_i A_i)}{\sum_1^2 A_i} = \frac{(2.25 \times 0.375 \times 0.19) + (15.87 \times 0.375 \times 7.935)}{2.25 \times 0.375 + 15.87 \times 0.375} = 6.97 \text{ in}$$

Unit moment of inertia (I_u):

$$\begin{aligned} I_u &= \sum (I_o + A_i d_i^2) \\ &= 2 \times \left\{ \left(\frac{15.87^3}{12} + 15.87 \times (7.935 - 6.97)^2 \right) + (2.25 \times 6.97^2) \right\} = 914.13 \text{ in}^3 \end{aligned}$$

Then the moment of inertia about an axis through G parallel to axis Z through the weld minimum effective throat is:

$$I = 0.707 h I_u = 0.707 \times (0.375) \times 914.13 = 242.36 \text{ in}^4$$

For the weld metal the normal stress at point A:

$$\sigma_x = \frac{Mc}{I} = \frac{35.4 (5) 6.97}{242.36} = 5.09 \text{ ksi}$$

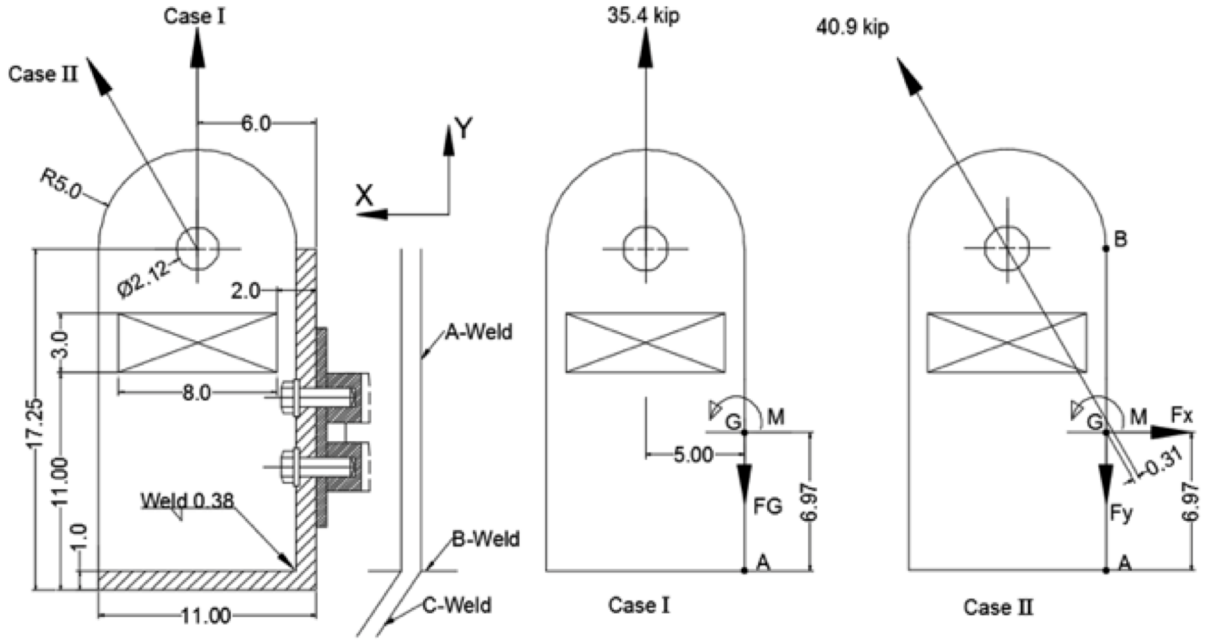


Figure 2.12.3-6. Standard Ear, Case I and Case II Weld Stresses

The shear stress is:

$$\tau_{xy} = \frac{F_G}{A} = \frac{35.4}{2(0.707)(2.25 \times 0.375 + 15.87 \times 0.375)} = 3.68 \text{ ksi}$$

The resulting von Mises stress in the weld metal is.

$$\sigma' = \sqrt{\sigma_x^2 + 3\tau_{xy}^2} = \sqrt{5.09^2 + 3(3.68)^2} = 8.16 \text{ ksi} < 23.7 \text{ ksi}$$

CALCULATION OF STRESS IN THE PARENT METAL:

The area subject to shear is:

$$A = 2 \times (0.375) \times (2.25 + 15.87) = 13.59 \text{ in}^2$$

Thus, the shear stress on the parent metal is:

$$\tau_{xy} = \frac{F_G}{A} = \frac{35.4}{13.77} = 2.6 \text{ ksi} < 13.7 \text{ ksi}$$

The section modulus of the ear plate at the weld interface is:

$$\frac{I}{C} = \frac{0.38 \times 914.33}{6.97} = 49.85 \text{ in}^3$$

Thus, the tensile stress at A in the parent metal is:

$$\sigma_x = \frac{35.4 (5)}{49.85} = 3.6 \text{ ksi}$$

$$\sigma' = \sqrt{\sigma_x^2 + 3\tau_{xy}^2} = \sqrt{3.6^2 + 3(2.6)^2} = 5.77 \text{ ksi} < 23.7 \text{ ksi}$$

Load Case II

Figure 2.12.3-6 (Case II) shows a free body diagram of the standard ear for Load Case II.

$$A = 2(0.707)(0.375)(2.25 + 15.87) = 9.61 \text{ in}^2$$

$$M = 40.9(0.31) = 12.68 \text{ k-in}$$

$$F_x = 20.5 \text{ kip}$$

$$F_y = 35.4 \text{ kip}$$

At the point B the bending stress and the tensile due to F_x add. For the weld metal the total normal stress is:

$$\sigma_x = \frac{F_x}{A} + \frac{Mc}{I} = \frac{20.5}{9.61} + \frac{12.68(16.25-6.97)}{242.36} = 2.62 \text{ ksi}$$

The shear stress is:

$$\tau_{xy} = \frac{F_y}{A} = \frac{35.4}{9.61} = 3.68 \text{ ksi}$$

Thus, the von Mises stress in the weld is:

$$\sigma' = \sqrt{\sigma_x^2 + 3\tau_{xy}^2} = \sqrt{2.62^2 + 3(3.68)^2} = 6.9 \text{ ksi} < 23.7 \text{ ksi}$$

The stresses in the parent metal are:

$$\begin{aligned}
 A &= 2 \times (0.375) \times (2.25 + 15.87) = 13.59 \text{ in}^2 \\
 T_{xy} &= \frac{35.4}{13.59} = 2.6 \text{ ksi} \\
 \sigma_x &= \frac{20.5}{13.59} + \frac{12.68}{49.85} = 1.77 \text{ ksi} \\
 \sigma' &= \sqrt{1.77^2 + 3(2.6)^2} = 4.85 \text{ ksi} < 23.7 \text{ ksi}
 \end{aligned}$$

- YIELDING OF ATTACHING BOLT AND SHEARING OF BOLT AND TAPPED THREAD

Bolt Loading Auxiliary Ear Design

For the auxiliary ear design, the external bolt force produced by the lifting condition is:

Load Case I

The moment applied to the bolts is:

$$M = 17.7(4.00) = 70.8 \text{ k-in}$$

The tensile stress σ_{tb} at the bottom of contact area due to the applied moment is:

$$\sigma_{tb} = \frac{Md/2}{I} = \frac{Md/2}{bd^3/12} = \frac{6M}{bd^2}$$

Where b and d are the base and height dimensions of the contact area. The tensile load on the bolt is the area A_{tb} of each fastener times σ_{tb} .

$$F_T = \frac{6M}{bd^2} A_{tb}$$

Where A_{tb} for the bottom row bolt is:

$$\begin{aligned}
 A_{tb} &= 3.00 \times (2.5 + 1.75) = 12.75 \text{ in}^2 \\
 F_T &= \frac{6(70.8)}{6.0 \times 9.5^2} \times 12.75 = 10.00 \text{ kip}
 \end{aligned}$$

Load Case II

The moment for this Load Case is reduced by the action of the horizontal component as follows:

$$M = 17.7 \times (4.54) - 10.2 \times (0.92 + 0.50 + 3.50 + 1.75) = 12.32 \text{ k-in. see}$$

Figure 2.12.3-1.

The tensile load on the bolt is:

$$F_T = \frac{6M}{bd^2} \times A_{tb} + \frac{F_H}{4} = \frac{6(12.32)(12.75)}{6.0(9.5)^2} + \frac{10.2}{4} = 1.74 + 2.55 = 4.29 \text{ kip}$$

Bolt Loading, Standard Ear Design

Load Case I and Case III (Slot Lift)

The moment applied to the bolt is:

$$M = 35.4(6.00) = 212.4 \text{ k-in}$$

$$A_{tb} = 3.00(3+1.75) = 14.25 \text{ in}^2$$

The tensile load F_t per bolt at the bottom row of bolts due to the applied moment is:

$$F_t = \frac{6MA_{tb}}{bd^2} = \frac{6(212.4)(14.25)}{6.0(10.0)^2} = 30.27 \text{ kip}$$

Load Case II

The moment for Load Case II is:

$$M = 35.4 (6.54) - 20.5 (0.92 + 7.75 + 3.50 + 1.75) = -53.84 \text{ k-in}$$

The tensile load F_t per bolt at the top row of bolts is:

$$A_{tb} = 3.00(3.5 + 1.75) = 15.75 \text{ in}^2$$

$$F_t = \frac{6(53.84)(15.75)}{6.0(10.0)^2} + \frac{20.5}{4} = 13.61 \text{ kip}$$

Load Case III ear base lift is not considered because the moment area is less than that of Load Case I and the load acts on the same directions as Load Case I.

Table 2.12.3-1 presents a summary of bolt loading for each of the ear designs (auxiliary and standard). Because the standard design under Load Case I, straight lift, imposes the largest tensile load on the bolt than in the other conditions, this load value (30.27 kip) is used in the analysis of the bolt.

Table 2.12.3-1. Bolt Loading Per Ear Design and Load Case

Ear Design	Bolt Loading (kip)			Yield Strength (ksi)	Shear Strength (ksi)
	Load Case				
	I	II	III (Slot Lift)		
Auxiliary	10	4.29	N/A	85	51
Standard	30.27	13.61	30.27	85	51

Bolt Analysis

Bolt and thread section properties use in the analyses for both internal and external threads are evaluated for a standard 1-8 UNC x 2-1/2 in bolt as follows.

Tensile stress area (A_t) for high strength bolt with $\sigma_{tb} > 100\text{ksi}$, as provided in *Machineries Handbook*, Reference 2-26, Page 1490 is:

$$A_t = \pi \left(\frac{E_{s_{min}}}{2} - \frac{0.16238}{n} \right)^2$$

where:

$$E_{s_{min}} = \text{Minimum pitch diameter} = 0.9188 \text{ inches}$$

$$n = \text{Number of threads per inch} = 8$$

$$A_t = \pi \left(\frac{0.9188}{2} - \frac{0.16238}{8} \right)^2 = 0.61 \text{ in}^2$$

Shear area of the external (A_s) and the internal (A_n) threads, *Machineries Handbook*, Reference 2-26, Page 1491.

$$A_s = \pi n L_e K_{n_{max}} \left[\frac{1}{2n} + 0.57735 (E_{s_{min}} - K_{n_{max}}) \right]$$

where:

$$n = 8$$

$$L_e = \text{Length of engagement} = 1.680 \text{ inches}$$

$$K_{n_{max}} = \text{Maximum minor diameter of internal thread} = 0.8795 \text{ inches}$$

$$A_s = \pi (8)(1.680)(0.8795) \left[\frac{1}{2(8)} + 0.57735 (0.9188 - 0.8795) \right] = 3.164 \text{ in}^2$$

$$A_n = \pi n L_e D_{s_{min}} \left[\frac{1}{2n} + 0.57735 (D_{s_{min}} - E_{n_{max}}) \right]$$

where:

$$D_{s_{min}} = \text{Minimum major diameter of external thread} = 0.9848 \text{ inches}$$

$$E_{n_{max}} = \text{Maximum pitch diameter of internal thread} = 0.9242 \text{ inches}$$

$$A_n = \pi (8)(1.680)(0.9848) \left[\frac{1}{2(8)} + 0.57735 (0.9848 - 0.9242) \right] = 4.05 \text{ in}^2$$

Bolt Preload

J.E. Shigley and L.D. Mitchell (Reference 2-27) recommend the bolt preload (F_i) be between 60% and 90% of the proof load. The proof load is equal to 85% of the yield strength (S_y) multiplied by the tensile stress area (A_t). For a torque of 600 ± 20 ft-lbs, the corresponding preload, proof load and percent of proof load are determined as follows:

$$F_i = T/(kd)$$

$$\% \text{ proof load} = [F_i / \text{proof load}] \times 100\%$$

Where:

$$T = \text{torque} = 600 \pm 20 \text{ ft-lb} = 7,200 \pm 240 \text{ in-lb}$$

$$d = \text{bolt thread nominal diameter} = 1.0 \text{ in} \quad (\text{GEH drawings 101E8718 and 105E9520})$$

$$k = \text{torque coefficient} = 0.2 \quad (\text{Reference 2-27})$$

$$\text{proof load} = \text{proof strength} \times A_t = 43,762 \text{ lbs}$$

$$\text{proof strength} = 0.85 S_y = 72,250 \text{ psi}$$

NEDO-33866 Revision 2
Non-Proprietary Information – Class I (Public)

$$A_t = \text{thread tensile area} = 0.6057 \text{ in}^2$$

$$S_y = \text{yield strength at room temperature} = 85,000 \text{ psi (Table 2.2-8)}$$

Table 2.12.3-2 summarizes the bolt preload, bolt proof load and % proof load for all three lifting ear bolt torque values. As indicated, maximum, nominal, and minimum torques produce loads within the recommended range of 60% to 90% of the proof load.

Table 2.12.3-2 Lifting Ear Bolt Percent Proof Load

Lifting Ear Bolt Torque	Torque Value (ft-lbs)	Bolt Preload (lb)	Proof Load (lb)	Percent Proof Load
Maximum	620	37,200	43,762	85%
Nominal	600	36,000		82%
Minimum	580	34,800		80%

Stresses produced by preload:

Bolt tension

$$\sigma = \frac{F_i}{A_t} = \frac{37,200}{0.606} = 61.42 \text{ ksi}$$

Bolt thread stripping

$$\tau = \frac{F_i}{A_s} = \frac{37,200}{3.164} = 11.76 \text{ ksi}$$

Tapped thread stripping

$$\tau = \frac{F_i}{A_n} = \frac{37,200}{4.054} = 9.18 \text{ ksi}$$

Minimum Bearing stress between cask and ear

$$\sigma_{ib} = \frac{(\# \text{ of bolt})(F_i)}{\text{Contact Area}} = \frac{4(34,800)}{6.0(10.0)} = 2.32 \text{ ksi}$$

The initial bearing pressure, σ_{ib} , previously calculated, is assumed to be uniform over the contact area. The bearing pressure should not be exceeded by tensile stress, σ_{tb} . Figure 2.12.3-7 shows the bearing stresses at the lifting ear contact region.

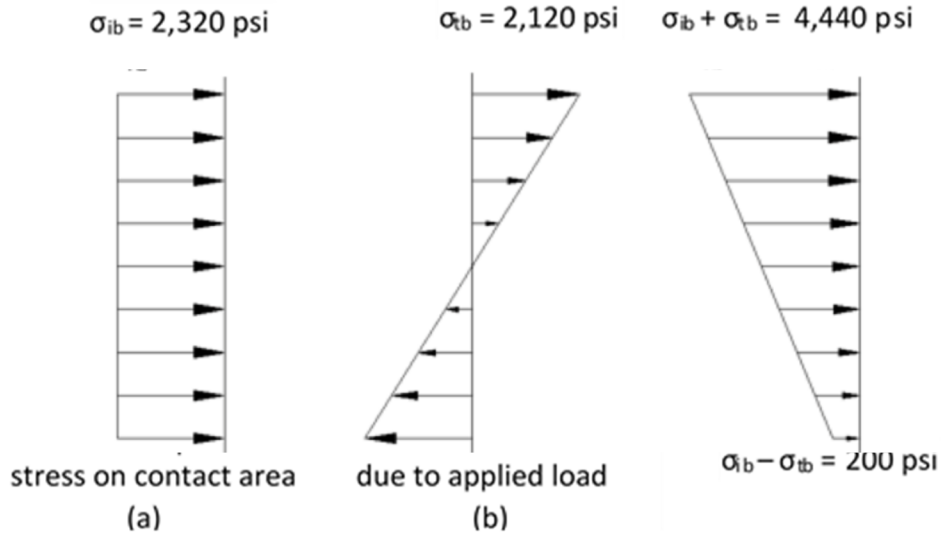


Figure 2.12.3-7. Lifting Ear Contact Bearing Stresses

$$\sigma_{tb} = \frac{6M}{bd^2} = \frac{6(212.4)}{6(10.0)^2} = 2.12 \text{ ksi}$$

$$\sigma_{ib} > \sigma_{tb}$$

The moment M (212.4 k-in) is produced by Load Case I or III on the standard ear design attaching bolt as previously calculated.

The nominal tensile stress, σ_t , in the bottom row bolts is:

$$\sigma_t = \frac{F_t}{A_t}$$

As previously calculated the tensile load for Load Case I is 30.27 kip per bolt.

$$\sigma_t = \frac{30.27}{0.606} = 49.95 \text{ ksi} < 85 \text{ ksi}$$

and the direct-shear component is:

$$\tau = \frac{35.4}{4(0.606)} = 14.6 \text{ ksi} < 51 \text{ ksi}$$

The interaction equation for the strength of a connection with bolts in combined shear and tension may be approximated by the elliptical relationship:

$$\left(\frac{\sigma_t}{\sigma_y}\right)^2 + \left(\frac{\tau}{0.6\sigma_y}\right)^2 \leq 1.0$$

$$\left(\frac{49.95}{85.0}\right)^2 + \left(\frac{14.60}{0.6(85)}\right)^2 \leq 1.0$$

$$0.43 \leq 1.0$$

Therefore, the selected bolts are adequate to carry the lifting load.

For the shearing of the bolt threads due to tensile load F_t .

$$\tau = \frac{F_t}{A_s} = \frac{30.27}{3.164} = 9.57 \text{ ksi} < 51.0 \text{ ksi}$$

For the shearing of the tapped threads due to tensile load F_t .

$$\tau = \frac{F_t}{A_n} = \frac{30.27}{4.054} = 7.47 \text{ ksi} < 51.0 \text{ ksi}$$

Bolt Fatigue Analysis

Bolt and Load Data:

1-8 UNC-2A, ASTM A193-B6

Yield Strength:	85 ksi (minimum)
Operating Temperature:	250°F
Modulus of Elasticity:	28.1 (10 ⁶) psi
Maximum Tensile Stress:	61.42 ksi (Preload)
Maximum Shear Stress:	14.6 ksi

(Shear neglects the reducing effect of friction between ear and cask body.)

The maximum cycle of stress is due to a combination of the preload stress, 61.42 ksi, and the shear stress (14.6 ksi) due to lifting. These give a maximum principal stress of:

$$\sigma_{\max} = \frac{61.42}{2} + \sqrt{\left(\frac{61.42}{2}\right)^2 + 14.6^2} = 64.71 \text{ ksi}$$

From ASME Section III NB 3232.3, the fatigue strength reduction factor to be used is 4.0. Because the fatigue curve (ASME Section III, Figure I-9.4 (Reference 2-18)) is based on modulus of elasticity of 30(10⁶) psi and the bolt has a modulus of elasticity of 28.1(10⁶) psi, the stress range is given by:

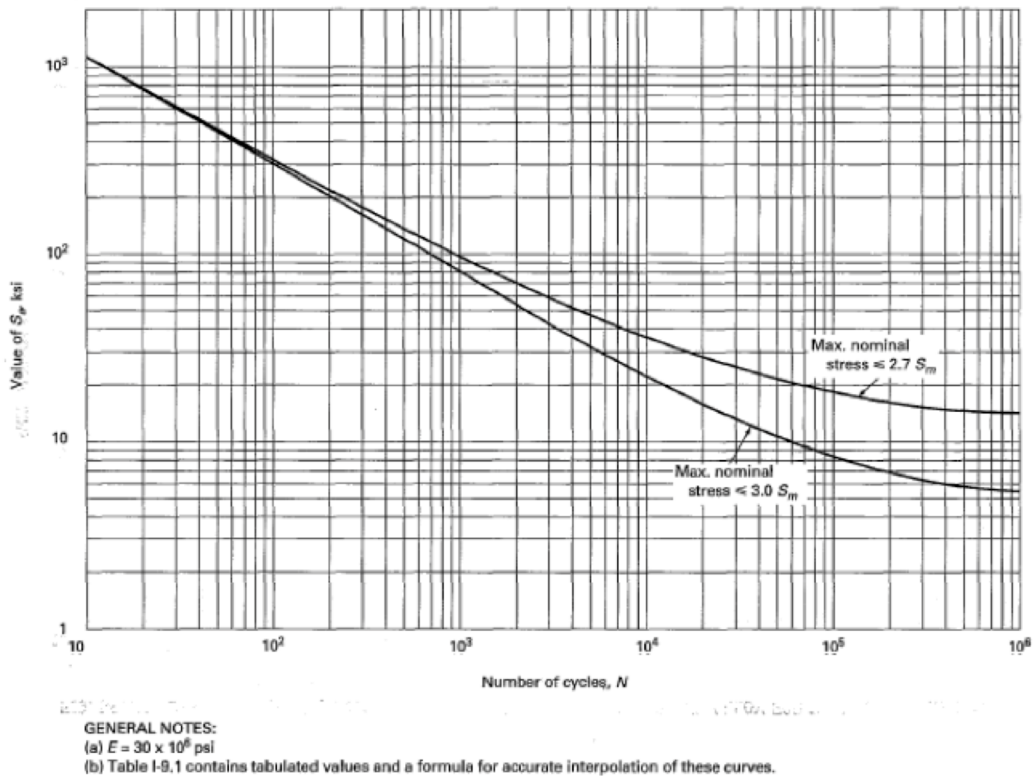
$$S = (64.71 \text{ ksi}) \times 4(30(10^6)/28.1(10^6)) = 276.34 \text{ ksi}$$

To select the correct fatigue curve, the stress intensity value, S_m , of 26.5 ksi is used at 250°F. Calculating the alternating stress:

$$S_a = \frac{1}{2} S = \frac{1}{2}(276.34) = 138.17 \text{ ksi}$$

Using the fatigue curve for a maximum nominal stress $\leq 2.7 S_m$ the fatigue limit is $\cong 530$ cycles as provided in Figure 2.12.3-8. Assuming an average of four ear lifts per usage and 12 usages per year, this gives a bolt life of:

$$\frac{530}{\left(\frac{12 \text{ usages}}{\text{year}}\right)\left(4 \frac{\text{cyc.}}{\text{usage}}\right)} = 11 \text{ yrs.}$$



2010 SECTION III, DIVISION 1 – APPENDICES

Figure 2.12.3-8. Design Fatigue Curves For High Strength Steel Bolting Above 700°F
 (from Reference 2-18)

- YIELDING OF CASK OUTER SHELL

The lifting ears are mounted to the outer shell of the cask on a mounting plate embedded to the cask. The mounting plate is embedded about 1.75 inches into the cask through the outer shell and the lead shield. However, 1 inch thickness of the outer shell and the maximum vertical load of 35.4 kip (standard ear) are conservatively considered for yielding due to the lifting load.

$$\sigma_c = \frac{F_c}{A} = \frac{35.4}{7.5} = 4.72 \text{ ksi}$$

where Area (A) = thickness of shell x width of mounting plate = 1 x 7.5 = 7.5 in²

$$\tau = \frac{F}{A_s} = \frac{35.4}{12.5} = 2.83 \text{ ksi}$$

where the shear area (A) = 2 x (6.25 x 1) = 12.5 in²

$$\sigma_b = \frac{Mc}{I} = \frac{247.8 \times 3.125}{152.59} = 5.07 \text{ ksi}$$

where M = 35.4 x 7 = 247.8 k-in,

NEDO-33866 Revision 2
Non-Proprietary Information – Class I (Public)

$$c = 6.25/2 = 3.125 \text{ in}$$

$$I = \frac{bh^3}{12} = \frac{7.5 \times 6.25^3}{12} = 152.59 \text{ in}^4$$

$$\sigma' = \sqrt{(4.72 + 5.07)^2 + 3 \times (2.83)^2} = 10.95 \text{ ksi}$$

• EXCESSIVE LOAD FAILURE

The lifting devices must be designed such that their failure under excessive load would not impair the ability of the package to meet other requirements of 10 CFR 71. In this section a margin of safety (MS) is determined for each of the lifting system components based on the results presented in Table 2.12.3-3.

Table 2.12.3-3. Summary of Ear Analysis for Model 2000

Condition	Stress Level (ksi)		Allowable (ksi) Based on Yield	MS(y) Aux./Std.	Allowable Based on Su	MS(U) Aux./Std.
	Auxiliary (Aux.)	Standard (Std.)				
Shear tearout of lift hole	6.02	8.98	14	1.33/0.56	26.18	3.35/1.92
Tensile failure of ear plate	4.82	17.7	23.7	3.92/0.34	68.6	13.23/2.88
Bearing of shackle pin on ear	10.2	17.7	23.7	1.32/0.34	68.6	5.73/2.88
Yielding of weld joint	9.2	8.16	23.7	1.58/1.9	68.6	6.46/7.41
Yielding of attaching bolt	---	61.42	85	0.38	110	0.79
Shearing of bolt thread	---	11.76	51	3.34	---	---
Shearing of tapped thread	---	9.18	14	0.53	26.18	1.85
Yielding of cask outer shell	---	10.95	23.7	1.16	68.6	5.26

Note:

Bolt and bolt thread stress levels are documented in Table 2.12.3-3 for standard ear because maximum bolt loading is documented during slot lift (Case III) of the standard ear (see Table 2.12.3-1).

The margins of safety MS(y) with respect to yield is calculated as follows:

$$MS(\text{yield}) = \frac{\text{Allowable based on yield strength}}{\text{Stress level}} - 1$$

The ear and cask shell material is ASTM 240 type 304 stainless steel. The margins of safety with respect to ultimate failure MS(U) are:

For shear tear-out of lifting hole

$$\text{Shear Strengths} = \frac{\sigma_{\text{ult}}}{2(1+\mu)} = \frac{68.6}{2(1.31)} = 26.18 \text{ ksi}$$

$$\tau = 8.98 \text{ ksi (Standard Ear, Load Case I)}$$

$$MS(U) = \frac{26.18}{8.98} - 1 = 1.92$$

For tensile failure of ear plate

$$\sigma_T = 17.7 \text{ ksi (Standard Ear, Load Case III)}$$

$$MS(U) = \frac{68.6}{17.7} - 1 = 2.88$$

For yielding of weld joints

$$\sigma' = 9.2 \text{ ksi (Auxiliary Ear, Load Case II)}$$

$$MS(U) = \frac{68.6}{9.2} - 1 = 6.46$$

For bolts

$$P_{ult} = 110 \times 0.606 = 66.66 \text{ kip}$$

$$F_t = 61.42(0.606) = 37.22 \text{ kip}$$

$$MS(U) = \frac{66.66}{37.22} - 1 = 0.79$$

For yielding of cask outer shell

$$\sigma' = 10.95 \text{ ksi}$$

$$MS(U) = \frac{68.6}{10.95} - 1 = 5.26$$

A review of the above margin of safety indicates that, under excessive loading, the ear attaching bolts will fail before the ear plates, ear welds or cask shell. Failure of the bolts assures that the ability of the package to meet any other regulatory requirements is not impaired.

- MODEL 2000 LID LIFTING LUG ANALYSIS

The lifting lug is covered during transport. It is shown by analysis that this lifting device complies with requirements of 10 CFR 71.45(a). The lifting lug is able to support three times the weight of the lid without yielding.

The weakest part of the lifting lug is the fillet weld, which attaches the stainless steel loop to the cask lid. Using the maximum shear stress theory the weld is determined to have a factor of safety of 1.76 when analyzed for lifting 3 times the weight of the lid.

The lifting lug is analyzed by considering the rigid frame shown in Figure 2.12.3-9. The analytical model has the same height and distance between the supports as the lifting lug.

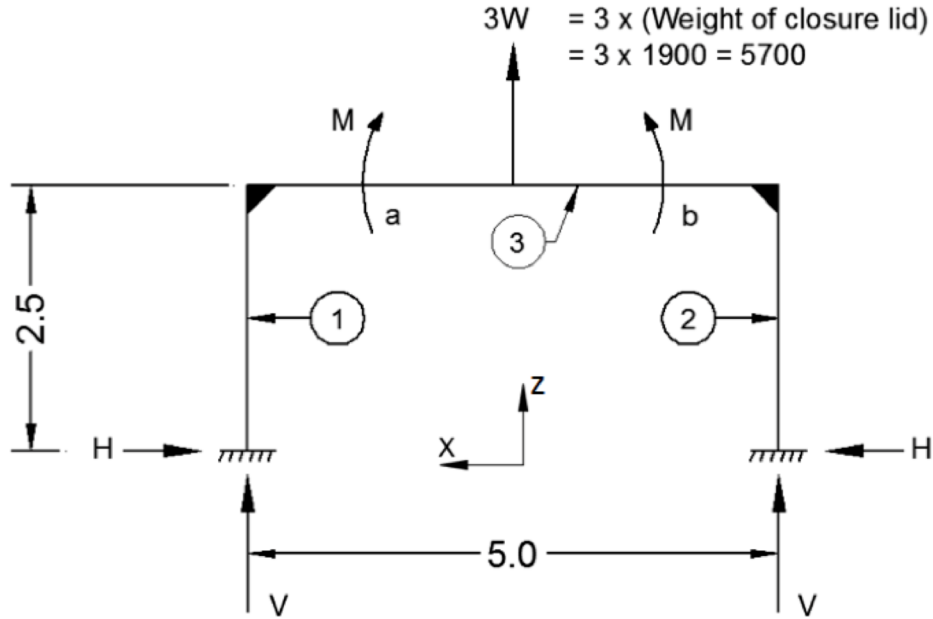


Figure 2.12.3-9. Analytical Model of Lifting Lug

The statically indeterminate forces and moments are obtained by solving the following set of equations from Reference 2-29.

$$\frac{-1/3HL^3_1}{I_1} + \frac{1/2M_1L^2_1}{I_1} = \frac{1/3HL^3_2}{I_2} - \frac{1/2M_2L^2_2}{I_2}$$

$$\frac{-1/2HL^2_1}{I_1} + \frac{M_1L_1}{I_1} = \frac{-1/3M_1L_3}{I_3} + \frac{1/6W(bL_3 - \frac{b^3}{L_3})}{I_3} - \frac{1/6M_2L_3}{I_3}$$

$$\frac{-1/2HL^2_2}{I_2} + \frac{M_2L_2}{I_2} = \frac{1/3M_2L_3}{I_3} + \frac{1/6M_1L_3}{I_3} - \frac{1/6W[2bL_3 + (\frac{b^3}{L_3}) - 3b^2]}{I_3}$$

And by symmetry:

$$M_1 = M_2 = M$$

$$H_1 = H_2 = H$$

$$V_1 = V_2 = V = 2,850 \text{ lb.}$$

Also,

$$L_1 = L_2 = 2.5$$

$$L_3 = 5.0$$

$$I_1 = I_2 = I_3$$

$$a = b = 2.5$$

Using substitution and solving the above equations simultaneously gives:

$$\begin{aligned} V &= 2,850 \text{ lb} \\ H &= 2,671 \text{ lb} \\ M &= 4,452 \text{ lb-in} \end{aligned}$$

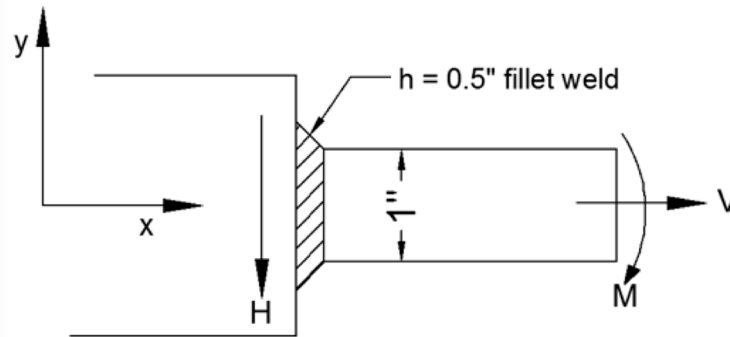


Figure 2.12.3-10. Loading on the Weld Area

The loading in the weld area is shown in Figure 2.12.3-10. The moment M produces a bending stress, σ_m , in the weld. This stress is assumed to act normal to the throat area (see Reference 2-27, P. 427).

The unit moment of inertia of the welds is from Reference 2-27, P. 429, given by:

$$I_u = \pi r^3$$

But the moment of inertia based on the weld throat is:

$$I = 0.707h\pi r^3$$

The normal stress in the weld is therefore given by:

$$\sigma = \frac{MC}{I} = \frac{MC}{0.707h\pi r^3}$$

The maximum stress occurs at the outer fibers where:

$$C = r$$

$$Z = 2\pi r$$

The maximum stress is therefore given by:

$$\sigma_m = \pm \frac{M}{0.707h\pi r^2}$$

From Reference 2-27, Equation (9.3), p. 417, the stress in the weld due to the force V is given by:

$$\tau_v = \frac{V}{0.707hZ}$$

Similarly, from Reference 2-27, Equation (a), p. 427, the stress in the weld due to the force H is given by:

$$\tau_H = \frac{H}{0.707hZ}$$

Figure 2.12.3-11 shows the stresses acting on the weld at the point where the bending moment is a maximum.

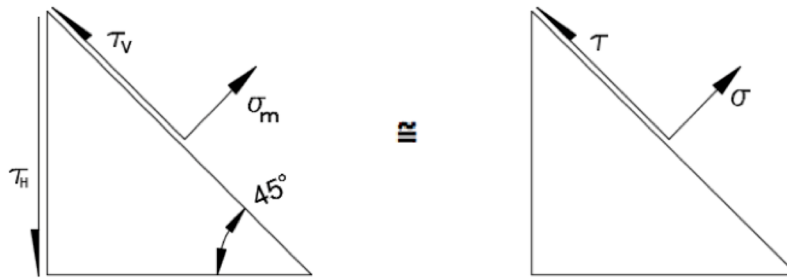


Figure 2.12.3-11. Stresses Acting on the Weld

$$\begin{aligned} \sigma &= \sigma_m = \frac{4452}{0.707 \times 0.5 \times \pi \times (0.5)^2} = 16,035.3 \text{ psi} \\ \tau &= \tau_v - \tau_H \cos 45^\circ \\ &= \frac{2,850}{0.707 \times 0.5 \times 2 \pi \times 0.5} - \frac{2,671}{0.707 \times 0.5 \times 2 \pi \times 0.5} \times 0.707 \\ \tau &= 2,566 - 1,700 = 866 \text{ psi} \end{aligned}$$

From Reference 2-27, p.31, the principal stresses are found using:

$$\begin{aligned} \sigma_1, \sigma_2 &= \frac{\sigma}{2} \pm \sqrt{\left(\frac{\sigma}{2}\right)^2 + \tau^2} \\ \tau_{\max} &= \pm \sqrt{\left(\frac{\sigma}{2}\right)^2 + \tau^2} \end{aligned}$$

Substituting for σ and τ yields

$$\begin{aligned} \sigma_1, \sigma_2 &= \frac{16,035.3}{2} \pm \sqrt{\left(\frac{16,035.3}{2}\right)^2 + 866^2} \\ &= 8,017.7 \pm 8064.3 \\ \sigma_1 &= 16,082 \text{ psi} \\ \sigma_2 &= -46.6 \text{ psi} \\ \tau_{\max} &= \pm 8064.3 \text{ psi} \end{aligned}$$

The maximum shear stress is applied to determine the likelihood of failure or safety.

$$\text{Allowable} = \tau_{\text{allowable}} = 0.6 S_y$$

Where S_y denotes the yield strength.
 The yield strength of stainless steel Type 304 is 23.7 ksi.

Substituting into equation (32)
 Allowable Stress = $0.6 \times 23.7 = 14.22$ ksi

$$\tau_{\max} = 8.06 \text{ ksi} \leq 14.22 \text{ ksi}$$

Therefore, the factor of safety is given by

$$\text{FS} = \frac{14.22}{8.06} = 1.76 \text{ (this is for lifting 3W)}$$

2.12.3.2. Tie-Down Analysis

The purpose and scope of this analysis is to demonstrate the structural integrity of the tie-down rib. The Model 2000 Transport Package is shipped normally by truck. Figure 2.12.3-12 shows the overall plan for tying the package to the vehicle. Eight wire ropes or chains tie the package to the vehicle: four connect to the upper tie-down ribs of the overpack, and the other four connect to the overpack base tie-down ribs. In addition, the base of the package is wedged to the truck bed to prevent sliding. Evaluation of the tie-down loading on the tie-down rib adjacent area consisted of the following:

- 1) Identification of the maximum tie-down member tension force due to loading.
- 2) Evaluation of the effect of the above force on the tie-down rib.

Classical hand calculation is used to identify the maximum tie-down member tension forces due to the combined loads. The results of this analysis were added to establish the maximum load. Table 2.12.3-3 gives a summary of each rope tie-down tension load for each force component and the total force. The maximum tie-down wire tension force is estimated to be 148.62 kips. This maximum load is then applied to the tie-down rib to determine the structural integrity of the tie-down rib by analyzing the following modes of failure:

- Shear tear-out of tie-down rib hole
- Bearing of shackle pin on ear
- Yielding of weld joints and parent metal

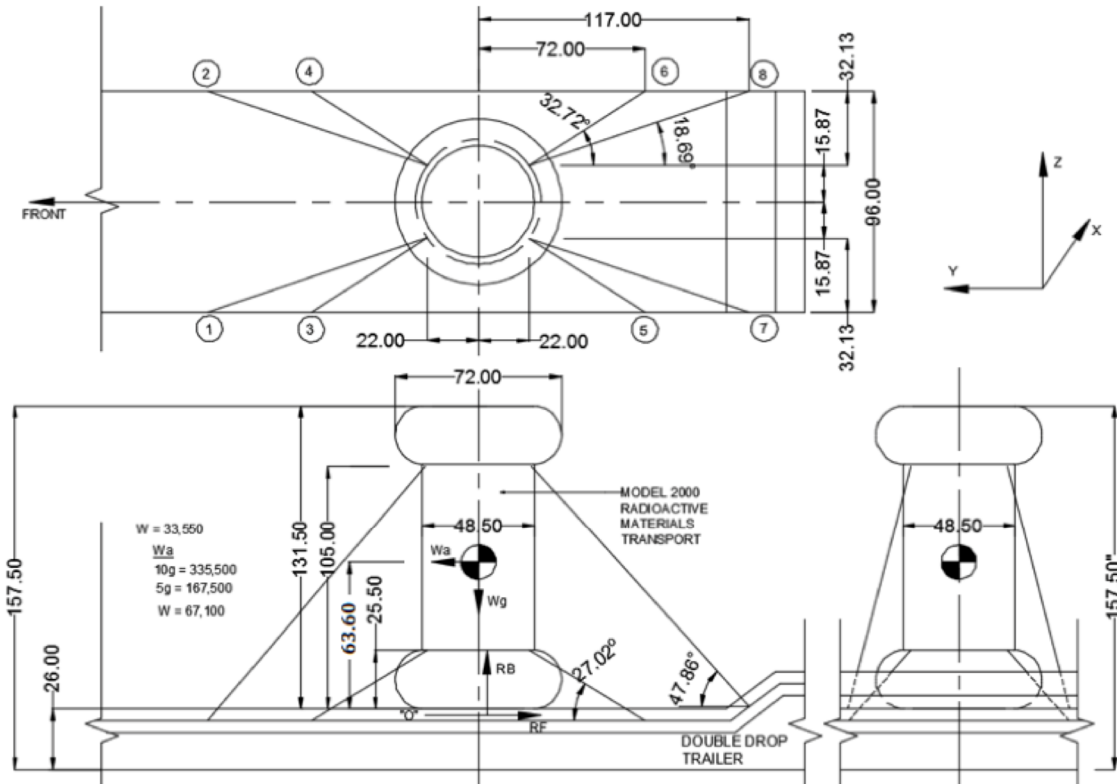


Figure 2.12.3-12. Tie-Down of Transport Package to Vehicle

• TIE-DOWN MEMBER TENSION FORCES

The package (wt. = 33,550 lb) is subject to accelerations of 10g longitudinal, 5g transverse, and 2g vertical (up) Per IAEA’s “Package stowage and retention” regulations. These accelerations result in the following forces acting on the C.G. of the cask:

$$\begin{aligned}
 F_{\text{long}} &= 33,550(10) = 335,500 \text{ lbf} \\
 F_{\text{trans}} &= 33,550(5) = 167,750 \text{ lbf} \\
 F_{\text{vert}} &= 33,550(2) = 67,100 \text{ lbf}
 \end{aligned}$$

In this calculation, each load is independently applied to the package and the tensile load on members for each case is calculated. The tensile loads are then added to calculate the maximum tension load on members.

10g Longitudinal

Because the base of the package is chocked, the 10g acceleration will cause it to rotate about point “o” counterclockwise (-x direction). This rotation will cause Ropes 1, 2, 3 and 4 to go slack and tension Ropes 5, 6, 7 and 8. From Figure 2.12.3-13.

$$\begin{aligned}
 F_7 &= F_8 \\
 F_5 &= F_6
 \end{aligned}$$

NEDO-33866 Revision 2
Non-Proprietary Information – Class I (Public)

The component forces for these ropes are:

$$\begin{aligned} F_{5y} &= F_{6y} = F_6 \cos 23.2^\circ \cos 32.7^\circ &= 0.774 F_6 \\ F_{5z} &= F_{6z} = F_6 \sin 23.2^\circ &= 0.394 F_6 \\ F_{7y} &= F_{8y} = F_8 \cos 46.3^\circ \cos 18.69^\circ &= 0.654 F_8 \\ F_{7z} &= F_{8z} = F_8 \sin 46.3^\circ &= 0.723 F_8 \end{aligned}$$

The reaction forces from chocking and friction (R_F) and bearing on the package base (R_B) are:

$$\begin{aligned} R_F &= F_{5y} + F_{6y} + F_{7y} + F_{8y} - W_a \\ R_B &= F_{5z} + F_{6z} + F_{7z} + F_{8z} + W_g \quad (\text{assuming } F_1 = F_2 = F_3 = F_4 = 0) \end{aligned}$$

The center of gravity is 63.60 inches.

$$\begin{aligned} \Sigma M_{ox} &= 0 = -W_a 63.60 + W_g 24.25 - R_B 24.25 + (F_{5y} + F_{6y}) 25.5 + (F_{7y} + F_{8y}) \\ &\quad 105.0 + (F_{5z} + F_{6z} + F_{7z} + F_{8z}) 46.25 \\ \Sigma M_{ox} &= -W_a 63.60 + W_g 24.25 - (F_{5z} + F_{6z} + F_{7z} + F_{8z} + W_g) 24.25 + \dots \\ &\quad \dots (F_{5y} + F_{6y}) 25.5 + (F_{7y} + F_{8y}) 105.0 + (F_{5z} + F_{6z} + F_{7z} + F_{8z}) 46.25 \\ &= -W_a 63.60 - [2 \times 0.394 F_6 + 2 \times 0.723 F_8] 24.25 + 2 \times 0.774 F_6 (25.5) + \dots \\ &\quad \dots 2 \times 0.654 F_8 (105.0) + [2 \times 0.394 F_6 + 2 \times 0.723 F_8] 46.25 \\ &= -W_a 63.60 - 19.1 F_6 - 35.1 F_8 + 39.5 F_6 + 137.3 F_8 + 36.4 F_6 + 66.9 F_8 \\ &= -W_a 63.60 + (-19.1 + 39.5 + 36.4) F_6 + (-35.1 + 137.3 + 66.9) F_8 \\ &= -(63.60) W_a + (56.8) F_6 + (169.1) F_8 \\ &\Rightarrow 2.134 (10^7) = (56.8) F_6 + (169.1) F_8 \end{aligned}$$

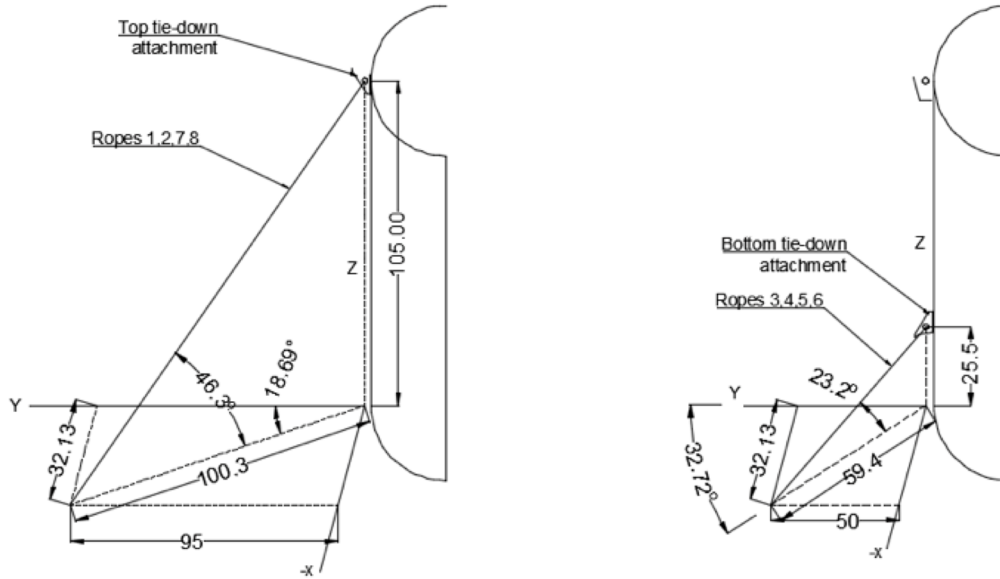


Figure 2.12.3-13. Tie-Down Wire Ropes

This cannot be solved for F6 and F8 so an additional equation relating F6 and F8 is required. By making certain assumptions, this equation can be obtained from consideration of the force and deflection (or extension) characteristics of the different length wire ropes. Figure 2.12.3-14 shows the extension of the ropes at small angle rotation. Assuming the ropes initially have no tension, the ratio of loads due to stretching of the ropes is:

$$\frac{F_7}{F_5} = \frac{\delta_7 EA}{\delta_5 EA} \frac{L_7}{L_5}$$

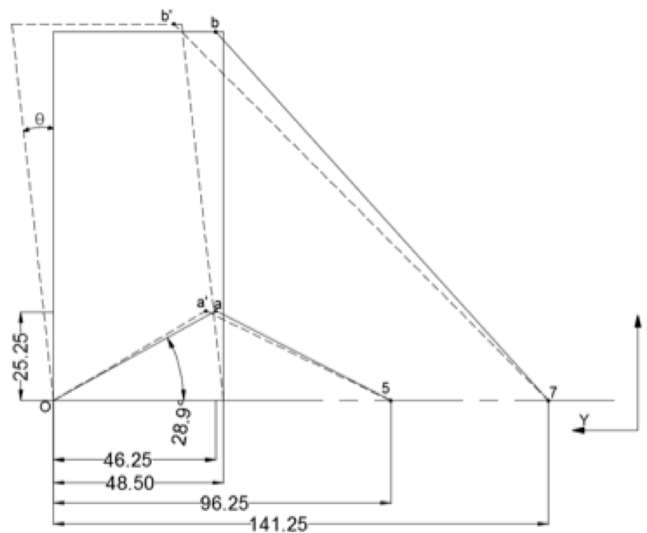


Figure 2.12.3-14. Wire Rope Extension at Small Angle (θ) Rotation

Because both ropes are of the same size and material,

$$\frac{F_7}{F_5} = \frac{\delta_7 L_5}{\delta_5 L_7}$$

For a rotation of θ° about point “O”, line 5 would be extended as follows

$$\delta_5 Z L_{5f} - L_{5i}$$

L_{5f} is the final length of rope 5 as shown in Figure 2.12.3-15.

$$L_{5i} = \sqrt{59.4^2 + 25.5^2} = 64.6 \text{ in}$$

$$\overline{oa'} = \overline{oa} = \sqrt{46.25^2 + 25.5^2} = 52.8 \text{ in}$$

Change in “a” in y direction is:

$$\overline{aa'_y} = 52.8[\cos 28.9^\circ - \cos(28.9 + \theta)]$$

Change in “a” in z direction is:

$$\overline{aa'_z}$$

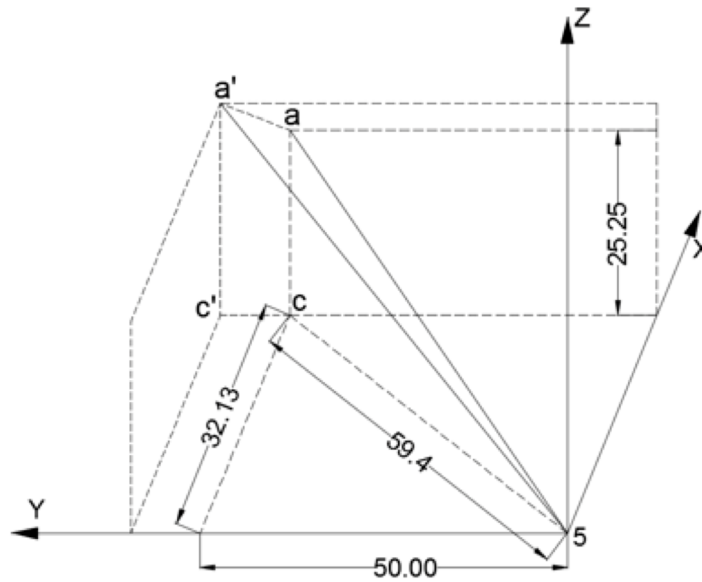


Figure 2.12.3-15. Final Length of Rope 5

$$L_{5f} = \sqrt{(25.5 + 52.8[\sin(28.9^\circ + \theta) - \sin 28.9^\circ])^2 + \dots + (32.13^2 + (50.0 + 52.8[\cos 28.9^\circ - \cos(28.9^\circ + \theta)])^2)}$$

To evaluate the effect of small rotations, L_{5f} will be evaluated for $\theta = 0.1^\circ$, $\theta = 1^\circ$ and $\theta = 10^\circ$.

NEDO-33866 Revision 2
Non-Proprietary Information – Class I (Public)

$$L_{5f_{.1^\circ}} = \sqrt{\frac{(25.5 + 52.8[\sin(29.0^\circ) - \sin 28.9^\circ])^2 + \dots}{32.13^2 + (50.0 + 52.8[\cos 28.9^\circ - \cos(29.0^\circ)])^2}}$$

$$= \sqrt{654.4 + 3,536.8} = 64.7 \text{ in}$$

$$L_{5f_{1^\circ}} = \sqrt{\frac{(25.5 + 52.8[\sin(29.9^\circ) - \sin 28.9^\circ])^2 + \dots}{32.13^2 + (50.0 + 52.8[\cos 28.9^\circ - \cos(29.9^\circ)])^2}}$$

$$= \sqrt{691.8 + 3,577.8} = 65.3 \text{ in}$$

$$L_{5f_{10^\circ}} = \sqrt{\frac{(25.5 + 52.8[\sin(38.9^\circ) - \sin 28.9^\circ])^2 + \dots}{32.13^2 + (50.0 + 52.8[\cos 28.9^\circ - \cos(38.9^\circ)])^2}}$$

$$= \sqrt{1,098.2 + 4,072.0} = 71.9 \text{ in}$$

A similar evaluation for line 7 yields:

$$L_{7i} = \sqrt{100.3^2 + 105^2} = 145.2 \text{ in}$$

$$\overline{ob} = \overline{ob'} = \sqrt{46.25^2 + 105^2} = 114.7 \text{ in}$$

Change in “b” in y direction is:

$$\overline{bb'_y} = 114.7[\cos 66.2^\circ - \cos(66.2 + \theta)]$$

Change in “b” in z direction is:

$$\overline{bb'_z} = 114.7 [\sin(66.2 + \theta) - \sin 66.2]$$

$$L_{7f} = \sqrt{\frac{(105 + 114.7[\sin(66.2 + \theta) - \sin 66.2])^2 + \dots}{32.13^2 + (95 + 114.7[\cos 66.2 - \cos(66.2 + \theta)])^2}}$$

Evaluation at $\theta = 0.1^\circ$, $\theta = 1^\circ$ and $\theta = 10^\circ$ gives:

$$L_{7f_{.1^\circ}} = \sqrt{\frac{(105 + 114.7[\sin 66.3 - \sin 66.2])^2 + \dots}{32.13^2 + (95 + 114.7[\cos 66.2 - \cos 66.3])^2}}$$

$$= \sqrt{11041.9 + 10,092.2} = 145.4 \text{ in}$$

$$L_{7f_{1^\circ}} = \sqrt{11,191.9 + 10,410.1} = 147.0 \text{ in}$$

$$L_{7f_{10^\circ}} = \sqrt{12,419.6 + 14,011.7} = 162.6 \text{ in}$$

Calculation of the ratio $\frac{L_f}{L_i}$ for each rope at each rotation value yields:

θ	Lf/Li	
	Rope 5	Rope 7
0.1°	1.002	1.001
1°	1.011	1.012
10°	1.113	1.120

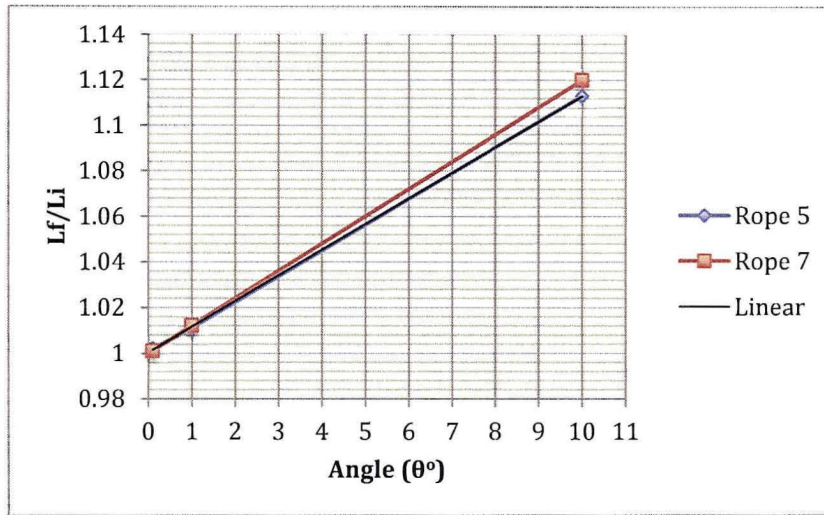


Figure 2.12.3-16. Final to Initial Rope Length Ratio per Small Angle Rotation

The fact that the ratios are the same for each rope and liner indicates that their derivation is correct. Their similarity and linearity would be expected from rigid body rotation.

Back to the relation between F_6 and F_8 (or F_5 and F_7), the ratio of loads due to stretching are for $\delta = 0.1^\circ$:

$$\begin{aligned} \frac{F_7}{F_5} &= \frac{\delta_7 L_5}{\delta_5 L_7} \\ \frac{F_7}{F_5} &= \frac{0.2 * 64.6}{0.1 * 145.2} = 0.8898... ** \\ L_5 &= 64.6 \\ L_7 &= 145.2 \\ \delta_5 &= L_5 f - L_5 i \\ &= 64.7 - 64.6 = 0.1 \\ \delta_7 &= 145.4 - 145.2 = 0.2 \end{aligned}$$

For $\theta = 10^\circ$

$$\frac{F_7}{F_5} = \frac{17.4}{7.3} = 1.061$$

Because the ropes cannot stretch 7.3 or 17.4 inches, this just shows that the ratio of forces in the ropes is fairly close at the two extremes. For the purpose of analysis, the value of 0.8898 will be used as this represents a more realistic elongation of the ropes.

$$F_7 = F_8 = 0.8898 F_5 = 0.8898 F_6$$

NEDO-33866 Revision 2
Non-Proprietary Information – Class I (Public)

$$F_6 56.8 + (0.8898 F_6) \times 169.1 = 2.134 (10^7)$$

$$\begin{aligned} F_5 &= F_6 = 102,960.00 \\ F_7 &= F_8 = 0.8898 F_6 = 91,614.00 \\ RF &= F_5y + F_6y + F_7y + F_8y - Wa \\ &= 0.774F_5 + 0.774F_6 + 0.654F_7 + 0.654F_8 - 335,500 = -56,287 \text{ lb} \end{aligned}$$

5g Transverse

This time the 5g acceleration will cause the package to rotate at a point 90° clockwise from point “o”. This will cause ropes 2, 4, 6 and 8 to go slack, and tension ropes 1, 3, 5 and 7. From symmetry the following assumptions can be made with reference to 2.12.3-11.

$$\begin{aligned} F_1 &= F_7 \\ F_3 &= F_5 \end{aligned}$$

The component forces for these ropes are:

$$\begin{aligned} F_{3x} &= F_{5x} = F_5 \cos 23.2^\circ \sin 32.7^\circ &= 0.497 F_3 \\ F_{3z} &= F_{5z} = F_5 \sin 23.2^\circ &= 0.394 F_3 \\ F_{1x} &= F_{7x} = F_7 \cos 46.3^\circ \sin 18.69^\circ &= 0.221 F_1 \\ F_{1z} &= F_{7z} = F_7 \sin 46.3^\circ &= 0.723 F_1 \end{aligned}$$

The reaction forces from chocking and friction (RF) and bearing on the package base (RB) are:

$$\begin{aligned} RF &= F_{5x} + F_{3x} + F_{7x} + F_{1x} - Wa \\ RB &= F_{5z} + F_{3z} + F_{7z} + F_{1z} + Wg \end{aligned}$$

RB is calculated assuming $F_2 = F_4 = F_6 = F_8 = 0$

$$\begin{aligned} \Sigma M_{ox} &= 0 = - Wa 63.60 + Wg 24.25 - RB 24.25 + (F_{5x} + F_{3x})25.5 + (F_{7x} + F_{1x}) \\ & \quad 105.0 + (F_{5z} + F_{3z} + F_{7z} + F_{1z}) 40.12 \end{aligned}$$

$$\begin{aligned} \Sigma M_{ox} &= - Wa 63.60 + Wg 24.25 - (F_{5z} + F_{3z} + F_{7z} + F_{1z} + Wg)24.25 + \dots \\ & \quad \dots (F_{5x} + F_{3x})25.5 + (F_{7x} + F_{1x})105.0 + (F_{5z} + F_{3z} + F_{7z} + F_{1z})40.12 \\ &= - Wa 63.60 - [2 \times 0.394F_3 + 2 \times 0.723F_1]24.25 + 2 \times 0.497F_3(25.5) + \dots \\ & \quad \dots 2 \times 0.221F_1 (105.0) + [2 \times 0.394F_3 + 2 \times 0.723F_1]40.12 \\ &= -Wa 63.60 - 19.1F_3 - 35.1F_1 + 25.3F_3 + 46.41F_1 + 31.6F_3 + 58F_1 \\ &= -Wa 63.60 + (-19.1 + 25.3 + 31.6) F_3 + (-35.1 + 46.41 + 58) F_1 \\ &= - (63.60) Wa + (37.8)F_3 + (69.31)F_1 \\ &=> 1.063 (10^7) = (37.8)F_3 + (69.3)F_1^* \end{aligned}$$

From equation** F_5 and F_7 are related as:

$$\begin{aligned} F_7 &= 0.8898F_5 \\ &= 0.8898F_3 = F_1 \\ &=> 1.063 (10^7) = (37.8)F_3 + (69.3)(0.8898F_3)^* \\ F_3 &= 106,874 \end{aligned}$$

NEDO-33866 Revision 2
Non-Proprietary Information – Class I (Public)

$$\begin{aligned} F_5 &= 106,874 \\ F_1 &= 95,096 \\ F_7 &= 95,096 \end{aligned}$$

$$\begin{aligned} \text{From above: } RF &= F_{5x} + F_{3x} + F_{7x} + F_{1x} - W_a \\ &= 0.497F_5 + 0.497F_3 + 0.221F_7 + 0.221F_1 - 167,100 = -18,835 \text{ lb} \end{aligned}$$

2g Vertical

During the 2g vertical load all 8 members are expected to experience tension, and all vertical components of the members will react. From symmetry, the following assumptions can be made with reference to Figure 2.12.3-13.

Assumption from symmetry: For the 2g vertical load, all ropes at the bottom (3,4,5,6) experience equal load and all ropes on top (1,2,7,8) experience equal load.

$$\begin{aligned} F_{5z} &= F_{4z} = F_{3z} = F_{6z} = \sin(23.2)F_3 = 0.394 F_3 \\ F_{7z} &= F_{2z} = F_{1z} = F_{8z} = \sin(46.3)F_1 = 0.723 F_1 \end{aligned}$$

Where Fz is the vertical component of the forces on the ropes.

$$\begin{aligned} \Sigma F_z &= 0 = (F_{5z} + F_{4z} + F_{3z} + F_{6z}) + (F_{7z} + F_{2z} + F_{1z} + F_{8z}) + W_g - W_a = 0 \\ &= 4 F_{5z} + 4 F_{7z} + W_g - W_a = 0 \\ &= 4 \times 0.394 F_3 + 4 \times 0.723 F_1 + W_g - 2W_g = 0 \\ &= 1.576F_3 + 2.892F_1 - W_g = 0 \\ &= 1.576F_3 + 2.892F_1 = 33,500 \end{aligned}$$

From above, $F_1 = 0.8898F_3$.

Hence $\Rightarrow \frac{1.576}{0.8898} F_1 + 2.892F_1 = 33,500$

$$\begin{aligned} \Rightarrow 1.771F_1 + 2.892F_1 &= 33,500 \\ &= 4.663F_1 = 33,500 \end{aligned}$$

$$\begin{aligned} \Rightarrow F_1 &= 7183.93 = F_2 = F_7 = F_8 \\ \Rightarrow F_3 &= 8073.65 = F_4 = F_5 = F_6 \end{aligned}$$

Table 2.12.3-4. Tie-Down Ropes Tension Forces

Rope No.	10W Long. (lb)	5W Transv. (lb)	2W Vert.(lb)	Total (lbf)
1	---	95,096	7,184	95,367
2	---	---	7,184	7,184
3	---	106,874	8,074	107,179
4	---	---	8,074	8,074
5	102,960	106,874	8,074	148,620^{max}
6	102,960	---	8,074	103,276
7	91,614	95,096	7,184	132,242
8	91,614	---	7,184	91,895
Friction	56,287	18,835	---	---

As documented in Table 2.12.3-4, the maximum cable tension force is 148.62 kip. This load value is used in subsequent tie-down analysis of the rib.

- TIE-DOWN RIB ANALYSIS

The tie-down ribs are triangular plate two inches thick supported at the short side by a 5 inch x 6.5 inch pad that is 0.5 inch thick. This plate is rolled to conform with the toroidal shell contour. The vertical edge of the tie-down rib is welded to a stiffening ring. The tie-down rib, pad and stiffening ring are fabricated from ASTM A240, Type [[]] material. The toroidal shell material is ASTM A403, Type 304 stainless steel; and the overpack outer shell, where the stiffening ring attaches, is fabricated from ASTM A240, SS304.

The maximum temperature, 249°F, of the overpack bottom toroidal shell, where the tie-down ribs will be attached, is used as a reference.

Several modes of failure are investigated for the components of the tie-down rib system. These modes of failure are:

- Shear tearout of tie-down rib hole
- Bearing of shackle pin on ear
- Yielding of weld joints and parent metal

- SHEAR TEAROUT OF TIE-DOWN RIB HOLE

Figure 2.12.3-17 shows a sketch of the tie-down rib with the rope tension force line of action and lines of failure in shear.

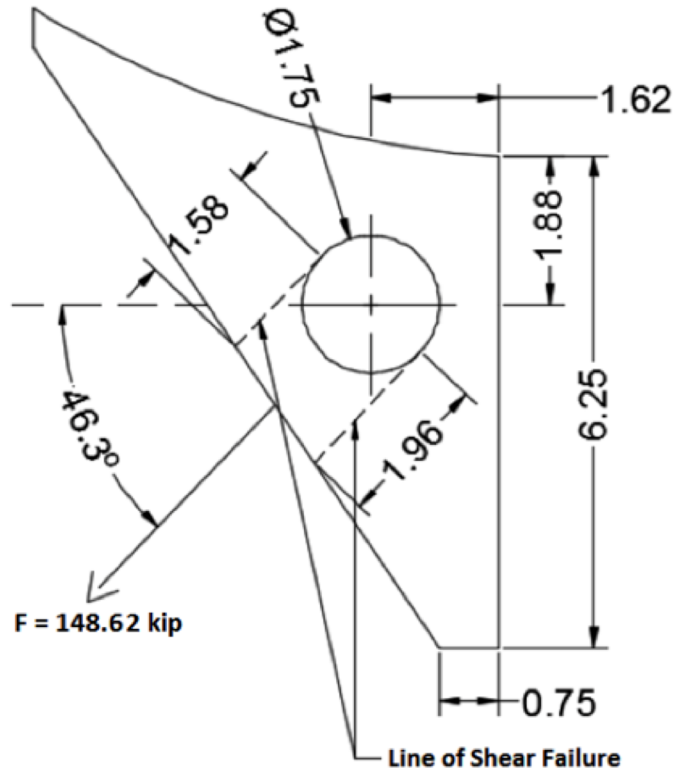


Figure 2.12.3-17. Tie-Down Rib Hole Loading

$$\tau = \frac{F}{A}$$

where $A = 2 \times (1.58 + 1.96) = 7.08 \text{ in}^2$

$$\tau = \frac{148.62}{7.08} = 20.99 \text{ ksi} < 27.12 \text{ ksi}$$

- BEARING OF SHACKLE PIN ON EAR

The bearing stress is computed assuming that the force is uniformly distributed over the projected contact area of the pin's 1.75-inch diameter. This gives for the stress:

$$\sigma = \frac{F}{A} = \frac{148.62}{2.0 \times 1.75} = 42.3 \text{ ksi}$$

$$\sigma = 42.5 \text{ ksi} < 45.2 \text{ ksi}$$

• YIELDING OF WELD JOINTS AND PARENT METAL

Figure 2.12.3-18 shows the approximate weld pattern for the top tie-down rib.

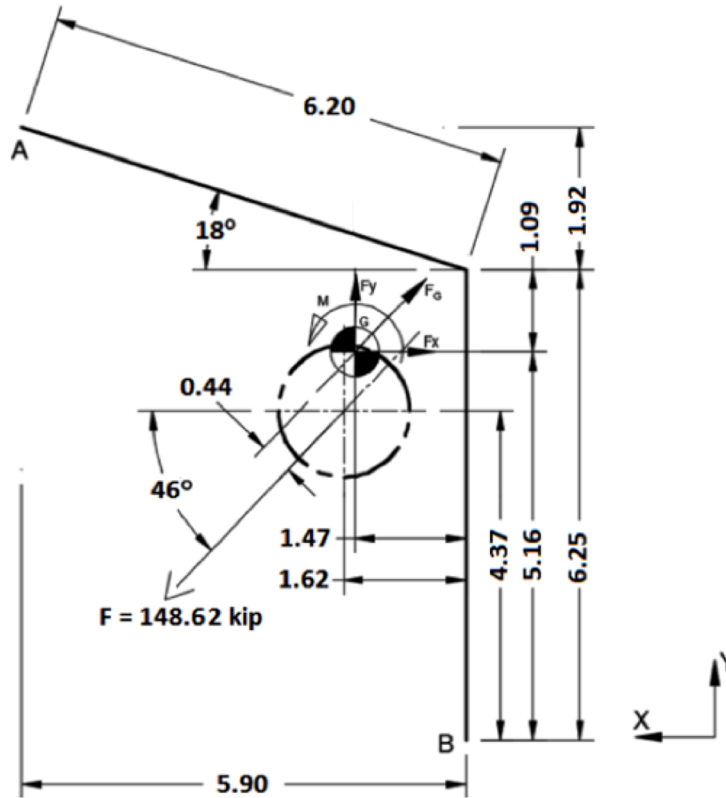


Figure 2.12.3-18. Weld Pattern of Top Tie Down Rib

Using the line load method (actual weld is 1/2 inch fillet 2 sides):

$$\begin{aligned}
 L &= 6.2 + 6.25 = 12.45 \text{ inches} \\
 \bar{X} &= \frac{\sum \bar{X}_i L_i}{\sum L_i} = \frac{6.2 \times \left(\frac{6.2 \cos(18^\circ)}{2}\right)}{12.45} = \frac{6.2 \times 2.95}{12.45} = 1.47 \text{ in} \\
 \bar{Y} &= \frac{\sum \bar{Y}_i L_i}{\sum L_i} = \frac{6.25 \times (6.25/2) + 6.2 \times \left(6.25 + \left(\frac{6.2 \sin(18^\circ)}{2}\right)\right)}{12.45} = 5.16 \text{ in} \\
 I_x &= \sum (I_o + Ad^2) \\
 &= \frac{6.25^3}{12} + 6.25 (5.16 - (6.25/2))^2 + \frac{6.2^3 \sin^2 18^\circ}{12} + \dots \\
 &\quad \dots 6.2(6.25 + \left(\frac{6.2 \sin(18^\circ)}{2}\right) - 5.16)^2 \\
 &= 74.13 \text{ in}^4/\text{in} \\
 I_y &= \frac{6.2^3 \cos^2(18^\circ)}{12} + 6.2(2.95 - 1.47)^2 + 6.25 (1.47)^2 \\
 &= 45 \text{ in}^4/\text{in}
 \end{aligned}$$

NEDO-33866 Revision 2
Non-Proprietary Information – Class I (Public)

$$\therefore I_z = I_x + I_y = 119.14 \text{ in}^4/\text{in}$$

There are two welds:

$$\begin{aligned}\therefore I_z &= 119.14 \times 2 = 238.28 \text{ in}^4/\text{in} \\ \therefore M_z &= F \times r = 148.62 \times 0.44 = 65.39 \text{ k-in.}\end{aligned}$$

$$F_x = F \cos \theta = 148.62 \cos 46^\circ = 103.24 \text{ kip}$$

$$F_y = F \sin \theta = 148.62 \sin 46^\circ = 106.91 \text{ kip}$$

∴ @ Point A:

$$P_x = \frac{F_x}{L} + \frac{M_{zy}}{I} = \frac{103.24}{2(12.45)} + \frac{(65.39)(6.25+1.92-5.16)}{(238.28)} = 4.97 \text{ k/in}$$

$$P_y = \frac{F_y}{L} + \frac{M_{zx}}{I} = \frac{106.91}{(24.9)} + \frac{(65.39)(6.2 \cos(18)-1.47)}{(238.28)} = 5.51 \text{ k/in}$$

$$P_z = 0$$

Total line load:

$$P_T = \sqrt{P_x^2 + P_y^2 + P_z^2} = 7.42 \text{ k/in.}$$

Shear stress in the effective throat area of the weld is:

$$S_v = \frac{7.42}{0.707t} = \frac{7.42}{0.707 \times 0.5} = 20.99 \text{ ksi} < 27.12 \text{ ksi (allowable base metal)}$$

Shear stress on the weld leg

$$S_t = \frac{7.42}{0.5} = 14.84 \text{ ksi}$$

∴ @ Point B:

$$P_x = \frac{103.24}{24.9} + \frac{(65.39)(5.16)}{(238.28)} = 5.56 \text{ kip}$$

$$P_y = \frac{106.9}{(24.9)} + \frac{(65.39)(1.47)}{(238.28)} = 4.7 \text{ k/in}$$

$$P_T = \sqrt{(5.56^2 + 4.7^2 + 0)} = 7.28 \text{ k/in}$$

$$S_v = \frac{7.28}{0.3535} = 20.59 \text{ ksi} < 27.12 \text{ ksi}$$

Shear stress on leg of weld:

$$S_t = \frac{7.28}{0.5} = 14.56 \text{ ksi} < 27.12 \text{ ksi}$$

The following analysis checks weld failure mode of weld attaching tie-down rib and gusset to overpack, refer to Figure 2.12.3-19.

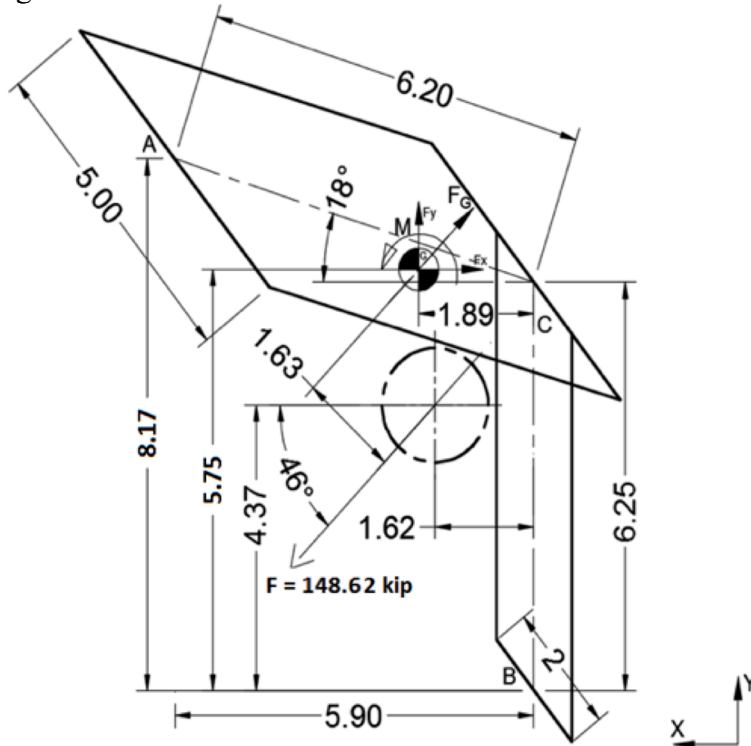


Figure 2.12.3-19. Weld Geometry of Tie-Down Rib and Gusset to Overpack

$$L = 5 + (6.2) \times 2 + 5 + 6.25 \times 2 = 34.9 \text{ inches}$$

$$\bar{X} = \frac{\sum \bar{X}_i L_i}{\sum L_i} = \frac{5 \times 6.2 \cos(18) + 12.4 \times \left(\frac{6.2 \cos(18)}{2}\right)}{34.9} = 1.89 \text{ in}$$

$$\bar{Y} = \frac{\sum \bar{Y}_i L_i}{\sum L_i} = \frac{5 \times (6.25 + 6.2 \sin(18)) + 12.4 \times \left(6.25 + \left(\frac{6.2 \sin(18)}{2}\right)\right) + 5 \times (6.25) + 12.5 \times \left(\frac{6.25}{2}\right)}{34.9} = 5.75 \text{ in}$$

$$\begin{aligned} I_z &= (5) \left[(6.2 \cos(18) - 1.89)^2 + (6.2 \sin(18) + 6.25 - 5.75)^2 \right] \\ &\quad + (12.4) \left[\left(\frac{6.2 \cos(18)}{2} - 1.89\right)^2 + \left(6.25 + \frac{6.2 \sin(18)}{2} - 5.75\right)^2 \right] \\ &\quad + (5) \left[(6.25 - 5.75)^2 + 1.89^2 \right] + (12.5) \left[1.89^2 + \left(\frac{6.25}{2} + (6.25 - 5.75)\right)^2 \right] + \frac{6.2^3}{12} + \frac{6.25^3}{12} \\ &= 339.77 \text{ in}^3 \end{aligned}$$

$$MZ = 148.62 \times 1.15 = 170.91 \text{ k-in.}$$

∴ @ Point A:

$$P_x = \frac{103.24}{34.9} + \frac{(170.89)(8.17 - 5.75)}{339.77} = 4.18 \frac{k}{in}$$

NEDO-33866 Revision 2
Non-Proprietary Information – Class I (Public)

$$P_Y = \frac{106.91}{34.9} + \frac{(170.55)(5.9-1.89)}{339.77} = 5.08 \frac{k}{in}$$

$$P_Z = 0$$

∴ Total line load:

$$P_T = \sqrt{4.18^2 + 5.08^2} = 6.58 \frac{k}{in}$$

Shear stress in the effective throat area of the weld is:

$$S_V = \frac{6.58}{0.707t} = \frac{6.58}{0.707 \times 0.5} = 18.60 \text{ ksi} < 27.12 \text{ ksi (allowable base metal)}$$

For a ½ inch fillet, shear stress in the weld leg is:

$$S_V = \frac{6.58}{(0.5)} = 13.15 \text{ ksi} < 27.12 \text{ ksi}$$

∴ @ Point B:

$$P_X = \frac{103.24}{34.9} + \frac{(170.91)(5.75)}{339.77} = 5.85 \frac{k}{in}$$

$$P_Y = \frac{106.91}{34.9} + \frac{(170.91)(1.89)}{339.77} = 4.02 \frac{k}{in}$$

$$P_Z = 0$$

∴ Total line load:

$$P_T = \sqrt{5.83^2 + 4.00^2} = 7.09 \frac{k}{in}$$

Shear stress in the effective throat area of the weld is:

$$S_V = \frac{7.09}{0.707t} = 20.07 \text{ ksi} < 27.12 \text{ ksi}$$

For a ½ inch fillet, maximum shear stress on the weld is:

$$S_V = \frac{7.09}{(0.5)} = 14.19 \text{ ksi} < 27.12 \text{ ksi}$$

The lower allowable stress for welds made to the A240 material is not a problem because of the direction of the applied load. The weld takes the load in tension. At Point C:

$$P_X = \frac{103.24}{34.9} + \frac{170.91(-0.5)}{339.77} = 2.71 \frac{k}{in}$$

$$P_Y = \frac{106.9}{34.9} + \frac{170.91(1.89)}{339.77} = 4.01 \frac{k}{in}$$

Forces acting in tension against the A240 are:

$$\begin{aligned} P_T &= P_X \sin \theta + P_Y \cos \theta \\ &= 2.71 \times \sin 18^\circ + 4.01 \times \cos 18^\circ = 4.65 \frac{k}{in} \\ S_t &= \frac{4.65}{0.5} = 9.31 \text{ ksi} < 23.7 \text{ ksi} \end{aligned}$$

• EXCESSIVE LOAD FAILURE

The tie-down system must be designed such that its failure under excessive load would not impair the ability of the package to meet the requirements of 10 CFR 71. The tie-down system is attached to the overpack structure; the cask (containment vessel) resides within the overpack without attachment to its inner surface. Therefore, failure of the tie-down will not affect the performance of the cask. The results are presented in Table 2.12.3-5.

Table 2.12.3-5. Tie-Down System Stress Analysis Results

Condition	Stress Level (ksi)	Allowable based on Yield Strength (ksi)	MS (y)	Allowable based on Ultimate Strength (ksi)	MS (U)
Shear tear-out of hole	20.99	0.6*45.2 = 27.12	0.29	36.95	0.76
Bearing of shackle pin	42.46	45.2	0.06	96.80	1.28
Yielding of weld joints	20.99	0.6*45.2 = 27.12	0.29	36.95	0.76

The tie-down rib and pin materials are type [[]] stainless steel.

The margins of safety (MS (y)) with respect to yield is calculated as follows:

$$MS \text{ (yield)} = \frac{\text{Allowable based on yield strength}}{\text{Stress level}} - 1$$

The margins of safety with respect to ultimate failure are:

Shear Strength:

$$\frac{\sigma_{ult}}{2(1+\mu)} = \frac{96.8}{2(1.31)} = 36.95 \text{ ksi}$$

Shear tear-out of tie-down rib hole

$$MS = \frac{36.95}{20.99} - 1 = 0.76$$

Bearing of shackle pin

$$MS = \frac{96.8}{42.46} - 1 = 1.28$$

Yielding of weld joints

$$MS = \frac{36.95}{20.99} - 1 = 0.76$$

2.12.4. Cask Closure Bolt Evaluation

2.12.4.1. Cask Lid Bolt Load Calculation

This section documents the cask lid bolt load calculations.

Cask Bolt Preload

The torque/preload relationship is defined as follows:

$$T = K \times D \times P_i \quad \text{Reference 2-14, Page 19}$$

Solving for P_i yields:

$$P_i = T / (K \times D)$$

NEDO-33866 Revision 2
Non-Proprietary Information – Class I (Public)

where

$$\begin{aligned}
 K &= \text{Torque friction coefficient} \\
 &= 0.15 \text{ (Reference 2-30)} \\
 D &= \text{Nominal bolt diameter (in)} \\
 &= 1.25 \text{ in} \\
 T &= 720 \pm 30 \text{ lb-in}
 \end{aligned}$$

The maximum cask bolt preload is:

$$P_{i \text{ Max}} = 750 \times 12 / (0.15 \times 1.25) = 48.00 \text{ kips}$$

Cask Bolt Applied Load: Non-Prying

The bolt non-prying load is defined as the sum of the non-prying tensile bolt force due to temperature, non-prying tensile bolt force due to pressure, axial load for gasket seating, and axial load for gasket operation for this calculation. The non-prying tensile bolt force due to temperature and non-prying tensile bolt force due to pressure can be easily calculated utilizing the parameters and formulas specified in NUREG-6007 (Reference 2-15). The axial load for gasket varies depending on the gasket material used and gasket width, which is the focus of the following evaluation.

Gasket Load

The formulas for the axial loads for gasket seating and gasket operation are given in Equation (1) and Equation (2), respectively (Reference 2-15, Table 4.2, page 13).

$$F_a = \frac{\pi D_{lg} b y}{N_b} \quad (1)$$

where

$$\begin{aligned}
 D_{lg} &= \text{Closure lid diameter at the location of the gasket load} \\
 &\quad \text{Reaction (in)} \\
 &= 29.25 \text{ in} \\
 b &= \text{Effective gasket surface seating width (in)} \\
 y &= \text{Minimum design seating stress (psi)} \\
 N_b &= \text{Total number of closure bolts} \\
 &= 15
 \end{aligned}$$

$$F_a = \frac{2 \pi D_{lg} b m (P_{li} - P_{lo})}{N_b} \quad (2)$$

$$\begin{aligned}
 m &= \text{Gasket factor for operating conditions} \\
 P_{li} &= \text{Pressure inside the closure lid (psi)} \\
 &= 30 \text{ psi} \\
 P_{lo} &= \text{Pressure outside the closure lid (psi)} \\
 &= 15 \text{ psi}
 \end{aligned}$$

Equations (1) and (2) use two experimentally determined constants, which are the gasket factor, m , and the minimum design seating stress, y . The gasket factor is taken into consideration for the axial load for gasket operation and is defined as the ratio of the required minimum gasket pressure to the pressure contained by the gasketed joint. Additionally, the seating stress is applied for the axial load for gasket seating and is defined as the minimum design seating stress of the gasket. Both of these constants are determined per Table E-1210-1 of the ASME Boiler and Pressure Vessel Code (B&PVC) Section III Division 1 Appendices (Reference 2-18, page 222).

Further, equation (1) and equation (2) both utilize the parameter b , which is the effective gasket or joint contact surface seating width. The effective gasket seating width is determined by first calculating the basic gasket seating width (b_o) per Table E-1210-2 of the ASME B&PVC Section III Division 1 Appendices (Reference 2-18). From Table E-1210-2, face sketch is used for the evaluation due to the fact that this sketch is the closest to the actual geometry as Figure B-1 depicts. It can be seen that b_o is a function of the variable w for face sketch, which is based upon the contact width between the flange facing and the gasket. Following, the effective gasket seating width is determined based off of the following criteria (Reference 2-18, page 223):

$$b = b_o, \text{ when } b_o \leq \frac{1}{4} \text{ in}$$

$$b = C_b \sqrt{b_o}, \text{ when } b_o > \frac{1}{4} \text{ in}$$

where

$$C_b = \text{effective width factor}$$

$$= 0.5 \text{ for U.S Customary calculations}$$

$$= 2.5 \text{ for SI calculations}$$

Once the effective gasket seating width is determined, both axial loads for gasket seating and gasket operation can be calculated by use of Equation (1) and Equation (2). For the calculations of this document, the parameters presented above are determined for soft aluminum. Furthermore, the seal detail drawing shown in Figure 2.12.4-1 is used to establish the contact width between the flange facing and the gasket (w) and is shown to be 0.872 inches (0.218 inches \times 4).

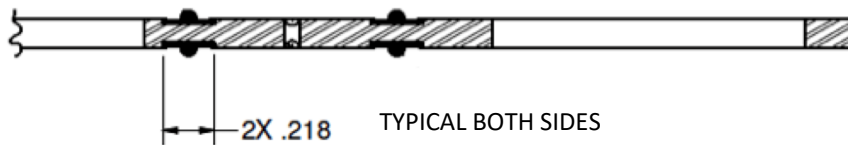


Figure 2.12.4-1. Seal with Contact Width Dimension

The gasket factor, minimum design seating stress, basic gasket seating width (b_o), and effective gasket width (b) are tabulated in Table 2.12.4-1 for the aluminum gasket material.

Table 2.12.4-1. Input Parameters

Material	Gasket Factor, m	Gasket Seating Stress, y (psi)	Basic Gasket Seating Width, b_o (in)	Effective Gasket Seating Width, b (in)
Aluminum	4.00	8800	.109	.109

The calculation for the basic gasket seating width (b_o) and effective gasket seating width (b) is determined by use of face sketch per Table E-1210-2. Therefore, the effective gasket width is:

$$b_o = \frac{w}{8} = \frac{.872 \text{ in}}{8} = .109 \text{ in}$$

Because b_o is less than $\frac{1}{4}$ in, b_o is equal to b .

With all parameters calculated, the axial loads due to gasket seating and gasket operation can be calculated.

The sections below provide a detailed analysis of the forces and moments that are subjected to the bolted joint of the Model 2000 cask during normal and accident conditions.

2.12.4.2. Lid Bolt Evaluation

2.12.4.2.1. Required Length of Engagement

For this analysis, a $1\frac{1}{4}$ -7 UNC-2A external thread with a $1\frac{1}{4}$ -7 UNC-2B internal thread is considered at an operating temperature of 150°F. The external thread material is ASTM A-540, Grade B22, Class 3 and the internal thread material is ASME SA-182, F304. Table 2.12.4-2 lists the required parameters needed for the analysis.

Table 2.12.4-2. Lid Bolt Evaluation Input Parameters

Parameter	Variable	Input	Units
Tensile Strength of External Thread at 150°F	S_{u1}	145*	ksi
Tensile Strength of Internal Thread at 150°F	S_{u2}	73	ksi
Minimum Pitch Diameter (External Thread)	$E_{s,min}$	1.1476	in
Minimum Major Diameter (External Thread)	$D_{s,min}$	1.2314	in
Maximum Pitch Diameter (Internal thread 2B)	$E_{n,max}$	1.1668	in
Maximum Major Diameter (Internal thread 2B)	$K_{n,max}$	1.123	in
Threads Per Inch	n	7	in
Bolt Pre-Load	P	82.8	kip

References:

Reference 2-30 Minimum Pitch Diameter: Table 3, Page 1827

Reference 2-30 Minimum Major Diameter: Table 3, Page 1827

Reference 2-30 Maximum Pitch Diameter (2B): Table 3, Page 1827

Reference 2-30 Maximum Minor Diameter (2B): Table 3, Page 1827

Based on these given inputs, it must be determined if the bolt will fail before the threads of either the internal or external fixtures or vice versa. To do this, the required length of engagement must be calculated and checked against the actual geometry. The length of engagement (L_e) is calculated as follows (Reference 2-30, Page 1536),

$$L_e = \frac{2A_t}{\pi(K_{n,max})(\frac{1}{2} + .57735n[E_{s,min} - K_{n,max}])}$$

NEDO-33866 Revision 2
Non-Proprietary Information – Class I (Public)

Where,

$$A_t = \text{Screw thread tensile stress area}$$

and A_t is given by the equation,

$$A_t = \pi \left[\frac{E_{s,\min}}{2} - \frac{0.16238}{n} \right]^2$$

The length of engagement (L_e) is for mating external and internal threads of the same strength. If the materials of the internal and external threads do not have the same strength, the relative strength (J) must be calculated to determine if the internal thread could strip before the bolt breaks. The relative strength is calculated as follows,

$$J = \frac{A_s \times S_{ut \text{ of external thread material}}}{A_n \times S_{ut \text{ of internal thread material}}}$$

where

$$A_s = \text{Shear area of external threads}$$

$$A_n = \text{Shear area of internal threads}$$

Also, the shear area of the external and internal threads are given by,

$$A_s = \pi n L_e K_{n,\max} \left[\frac{1}{2n} + .57735(E_{s,\min} - K_{n,\max}) \right]$$

and,

$$A_n = \pi n L_e D_{s,\min} \left[\frac{1}{2n} + .57735(D_{s,\min} - E_{n,\max}) \right]$$

where

$$n = \text{number of threads per inch}$$

If the relative strength is calculated to be less than or equal to 1, then the length of engagement (L_e) is sufficient to prevent stripping of the internal thread. If the relative strength is calculated to be greater than 1, then the required length of engagement is calculated by taking the product of the J factor and the length of engagement as given is:

$$Q = J L_e$$

where

$$Q = \text{Required length of engagement}$$

Once the required length of engagement is calculated, this value is checked against the actual geometry to determine if the internal threads will strip before the bolt breaks or vice versa. Table 2.12.4-3 presents the results.

Table 2.12.4-3. Calculation of Required Length of Engagement at 150°F

Parameter	Variable	Result	Units
Tensile stress area of bolt	A_t	0.952	in ²
Effective length	L_e	0.901	in
Shear area of internal threads	A_n	2.652	in ²
Shear area of external threads	A_s	1.905	in ²
Relative strength of external/internal threads	J	1.427	--
Required length of engagement if $J > 1$	Q	1.285	in

Looking at the actual geometry, the engagement = 3.00 inches (lid bolt length) – 1.625 inches (flange + seal) = 1.375 inches. At 150°F, the required length of engagement is less than the engagement of the geometry. Therefore, a thread engagement of 1.375 inches will ensure that the threads of either the internal or external fixture will not strip before the bolt fails for a Class 2A bolt in 2B threads.

2.12.4.2.2. Applied Load Analysis

The maximum load on the bolt to break the threaded portion is determined by taking the product of the ultimate tensile strength of the external thread and the bolt thread tensile stress area (Reference 2-30).

$$\begin{aligned}
 P_{\max} &= S_u A_t \\
 &= (145 \text{ ksi})(.952 \text{ in}^2) \\
 P_{\max} &= 138 \text{ kip}
 \end{aligned}$$

Now that the maximum load has been calculated, the minimum thread engagement, L_e , based on the applied pre-load is:

$$\begin{aligned}
 P &= \sigma A_n \\
 &= \text{bolt pre-load} \\
 &= 82.8 \text{ kip} \\
 &= \text{Tensile strength of internal thread} \\
 A_n &= \text{Internal thread shear area (Class 2A + 2B)}
 \end{aligned}$$

From Reference 2-30:

$$P = \sigma \times \pi \times n \times L_e \times D_{s,\min} \times [1/2n + .57735(D_{s,\min} - E_{n,\max})]$$

Solving for the effective length:

$$L_e = P / (\sigma \times \pi \times n \times D_{s,\min} \times [1/2n + .57735(D_{s,\min} - E_{n,\max})])$$

Solving, the minimum thread engagement is 0.3852 inches at an operating temperature of 150°F. accordingly, calculating the product of the effective length and the number of threads per inch, the minimum thread engagement to prevent internal 2B thread stripping is approximately three threads.

2.12.4.2.3. Bolt Stress Analysis

The cask lid of the Model 2000 cask is fastened to the cask flange by way of 15 uniformly spaced ASTM A540, Grade B-22, Class 3 socket head screws. Table 2.12.4-4 provides the input parameters that are to be used in the analysis at an operating temperature of 500°F.

Table 2.12.4-4. Model 2000 Stress Analysis Design Input Parameter

Parameter	Variable	Input	Units
Number of Bolts	N_b	15	--
Lid Diameter at Bolt Circle	D_{lb}	32.25	in
Lid Diameter at Gasket	D_{lg}	29.25	in
Nominal Bolt Diameter	D_b	1.25	in
Lid Diameter at Inner Edge	D_{li}	28	in
Lid Diameter at Outer Edge	D_{lo}	34.75	in
Equivalent Thickness of Lid	t_l	7.89	in
Thickness of Lid Flange	t_{lf}	1.5	in
Thickness of Cask Wall	t_c	6	in
Bolt Length Between the Top and Bottom of Closure Lid at Bolt Circle	l_b	1.5	in
Bolt Engagement Length	BEL	1.625	in
Bolt Moment of Inertia/Cir	XIB	0.018	in ³
Young's Modulus For Lid	E_l	25900000	psi
Young's Modulus For Cask	E_c	25900000	psi
Young's Modulus For Bolt	E_b	27400000*	psi
Poisson's Ratio For Lid	N_{ul}	0.31	--
Poisson's Ration For Cask	N_{uc}	0.31	--
Lid Thermal Expansion Coefficient	a_l	9.70E-06	1/°F
Bolt Thermal Expansion Coefficient	a_b	7.30E-06*	1/°F
Weight of Cask Payload	W_C	5450	lb
Weight of Cask Lid	W_l	1900	lb
Dynamic Load Factor	DLF	1	--
Preload Torque	Q_{NOM}	720	lb-ft
Preload Torque Tolerance	Q_{TOL}	30	lb-ft
Maximum Preload Torque	Q_{MAX}	9000	lb-in
Minimum Preload Torque	Q_{MIN}	8280	lb-in
Nut Factor For Preload Torque	K_q	0.15	--
Gasket Seating Width	G_b	0.109	in
Gasket Seating Stress	G_y	8800	psi
Gasket Factor	G_m	4	--
Wall Thermal Expansion Coefficient	a_c	9.70E-06	1/°F
Basic Allowable Stress Limit	S_m	7.71E+04	psi
Minimum Yield Strength	S_y	115700	psi
Minimum Ultimate Strength	S_u	145000	psi
Pressure Inside Closure Lid	P_{li}	30	psi

NEDO-33866 Revision 2
Non-Proprietary Information – Class I (Public)

Parameter	Variable	Input	Units
Pressure Outside the Closure Lid	P _{lo}	15	psi
Pressure Inside the Cask Wall	P _{ci}	30	psi
Pressure Outside the Cask Wall	P _{co}	15	psi
Temperature Change of the Closure Lid	T _l	117.5	°F
Temperature Change of the Closure Bolt	T _b	111.9	°F
Temperature Change of the Cask Wall	T _c	118.0	°F
Temperature Change of Inner Surface of Closure Lid	T _{li}	116.8	°F
Temperature Change for Outer Surface of Closure Lid	T _{lo}	118.1	°F
Maximum rigid body impact acceleration (g)	a _i	25**	--
Impact angle between the cask axis and the target surface	xi	90°	--
Maximum axial vibration acceleration (g) at the cask support	ava	2	--
Maximum transverse vibration acceleration (g) at the cask support	avt	5	--
Vibration transmissibility of acceleration between the cask support and the closure lid	VTR	1	--

References:

- Reference 2-31 Gasket Seating Width: Table E-1210-2
- Reference 2-31 Gasket Seating Stress: Table E-1210-1
- Reference 2-31 Gasket Factor: Table E-1210-1
- Reference 2-15 Basic Allowable Stress Limit: Table 6.1, Page 28
- Reference 2-1 Maximum Axial Vibration Acceleration (g) at the cask support
- Reference 2-1 Maximum Transverse Vibration Acceleration (g) at the cask support
- Reference 2-15 Vibration transmissibility of acceleration between the cask support and the closure lid

Notes:

- * Grade B21 bolt properties used because temperature dependent values could not be found for Grade B22.
- ** Section 2.12.1, Figure 2.12.1.11-30 presents the justification for the reduced impact acceleration during the HAC end drop.

NUREG/CR-6007 (Reference 2-15) is used to accurately verify whether or not the closure bolts can effectively hold up to the various loads in both normal conditions of transport and hypothetical accident conditions. This includes forces and moments due to pressure, temperature, vibration, impact, preload, gasket, puncture, and prying. Also, NUREG/CR-6007 gives procedures for combining loads and stress limits that must be met. Loads include the axial force (F_a), shear force (F_s), fixed-edge closure-lid force (F_f), fixed edge closure lid moment (M_f), and also torsional moments (M_t) that are created by the torque wrench in the preload and gasket seating operations. All of which are elaborated on in the following sections.

2.12.4.2.4. Forces/Moments Generated By Preload

Found in Table 4.1 in NUREG/CR-6007, are the bolts loads due to use of a torque wrench. The non-prying axial bolt force per bolt is given by the equation,

$$F_a = Q / (K_q \times D_b)$$

The torsional bolt force per bolt is defined by the formula,

$$M_t = 0.5 Q$$

2.12.4.2.5. Forces/Moments Generated By Gasket Loads

Per Table 4.2 in NUREG/CR-6007, are the formulas for calculating the forces and moments generated by gasket loads by utilization of a torque wrench. The axial force produced by the gasket seating operation is evaluated by use of the following equation,

$$F_a = \frac{\pi \times D_{lg} \times G_b \times G_y}{N_b}$$

and the torsional bolt moment due to the seating operation is,

$$M_t = \frac{0.5 \times \pi \times K_q \times D_b \times D_{lg} \times G_b \times G_y}{N_b}$$

Also, The non-prying tensile bolt force per bolt produced by the operating gasket seating is determined by,

$$F_a = \frac{2 \times \pi \times D_{lg} \times G_b \times G_m (P_{li} - P_{lo})}{N_b}$$

2.12.4.2.6. Forces/Moments Generated By Pressure Loads

Table 4.3 in NUREG/CR-6007 is applied to determine the moments and forces that are generated due to the pressure difference between the inside and outside of the cask. The associated equation for the axial force due to pressure loads is,

$$F_a = \frac{\pi \times D_{lg}^2 \times (P_{li} - P_{lo})}{4 \times N_b}$$

where

$$\begin{aligned} P_{li} &= \text{Pressure inside the closure lid} \\ &= 30 \text{ psi} \\ P_{lo} &= \text{Pressure outside the closure lid} \\ &= 15 \text{ psi} \end{aligned}$$

The shear bolt force per bolt is then,

$$F_s = \frac{\pi \times E_t \times t_t \times (P_{li} - P_{lo}) \times D_{fb}^2}{2 \times N_b \times E_c \times t_c \times (1 - \nu_{ul})}$$

where

$$\begin{aligned} P_{ci} &= \text{Pressure inside the cask wall} \\ &= 30 \text{ psi} \\ P_{co} &= \text{Pressure outside the cask wall} \\ &= 15 \text{ psi} \end{aligned}$$

The fixed-edge closure-lid force generated by internal pressure is,

$$F_f = \frac{D_{lb} (P_{li} - P_{lo})}{4}$$

and the fixed-edge moment is,

$$M_f = \frac{D_{lb}^2 (P_{li} - P_{lo})}{32}$$

2.12.4.2.7. Forces/Moments Generated By Temperature Loads

Table 4.4 of NUREG/CR-6007 gives the formulas for bolt forces/moments generated by thermal expansion difference between the closure lid, bolt, and wall. The axial force due to a temperature difference between the closure bolt and lid is:

$$F_a = \frac{1}{4} \times \pi \times D_b^2 \times E_b \times (\alpha_l \times T_l - \alpha_b \times T_b)$$

where

$$\begin{aligned} T_l &= \text{Temperature change of the closure lid} \\ &= 117.5^\circ\text{F} \end{aligned}$$

$$\begin{aligned} T_b &= \text{Temperature change of the closure bolt} \\ &= 111.9^\circ\text{F} \end{aligned}$$

The shear force acting on each bolt is given by,

$$F_s = \frac{\pi \times E_l \times t_l \times D_{lb} \times (a_l \times T_l - a_c \times T_c)}{N_B \times (1 - N_{ul})}$$

where,

$$\begin{aligned} T_c &= \text{Temperature change of the cask wall} \\ &= 118^\circ\text{F} \end{aligned}$$

Fixed-edge force and fixed-edge moment due to temperature difference between the inner and outer surface of the closure lid is determined by use of the following equations.

$$F_f = 0 \text{ lb/bolt}$$

$$M_f = \frac{E_l \times a_l \times t_l^2 \times (T_{lo} - T_{li})}{12 \times (1 - N_{ul})}$$

where,

$$\begin{aligned} T_{lo} &= \text{Temperature change of the outer surface of the closure lid} \\ &= 118.1^\circ\text{F} \end{aligned}$$

$$\begin{aligned} T_{li} &= \text{Temperature change of the inner surface of the closure lid} \\ &= 116.8^\circ\text{F} \end{aligned}$$

2.12.4.2.8. Forces/Moments Generated By Impact Loads

For this evaluation, the loads created by impact are analyzed for a cask with a protected closure lid and are found via Table 4.5 in NUREG/CR-6007. As follows, the non-prying tensile bolt force per bolt due to impact is:

$$F_a = \frac{1.34 \times \sin(\alpha_i) \times DLF \times a_i \times (W_l - W_c)}{N_b}$$

Further, the shear bolt force per bolt is evaluated using,

$$F_s = \frac{\cos(\alpha_i) \times a_i \times W_l}{N_b}$$

Accordingly, the fixed-edge force and fixed-edge moment are defined by:

$$F_f = \frac{1.34 \times \sin(\alpha) \times DLF \times a_i \times (W_1 - W_c)}{\pi \times D_{1b}}$$

and,

$$M_f = \frac{1.34 \times \sin(\alpha) \times DLF \times a_i \times (W_1 - W_c)}{8\pi}$$

2.12.4.2.9. Forces/Moments Generated By Vibration Loads

Looking at Table 4.8 in NUREG/CR-6007, the loads that are generated due to vibration are outlined. The tensile bolt force per bolt due to vibration is:

$$F_a = \frac{VTR \times a_{va} \times W_1}{N_b}$$

The shear bolt force per bolt is calculated by use of the equation,

$$F_s = \frac{VTR \times a_{vt} \times W_1}{N_b}$$

The fixed-edge force and fixed edge moment are:

$$F_f = \frac{VTR \times a_{va} \times W_1}{\pi \times D_{1b}}$$

and,

$$M_f = \frac{VTR \times a_{va} \times W_1}{8\pi}$$

2.12.4.2.10. Prying Action Forces Generated by Applied Loads

Table 2.1 of NUREG/CR-6007 lays out the analysis to evaluate the axial bolt force per bolt caused by prying action of the lid is:

$$F_{ap} = \left(\frac{\pi D_{1b}}{N_b} \right) \left[\frac{\frac{2 \times M_f}{D_{1o} - D_{1b}} - C1(B - F_f) - C2(B - P)}{C1 + C2} \right]$$

where

$$C1 = 1$$

$$C2 = \left(\frac{8}{3(D_{1o} - D_{1b})^2} \right) \left(\frac{E_l \times t_l^3}{1 - \nu_{ul}} + \frac{(D_{1o} - D_{1l}) E_{lf} \times t_{lf}^3}{D_{1b}} \right) \left(\frac{L_b}{N_b D_b^2 E_b} \right)$$

$$L_b = \text{Bolt length between the top and bottom surfaces of the closure lid at the bolt circle}$$

$$= 1.5 \text{ in}$$

$$B = F_f \text{ if } F_f > P, \text{ otherwise } B = P$$

It should be noted that the fixed-edge force and fixed-edge moment are inputs from Table 4.2, 4.3 and 4.8 for NCT and Table 4.2, 4.3 and 4.5 for HAC.

2.12.4.2.11. Bending Bolt Moment Generated by Applied Loads

Located in Table 2.2 of NUREG/CR-6007 is the formula for calculating the bending bolt moment per bolt caused by the rotation or bending of the closure lid and is:

$$M_{bb} = \left(\frac{\pi D_{1b}}{N_b} \right) \left(\frac{K_b}{K_b + K_l} \right) M_f$$

where

$$K_b = \left(\frac{N_b}{L_b}\right) \left(\frac{E_b}{D_{1b}}\right) \left(\frac{D_b^4}{64}\right)$$

$$K_l = \frac{E_l t_l^3}{3 \left[(1 - N_{ul}^2) + (1 - N_{ul})^2 \left(\frac{D_{1b}}{D_{1o}}\right) \right] D_{1b}}$$

Once again, it should be noted that the fixed-edge force and fixed-edge moment are inputs from Table 4.2, 4.3 and 4.8 for NCT and Table 4.2, 4.3 and 4.5 for HAC.

2.12.4.2.12. Calculation of Total Loads and Bolt Stresses

In order to accurately combine tensile bolt forces, Table 4.9 of NUREG/CR-6007 is applied. To calculate the total non-prying axial load, the axial bolt force from Tables 4.3-4.8 is summed. The same process is used to determine the total fixed-edge force and fixed-edge moment. Further, the bolt stresses can be formulated from Table 5.1 of NUREG/CR-6007. Calculating the average bolt direct stress caused by the tensile bolt force is:

$$S_{ba} = 1.2732 F_a / D^2$$

and the average bolt shear stress is formulated as,

$$S_{bs} = 1.2732 F_s / D^2$$

The maximum bending stress and maximum shear stress are represented as,

$$S_{bb} = 10.186 M_{bb} / D^3$$

$$S_{bt} = 5.093 M_t / D^3$$

Where F_a , F_s , M_{bb} , and M_t all represent total values of the tensile bolt force, shear bolt force, bending bolt moment, and torsional bolt moment respectively.

2.12.4.2.13. Limits on Bolt Stresses

Table 6.1 of NUREG/CR-6007 gives the acceptance criteria for normal conditions of transport. The acceptance criteria state that the average stress must be less than the allowable stress in tension. For shear, the average stress must be less than 60 percent of the allowable stress. In addition, the sum of the squares of the stress ratio for average tensile stress and stress ratio for average shear stress must be less than one. Further, the maximum stress intensity must be less than 1.35 times the allowable stress for bolts having a minimum tensile strength greater than 100 ksi and 1.5 times for bolts having a minimum tensile strength less than 100 ksi.

Looking at Table 6.3 for HAC, the average stress in tension must be less than the smaller of $0.7S_u$ or S_y at temperature. The average stress in shear must be less than the smaller of $0.42S_u$ or $0.6S_y$ at temperature. Furthermore, the sum of the squares of the stress ratio for average tensile stress and stress ratio for average shear stress must be less than one.

2.12.4.2.14. Analytical Results

Forces and Moments

The forces and moments that the Model 2000 Transport Package closure lid, wall, and bolt are subjected to during normal conditions of transport and hypothetical accident conditions are shown in Table 2.12.4-5 and Table 2.12.4-6, respectively.

Table 2.12.4-5. Forces/Moments Results (NCT)

Load Condition	Forces/Moments	Variable	Magnitude	Units
PRESSURE	Non-Prying Tensile Bolt Force	F _a	671.96	lb
	Shear Bolt Force Per Bolt	F _s	3113.55	lb
	Fixed-Edge Closure-Lid Force	F _f	120.94	lb
	Fixed-Edge Closure-Lid Moment	M _f	487.53	lb-in
TEMPERATURE	Non-Prying Tensile Bolt Force	F _a	10856.79	lb
	Shear Bolt Force Per Bolt	F _s	-9701.92	lb
	Fixed-Edge Closure-Lid Force	F _f	0	lb
	Fixed-Edge Closure-Lid Moment	M _f	2455.49	lb-in
VIBRATION	Non-Prying Tensile Bolt Force	F _a	253.33	lb
	Shear Bolt Force Per Bolt	F _s	633.33	lb
	Fixed-Edge Closure-Lid Force	F _f	37.51	lb
	Fixed-Edge Closure-Lid Moment	M _f	151.2	lb-in
PRELOAD	Non-Prying Tensile Bolt Force Per Bolt	F _a	48000	lb
	Torsional Bolt Moment Per Bolt	M _t	4500	lb-in
GASKET	Axial Load For Gasket Seating	F _a	5876.16	lb
	Axial Load For Gasket Operation	F _a	80.13	lb
	Torque Due to Gasket	M _t	550.89	lb-in
PRYING	Axial Load Due to Prying	F _a	-2339.42	lb
	Bending Moment Due to Prying	M _{bb}	9.99	lb-in

Table 2.12.4-6. Forces/Moments Results (HAC)

Load Condition	Forces/Moments	Variable	Magnitude	Units
PRESSURE	Non-Prying Tensile Bolt Force	F _a	671.96	lb
	Shear Bolt Force Per Bolt	F _s	3113.55	lb
	Fixed-Edge Closure-Lid Force	F _f	120.94	lb
	Fixed-Edge Closure-Lid Moment	M _f	487.53	lb-in
TEMPERATURE	Non-Prying Tensile Bolt Force	F _a	10856.79	lb
	Shear Bolt Force Per Bolt	F _s	-9701.92	lb
	Fixed-Edge Closure-Lid Force	F _f	0	lb
	Fixed-Edge Closure-Lid Moment	M _f	2455.49	lb-in
IMPACT	Non-Prying Tensile Bolt Force	F _a	16415.00	lb
	Shear Bolt Force Per Bolt	F _s	0	lb
	Fixed-Edge Closure-Lid Force	F _f	2430.26	lb
	Fixed-Edge Closure-Lid Moment	M _f	9796.98	lb-in
PRELOAD	Non-Prying Tensile Bolt Force Per Bolt	F _a	48000	lb
	Torsional Bolt Moment Per Bolt	M _t	4500	lb-in
GASKET	Axial Load For Gasket Seating	F _a	5876.16	lb
	Axial Load For Gasket Operation	F _a	80.13	lb
	Torque Due to Gasket	M _t	550.89	lb-in
PRYING	Axial Load Due to Prying	F _a	-2149.02	lb
	Bending Moment Due to Prying	M _{bb}	41.13	lb-in

2.12.4.2.15. Total Loads and Bolt Stresses Results

Now that all of the forces and moments have been calculated for both NCT and HAC, the loads can be combined appropriately to determine the total loads. Additionally, the bolt stresses can be calculated from the total loads. The results are displayed below for NCT and HAC in Table 2.12.4-7 and Table 2.12.4-8 respectively.

Table 2.12.4-7. Total Loads/Bolt Stresses (NCT)

Total Loads/ Bolt Stresses	Variable	Magnitude	Units
Total Bolt Axial Load	F _a	63318.83	lb
Total Bolt Shear Load	F _s	-5995.04	lb
Total Bolt Bending Moment	M _b	3094.22	lb-in
Total Bolt Torsional Moment	M _t	4500	lb-in
Average Bolt Direct Stress	S _{ba}	65335.10	psi
Average Bolt Shear Stress	S _{bs}	-6144.66	psi
Maximum Bending Stress	S _{bb}	22994.83	psi
Maximum Shear Stress	S _{bi}	16720.98	psi
Maximum Stress Intensity	S _{bt}	90827.37	psi

Table 2.12.4-8. Total Loads/Bolt Stresses (HAC)

Total Loads/ Bolt Stresses	Variable	Magnitude	Units
Total Bolt Axial Load	F _a	79670.89	lb
Total Bolt Shear Load	F _s	-6588.37	lb
Total Bolt Bending Moment	M _b	12781.13	lb-in
Total Bolt Torsional Moment	M _t	4500	lb-in
Average Bolt Direct Stress	S _{ba}	82207.87	psi
Average Bolt Shear Stress	S _{bs}	-6798.17	psi
Maximum Bending Stress	S _{bb}	94983.60	psi
Total Bolt Shear Stress	S _{bt}	16720.98	psi

2.12.4.2.16. Limits on Bolt Stresses Results

Accordingly, the code evaluation is conducted using the information given in the previous subsection and the appropriate tables from NUREG/CR-6007 for both NCT and HAC. Per Table 6.1 of NUREG/CR-6007, the limits for NCT are evaluated as,

$$S_{ba} < S_u$$

$$65335.10 \text{ psi} < 77,130 \text{ psi}$$

and,

$$S_{bs} < 0.6S_u$$

$$-6144.66 \text{ psi} < 46278 \text{ psi}$$

also,

$$R_t^2 + R_s^2 < 1$$

$$(0.8474)^2 + (-0.1328)^2 < 1$$

where,

$$R_t = \text{Stress ratio for average tensile stress}$$

$$R_s = \text{Stress ratio for average shear stress}$$

Per Table 6.3 of NUREG/CR-6007, the limits for HAC are evaluated as,

$$S_{ba} < 0.7S_u$$

$$82207.87 \text{ psi} < 101500 \text{ psi}$$

and,

$$S_{bs} < 0.42S_u$$

$$-6798.17 \text{ psi} < 60900 \text{ psi}$$

also,

$$R_t^2 + R_s^2 < 1$$

$$(0.8099)^2 + (-0.1116)^2 < 1$$

2.12.4.2.17. Fatigue Analysis

The fatigue analysis considers vibration and operating stresses, which come from the NCT bolt stress. Included in the operating stress are the pressure, preload, gasket load, and temperature stresses. Therefore, the loads are:

$$S_{\text{Operating}} = 67487.62 \text{ psi}$$

$$S_{\text{Vibration}} = 261.40 \text{ psi}$$

Using ASME Code, Section III, NB-3232.3 (Reference 2-32, page 91), the alternating stresses can be found by the equation below,

$$S_{\text{a-Operating}} = \text{RF} \times S_{\text{Operating}} \left(\frac{E_{\text{dc}}}{E_{\text{a}}} \right)^U$$

$$S_{\text{a-Vibration}} = \text{RF} \times S_{\text{Vibration}} \left(\frac{E_{\text{dc}}}{E_{\text{a}}} \right)^U$$

where

$$\text{RF} = \text{Fatigue Strength Reduction Factor (Reference 2-32)}$$

$$E_{\text{dc}} = \text{Modulus of Elasticity on Design Fatigue Curve (Reference 2-18, Figure I-9.4, page 12)}$$

$$E_{\text{a}} = \text{Modulus of Elasticity used in the Analysis}$$

$$U = \text{Cumulative Usage Factor}$$

$$U = 1 \text{ (Reference 2-32)}$$

Applying ASME Section III, Figure I-9.4, the fatigue limit for maximum nominal stress $\leq 2.7 S_m$ for the loads of this analysis are,

$$N_{\text{a-Operating}} = 466 \text{ Cycles}$$

$$N_{\text{a-Vibration}} = 10^{11} \text{ Cycles}$$

The above values are accurately calculated by interpolating the tabular data given in ASME Section III, Table I-9.0 (Reference 2-18, page 2). Assuming 10^7 cycles for vibration load and 190 transports:

$$N_{\text{Operating}} = 190 \text{ Cycles}$$

The accumulative usage is then,

$$R = \left(\frac{N_{\text{Operating}}}{N_{\text{a-Operating}}} \right) + \left(\frac{N_{\text{Vibration}}}{N_{\text{a-Vibration}}} \right)$$

Shown in Table 2.12.4-9 are the results from the analysis.

Table 2.12.4-9. Fatigue Analysis Results

Parameter	Variable	Value	Units
Vibration Stress	$S_{\text{vibration}}$	261.40	psi
Operating Stress	$S_{\text{operating}}$	67487.62	psi
Fatigue Strength Reduction Factor	RF	4	--
Cumulative Usage Factor	U	1	--
E given on design curve	E_{dc}	30000000	psi
E used in analysis	E_{a}	27400000	psi
Ratio of Modulus of Elasticity	E_{ratio}	1.09	--
Alternating Stress due to Vibration	$S_{\text{a-Vibration}}$	572.41	psi
Alternating Stress due to Operating	$S_{\text{a-Operating}}$	147783.10	psi
Number of Alt. Cycles due to Vibration	$N_{\text{a-Vibration}}$	1E+11	--
Number of Alt. Cycles due to Operating	$N_{\text{a-Operating}}$	466	--
Number of Cycles for Vibration Load	$N_{\text{Vibration}}$	1.00E+07	--
Number of Cycles for Operating Load	$N_{\text{Operating}}$	190	--
Accumulative Usage	R	0.4078	--

Because the accumulative usage is less than one, it is acceptable to have up to 190 transports before all bolts are replaced. After 190 transports, all bolts must be replaced.

2.12.5. Model 2000 Scale Model Drop Test Report

Model 2000 Drop Test Report No. 87-08-01 is provided in the following pages.